Geochemical and Physical Water Mass Properties and Halocarbon Ventilation in the Southern Canadian Basin of the Arctic Ocean

By

Fiona McLaughlin
B.Sc., University of Victoria, 1972

A Thesis Submitted in Partial Fulfillment of the Requirements for the Degree of

MASTERS OF SCIENCE

in the School of Earth and Ocean Sciences

We accept this thesis as conforming to the required standard

[redacted]

Dr James Bishop, Supervisor (School of Earth and Ocean Sciences)

[redacted]

Dr. Michael Whiticar, Departmental Member (School of Earth and Ocean Sciences)

[redacted]

Dr. Eddy Carmack, Departmental Member (School of Earth and Ocean Sciences)

[redacted]

Dr Robie Macdonald, Outside Member (Institute of Ocean Sciences)

[redacted]

Dr. Frank Robinson, External Examiner (Department of Chemistry)

Supervisor: Dr. James Bishop

Abstract

Temperature, salinity, nutrients, oxygen, and halocarbon data collected in the Arctic Ocean reveal a frontal structure previously unrecognized in the hydrography of the Canadian Basin. Samples were collected in 1993 on a 1300-km section extending from the Beaufort Sea in the Canada Basin to the East Siberian Sea in the Makarov Basin and reveal a lateral boundary between water masses of Atlantic and Pacific origin. The term water mass assembly is introduced to describe the basic arrangement or vertical stacking of water masses found in the Arctic Ocean, recognizing that water mass components within each assembly may differ from basin to basin. Because the presence or absence of Pacific origin water is a key characteristic distinguishing the two assemblies (EA and WA), the water mass boundary between the two assemblies is referred to as the Atlantic/Pacific front. Earlier research indicated that water masses in the Arctic Ocean were separated by a front located above the Lomonosov Ridge. Although all stations from the Canada Basin display classic WA assembly characteristics, the Makarov Basin station shows EA assembly characteristics in the upper and Atlantic layers and a WA assembly deep layer. This suggests a relocation in the position of the Atlantic/Pacific boundary away from the Lomonosov Ridge. Further, data show the transition region between the Atlantic and deep layers

is fresher in the Makarov Basin than corresponding water in either the Canada or Eurasian basins, implying a source of cold, low-salinity water, perhaps from Eurasian shelves. The front separating these two assemblies now lies above the Mendeleyev Ridge and is marked by large lateral gradients in all measured properties. In particular, the penetration of anthropogenic halocarbons is 2 to 3 times deeper and the apparent ages are younger in the Makarov Basin than in the Canada Basin, implying enhanced rates of ventilation and more vigorous circulation.

Examiners:

[redacted]

Dr James Bishop, Supervisor (School of Earth and Ocean Sciences)

[redacted]

Dr. Michael Whiticar, Departmental Member (School of Earth and Ocean Sciences)

[redacted]

Dr. Eddy Carmack, Departmental Member (School of Earth and Ocean Sciences)

[redacted]

Dr Robie Macdonald, Outside Member (Institute of Ocean Sciences)

[redacted]

Dr. Frank Robinson, External Examiner (Department of Chemistry)

Table of Contents

List of Tables

List of Figures

Chapter 4

Chapter 5

Chapter 1: Introduction

Nansen, in his 1902 discussion of the **Fram** expedition, reasoned that because pathways of communication exist between the Arctic Ocean and the world ocean through Fram Strait, Bering Strait and the Canadian Archipelago, a relationship must exist among the North Polar Basin, ocean circulation and global climate. One hundred years later, general climate models (GCMs) suggest that the Arctic Ocean is sensitive to changes in global climate, and may, in fact, influence the global thermohaline circulation (Manabe and Stouffer, 1988; Walsh and Crane, 1992). Recent analysis of ice core data from the Greenland Ice Cap confirm that the arctic is sensitive to climate change (Cuffey et al., 1995).

Freshwater export from the Arctic Ocean via Fram Strait and the Canadian Archipelago is believed to condition northern latitude convection and the water mass transformation that drives global overturning in the ocean (Aagaard and Carmack, 1989). This convection in the Greenland, Iceland, Norwegian and Labrador seas, and the global circulation that results, has been linked to fluctuations in the northern European climate. Periods of weaker thermohaline forcing have been also associated with major climatic disturbances in the paleoclimate record (Broecker et al., 1985), which likewise suggest that perturbations in freshwater export from the Arctic Ocean influence regional and global climate. Increased freshwater export supplies additional buoyancy to North Atlantic water and weakens convection, perhaps to the point where convection sites and regions of ice cover are moved further south; conversely, decreased freshwater export strengthens convection and moves convection sites and regions of ice cover northward (Aagaard and Carmack, 1994). Understanding Arctic Ocean circulation and the mechanisms by which it

receives, modifies and exports various water masses is therefore critical to developing reliable models of climate change.

Arctic Ocean circulation is also an important factor in determining how contaminants such as organochlorines are transported. Carried by atmospheric and oceanic currents far from their southern agricultural and industrial application sites, these contaminants are found ubiquitously in arctic snow, ice, water, biota, and sediments. That many of these compounds bioaccumulate and biomagnify in the foodweb is of immense concern to those northern residents whose diets are chiefly comprised of country foods such as fish, seal, whale, and walrus.

Water mass circulation and estimates of renewal and transport rates within the Arctic Ocean have historically been inferred from analysis of physical and natural geochemical tracer distributions. Recently, anthropogenic tracers such as the suite of halocarbons CFC-11, CFC-12, CFC-113 and CCl_4, have proven valuable as time-dependent tracers of ocean circulation (Gammon et al., 1982; Bullister and Weiss, 1983; Krysell and Wallace, 1988, Wallace et al., 1992). Halocarbons enter the ocean from the atmosphere by gas exchange and their concentrations in surface water reflect existent atmospheric concentrations. Because atmospheric concentrations have been increasing with time, however, measurements of these compounds and their ratios in the water column provide estimates of apparent ages, where apparent age is a measure of the time elapsed since the water parcel last equilibrated with the atmosphere. Halocarbon concentrations provide information about oceanic ventilation on time scales ranging from one to 70 years, whereas halocarbon ratios provide information on time scales ranging from one to 50 years because of the different release histories associated with each halocarbon.

Prior to the mid 1980s, description of the Arctic Ocean interior water mass characteristics and circulation were based on relatively sparse data, limited in geographic, temporal, and geochemical dimensions. Similarly, data on contaminant burdens were limited in both number of stations sampled geographically, as well as by analysis of sample matrix (ice, water, biota and sediment). Historically, these data were generally collected by North American scientists at ice camps located mainly in the Canadian Basin. Other arctic data, collected by Soviet scientists prior to the mid-1980s, remained generally unavailable or appeared only in atlas form. In summary, the Arctic Ocean, as portrayed in the literature up to the mid-1980s, was described as a homogeneous, low energy ocean whose circulation patterns were studied on a regional basis. The Arctic Ocean's physical and geochemical characteristics to this time were reviewed respectively by Carmack (1990) and Jones et al. (1990).

In response to climate and contaminant issues, increased international efforts to collect physical, geochemical, transient tracer and contaminant samples from the interiors of the principal Arctic Ocean basins have been undertaken since 1987. These research programs have been made possible by research-capable icebreakers that can penetrate the high reaches of this ice-covered ocean. In 1987, physical and geochemical tracer samples across the Nansen Basin were collected aboard the German icebreaker **Polarstern**, an expedition which completed the first scientific crossing of an Arctic Ocean sub-basin. Four years later in 1991, as part of a joint Swedish, German and American expedition aboard the Swedish **Oden,** water column samples were collected across the Nansen and Amundsen basins and at a small number of stations in the Makarov Basin. Each of these expeditions were focussed primarily on the Eurasian Basin, and provided information about circulation

in this region.

Data collected during the Canada and Russia East Siberian Sea expedition in 1993 aboard the **CCGS Henry Larsen** icebreaker provided new information about water mass circulation in the southern Canadian Basin. This cruise (**Larsen-93**) collected a full suite of modern geochemical parameters along a 1300 km section extending from the Canada Basin to the Makarov slope. Physical, geochemical and tracer measurements obtained during this cruise provide the principal data for this thesis. The purpose of the following discussion is to present findings from the **Larsen-93** expedition which pertain to water mass boundaries, ocean circulation, and ventilation.

The structure of the thesis is as follows. Chapter 1 presents a general overview of the Arctic Ocean, its bathymetry, currents and freshwater inflows, water mass layers and circulation. Chapter 2 defines the **Larsen-93** study area, presents the geochemical measurements obtained, and describes the methods of halocarbon sampling and analysis. Chapter 3 discusses water mass characteristics based on five basin stations, introduces the term <u>water mass assemblies</u>, and identifies the distinct nature of two different assemblies found in the Arctic Ocean—labelled as the Western Arctic (WA) and Eastern Arctic (EA) assemblies. **Larsen-93** geochemical tracer data presented in this chapter reveal a previously unobserved Atlantic/Pacific water mass boundary, or front, within the Canadian Basin. This finding suggests that the Atlantic/Pacific front has shifted from a location above the Lomonosov Ridge, as observed in the late 1970s, to a location above the Mendeleyev Ridge, as observed in 1993 (McLaughlin et al., 1996). Chapter 4 presents halocarbon tracer data and estimates of apparent ages and dilution factors of waters found in five basin stations. The apparent ages of waters in the Canada and Makarov basins are compared to illustrate differences in ventilation in

waters found on either side of the Atlantic/Pacific front. Chapter 5 examines physical and geochemical properties from three shelf/slope stations for corroborative evidence of the Atlantic/Pacific front, as well as for evidence of shelf processes. The thesis concludes with Chapter 6, a summary chapter which states the general findings of this research and some of the questions raised by these findings that warrant further study.

1.1 Physical Description of the Arctic Ocean

This section presents a general overview of the Arctic Ocean, including its bathymetry, currents, water mass layers and circulation. The Arctic Ocean is approximately 10 x 10^6 km^2 in area and 17 x 10^6 km^3 in volume when the Barents Sea, Kara Sea and waters of the Canadian Archipelago are included. It is an ocean almost entirely surrounded by land (hence its description in some writings as mediterranean), connected to the Atlantic Ocean through Fram Strait and the Canadian Archipelago, and to the Pacific Ocean through Bering Strait (Figure 1). Approximately one-third of the Arctic Ocean's area consists of broad (600-800 km) shallow (30-200 m) shelves located primarily north of Eurasia along the Barents, Kara, Laptev, East Siberian and Chukchi seas, and north of Canada along the Beaufort Sea. In summer, these shelves are regions of open water and high biological productivity; in winter, they are regions of sea-ice production and potential dense water formation.

1.2 Bathymetry

Water mass circulation in the Arctic Ocean is closely tied to its complex bathymetry (see Figure 1) with much of the transport occurring along ocean boundaries and ridges (Aagaard, 1989). The relationship between bathymetry and circulation is strong in the Arctic Ocean because the

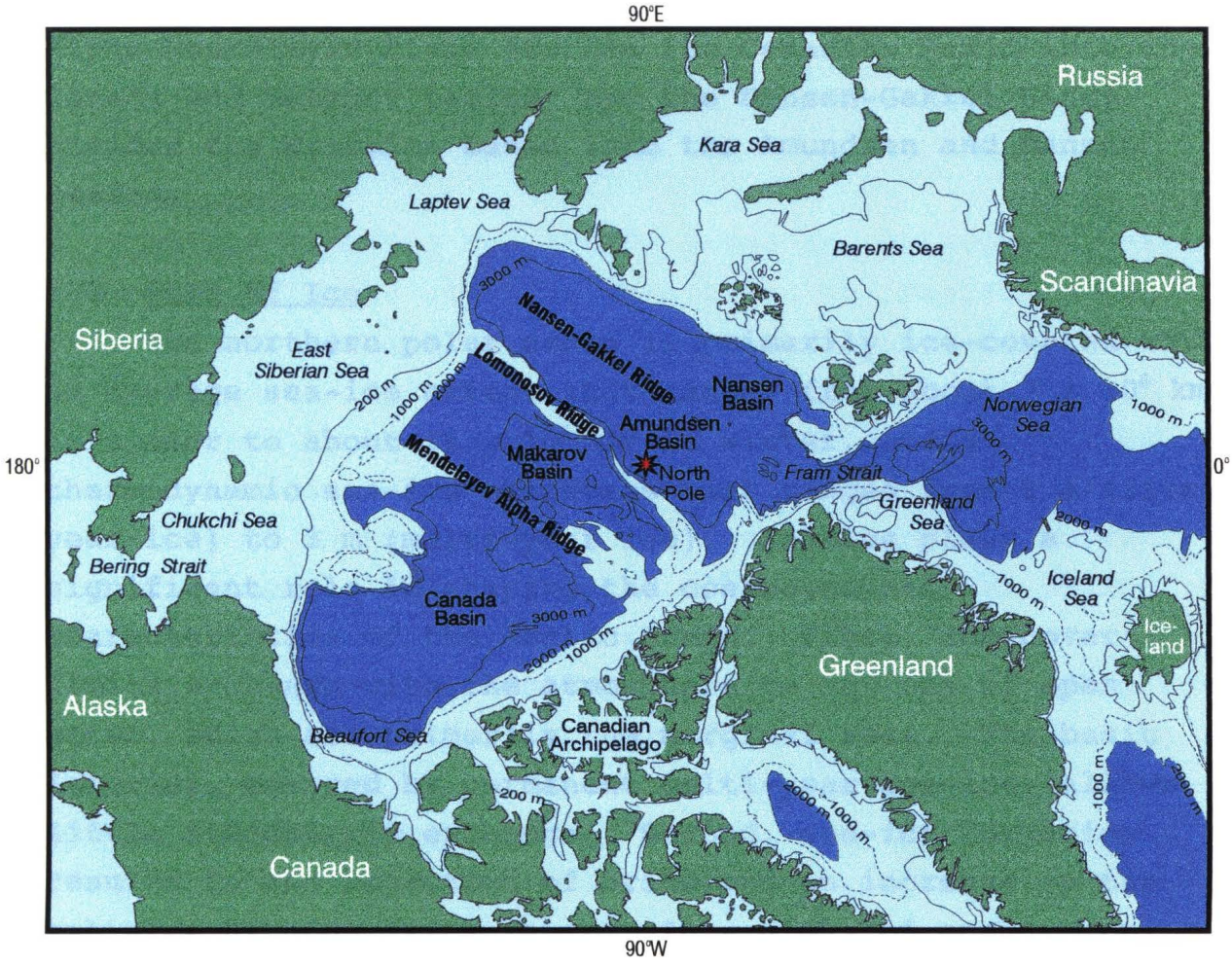
90°E
180°
0°
90°W
Russia
Kara Sea
Laptev Sea
Barents Sea
Scandinavia
Siberia
East
Siberian Sea
Nansen-Gakkel Ridge
Lomonosov Ridge
Nansen
Basin
Amundsen
Basin
Makarov
Basin
North
Pole
Mendeleyev Alpha Ridge
Fram Strait
Norwegian
Sea
Greenland
Sea
Chukchi Sea
Bering Strait
Canada
Basin
Iceland
Sea
Ice-
land
Greenland
Alaska
Beaufort Sea
Canadian
Archipelago
Canada
3000 m
2000 m
1000 m
200 m

Figure 1

latitudinal variation of the Coriolis parameter (Beta effect) at high latitudes is small (Schlosser et al., 1995). The Arctic Ocean interior is divided by the Lomonosov Ridge (sill depth 1500 m) into two main basins, the Canadian (maximum depth 3800 m) and Eurasian basins (maximum depth 4200 m). These basins are further divided by ridges: the Alpha-Mendeleyev Ridge divides the Canadian Basin into the Canada and Makarov basins; and the Nansen-Gakkel Ridge divides the Eurasian Basin into the Amundsen and Nansen basins.

1.3 Role of Ice

The northern polar ocean is primarily ice-covered with an average sea-ice extent that ranges from about 7 x 10^6 km^2 in summer to about 14 x 10^6 km^2 in winter, and a thermodynamic sea-ice thickness that ranges from 2 m (first-year ice) to 3 m (multi-year ice). Sea-ice plays a significant role in shaping the oceanographic characteristics of the Arctic Ocean. First, ice-cover limits exchange with the atmosphere to regions of open water, which are primarily the marginal seas. The basin interior, covered by permanent multi-year sea-ice, allows little atmospheric exchange. Second, sea-ice formation results in the rejection of brine and an increase in the salinity of underlying water. In regions of open water (polynyas), repeated ice formation may result in the formation of dense bottom water. Dense bottom water – water dense enough to sink to the bottom of a shelf and flow into the basin interior at a depth determined by its density – is believed responsible for maintenance and ventilation of the arctic halocline (Aagaard et al., 1981; Melling and Lewis, 1982). Production of bottom water may require upwelling to precondition shelf waters and may not occur every year (Melling, 1993). Third, sea-ice is carried by two main

surface currents. Sea-ice and surface waters are carried by the Transpolar Drift from regions near the Laptev Sea across the Eurasian Basin toward Fram Strait (Figure 2). In the Canadian Basin, sea-ice and surface waters are carried by the anticyclonic Beaufort Gyre. These surface currents also provide a mechanism for transporting contaminants which are incorporated into the ice structure as ice forms on shallow shelves.

1.4 Currents

Waters entering the Arctic Ocean are principally from the north Atlantic via Fram Strait and the Pacific Ocean via Bering Strait (see Figure 2). On the eastern side, the Arctic Ocean is linked with the Greenland, Norwegian and Iceland seas by two main currents that flow through Fram Strait, a passage 600 km wide with a sill depth of 2600 m. The first of these currents, the West Spitsbergen Current (WSC) transports 2-8 Sv (1 Sv = 10^6 m^3/s) of warm, saline Atlantic origin water into the Arctic Ocean, some of which recirculates in the Greenland Sea, some of which enters the Arctic Ocean around Spitsbergen (Fram Strait branch, FSB), and some of which, near the Yermak Plateau, is modified and enters both as deep water and as water that recirculates (Manley, 1995). Atlantic water also enters the Arctic Ocean by throughflow from the southwest across the Barents Sea (Barents Sea Branch, BSB). In crossing the Barents Shelf, Atlantic origin water is modified by mixing with surrounding water, by cooling, and by ice formation; processes described by Midttun (1985) which produce dense bottom water in the Barents Sea. About 1-3 Sv of this modified dense water enters the Arctic Ocean through the strait between Novaya Zemlya and Frans Josef Land down the St. Anna Trough (Loeng et al., 1995). Variability in the density and volume of the outflow of the Barents Sea Branch may influence water mass

Ice Motion and Subsurface Currents

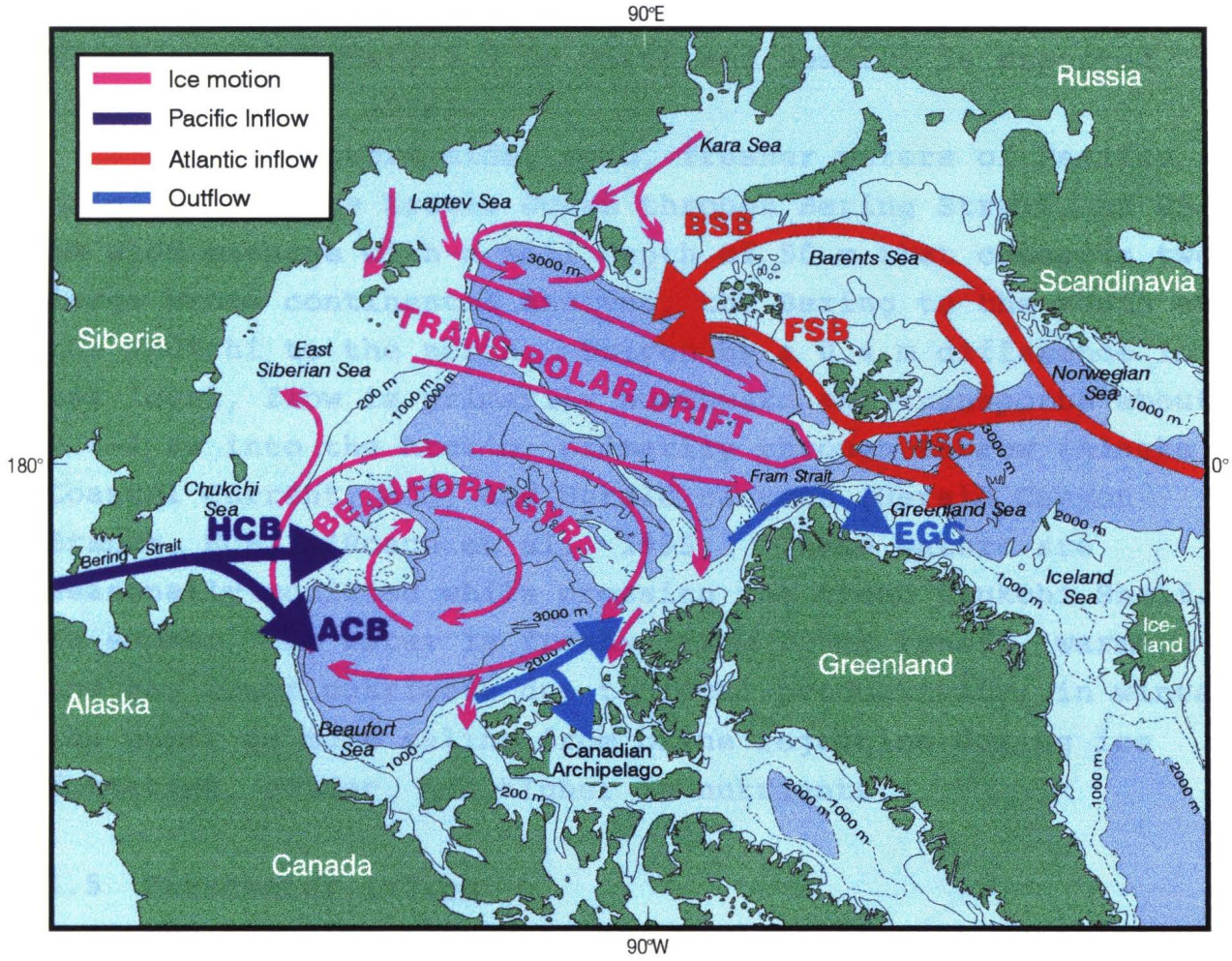

Figure 2

circulation and basin water mass characteristics.

The second of the currents through Fram Strait, the East Greenland Current (EGC), exports about 3 Sv water and 4000-5000 km^3/yr (0.13-0.16 Sv) of sea-ice (Foldvik et al., 1988; Vinje and Finnekasa, 1986). The Arctic Ocean is also linked to the North Atlantic by the Canadian Archipelago, a group of channels and straits about 200-300 m deep, through which approximately 1.7 Sv water and sea-ice is exported (Fissel et al., 1982).

On the western side, cold, fresher waters of Pacific origin enter the Arctic Ocean through Bering Strait, an 85 km wide passage with a sill depth of 50 m that connects two large broad continental shelves, the Bering to the south and the Chukchi to the north. Driven by a 0.4 m difference in sea level, flow is primarily northward and transports about 0.8-1 Sv into the Arctic, primarily through Barrow (Alaska Coastal Current, ACC) and Herald canyons (Herald Canyon Branch, HCB), (Roach et al., 1995). These waters are seasonally modified while crossing the broad Chukchi Shelf. In summer, the water is fresher from river runoff, warmer, and has lower nutrients due to local productivity; in winter the water is more saline from brine rejection during ice formation, colder, and higher in nutrients.

1.5 Freshwater Inflow

The Eurasian Arctic is the world's largest drainage basin, and collects water from an area more than half the size of the Arctic Ocean (Milliman and Meade, 1983). Together, the Eurasian and North American rivers (Figure 3) deliver an annual freshwater streamflow of 3300 km^3/yr (0.1 Sv) into the Arctic Ocean (Aagaard and Carmack, 1989). An additional 1500-2000 km^3/yr (0.05-0.06 Sv) enters as the freshwater component of Bering Strait inflow (where freshwater is determined relative to salinity S=34.80;

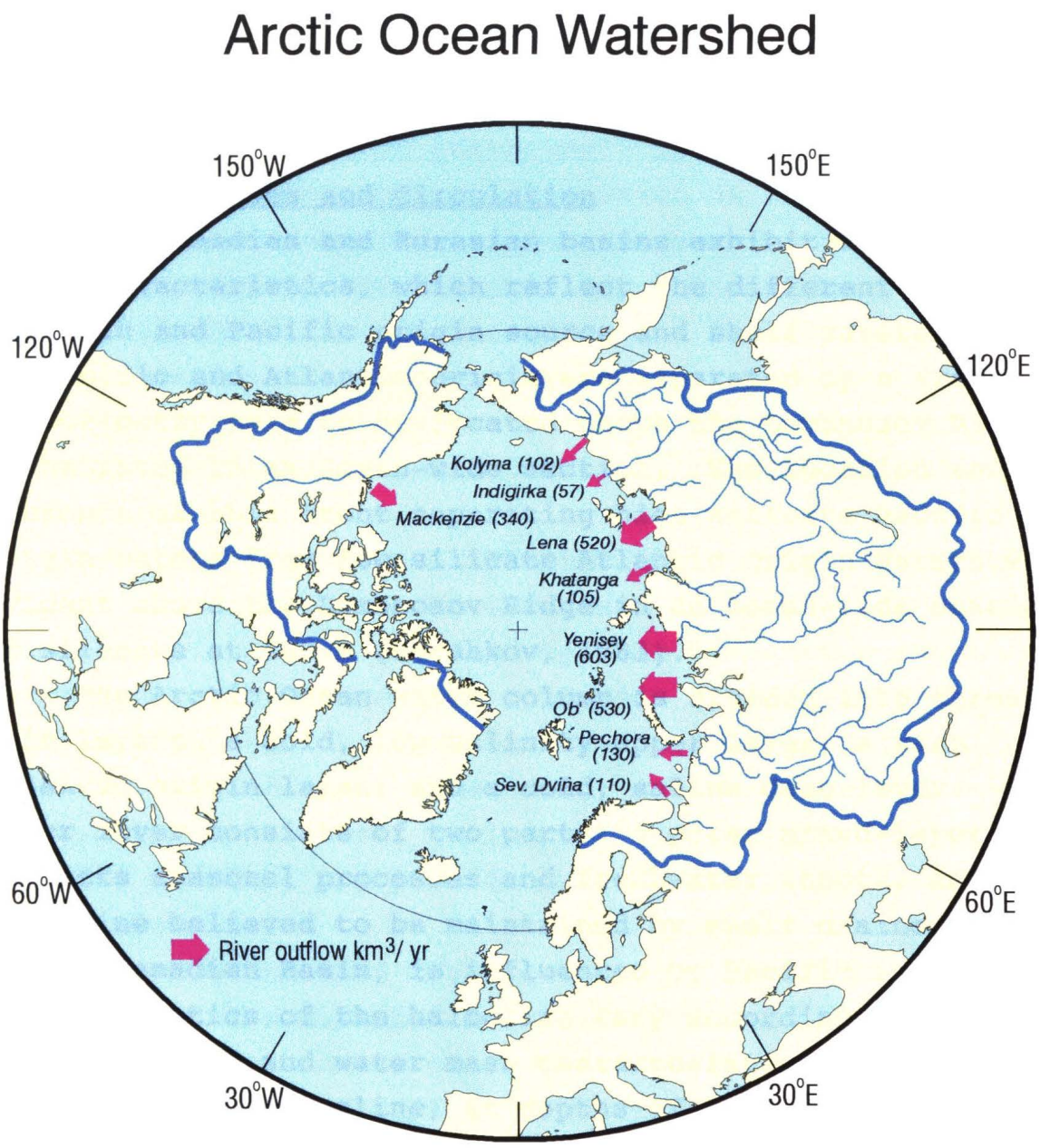
Arctic Ocean Watershed
150°W
150°E
120°W
120°E
60°W
60°E
30°W
30°E
Kolyma (102)
Indigirka (57)
Mackenzie (340)
Lena (520)
Khatanga (105)
Yenisey (603)
Ob' (530)
Pechora (130)
Sev. Dvina (110)
River outflow km3/ yr

Figure 3

Coachman et al., 1975, Aagaard and Carmack, 1989). This large freshwater inflow creates a stable salt-stratified system within the Arctic Ocean which limits the depth of thermal convection during winter and allows the formation of a stable ice cover.

1.6 Water Masses and Circulation

The Canadian and Eurasian basins exhibit distinct water mass characteristics, which reflect the different inflows of Atlantic and Pacific origin source and shelf waters. Waters of Pacific and Atlantic origin are separated by a front, historically held to be located above the Lomonosov Ridge as illustrated in an ocean-wide section. The location and presence of this front separating high silicate Pacific origin waters from low silicate Atlantic origin waters was evident above the Lomonosov Ridge in an ocean-wide section of silicate at 100 m (Gorshkov, 1983).

The Arctic Ocean water column is divided into three main layers: a cold, low salinity upper layer; a warm Atlantic origin layer; and a cold, saline deep layer. The upper layer consists of two parts: a polar mixed-layer that reflects seasonal processes and freshwater inputs; and a halocline believed to be maintained by shelf drainage and, in the Canadian Basin, is influenced by Pacific inflow. Characteristics of the halocline vary according to basin, both in volume and water mass characteristics. In the Eurasian Basin halocline, at depths of 20-120 m, temperature is uniformly colder than -1.5 °C and salinity increases rapidly from S=32 to S=34.2. The Canadian Basin halocline, in contrast, extends deeper in the water column to depths of 200 m or more, and shows three temperature features over a salinity range from S=30 to S=34.4. The first feature is a temperature minimum near S=31.6 due to winter cooling. Next there is a temperature maximum near S=32.4 and a temperature

minimum at S=33.1, due respectively to summer and winter inflow of Pacific origin water through Bering Strait (Coachman and Barnes, 1961; Macdonald et al., 1989). The Atlantic layer is found in both basins and characterized by a temperature maximum. Again, differences between basins are evident in the core characteristics of this layer; in the Eurasian Basin, temperatures reach as high as 2 °C at salinities near S=34.90 at about 250 m. In the Canadian Basin, the core of the Atlantic layer is colder (0.5 °C), fresher (S=34.84) and deeper (400 m). Finally, the characteristics of the deep layer differ in each basin; Eurasian Basin deep waters are colder and less saline than those of the Canadian Basin. This is because the Lomonosov Ridge divides and isolates the circulation of the deep layer into the two main basins. Whether the Canadian Basin deep waters are formed from the Greenland and Barents seas (see Swift et al., 1983), modified by near-boundary dense water formation and flow over the Lomonosov Ridge (Aagaard et al., 1985), or whether the Canadian Basin deep layer is relict water from a different climatology (Macdonald and Carmack, 1991), remains unclear. Collection and analysis of tracer data (^{14}C and ^{39}Ar) may provide better understandings about these questions.

Interpretation of transient tracer measurements, primarily in the Eurasian Basin in 1987 and 1991, has confirmed the soundness of earlier ideas and has advanced our understanding of Arctic Ocean circulation. Analysis of 1991 halocarbon data, for example, suggested that circulation below the halocline is strongly influenced by topography and identified three mid-basin return flows of the Atlantic layer; one over the Nansen-Gakkel Ridge, one over the Lomonosov Ridge, and one from the Canadian Basin (Rudels et al., 1994). Based on observations from the Eurasian Basin, Rudels et al. (1994) proposed a circulation

scheme of the Atlantic layer in the entire Arctic Ocean which shows flow along the basin perimeters and along the ridges dividing the basins. Anderson et al. (1994) further suggested that communication between the Canadian and Eurasian basins occurs mostly along the southern boundaries (around basin perimeters), and that circulation around the Canadian Basin perimeter appears weaker than circulation around the Eurasian Basin.

References:

Aagaard, K., A synthesis of the Arctic Ocean circulation, Rapp. P.-v. Reun., Cons. int. Explor. Mer, 188, 11-22, 1989.

Aagaard, K., J. H. Swift and E. C. Carmack, Thermohaline circulation in the Arctic Mediterranean Seas, J. Geophys. Res., 90, 4833-4846, 1985.

Aagaard, K., L. K. Coachman, and E. C. Carmack, On the halocline of the Arctic Ocean, Deep-Sea Res., 28, 529-545, 1981.

Aagaard, K. and E. C. Carmack, The role of sea ice and other fresh water in the Arctic circulation, J. Geophys. Res., 94, 14485-14498, 1989.

Aagaard, K. and E. C. Carmack, "The Arctic Ocean and climate: a perspective" in The Polar Oceans and Their Role in Shaping the Global Environment: the Nansen Centennial Volume, O. M. Johannessen, R. D. Muench and J. E. Overland, eds., Geophysical Monograph 85, American Geophysical Union, 1994.

Anderson, L. G., E. P. Jones, K. P. Koltermann, P. Schlosser, J. H. Swift and D. R. W. Wallace, The first oceanographic section across the Nansen Basin in the Arctic Ocean, Deep-Sea Res., 36, 475-482, 1990.

Anderson, L. G., G. Bjork, O. Holby, E. P. Jones, G. Kattner, K. P. Koltermann, B. Liljeblad, R. Lindegren, B. Rudels and J. H. Swift, Water masses and circulation in the Eurasian Basin: Results from the ODEN 91 expedition, J. Geophys. Res., 99, 3273-3283, 1994.

Bullister, J. L. and R. C. Weiss, Anthropogenic chlorofluorocarbons in the Greenland and Norwegian Seas, Science, 221, 265-268, 1983.

Broecker, W. S., D. M. Peteet and D. Rind, Does the ocean-atmosphere system have more than one stable mode of operation?, Nature, 315, 21-26, 1985.

Carmack, E. C.,"Large-scale physical oceanography of polar oceans" in Polar Oceanography, Part A:Physical Science, Walker O. Smith, Jr., ed., Academic Press, San Diego, 1990.

Coachman, L.K., and C. A. Barnes, The contribution of Bering Sea water to the Arctic Ocean, Arctic, 14, 146-161, 1961.

Coachman, L. K., K. Aagaard and R. B. Tripp, Bering Strait: The Regional Physical Oceanography, University of Washington Press, Seattle, 1975.

Cuffey, K. M., G. D. Clow, R. B. Alley, M. Stuiver, E. D. Waddington and R. W. Saltus, Large Arctic temperature change at the Wisconsin-Holocene glacial transition, Science, 270, 455-458, 1995.

Fissel, D. B., D. D. Lemon and J. R. Birch, Major features of the summer near-surface circulation of western Baffin Bay, 1978 and 1979, Arctic, 35, 180-200, 1982.

Foldvik, A., K. Aagaard and T. Torresen, On the velocity field of the East Greenland Current, Deep Sea Res., 35, 1335-1354, 1988.

Gammon, R. H., J. Cline and D. Wisegarver, Chlorofluoromethanes in the northeast Pacific Ocean: measured vertical distributions and applications as transient tracers of upper ocean mixing, J. Geophys. Res., 87, 9441-9454, 1982.

Gorshkov, S. G., World Ocean Atlas, 3, Arctic Ocean, Pergamon Press, New York, 1983.

Jones, E. P., D. M. Nelson and P. Treguer, "Chemical Oceanography" in Polar Oceanography, Part B:Chemistry, Biology and Geology, Walker O. Smith, Jr., ed., Academic Press, San Diego, 1990.

Krysell, M. and D. W. R. Wallace, Arctic Ocean ventilation studied with a suite of anthropogenic halocarbon tracers, Science, 242, 746-749, 1988.

Loeng, H., V. Ozhigin and B. Adlandsvik, Water Fluxes through the Barents Sea, ICES C.M. 1995, 8p, 1995.

Macdonald, R. W., E. C. Carmack, F. A. McLaughlin, K. Iseki, D. M. Macdonald and M. C. O'Brien, Composition and modification of water masses in the Mackenzie shelf estuary, J. Geophys. Res., 94, 18057-18070, 1989.

Manabe, S. and R. J. Stouffer, Two stable equilibria of a coupled ocean-atmosphere model, J. Climate, 1,841-866, 1988.

Manley, T. O., Branching of Atlantic Water within the Greenland-Spitsbergen Passage: an estimate of recirculation, J. Geophys. Res., 100, C10, 20627-20634, 1995.

McLaughlin, F. A., E. C. Carmack, R. W. Macdonald and J. K. B. Bishop, Physical and geochemical properties across the Atlantic/Pacific water mass front in the Southern Canadian Basin, J. Geophys. Res., 101, 1183-1197, 1996.

Melling, H. The formation of a halocline shelf front in wintertime in an ice-covered arctic sea, Cont. Shelf Res., 13, 1123-1147, 1993.

Midttun, L., Formation of dense bottom water in the Barents Sea, Deep-Sea Res., 32, 1233-1241, 1985.

Milliman, J. D. and R. H. Meade. World-wide delivery of river sediment to the oceans. J. Geology, 91, 1-21, 1983.

Roach, A. T., K. Aagaard, C. H. Pease, S. A. Salo, T. Weingartner, V. Pavlov and M. Kulakov, Direct measurements of transport and water properties through the Bering Strait, J. Geophys. Res., 100, 18443-18457, 1995.

Rudels, B., E. P. Jones, L. G. Anderson, and G. Kattner, "On the intermediate waters of the Arctic Ocean" in The Polar Oceans and Their Role in Shaping the Global Environment: the Nansen Centennial Volume, O. M. Johannessen, R. D. Muench and J. E. Overland, eds., Geophysical Monograph 85, American Geophysical Union, 1994.

Schlosser, P., J. H. Swift, D. Lewis and S. Pfirman, The role of the large-scale Arctic Ocean circulation in the transport of contaminants, Deep Sea Res., 42, 1-27, 1995.

Swift, J. H., T. Takahashi and H. D. Livingston, The contribution of the Denmark Strait overflow to the deep North Atlantic, J. Geophys. Res., 88, 5981-5986, 1983.

Vinje, T. K. and O. Finnekasa, The ice transport through the Fram Strait., Skr., Nor. Polarinst., 186, 1-39, 1986.

Wallace, D. W. R., P. Schlosser, M. Krysell and G. Bonisch, Halocarbon ratio and tritium/^{3}He dating of water masses in the Nansen Basin, Arctic Ocean, Deep-Sea Res., 39, S435-S458, 1992.

Chapter 2: Research Area and Methodology

This chapter begins with a description of the research area and lists the physical and geochemical parameters measured. Following this is a discussion of the methods of halocarbon sampling and analysis used in this research. Lastly, the quality of the halocarbon data is examined by reporting sample accuracy obtained by analyzing duplicate samples, and measurement precision obtained by analyzing standards as unknowns. Estimates of oceanographic consistency in both geographic and temporal dimensions is presented by comparing data obtained from geographically-similar stations and from one station in different years.

2.1 Research Area

In late August 1993, the Canada/Russia East Siberian Sea expedition left Tuktoyaktuk, N. W. T., aboard the **CCGS Henry Larsen**, and began a section that stretched 1300 km from the Beaufort Sea in the Canada Basin to the East Siberian Sea in the Makarov Basin. En route, the cruise crossed the Northwind Ridge and Plain, as well as the Chukchi Plain and Shelf, and collected samples from eight stations situated at deep basin, slope, and shelf locations (Figure 1).

Description of the physical and geochemical samples collected and analyzed during the cruise appears in Macdonald et al. (1994) and is summarized in Chapter 3. Physical and geochemical data are tabulated in the Appendix. Table 1 reports the error estimates and calibration details for these measurements. The pooled variance (s_p) is calculated as:

$$s_p = [(v_1 s^2_1 + \ldots + v_i s^2_i)/(v_1 + \ldots + v_i)]^{1/2}$$

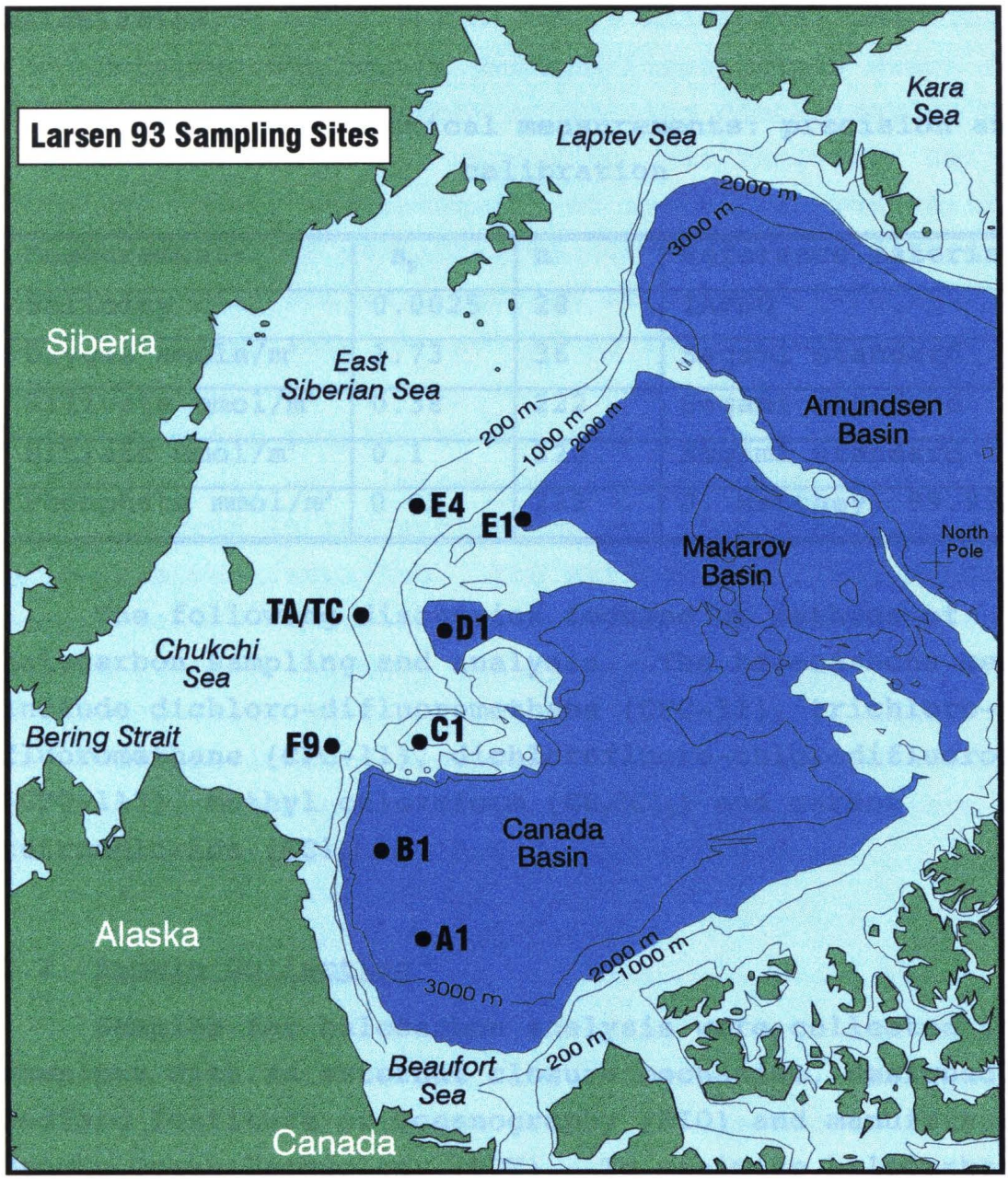
Larsen 93 Sampling Sites
Laptev Sea
Kara Sea
2000 m
3000 m
Siberia
East Siberian Sea
200 m
1000 m
2000 m
Amundsen Basin
E4
E1
Makarov Basin
North Pole
TA/TC
D1
Chukchi Sea
Bering Strait
F9
C1
Canada Basin
B1
Alaska
A1
2000 m
1000 m
3000 m
200 m
Beaufort Sea
Canada

Figure 1

where $v_i = n_i - 1$ degrees of freedom, and n_i and s_i refer to the number of replicates and the standard deviation of the components used in the pooled standard deviation calculation.

Table 1: Geochemical measurements: precision and calibration

Measurement:	s_p	n	Reference material
Salinity	0.0025	28	IAPSO
Oxygen mmole/m^3	1.73	36	Sagami standard
Silicate mmol/m^3	0.38	222	Sagami standard
Nitrate mmol/m^3	0.1	220	Sagami standard
Phosphate mmol/m^3	0.02	222	J. Matthey, 99.999% purity

The following discussion focuses on methods of halocarbon sampling and analysis. The halocarbons measured include dichloro-difluoromethane (CFC-12), trichloro-fluoromethane (CFC-11), dichlorofluoro-chlorodifluoroethane (CFC-113), methyl chloroform (CH_3CCl_3) and carbon tetrachloride (CCl_4).

2.2 Sample Collection

Samples for halocarbon analysis were collected in water samplers with an external closure mechanism, designed at Bedford Institute of Oceanography (BIO) and manufactured by Brooke Ocean Technology (BOT). To minimize halocarbon contamination, the seawater sample was in contact only with polyvinylchloride (PVC, bottle walls and end caps) and polyurethane (seals). All PVC tubing was baked at about 300 °C before machining to outgas potential halocarbon contamination. Vents and stopcocks were also made of PVC and installed with PVC glue. Prior to sampling, water

samplers were attached to a rosette frame and aired during the transit from Tuktoyaktuk to the first station. To ensure the water samplers were well rinsed, water was collected from eight casts before halocarbon sampling began.

A halocarbon sample was the first sample drawn from the BOT water sampler, thereby minimizing contamination with air that entered the bottle when water was removed. Before sampling began, the integrity of the sample was verified by opening the water sampler stopcock—no flow comfirmed all apertures were sealed. Samples were drawn into 100 ml glass syringes which were pre-wetted by filling with seawater several hours before sampling. Samples were transferred from the water sampler to the syringe in a way to ensure no bubbles of air were introduced into the sample; when bubbles were observed in the syringe at any time, the sampling procedure was restarted. The syringe was first rinsed with sample water, rinsed with about 30 ml of sample three times, then filled to 100 ml. The syringe was capped by a stainless steel Luer fitting and stored until analysis by immersing it in cold seawater to prevent air contamination. Samples were collected from a pair of water samplers closed at the same depth six times during the cruise.

2.3 Analytical Method

Halocarbons were analyzed using a purge and trap technique (Wallace et al., 1994, Figure 2). The system consisted of an extraction board, an electronic interface box, gas chromatograph (GC), and a computer. The extraction board consisted of: electronically actuated Valco valves which controlled the flow; a calibrated glass volume for sample introduction; a glass stripper cell; a water removal trap (magnesium perchlorate); and a trapping column. Trap temperatures were regulated and monitored by ceramic resistance temperature devices (RTDs) and Omega temperature

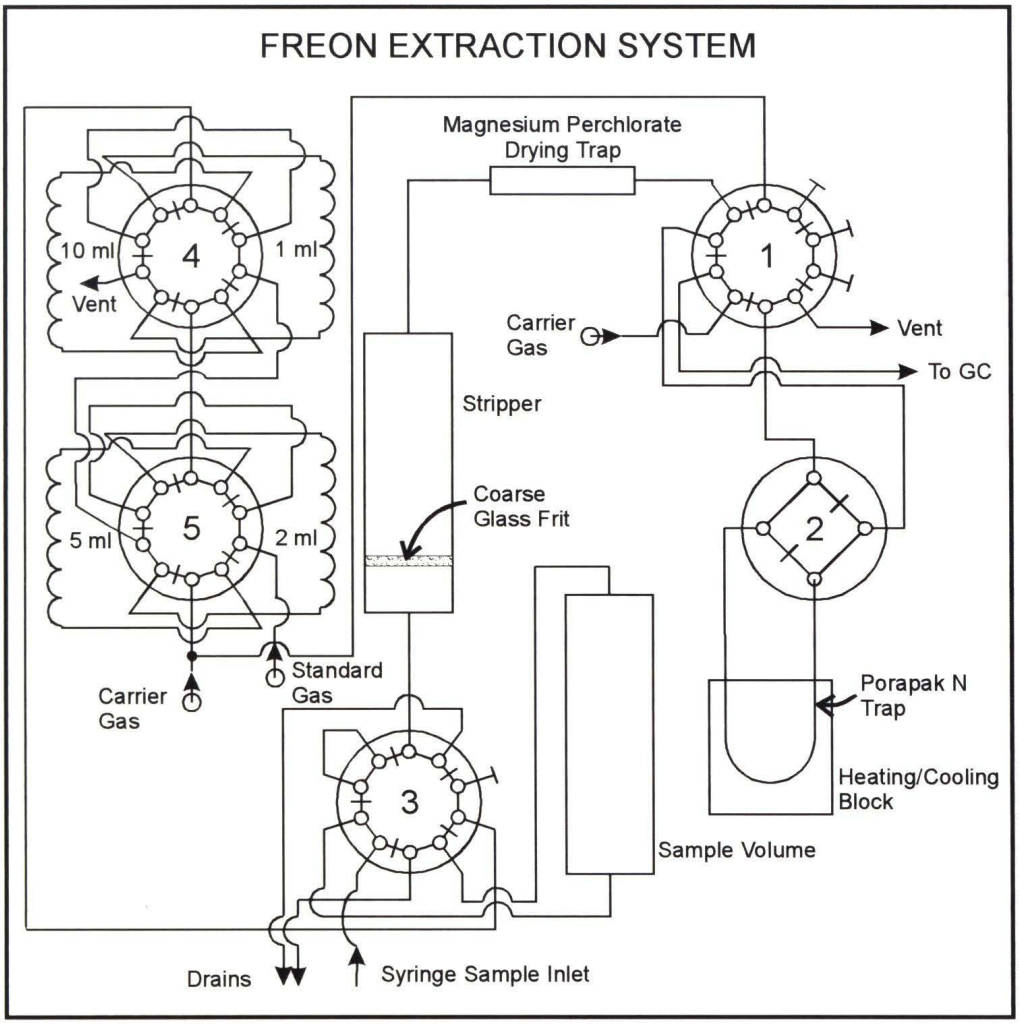
FREON EXTRACTION SYSTEM
Magnesium Perchlorate
Drying Trap
10 ml
4
1 ml
Vent
1
Carrier
Gas
Vent
To GC
Stripper
Coarse
Glass Frit
5 ml
5
2 ml
2
Standard
Gas
Carrier
Gas
Porapak N
Trap
Heating/Cooling
Block
3
Sample Volume
Drains
Syringe Sample Inlet

Figure 2

controllers. All valve switching and temperature control of the trap were operated automatically via the interface box, according to a timetable written in the Waters/Millipore chromatography software program "Baseline." Carrier gas flow was supplied by two nitrogen tanks (UHP grade)--one for stripping the sample and one for maintaining flow through the GC. To remove contamination, an oxygen removal trap (Oxytrap) and a molecular sieve trap (13X mesh size 80/100 mesh, length 1/4" o.d. x 10 ft) were installed in each nitrogen line. Flow rates were regulated by Omega flow controllers.

Blanks were run at the beginning of each day before analysis began to ensure that neither of the two standard analysis valve configurations was contaminated, and to ensure there were no leaks in the system. The system was calibrated by analyzing six to eight volumes of halocarbon gas standard (BNL, discussed below)—volumes from 1 to 15 ml were determined by combining four calibrated loop volumes (1.0, 2.0, 5.0 and 10.0 ml, Valco). Volumes were selected to calibrate the system over the range of expected sample concentrations.

Seawater samples were injected into the calibrated volume (about 24 ml) through a three-way Hamilton valve fitted with a Luer port for injection. The volume was filled by overflowing twice and then isolated. Sufficient sample (about 30 ml) was retained in the syringe in case a replicate analysis was required. The sample was then transferred by nitrogen flow from the calibrated volume to the stripper chamber. The stripper had one sintered glass frit at the inlet to maximize bubble formation and stripping efficiency. A second frit at the outlet minimized water vapour transfer. The sample was purged for four minutes at 60 ml/min to remove halocarbons. Based on prior experiments, these conditions yielded an extraction

efficiency greater than 99% for all compounds measured, and no breakthrough of CFC-12 was detected (the first halocarbon to elute). Purged halocarbons were first passed through a magnesium perchlorate trap to remove water vapour, and then collected on a cold (less than 10 °C) Porapak N trap (80/100 mesh, 1/8" i.d. x 22 cm). Trap temperature was maintained by a refrigerated recirculating water bath. After four minutes, the trap was isolated and heated to 170 °C for three minutes. GC carrier gas flow was then directed to backflush the trap and sweep the halocarbons onto the GC column. During this time the stripper chamber was drained and flushed with nitrogen from the purging gas flow.

A Hewlett-Packard 9860 GC was used to separate and detect the suite of halocarbons. The GC was equipped with a wide bore DB-624 column (75 m x 0.53 mm o.d.; 3.0 mm film thickness; flow rate 16 ml/min) and a ^{63}Ni electron capture detector heated to 300 °C. The program for controlling the GC was initiated at the beginning of analysis under the following conditions: the GC column was held at 40 degrees for nine minutes, heated to 60 °C at 5 °C/min, heated to 120 °C at 20 °C/min, then held at 120 °C for two minutes. The GC gas flow was directed through the trap and onto the GC column for one minute to transfer the halocarbons of interest. Then the valves were switched to direct flow through the GC column only. At the same time, the stripper gas flow was directed through the heated trap for three minutes to clean the trap. Twelve minutes after analysis began, the trap was cooled in preparation for the next sample. Data were acquired, stored, and processed using Baseline on a Toshiba 3200 computer. Three calibration curves were produced from each series of standards and the most appropriate curve was selected to calculate sample halocarbon concentrations. For example, the full calibration curve was used to calculate concentration of a

sample with a high response (area), and a calibration curve that included only the lowest three standard concentrations was used for a sample with a low response (see Appendix for calibration curves).

A typical chromatogram is presented in Figure 3 to show the elution order of the halocarbons. The chromatogram also show the presence of other peaks that elute near CFC-113. Methyl iodide, a naturally produced compound, elutes immediately after CFC-113. In addition, contaminant peaks arising from water breakthrough to the DB-624 column also elute in this region of the chromatogram. These peaks have the potential to interfere with the quantitation of CFC-113 and cause changes in the CFC-113 blank.

2.4 Standards, Accuracy, and Precision

A compressed gas standard containing CFC-11, CFC-12, CFC-113, CH_3CCl_3, and CCl_4 was purchased from Brookhaven National Laboratory (BNL). The standard was stored in an acid washed Aculife-4 aluminum cylinder (Scott Specialty Gases), and calibrated before and after the expedition to verify the stability of all compounds, particularly CCl_4. This standard was one of a group of standards prepared in July 1993 under the supervision of Jim Happell at BNL. One tank (#ALM-032396), used to intercalibrate the other standards, was sent to NOAA's Climate Monitoring and Diagnostic Laboratory (CMDL) in Boulder, Colorado for calibration. Two years later, the tank was recalibrated at CMDL and also sent to Scripps Institution of Oceanography for calibration, where concentrations were reported on the SIO 1993 scale. The results are reported in Table 2, and the uncertainty refers to one standard deviation.

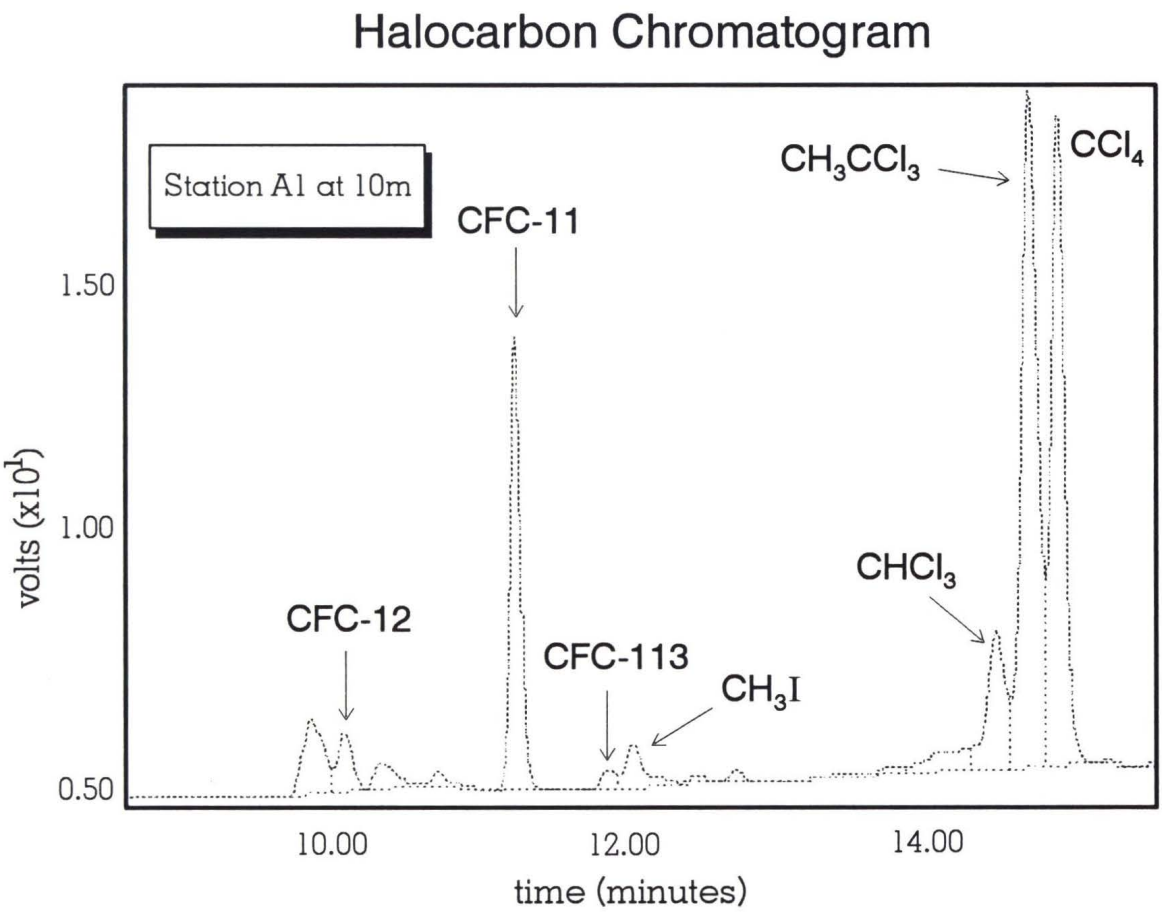
Halocarbon Chromatogram
Station A1 at 10m
CFC-11
CH_3CCl_3
CCl_4
$CHCl_3$
CFC-12
CFC-113
CH_3I
1.50
1.00
0.50
volts (x10^4)
10.00
12.00
14.00
time (minutes)

Figure 3

Table 2: Calibration concentrations (ppt)

#ALM	CMDL 1993	CMDL 1995	SIO 1995
CFC-12	505.5 ± 2.2	506.2 ± 10.0	504.4 ± 0.4
CFC-11	266.2 ± 1.1	268.4 ± 3.0	262.8 ± 0.2
CFC-113	94.6 ± 2.0	80.6 ± 2.0	80.44 ± 0.15
CH_3CCl_3	132.3 ± 2.1	133.5 ± 2.0	120.5 ± 0.3
CCl_4	104.7 ± 1.3	109.6 ± 3.0	108.9 ± 0.2

Values found in Table 2 confirm that standards remained stable over two years, and that no change occurred within the limits of measurement. An apparent change in CFC-113 concentration was attributed to contamination in the CMDL system during the 1993 calibration (Jim Happell, personal communication). The difference between CH_3CCl_3 values may be attributed to both CMDL and SIO reporting a 5% difference in their current absolute calibration (Jim Happell, personal communication).

The IOS standard (#ALM-032399) was intercalibrated with tank #ALM-032396 in July, 1993 and in March, 1995. The total uncertainty reported for the intercalibrated values was calculated from the propagation of the uncertainty associated with the calibration curve at the 95% confidence level, together with the uncertainty of five replicate injections of the standard. IOS standard concentrations are given in Table 3. Calculated values are based on the amount of halocarbon added to the cylinder during the gravimetric preparation of the standard and intercalibrated values are based on the CMDL scale. **Larsen-93** halocarbon concentrations will be reported throughout this discussion using the 1995 intercalibrated CMDL scale.

Table 3: IOS Halocarbon Standard Concentrations (ppt)

#ALM-032399	By weight	CMDL Intercal
CFC-12	128.5 ± 1.7	131.5 ± 2.7
CFC-11	308.7 ± 2.3	319.5 ± 6.1
CFC-113	67.4 ± 1.1	70.3 ± 2.4
CH_3CCl_3	1194.3 ± 7.0	1214.7 ± 26.7
CCl_4	381.4 ± 2.8	392.6 ± 10.4

2.4.1 Seawater sample analysis

Duplicate samples, primarily deep water samples with concentrations near blank levels, were collected to provide estimates of analytical precision for each halocarbon. The standard deviations for these duplicate seawater halocarbon measurements are found in Table 4.

Table 4: Sample analysis precision

	Standard deviation (s_p)	n
CFC-12	0.013	6
CFC-11	0.012	5
CFC-113	0.013	5
CH_3CCl_3	0.50	5
CCl_4	0.14	5

Typical concentrations and error estimates are illustrated in Figure 4 which show halocarbon profiles of samples collected at Station A1.

Estimates of accuracy were determined by analysis of standards as unknowns. Percent accuracies, determined by comparing a measured concentration to a known standard concentration, are presented in Table 5.

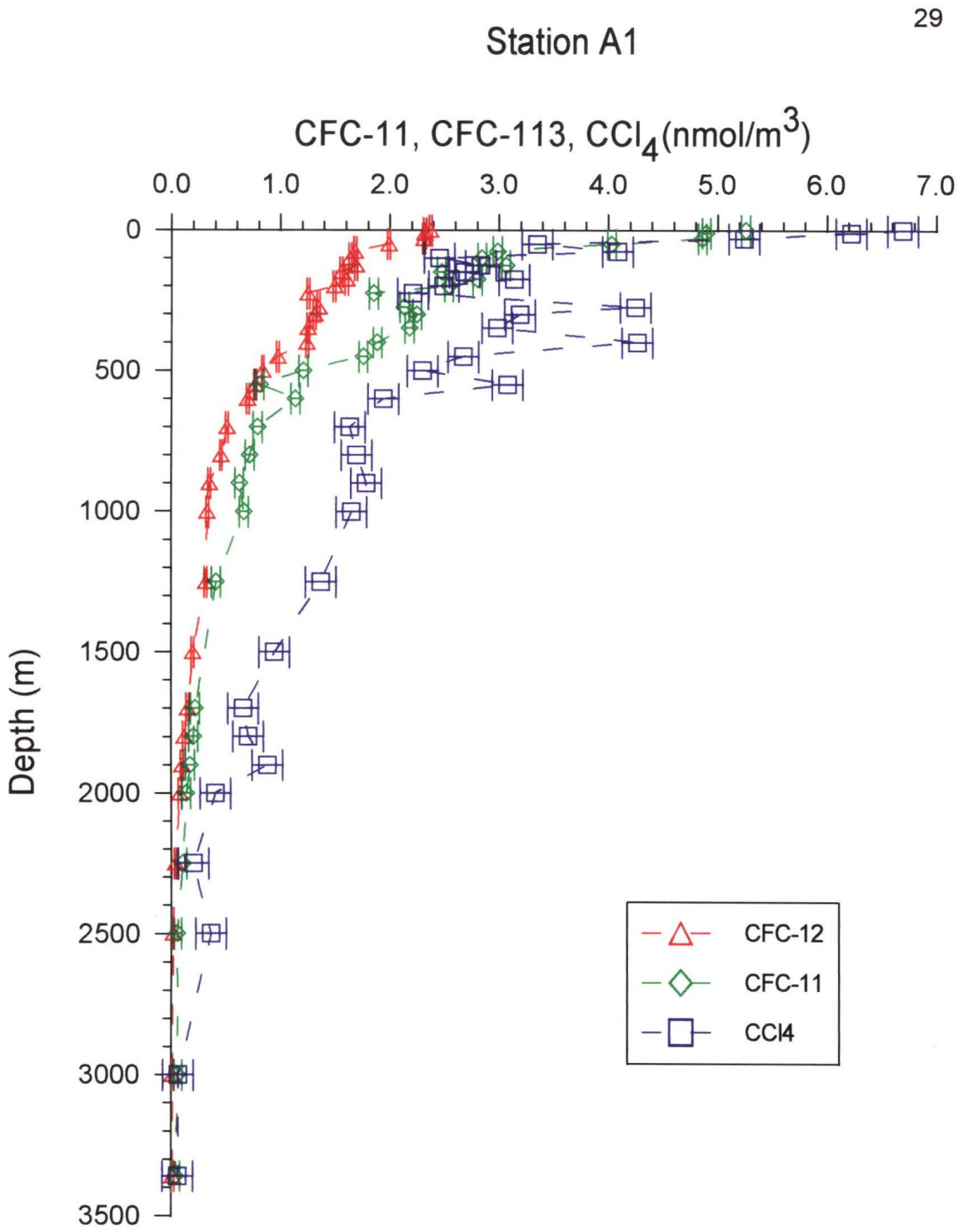
Station A1
CFC-11, CFC-113, CCl_4(nmol/m^3)
0.0
1.0
2.0
3.0
4.0
5.0
6.0
7.0
0
500
1000
1500
2000
2500
3000
3500
Depth (m)
CFC-12
CFC-11
CCl4

Figure 4

Table 5: Accuracy estimates

	Percent ± 1σ	n
CFC-12	100.9% ± 0.18	5
CFC-11	98.6% ± 3.28	5
CFC-113	96.9% ± 1.59	5
CH_3CCl_3	105.9% ± 19.6	5
CCl_4	103.3% ± 4.95	5

CFC-12 and CFC-11 accuracies meet WOCE data quality accuracy criteria (1-2%), whereas CFC-113 and CCl_4 are close to meeting these criteria.

2.4.2 Oceanographic consistency

Larsen-93 halocarbon measurements were evaluated by comparing data obtained at stations located in geographic proximity and influenced by similar oceanographic processes. Stations A1 and B1 were situated 990 km apart in the Canada Basin, the former at 3360 m depth and the latter at 3420 m. Although the origin of the water mass layers found at these stations were similar, differences in physical and geochemical properties were found in the upper layer. These differences can be explained geographically as Station B1 was sited between Herald and Barrow canyons, close to the main source of Pacific origin waters, whereas Station A1 was located further downstream of inflow from both canyons. Differences in temperature between Stations A1 and B1 at salinities from S=27 to S=34 in the upper layer are illustrated in Figure 5a. Because halocarbon solubility is a function of temperature, comparisons of halocarbon concentrations were not made in the upper layer. However, oceanographic consistency with respect to temperature was demonstrated between S=34.90 to S=34.95 in the Atlantic and

Figure 5a:Canada Basin spatial and temporal variability

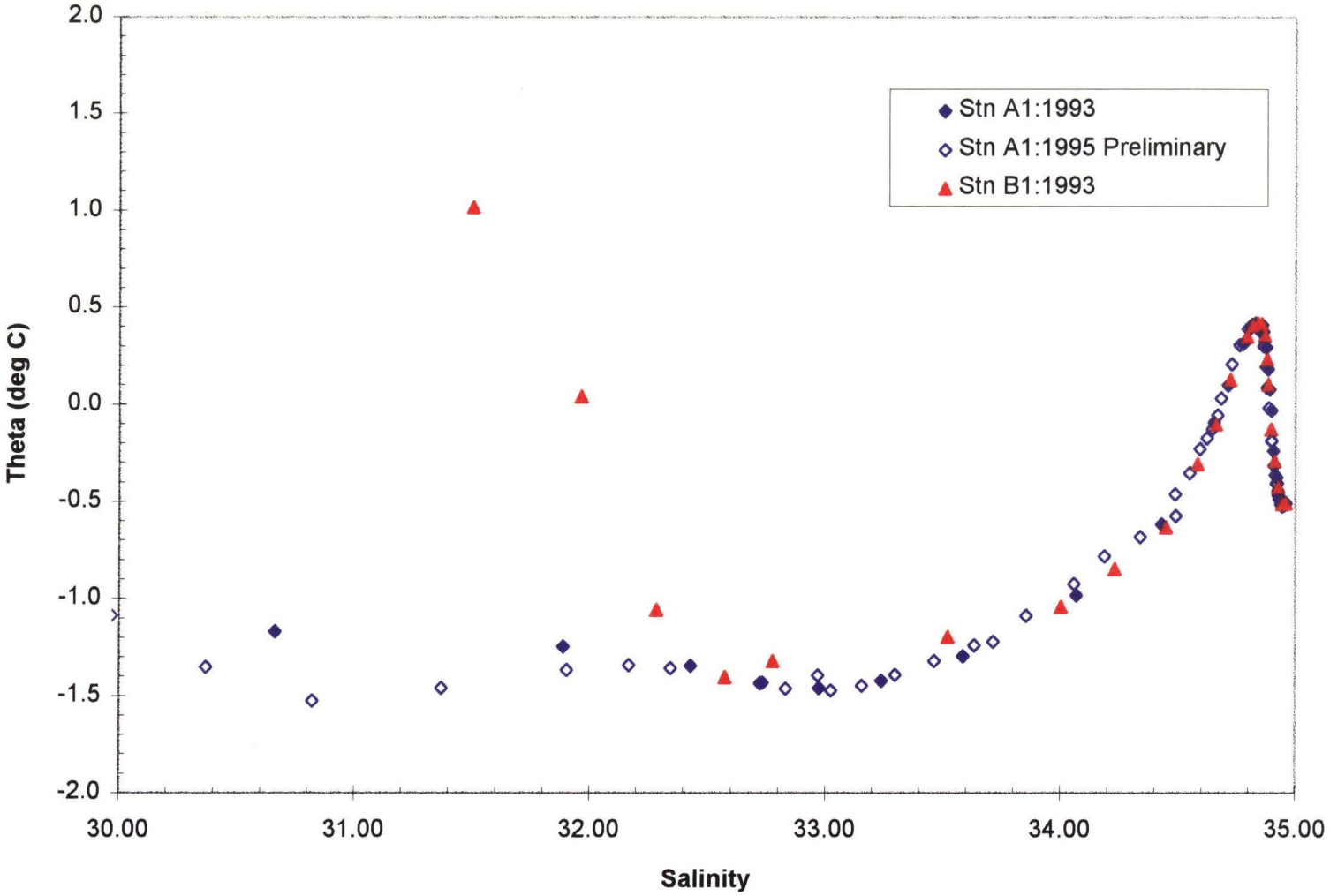

Figure 5b:Canada Basin spatial and temporal variability

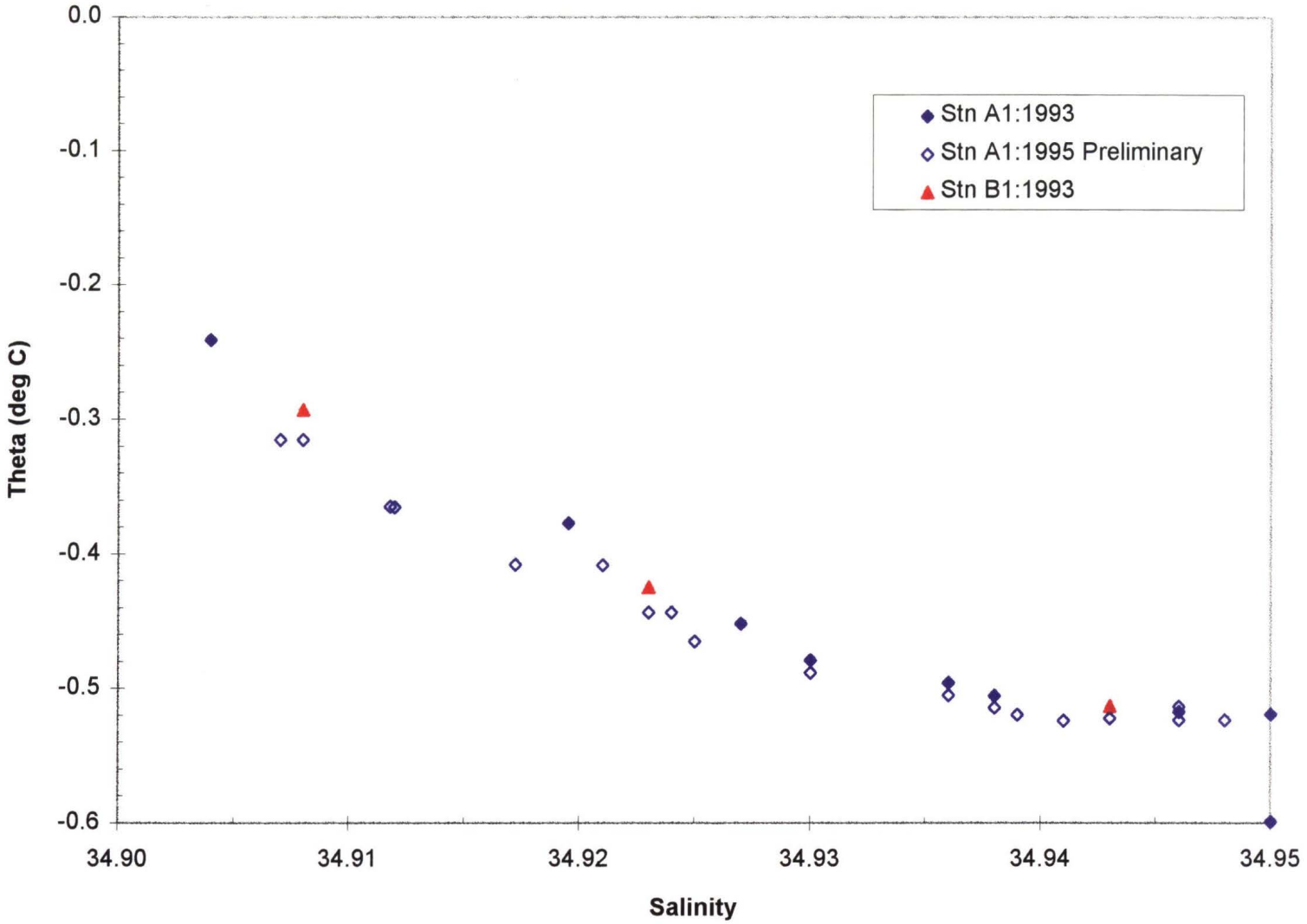

deep layers where a relationship between temperature and salinity is apparent (Figure 5b).

Accordingly, halocarbon profiles from Stations A1 and B1 were examined for oceanographic consistency in a restricted range from 1250 m to 2250 m between salinities S=34.90 to S=34.95. Halocarbon concentrations from Stations A1 and B1 were first compared to estimate the spatial variability of halocarbons. Then, because property-property consistency has proven useful elsewhere in validating data quality[1], this approach was next applied. A halocarbon-salinity property pair was selected because halocarbons enter the water column through gas exchange at the surface and are carried to depth by mixing and spreading along isopycnal surfaces. Property-property consistency was examined by applying a least squares linear regression analysis to halocarbon-salinity data from Stations A1 and B1.

To determine the spatial variability of halocarbon measurements, data from Stations A1 and B1 were sorted according to salinity, and the standard deviation of the difference between each pair of measurements was calculated. These results, presented in Table 6, define the spatial consistency of **Larsen-93** halocarbon data in the Canada Basin at Stations A1 and B1. The standard deviation provides a means by which to compare halocarbon data collected at other locations. Although the geographic standard deviation is larger than the estimate of precision determined by

---

[1]Confidence in measurements is obtained when properties that behave similarly, or are influenced by similar processes, demonstrate a linear relationship. For example, confirmation that cadmium analytical techniques had overcome contamination problems could not be obtained until property-property consistency was established between cadmium and phosphate, a geochemical property that undergoes the same uptake and regeneration biogeochemical processes as cadmium (Boyle et al., 1976).

replicate analyses (values in brackets in Table 6 for comparison), it is more representative of the uncertainty of each halocarbon measurement because it extends over a larger concentration range. It may, however, include environmental differences and thus provides a worst-case estimate.

Table 6: Standard deviation of the difference between halocarbon measurements at Stations A1 and B1

	s_p	n
Salinity	0.0025 (cf 0.0025)	3
CFC-12	0.04 (cf 0.013)	3
CFC-11	0.07 (cf 0.012)	2
CFC-113	0.14 (cf 0.013)	3
CH_3CCl_3	0.73 (cf 0.50)	3
CCl_4	0.08 (cf 0.14)	3

To determine property-property consistency, halocarbon-salinity data were examined using a least squares linear regression analysis whereby all uncertainty is assigned to the halocarbon measurements. This assumption is reasonable because the precision of salinity measurements is better than the precision of halocarbon measurements. Findings of the linear regression analysis are summarized in Table 7, where S_{ey} is the standard error for the y estimate and r^2 is the coefficient of determination. Slope and intercept values were used to calculate halocarbon concentration from salinity. The relationship between the measured value and calculated value for each halocarbon is also illustrated in Figures 6 to 10, and the standard deviations of differences between these numbers are included in Table 7.

Figure 6:
CFC-12 Oceanographic Variability

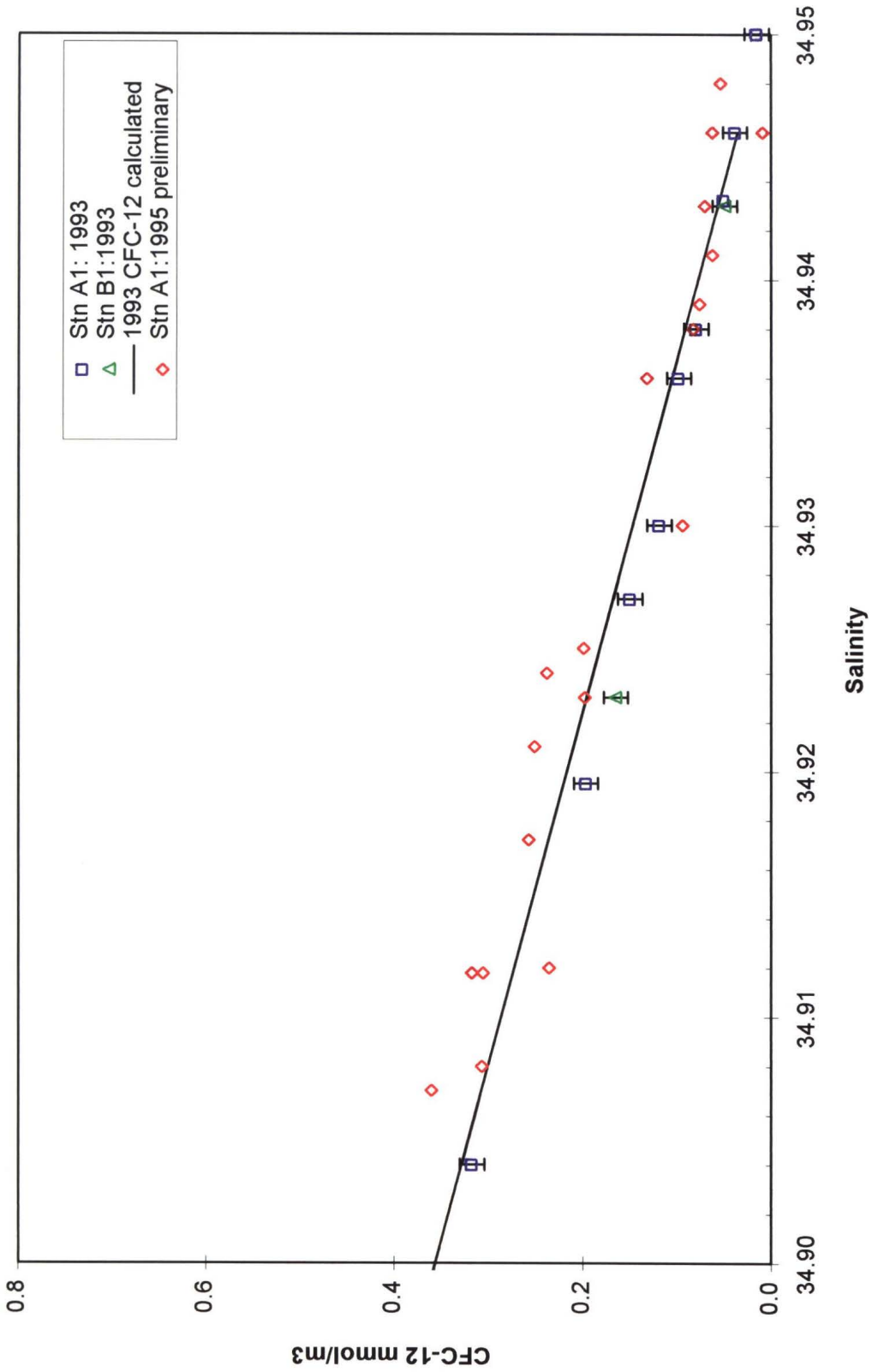

Figure 7:
CFC-11 Oceanogaphic Variability

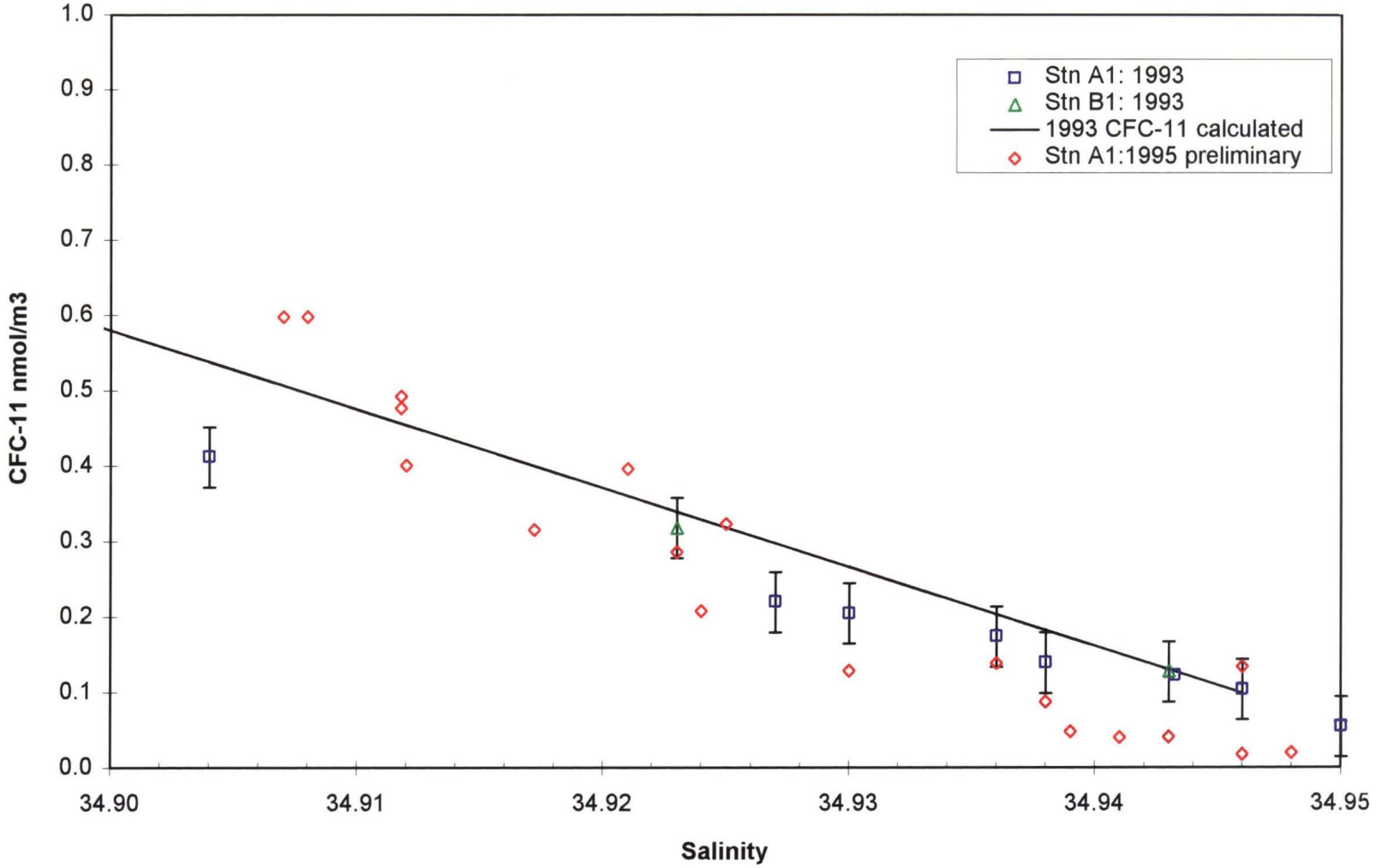

Figure 8:
CFC-113 Oceanographic Variability

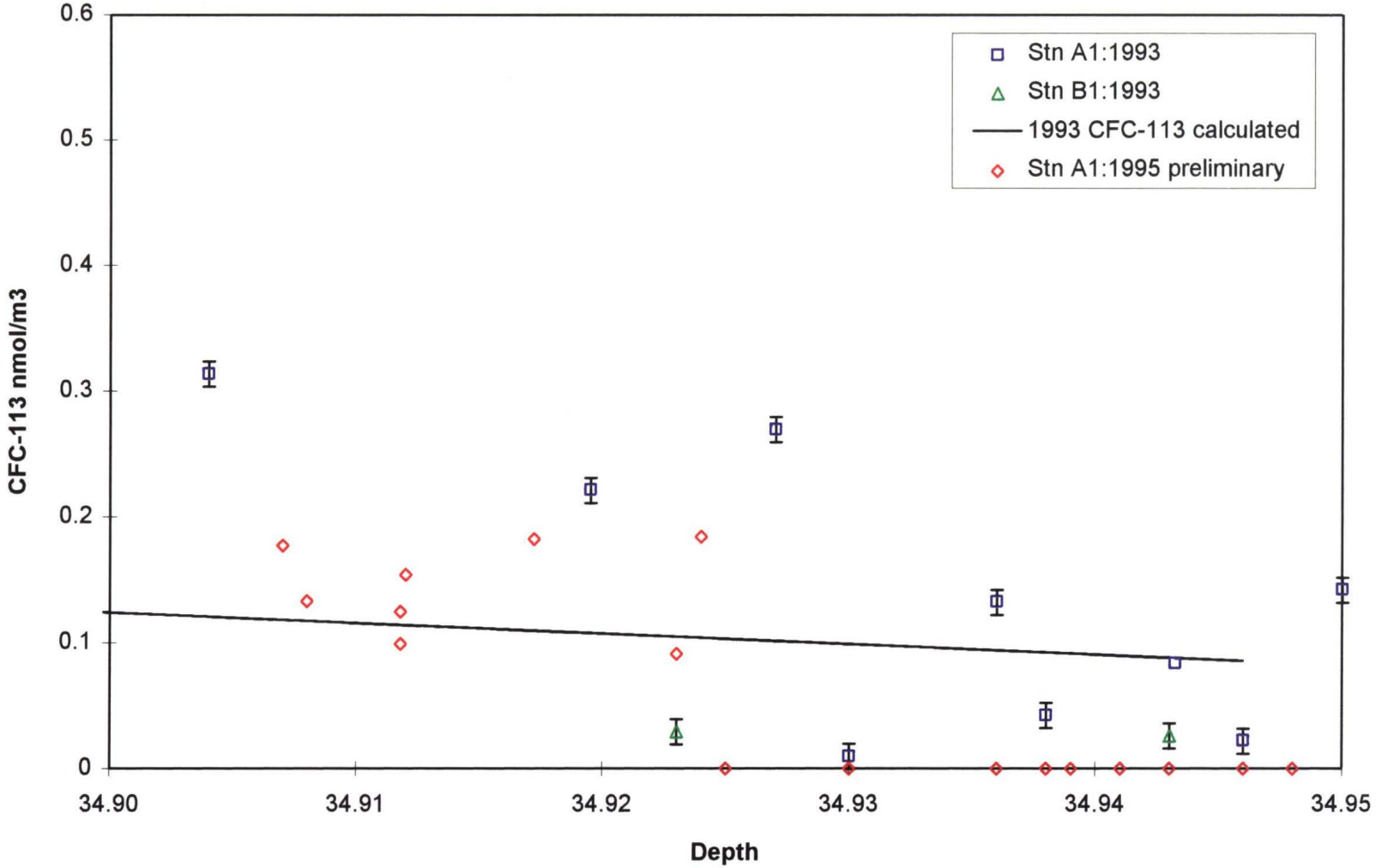

Figure 9:
CH_3CCl_3 Oceanographic Variability

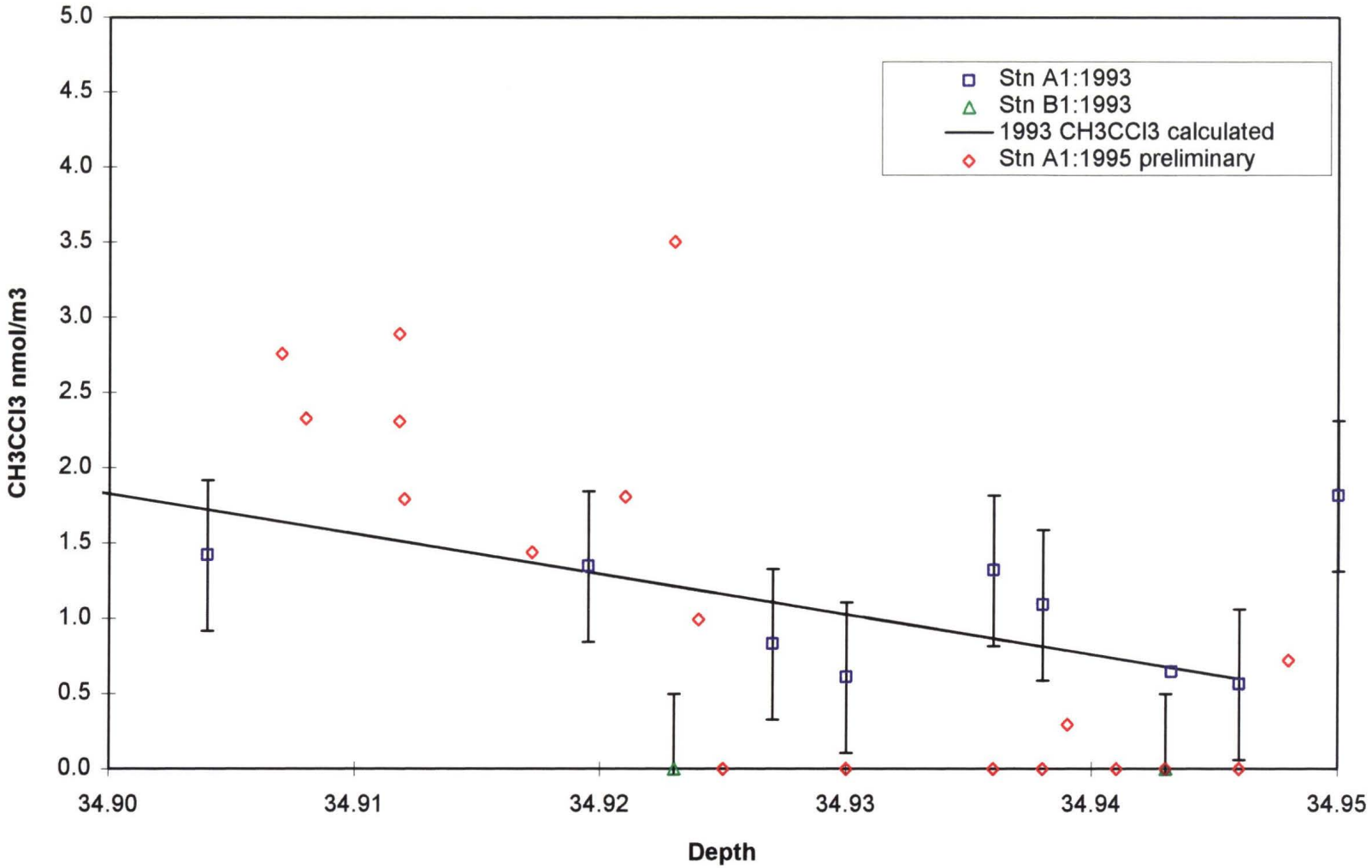

Figure 10:
CCl_4 Oceanographic Variability

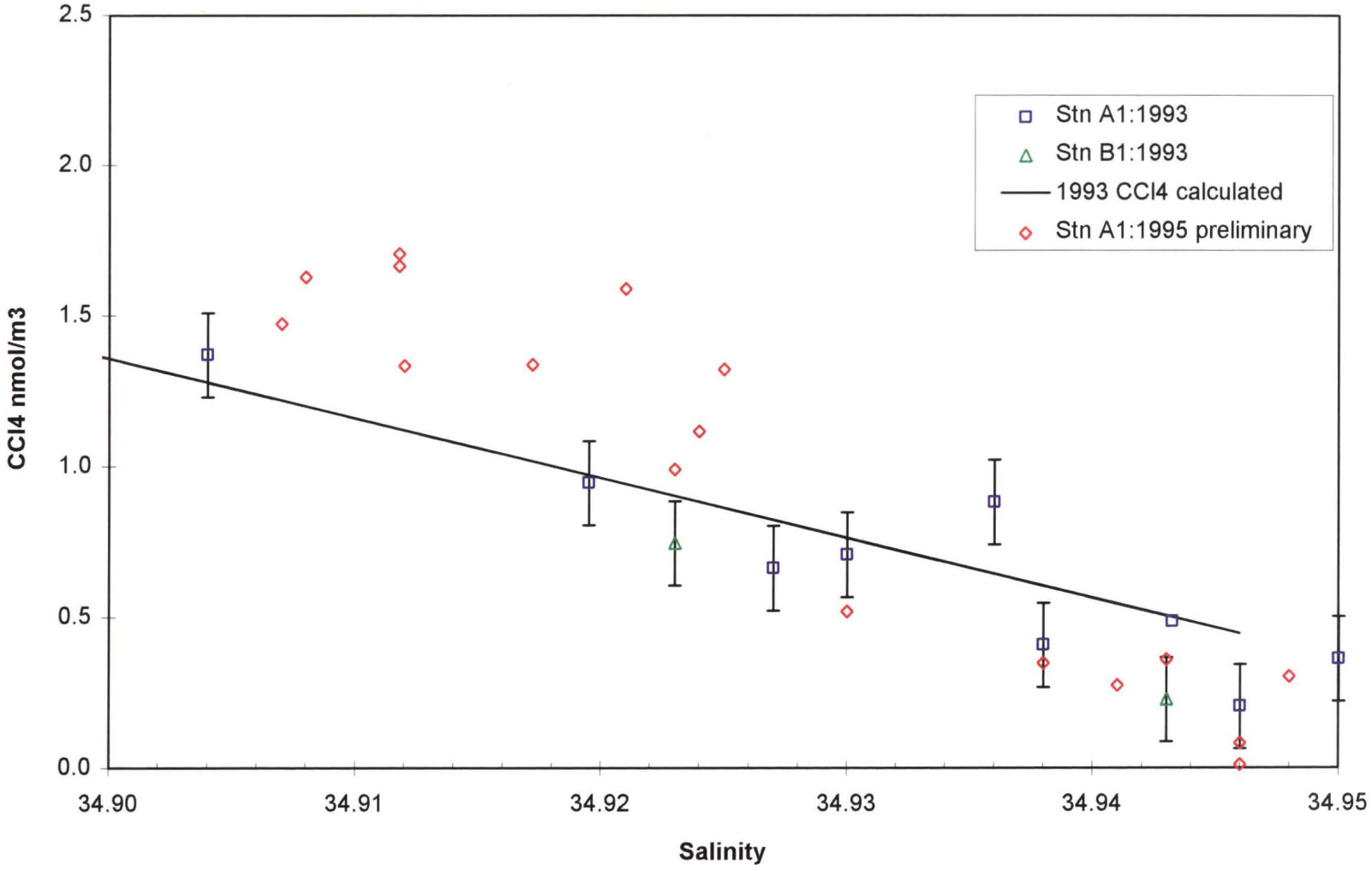

Table 7: Linear regression analysis: Stations A1 and B1

wrt Salinity	S_{ey}	r^2	n	s_p
CFC-12	0.01	0.99	10	0.01
CFC-11	0.05	0.94	9	0.04
CFC-113	0.11	0.14	10	0.07
CH_3CCl_3	0.51	0.15	10	0.43
CCl_4	0.16	0.87	10	0.12

As illustrated in Figures 6 to 10, all halocarbon measurements except CFC-113 and CH_3CCl_3 display strong relationships with salinity which validates the **Larsen-93** halocarbon measurements. The CFC-113/salinity data do not show a strong relationship (low r^2 value) because of two factors; the age of the Atlantic and deep layer waters, and CFC-113's shorter production history. CFC-113 values were barely detectable in the Atlantic layer and were at, or below, detection limits in the deep layer. This finding however, does not invalidate CFC-113's use because CFC-113 is only applied to estimate the age of young waters. Young waters in the upper layer were not evaluated in this analysis. The lower CH_3CCl_3 coefficient of variation reported here suggests that CH_3CCl_3 may not be as useful as a tracer.

The variability of halocarbon data over time was examined next by comparing data collected at Station A1 in 1993 with data collected at Station A1 in 1995. In 1995, halocarbon data were collected with the same extraction technique and used two systems for measurement, one with a Hewlett-Packard GC and one with a Varian GC. Temporal variability at Station A1 was first examined by comparing theta and salinity properties from 1993 and 1995 (Figures 5a and 5b). These figures illustrate that temporal continuity at Station A1 exists at salinities greater than S=34.92.

Halocarbon concentrations for samples collected at Station A1 in 1995 are shown in profile in Figure 11 and are plotted against salinity in Figures 6 to 10. These data along with data from **Larsen-93** were paired according to their salinity, and the standard deviation of their differences was obtained. Table 8 presents a comparison of salinity and halocarbon data from depths greater than 1500 m at salinities greater than 34.92.

Table 8: Comparison of Station A1 halocarbon data: 1993 and 1995

>1500 m	s_p	n
Salinity	0.0010	9
CFC-12	0.05 (0.04, 0.013)	9
CFC-11	0.06 (0.07, 0.012)	7
CFC-113	0.05 (0.14, 0.013)	7
CH_3CCl_3	0.68 (0.73, 0.50)	8
CCl_4	0.13 (0.08, 0.14)	8

The standard deviations, reported in Table 8, show that the magnitude of temporal variation below 1500 m at Station A1 is similar to the magnitude of geographical variation found below 1250 m between Stations A1 and B1 in the Canada Basin. Although the values are greater than the variation based on replicate analyses, they provide a basis for comparison when determining whether a change in ventilation has occurred.

The preceding tables thus demonstrate that **Larsen-93** halocarbon data are oceanographically consistent in terms of geography within the Canada Basin, and that they are also consistent in terms of time, from 1993 to 1995 at depths below 1500 m. This analysis describes waters in the Canada Basin as relatively homogeneous along constant density

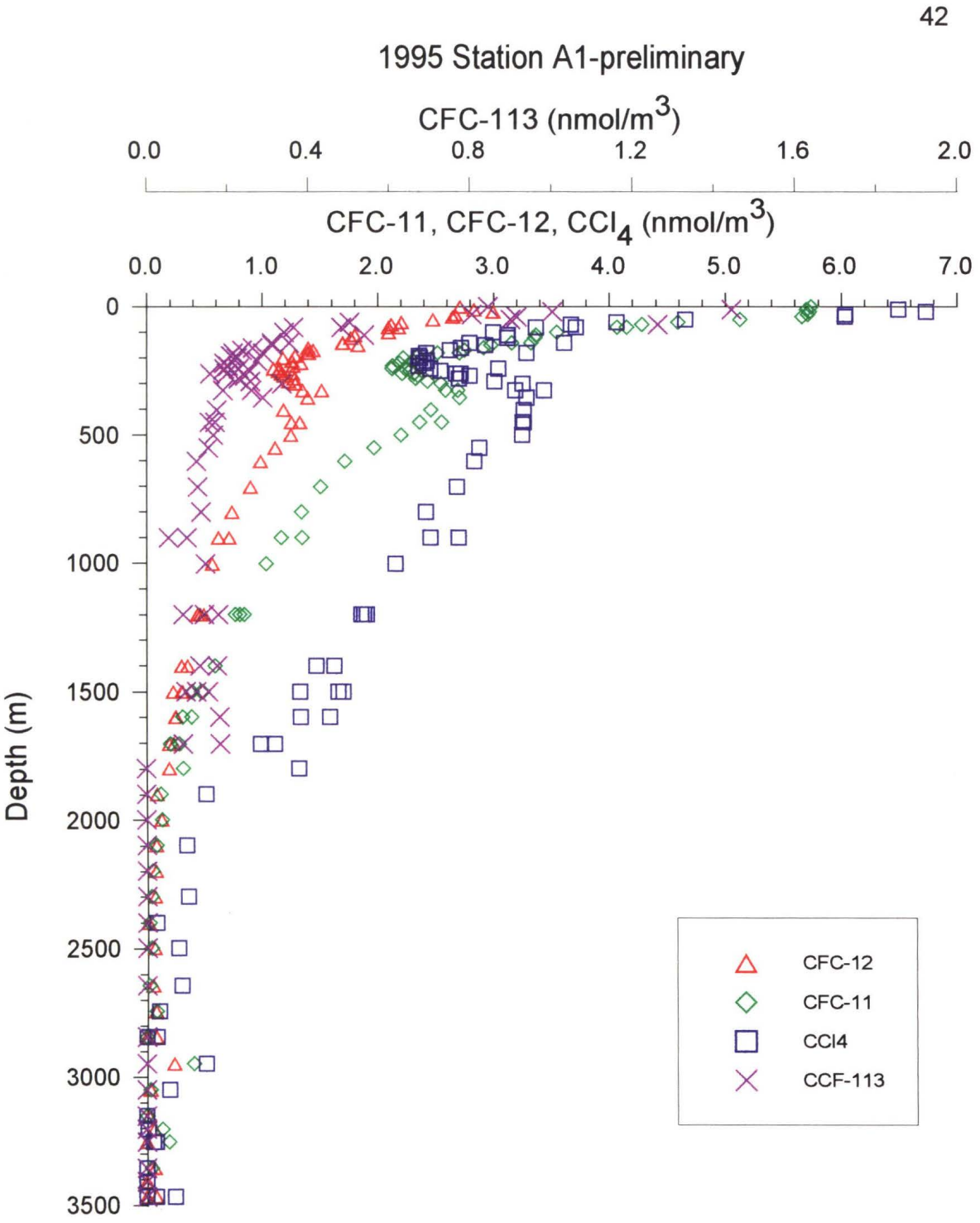
1995 Station A1-preliminary
CFC-113 (nmol/m3)
0.0
0.4
0.8
1.2
1.6
2.0
CFC-11, CFC-12, CCl4 (nmol/m3)
0.0
1.0
2.0
3.0
4.0
5.0
6.0
7.0
Depth (m)
0
500
1000
1500
2000
2500
3000
3500
CFC-12
CFC-11
CCl4
CCF-113

Figure 11

surfaces, a finding that agrees with historical views of Canada Basin waters. This analysis further suggests that processes which influence ventilation of subsurface waters below 1500 m did not change during the period 1993 to 1995. Finally, with these measurements of accuracy and precision now determined, **Larsen-93** halocarbon data can now be compared and analyzed.

References:

Boyle, E. A., F. Sclater and J. M. Edmond, On the geochemistry of cadmium, Nature, 263, 42-44, 1976.

Wallace, D.W.R., P. Beining, and A. Putzka, Carbon tetrachloride and chlorofluorocarbons in the south Atlantic Ocean, 19°S, J. Geophys. Res., 99, 7803-7819, 1994.

Chapter 3: Defining the Atlantic/Pacific Water Mass Boundary

Chapter 3 examines water mass properties based primarily on physical and geochemical measurements made at five basin stations in the Canadian Basin. The description that follows is that which appears as "Physical and Geochemical Properties Across the Atlantic/Pacific Water Mass Front in the Southern Canadian Basin", in the Journal of Geophysical Research, Vol. 101, pages 1183-1197, 1996.

Abstract

Temperature, salinity, nutrients, oxygen, and halocarbon data collected in the Arctic Ocean reveal a frontal structure previously unrecognized in the hydrography of the Canadian Basin. Samples were collected on a 1300-km section extending from the Beaufort Sea in the Canada Basin to the East Siberian Sea in the Makarov Basin. These data, collected in 1993 aboard the **CCGS Henry Larsen**, reveal a lateral boundary between water masses of Atlantic and Pacific origin. The term water mass assembly is introduced to describe the basic arrangement or vertical stacking of water masses found in the Arctic Ocean, recognizing that water mass components within each assembly may differ from basin to basin. Using historical data, two primary water mass assemblies are defined, each consisting of three layers: an upper layer, an Atlantic layer, and a deep layer. These two assemblies are marked by important differences. One assembly, here defined as the Western Arctic (WA) assembly, is characterized by an upper layer of relatively fresh, high-nutrient water of Pacific origin; below this, by an Atlantic layer with a core temperature generally below

0.5°C; and finally, by a deep layer of higher salinities and colder temperatures (about -0.5°C) than found in the overlying Atlantic layer. The second assembly, here defined as Eastern Arctic (EA) assembly, is characterized by the absence of Pacific water in the upper layer; below this, by an Atlantic layer core as warm as 2° to 3°C; and by a colder (about -0.9°C) deep layer. Because the presence or absence of Pacific origin water is a key characteristic distinguishing the two assemblies, we will refer to the water mass boundary between the two assemblies as the Atlantic/Pacific front. Earlier research indicated that water masses in the Arctic Ocean were separated by a front above the Lomonosov Ridge into the Canadian and Eurasian basins. Although all **Larsen-93** stations from the Canada Basin (A1-D1) display classic WA assembly characteristics, the Makarov Basin station (E1) shows EA assembly characteristics in the upper and Atlantic layers and a WA assembly deep layer. This suggests a relocation in the position of the Atlantic/Pacific boundary away from the Lomonosov Ridge. Further, **Larsen-93** data show the transition region between the Atlantic and deep layers is fresher in the Makarov Basin than corresponding water in either the Canada or Eurasian basins, implying a source of cold, low-salinity water, perhaps from the Laptev and East Siberian shelves. The front separating these two assemblies lies above the Mendeleyev Ridge and is marked by large lateral gradients in all measured properties. In particular, the penetration of anthropogenic halocarbons is 2 to 3 times deeper in the Makarov Basin than in the Canada Basin, implying enhanced rates of ventilation. This suggests that direct exchange between the Canadian and Eurasian basins has occurred recently near the perimeter and that physical and chemical properties, including contaminants, may have been transported by boundary currents more quickly from one basin to the other.

3.1 Introduction

The principal waters entering the Arctic Ocean are from the North Atlantic via Fram Strait and the Barents Sea, and the North Pacific via Bering Strait. Within the Arctic interior, these waters join the large-scale circulation and are subsequently modified by processes of air/sea/ice interaction, river inflow, and exchange with surrounding shelves. However, little is known about either the lateral boundaries (fronts) separating the primary water masses, or the relative rates of water mass modification and ventilation. Discussion of these topics has been limited both by the small number of sampling sites and by the fact that modern geochemical tracer techniques have only recently been applied (see Jones et al. (1990), for review). Such research is required to determine the formation sites, rates, and spreading pathways of water masses within the Arctic system. This paper presents new data which describe the frontal structure separating waters of Pacific and Atlantic origin within the southern Canadian Basin and their relative rates of ventilation.

Water mass circulation and distributions in the Arctic Ocean are strongly connected to its complex bathymetry (Aagaard, 1989). The ocean interior is divided by the Lomonosov Ridge into two main basins, the Canadian Basin and the Eurasian Basin. These main basins are further divided: the Canadian Basin by the Alpha-Mendeleyev Ridge into the Canada and Makarov basins; and the Eurasian Basin by the Nansen-Gakkel Ridge into the Nansen and Amundsen basins. These basins are, in turn, surrounded by broad (600-800 km), shallow (30-200 m) continental shelves, found primarily north of Europe and Asia along the Barents, Kara, Laptev, and East Siberian seas. Current understanding of Arctic circulation holds that the two main basins maintain distinct circulations separated by a front in the central region over

the Lomonosov Ridge (Anderson et al., 1994). Furthermore, Eurasian Basin waters are relatively well ventilated while Canadian Basin deep waters are older and more isolated (Ostlund, 1982; Macdonald et al., 1993).

The vertical layering of Arctic water masses is largely determined by the distribution of salinity, the structure of which has been variously described (see Jones et al. (1990), and Carmack (1990), for reviews). This stratification is due to the combined effects of river inflow, seasonal ice melt and, in the western Arctic, the additional input of relatively fresh water of Pacific origin through Bering Strait. The surrounding continental shelves, especially those north of Europe and Asia, are also sites of seasonal ice formation and melting that contribute to the physical and geochemical characteristics of water in the central basins (Aagaard et al., 1981; Melling and Lewis, 1982; Jones and Anderson, 1986; Cavalieri and Martin, 1994). The combined effects of circulation and proximity to these freshwater sources provide the potential for horizontal variation in water column structure and regional differences in residence time and ventilation across the Arctic Ocean (Aagaard and Carmack, 1989; Schlosser et al., 1994).

This paper combines temperature and salinity data from **Larsen-93** and the historical record to describe the basic arrangement of water masses in the Arctic Ocean using the term water mass assembly (section 3.1). Property-property plots of **Larsen-93** geochemical data are then used to define further the two water mass assemblies and to show the transition from one assembly to the other (section 3.2). In addition, the structure of the boundary separating these two assemblies within the southern Canadian Basin is illustrated using vertical sections (section 3.3). Finally, the relative rates of ventilation are shown using vertical plots and section data (section 3.4).

3.2 Methods

During a cruise on the **CCGS Henry Larsen** from August 23 to September 25, 1993, samples were collected from eight geochemistry stations, five of which form a section across the Canadian Basin (Figure 1). Water samples were collected in 10-L Niskin-type bottles designed at the Bedford Institute of Oceanography. The bottles were mounted on a General Oceanics rosette together with a Falmouth conductivity-temperature-depth (CTD) profiler. Measurements of temperature, pressure, and conductivity were made on both downcasts and upcasts; sample bottles were tripped on the upcast. Temperatures were converted to potential temperatures (Θ) according to the algorithms published by Fofonoff and Millard (1983). Subsamples were drawn for salinity (S), oxygen, nutrients, and halocarbons. Salinities were determined after the cruise from conductivity measurements using a Guildline Portasal salinometer and standardized against Standard Sea Water, IAPSO Batch P118 (pooled variance S_p=0.0025, n=28). The remaining parameters were analyzed on board: oxygen by the Carpenter-Winkler method (S_p=1.73 mmol m^{-3}, n=36), nutrients by standard AutoAnalyzer Technicon methods for silicate and nitrate, and a modified method for phosphate ($Si(OH)_4$: S_p=0.38 mmol m^{-3}, n=222; NO_3: S_p=0.1 mmol m^{-3}, n=220; PO_4: S_p=0.02 mmol m^{-3}, n=222). Halocarbons were analyzed using an extraction and trapping system (see Wallace et al., 1994) combined with a Hewlett-Packard gas chromatograph electron capture detector:

CFC-12: S_p=0.013 nmol m^{-3}, n=5;

CFC-11: S_p=0.012 nmol m^{-3}, n=5;

CFC-113: S_p=0.013 nmol m^{-3}, n=6;

CCl_4: S_p=0.14 nmol m^{-3}, n=5.

A complete discussion of methods is reported by Macdonald

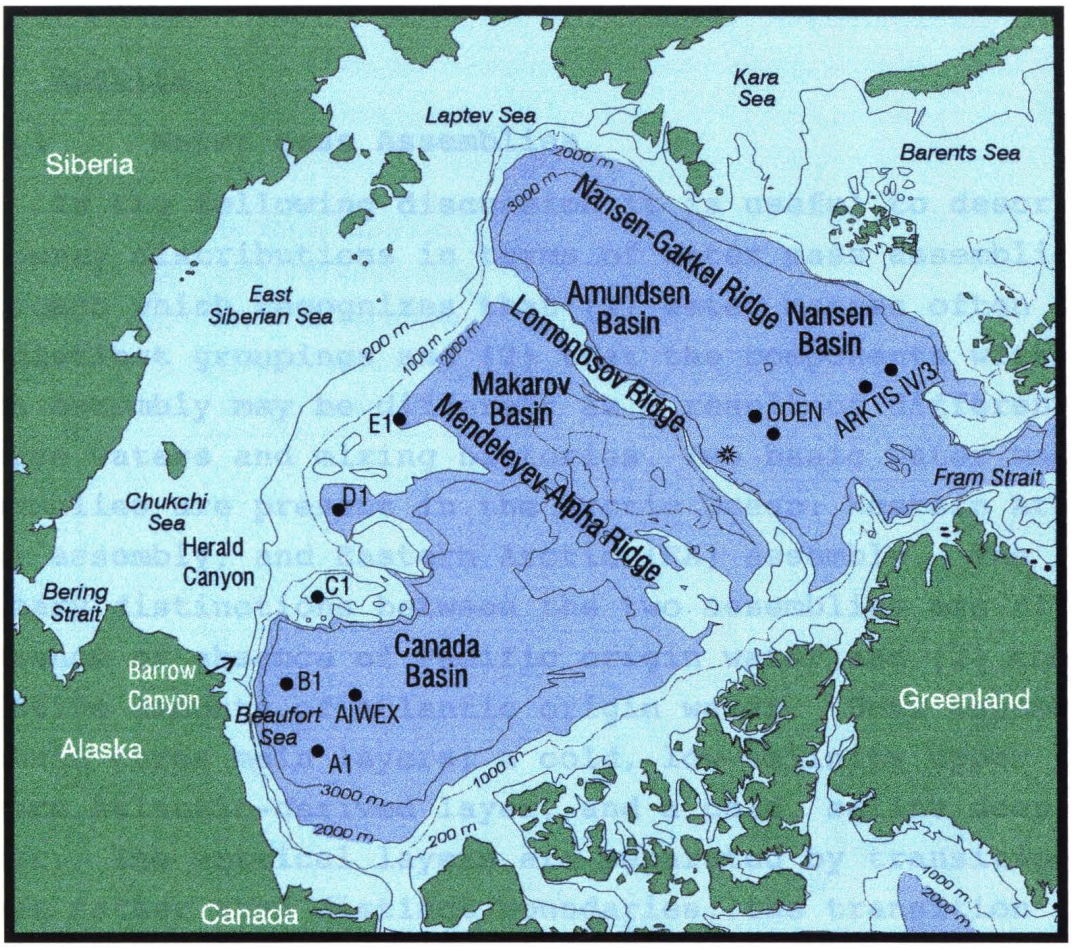
Siberia
Laptev Sea
Kara Sea
Barents Sea
Nansen-Gakkel Ridge
Amundsen Basin
Nansen Basin
East Siberian Sea
Lomonosov Ridge
Makarov Basin
Mendeleyev-Alpha Ridge
E1
ODEN
ARKTIS IV/3
Fram Strait
Chukchi Sea
Herald Canyon
D1
C1
Bering Strait
Canada Basin
Barrow Canyon
B1
AIWEX
Beaufort Sea
A1
Alaska
Greenland
Canada
2000 m
3000 m
1000 m
200 m

Figure 1

et al. (1995). Note: For comparison to other published data, the SI unit millimoles per cubic meter is numerically equivalent to micromoles per liter and can be converted to micromoles per kilogram by dividing by 1.03.

3.3 Results

3.3.1 Water Mass Assemblies

In the following discussion it is useful to describe property distributions in terms of water mass assemblies, an approach which recognizes that (1) water masses often occur in distinct groupings and (2) that the components within each assembly may be different as a result of different source waters and mixing histories. Two basic water mass assemblies are present in the Arctic Ocean: Western Arctic (WA) assembly, and Eastern Arctic (EA) assembly. The primary distinctions between the two assemblies are (1) the presence or absence of Pacific origin water and (2) the relative amounts of Atlantic origin water. Both assemblies contain three main layers; a cold, low-salinity upper layer, a warm Atlantic-derived layer, and a cold, saline deep layer. The vertical layers are separated by transition zones rather than distinct boundaries: the transition between the upper and Atlantic layers is marked by an inverse thermocline in which temperature increases rapidly with depth; the transition between the Atlantic and deep layers is marked by a relatively weak thermocline in which temperature decreases with depth.

The structure of the two assemblies is evident in a plot of Θ versus S showing the upper, Atlantic, and deep layers (Plate 1). **Larsen-93** data (Station A1, Canada Basin and Station E1, Makarov Basin) are combined with historical data to describe the two main water mass assemblies; characteristics of the WA assembly are defined by Arctic

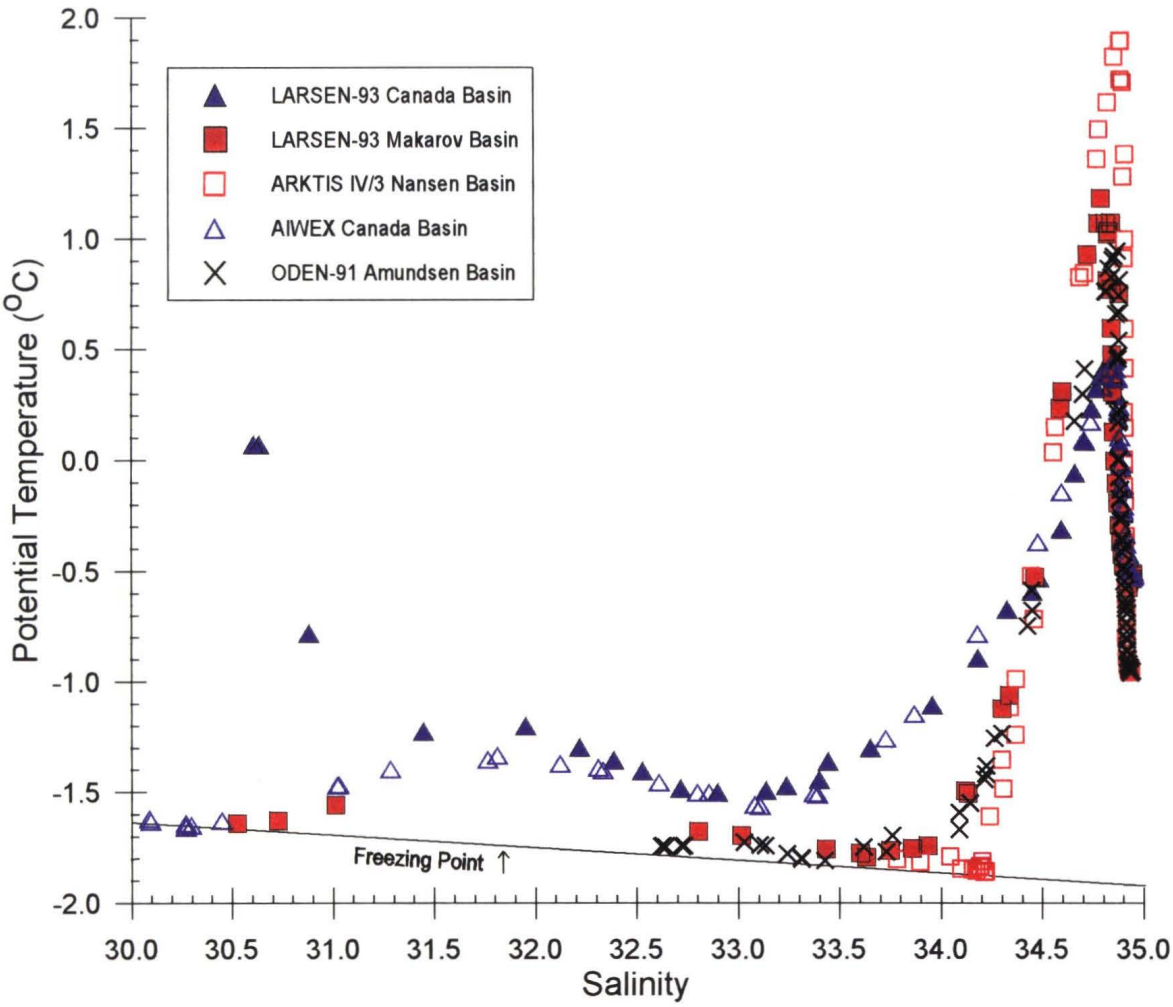
LARSEN-93 Canada Basin
LARSEN-93 Makarov Basin
ARKTIS IV/3 Nansen Basin
AIWEX Canada Basin
ODEN-91 Amundsen Basin
Freezing Point ↑
Potential Temperature (°C)
Salinity
2.0
1.5
1.0
0.5
0.0
-0.5
-1.0
-1.5
-2.0
30.0
30.5
31.0
31.5
32.0
32.5
33.0
33.5
34.0
34.5
35.0

Plate 1a

Internal Wave Experiment (AIWEX) (1985) data from the Canada Basin and characteristics of the EA are defined by ARKTIS IV/3 (1987) data from the Nansen Basin and ODEN-91 (1991) data from the Amundsen Basin.

The upper layer in both assemblies consists of a polar mixed layer, reflecting seasonal freshwater inputs and winter mixing, and beneath this, a cold halocline influenced by lateral inputs from the shelves and adjacent seas. The mixed layer of the WA assembly is generally fresher than that of the EA (cf. Coachman and Aagaard, 1974). These differences are due to conditions such as residence time and proximity to freshwater sources and sinks.

Below this seasonally mixed layer, differences between the EA and WA assemblies are particularly evident. The cold halocline of the WA assembly differs from that of the EA by the presence of Pacific origin water. The halocline of the WA assembly extends deeper in the water column (30 to 200 m depth) and shows two distinct features: the first, found at 50 to 80 m, is a potential temperature maximum (Θ_{max}) between salinities S=31 and S=32; and the second, found at about 150 m, is a potential temperature minimum (Θ_{min}) near S=33.1. In contrast, in the EA halocline (20 to 120 m depth), the Θ/S curve is flat and lies close to the freezing point line; temperature generally decreases between the upper (S=32.7) and lower (S=34.2) regions of the halocline. Also, the lower region of the halocline within the EA assembly remains cold up to S=34.2, while that in the WA warms slowly from S=33.1 to S=34.4. This latter difference suggests either a different mixing history or the presence of another water mass which bridges the cold, nutrient-rich water of the middle halocline of the WA assembly with underlying thermocline water. Possible sources for such water include a modified variety of Atlantic water from the Barents Sea branch or drainage from the Siberian shelves. Generally,

the halocline of the EA assembly in the Amundsen Basin is fresher and has a larger salinity range (S=32.6 to S=34.2) than that found in the Nansen Basin (S=33.7 to S=34.2), reflecting runoff from the Laptev and Kara seas.

Waters of Pacific origin entering through Bering Strait via Barrow and Herald canyons are believed responsible for halocline features within the upper layer of the Canadian Basin (cf. Coachman and Aagaard, 1974; A.F. Treshnikov, Oceanography of the Arctic Basin, unpublished manuscript, 1959), although modification of properties by shelf processes occurs (Jones et al., 1991). The Pacific inflow, comprised of nutrient-rich Gulf of Anadyr water, Bering Shelf water, and fresher Alaskan Coastal water, bifurcates upon entering the Chukchi Sea. The eastern branch of Alaskan Coastal waters is further freshened on its way to Barrow Canyon, while the western branch of Gulf of Anadyr and Bering Shelf waters is also modified while crossing the large Chukchi Shelf before entering the Arctic Ocean via Herald Canyon. Coachman and Barnes (1961) referred to the (S=31 to S=32, Θ_{max}) and (S=33.1, Θ_{min}) features as Bering Sea Summer Water and Bering Sea Winter Water, respectively, while Jones and Anderson [1986] referred to the (S=33.1, Θ_{min}) feature as Upper Halocline Water. Jones and Anderson (1986) called the lower region of the halocline, marked by a local minimum in NO (a quasi-conservative property defined as $9NO_3 + O_2$ by Broecker (1974)), Lower Halocline Water and proposed that this water derives from the Barents and Kara seas. We note that a sharp break occurs in the Θ/S plots at S=34.2 in the EA assembly and at S=34.4 in the WA assembly, coincident with the NO minimum in each assembly. This lateral change in the NO minimum layer across the front will be discussed further below.

The inverse thermocline (Θ increasing with depth) represents a transition between the cold halocline waters

above and the warm Atlantic layer below. In both assemblies this transition zone also has unique characteristics, primarily due to a difference in $\Delta\Theta/\Delta S$ slope, as seen in Plate 1b. The slope of the thermocline in the WA assembly is shallower, ($\Delta\Theta/\Delta S=3.4$) than the slope of the halocline in the EA assembly ($\Delta\Theta/\Delta S=5.8$). This slope difference is important as it signifies the stability of the thermocline region relative to isopycnals; the steep $\Delta\Theta/\Delta S$ slope of the EA is more closely aligned with isopycnals, close to the critical slope for the onset of the cabelling instability (Foster and Carmack, 1976). Another difference between these two assemblies is the depth at which the thermocline begins. It is deeper in the water column in the WA assembly (about 200 m) than in the EA assembly (about 120 m).

Next in the assembly structure is the Atlantic layer with a core marked by a potential temperature maximum. Although Atlantic water is present in both assemblies, it is cooler ($\Theta=0.5°C$) and fresher ($S=34.84$) in the WA assembly than in the EA assembly which has temperatures as high as 2°C and salinities near $S=34.90$. Again, the core of Atlantic water is deeper in the WA assembly (about 400 m) than in the EA assembly (about 250 m).

Within each assembly, the transition zone to the deep layer lies under the Atlantic layer and extends down to the depth at which potential temperatures become near-isothermal, that is, at about -0.4°C in the WA assembly and -0.8°C in the EA assembly (Plate 1c). In the upper portion of this domain, waters at a given temperature in the Canadian Basin are less saline than those of the Eurasian Basin; at $S=34.92$ and $\Theta=-0.4°C$ the Θ/S lines cross and Canadian Basin deep waters remain near-isothermal, whereas those of Eurasian Basin continue to cool to temperatures below -0.9°C. This cross-over point on the Θ/S plot likely reflects the sill depth of the Lomonosov Ridge. In

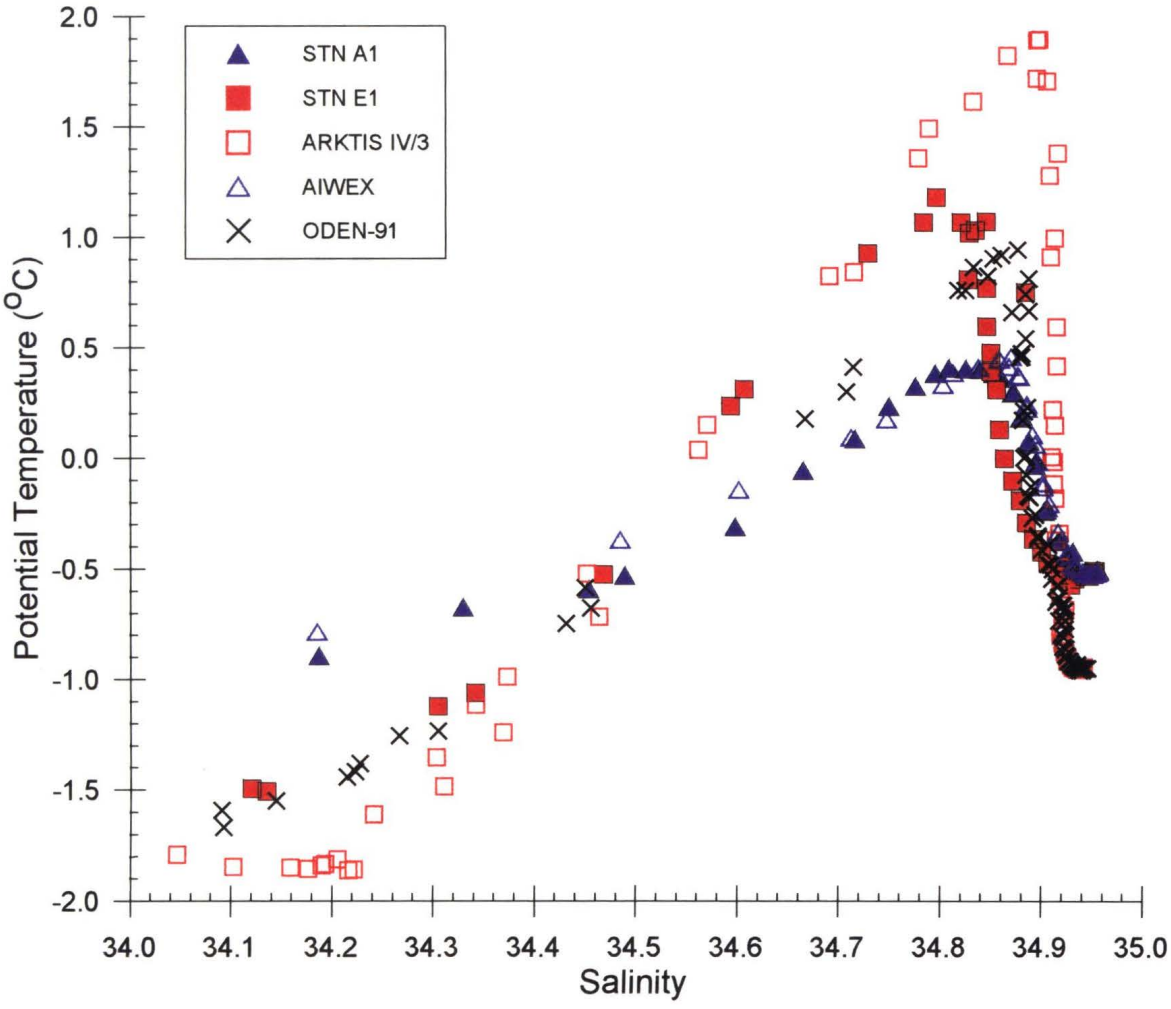
STN A1
STN E1
ARKTIS IV/3
AIWEX
ODEN-91
Potential Temperature (°C)
2.0
1.5
1.0
0.5
0.0
-0.5
-1.0
-1.5
-2.0
34.0
34.1
34.2
34.3
34.4
34.5
34.6
34.7
34.8
34.9
35.0
Salinity

Plate 1b

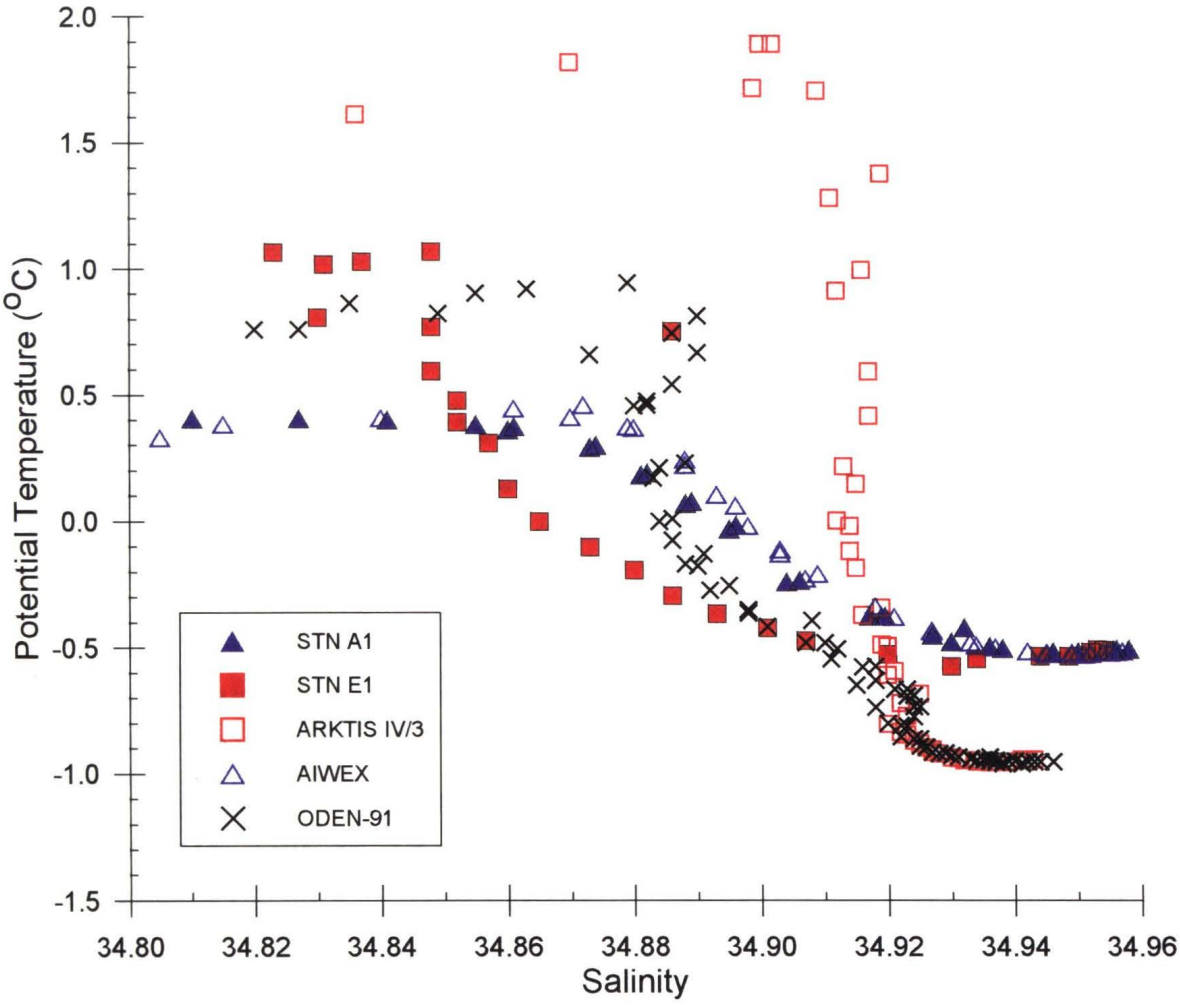
2.0
1.5
1.0
0.5
0.0
-0.5
-1.0
-1.5
Potential Temperature (°C)
34.80
34.82
34.84
34.86
34.88
34.90
34.92
34.94
34.96
Salinity
STN A1
STN E1
ARKTIS IV/3
AIWEX
ODEN-91

Plate 1c

addition, as Plate 1c suggests, the transition water of the EA assembly may be divided into Nansen and Amundsen Basin components; water in the Nansen Basin is warmer and more saline than that in the Amundsen Basin. Similarly, the transition water of the WA assembly may be divided into Makarov and Canada Basin components, the Makarov Basin being cooler and less saline than the Canada Basin.

At potential temperatures between 0.4°C and -0.4°C, water in the Makarov Basin (Station E1) is less saline than corresponding water in either the Nansen and Amundsen basins to the west or the Canada Basin to the east. This local minimum in salinity at salinities between S=34.84 and S=34.88 and depths between 600-1800 m implies an advective source of cold, relatively fresh shelf water from the Eurasian continental shelf, perhaps either the Laptev or East Siberian seas. Also, this relatively fresh deep water does not appear to influence the more saline deep waters of the Canada Basin, and may circulate within the Makarov Basin.

The final layer in both assemblies is deep water where distinctions between the EA and WA assemblies are also evident. Deep waters of the WA assembly are warmer ($-0.4 < °C < -0.5$) and more saline (S=34.96) than those of the EA assembly ($-0.8 < °C < -0.9$; S=34.94).

From the above description of the two water mass assemblies and a comparison of the **Larsen-93** stations in Plates 1a-1c, it is apparent that Station A1 in the Canada Basin has characteristics exclusively belonging to the WA assembly. Station E1 in the Makarov Basin, however, lacks Pacific influence in the upper layer, exhibits a steeper $\Delta\Theta/\Delta S$ slope, and reveals a warmer Atlantic layer, all of which are characteristic of the EA assembly. The lower transitional zone between the Atlantic and deep layers is fresher than either the Eurasian and Canada basins and is

suggestive of local, shelf-modified inputs. However, water below 2000 m, the approximate sill depth of the Lomonosov Ridge, clearly shows WA assembly characteristics. The presence of the two distinct assemblies in the Canadian Basin, the WA at Station A1 and the EA at Station E1, points to a front located between these two stations. This Atlantic/Pacific front is marked by a relocation of EA assembly eastward into the Canadian Basin to at least the deep layer, and a corresponding westward displacement of Pacific water.

3.3.2 Geochemical Correlation Diagrams

The Atlantic/Pacific boundary may be further characterized by examining geochemical data. Silicate, nitrate, phosphate, oxygen, NO,and NO/PO are examined to define characteristics of the two water mass assemblies. Stations A1 and E1, shown earlier to represent the two assemblies, are used to define the geochemical characteristics of the WA and EA assemblies, respectively.

Three property-property diagrams (Plates 2a-2c) illustrate silicate, nitrate, and phosphate plotted against salinity. At Station A1, all three nutrients are low in near-surface waters due to biological uptake. They increase to a mid-depth maximum in the middle region of the halocline due to the presence of nutrient-rich Pacific origin water (S=33.1), and then decrease to a minimum in the Atlantic layer due to low nutrient Atlantic origin water (S=34.8 to S=34.9). Finally, nutrients increase through the lower transition zone to a local maximum in the deep layer. At Station E1, however, the lack of a nutrient maximum reflects the absence of Pacific origin waters within the entire halocline; not only are there differences at salinities near S=33.1 but also at salinities near S=34.4.

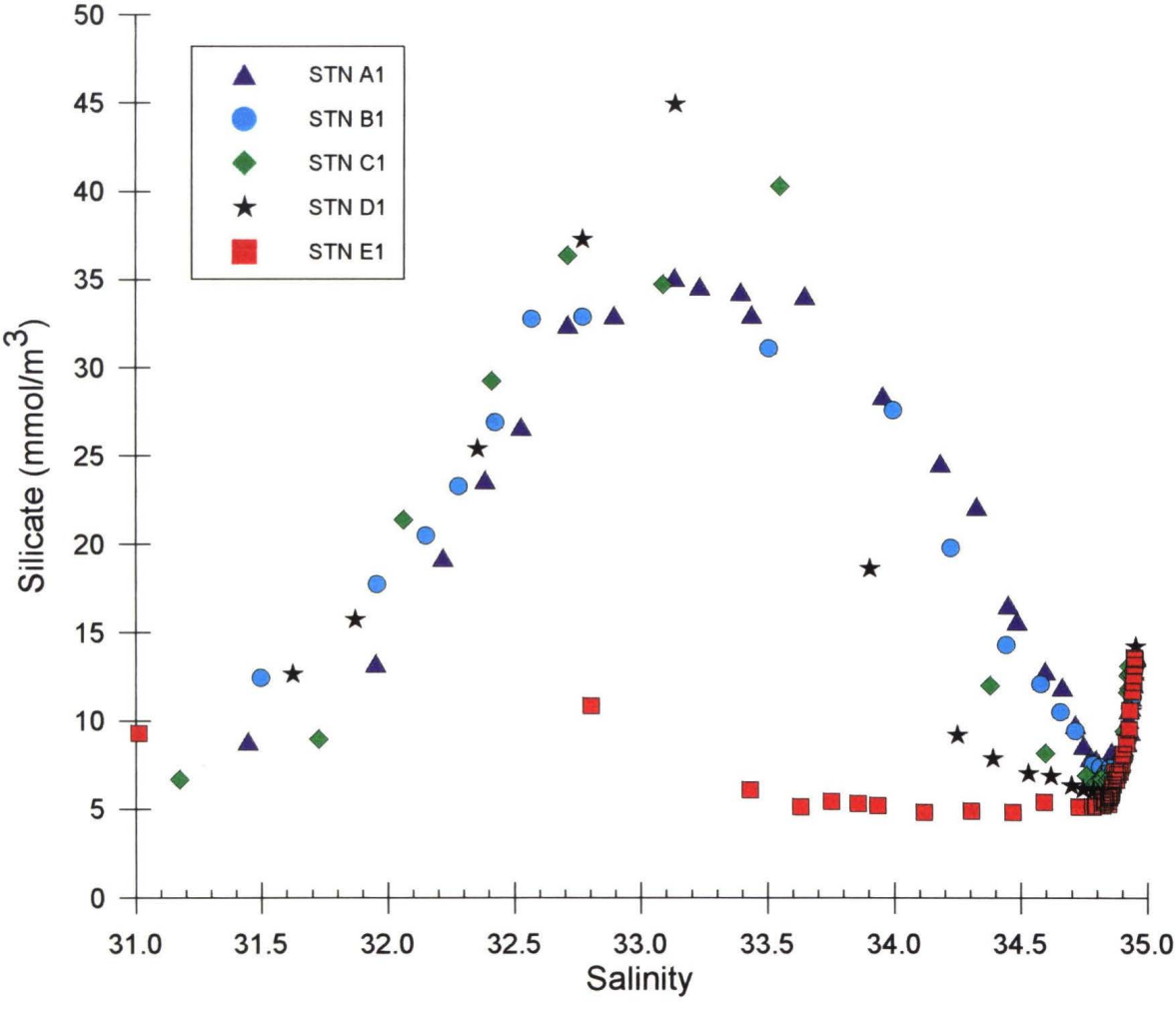
STN A1
STN B1
STN C1
STN D1
STN E1
Silicate (mmol/m3)
Salinity
0
5
10
15
20
25
30
35
40
45
50
31.0
31.5
32.0
32.5
33.0
33.5
34.0
34.5
35.0

Plate 2a

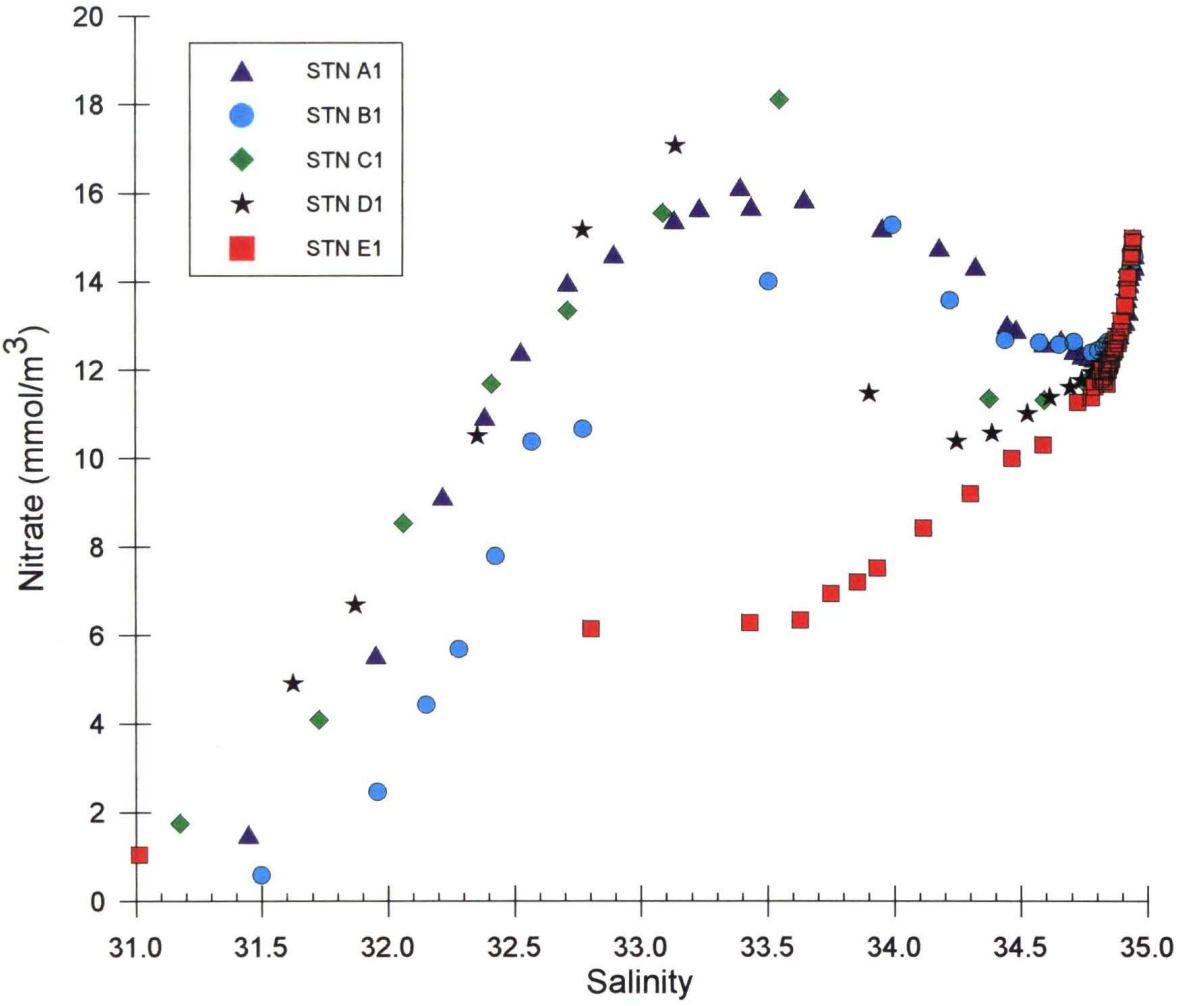
STN A1
STN B1
STN C1
STN D1
STN E1
Nitrate (mmol/m3)
Salinity
0
2
4
6
8
10
12
14
16
18
20
31.0
31.5
32.0
32.5
33.0
33.5
34.0
34.5
35.0

Plate 2b

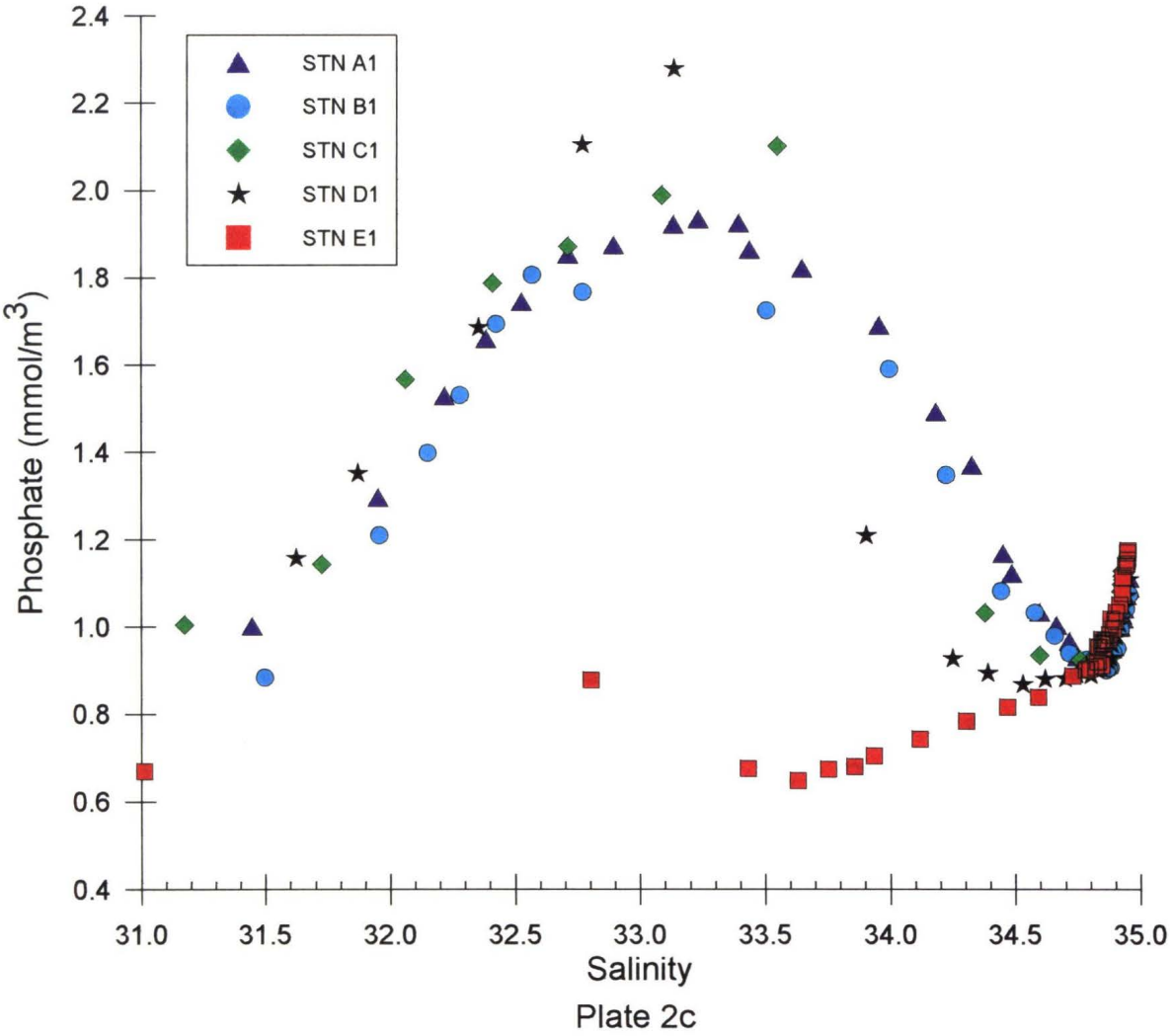
STN A1
STN B1
STN C1
STN D1
STN E1
Phosphate (mmol/m3)
2.4
2.2
2.0
1.8
1.6
1.4
1.2
1.0
0.8
0.6
0.4
31.0
31.5
32.0
32.5
33.0
33.5
34.0
34.5
35.0
Salinity

Plate 2c

Shelf inputs are suggested by a comparison of silicate data obtained in the Nansen Basin with two regions of the water mass assembly at Station E1 in the Makarov Basin (Figure 2). The first is the occurrence of higher silicate at salinities between S=33.6 and S=34 at Station E1 and may be due to input from the Siberian shelves as proposed by Jones and Anderson (1986) and Wilson and Wallace (1990). The second difference is in the lower thermocline transition zone between S=34.84 and S=34.9, where silicate levels at a given salinity are higher at Station E1 than in the Nansen Basin. A shelf source, contributing silicate to this transition zone, corroborates the interpretation of the Θ/S plot (Plate 1c) which proposed an advective source of cold, relatively fresh shelf water from the Laptev or East Siberian seas.

The oxygen-salinity diagram (Plate 3) similarly characterizes the two water mass assemblies at Stations A1 and E1. At Station A1, there are high oxygen levels in surface waters due to air/sea exchange. Oxygen then decreases rapidly to salinities near S=33.1 (corresponding to the nutrient maximum of Pacific origin waters), remains relatively constant to salinities near S=33.8, and decreases to a minimum at salinities near S=34.3. Oxygen then increases to a local maximum near the core of the Atlantic layer and decreases through the lower transition zone to a minimum at depth. At Station E1, oxygen shows similar high levels in the near surface, decreases to a local minimum in the lower halocline at S=34.7, increases slightly in the Atlantic layer, then decreases to a minimum in the deep layer. Unlike Station A1, the oxygen minimum at Station E1 is not a pronounced feature. The decrease from surface waters to the minimum at Station A1 is about 120 mmol m^{-3}, in contrast to a decrease of 45 mmol m^{-3} at Station E1. Similarly, the increase between the lower halocline and the

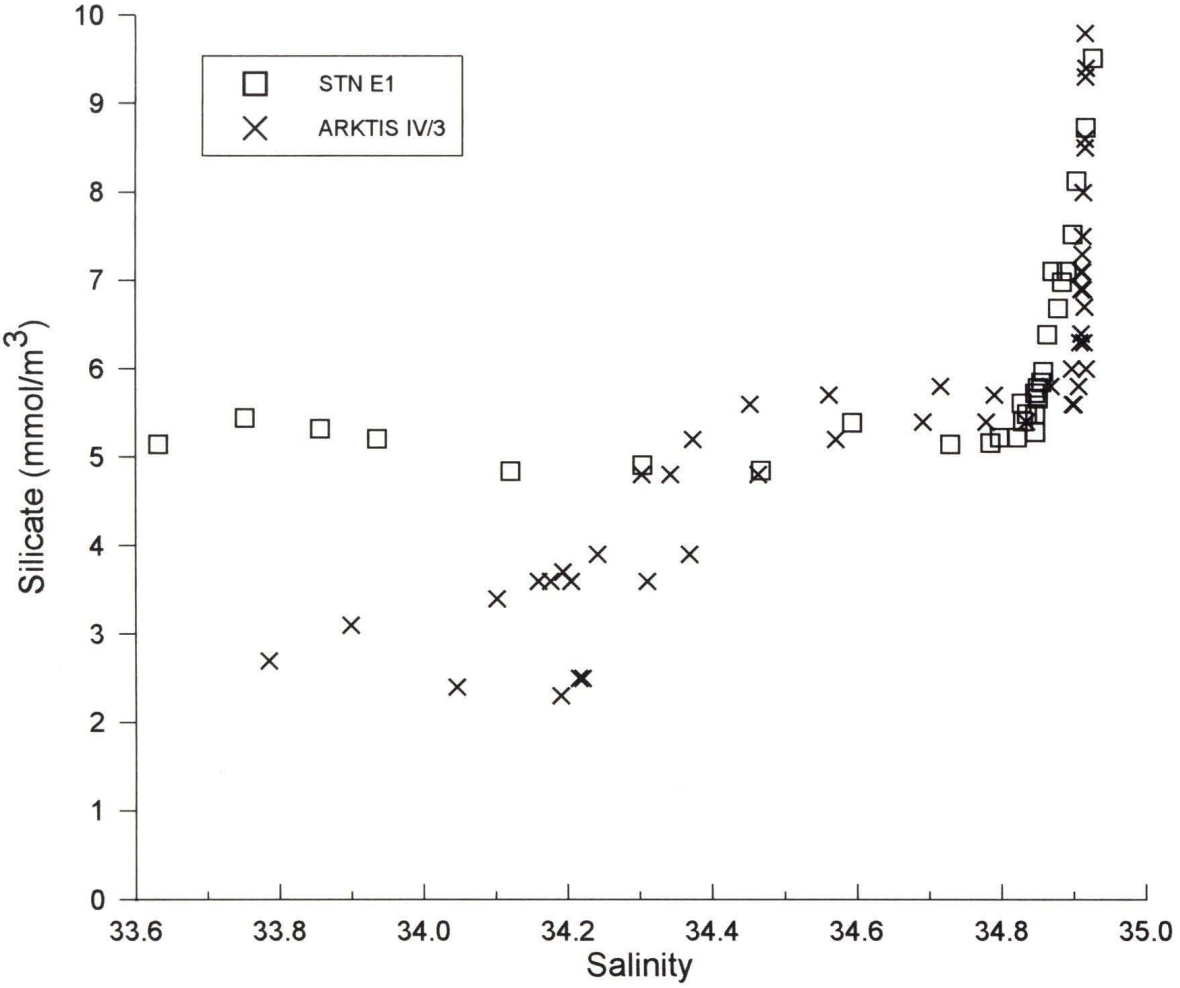
STN E1
ARKTIS IV/3
Silicate (mmol/m3)
Salinity
0
1
2
3
4
5
6
7
8
9
10
33.6
33.8
34.0
34.2
34.4
34.6
34.8
35.0

Figure 2

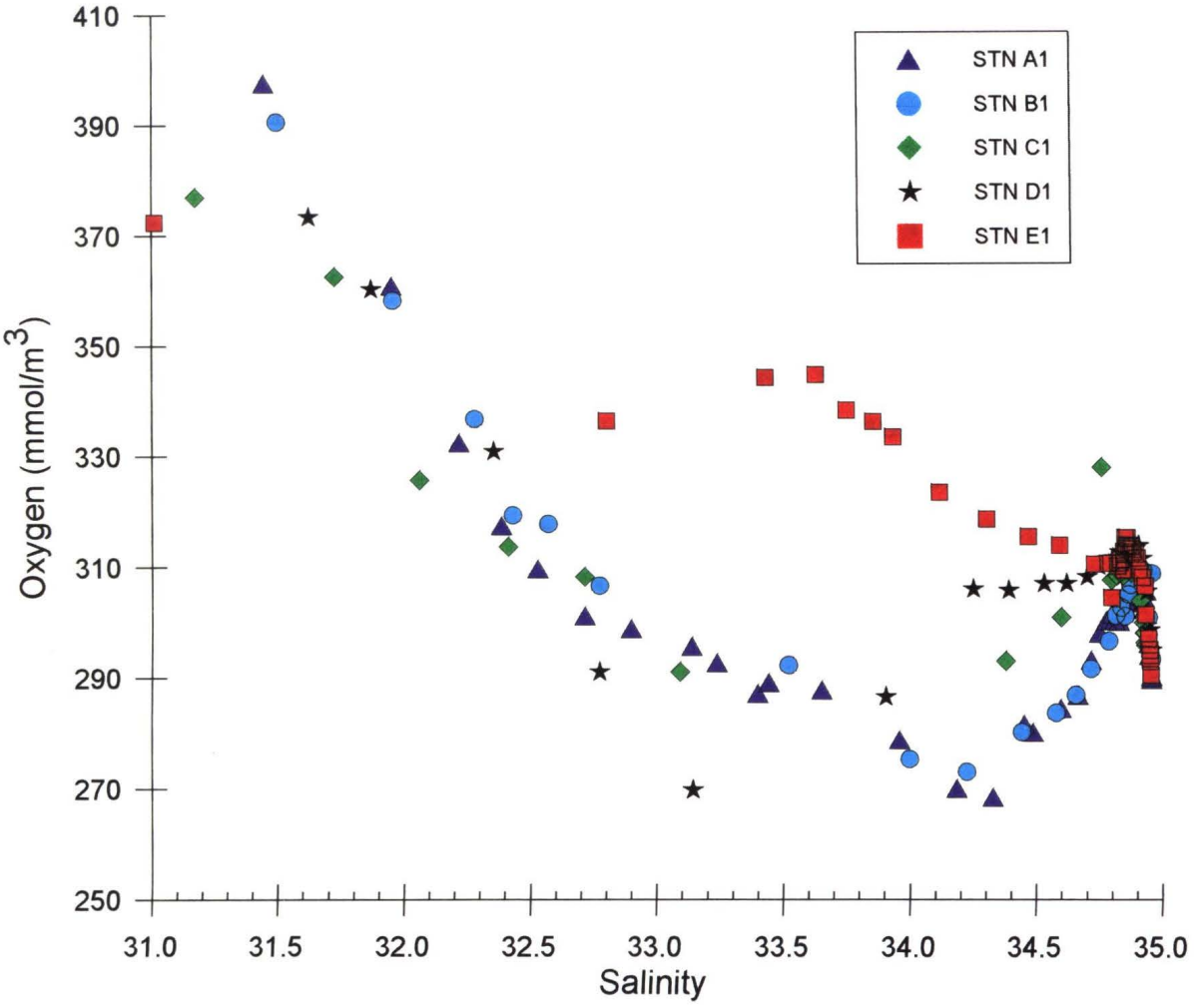
410
390
370
350
330
310
290
270
250
Oxygen (mmol/m3)
31.0
31.5
32.0
32.5
33.0
33.5
34.0
34.5
35.0
Salinity
STN A1
STN B1
STN C1
STN D1
STN E1

Plate 3

Atlantic layer is 35 mmol m^{-3} at Station A1, compared to 3 mmol m^{-3} at Station E1. The major difference between these two stations is again due to either the presence or absence of Pacific origin waters. The low oxygen found in the halocline of the WA assembly near S=33.1 at Station A1 may be explained by the depletion of oxygen in Pacific origin waters as they transit the highly productive Chukchi shelf. Oxygen then decreases further to a minimum at salinities near S=34.3, suggesting an additional shelf-derived water mass in the lower region of the WA assembly halocline, as noted in the Θ/S discussion.

The plot of NO versus salinity (Plate 4) again shows differences between WA and EA assemblies in the entire halocline region. At Station A1, NO increases to a maximum of 430 mmol m^{-3} in the WA assembly near S=33.2, decreases to a minimum of 395 mmol m^{-3} between S=34.3 and S=34.5, then increases to high levels in the Atlantic layer. At Station E1, NO increases to a maximum of 400 mmol m^{-3} at S=33.6, decreases slightly to a minimum of 399 mmol m^{-3} near S=34.2, then increases to high Atlantic layer levels. Three distinctions between the assemblies are evident: (1) the salinity at which the minimum occurs (S=34.3 to S=34.5 in the WA assembly and S=34.2 in the EA assembly), (2) the silicate concentrations at these salinities (near 20 mmol m^{-3} in the WA assembly and 7 mmol m^{-3} in the EA assembly), and (3) a small difference in the NO minimum (395 mmol m^{-3} in the WA assembly versus 399 mmol m^{-3} in the EA assembly). These differences are due to the presence of Pacific origin waters at Station A1 and the absence of Pacific origin waters by Atlantic origin waters at Station E1. Jones and Anderson (1986) proposed that low NO waters in the lower region of the halocline originate in the Barents and Kara seas. That NO values are lower in the WA assembly than in the EA assembly, where the signal is presumed to originate, is

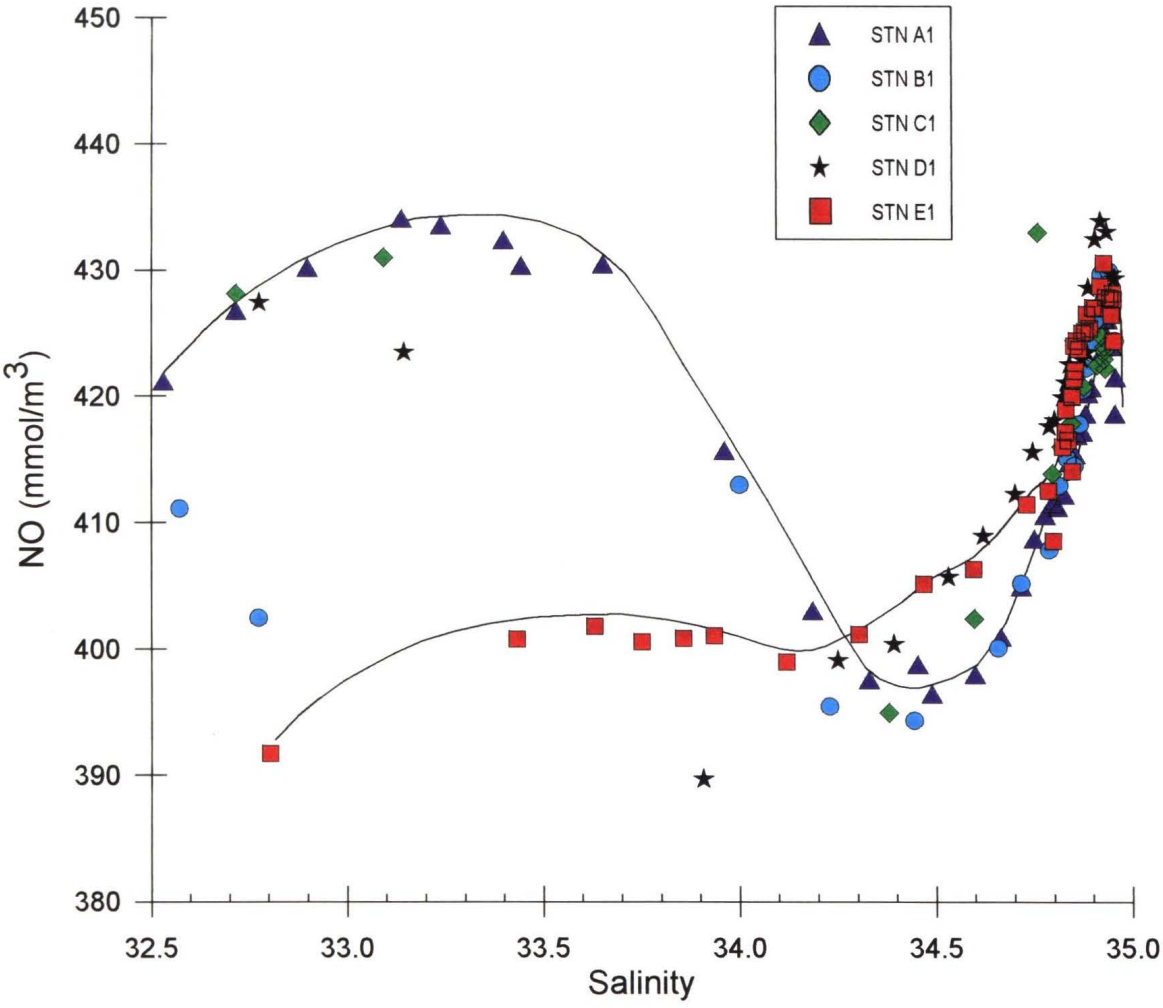
STN A1
STN B1
STN C1
STN D1
STN E1
NO (mmol/m3)
450
440
430
420
410
400
390
380
32.5
33.0
33.5
34.0
34.5
35.0
Salinity

Plate 4

seemingly at odds with this hypothesis. Although both assemblies have a low NO signal at the base of the upper layer, it is clear that the low NO water in the WA assembly is not purely of Barents and Kara sea origin but rather has been further modified. Salmon and McRoy (1994) reexamined historical data noting an inhomogeneity in the silicate levels in the lower region of the central Arctic halocline and concluded that the low NO waters in the Canada Basin are different. They named this water Canada Lower Halocline Water and suggested the process of interleaving Chukchi Sea water during winter with Barents and Kara Sea low NO water could produce this water. The source of the low NO in the lower region of the halocline in the WA assembly is unclear (cf. Rudels et al., 1991) and awaits wintertime measurements of these properties along the Eurasian shelves.

The last geochemical property to characterize the features of the two Arctic assemblies is the NO/PO ratio, used by Wilson and Wallace (1990) to identify shelf water sources (where $PO=135PO_4+O_2$ as defined by Broecker (1974)). They concluded that shelf seas have distinct NO/PO ratios: the Barents Sea ratio=1.0, Laptev Sea ratio=0.90-0.95, East Siberian Sea ratio=0.65-0.75, and Chukchi Sea ratio=0.75-0.85. As shown in Plate 5, the NO/PO ratio in the top 30 m at Station E1 is 0.84, indicative of Chukchi Sea shelf inputs in the mixed layer. This is evidence of the displacement of Pacific origin waters, for example, the top 30 m is the only remnant of Pacific origin water, the remainder having been replaced by waters of Atlantic origin. Deeper in the water column at Station E1, at salinities S=33.5, the ratio is about 0.93, implying an Atlantic/Barents/Laptev sea influence. In contrast, the NO/PO ratio at Station A1 is about 0.78 at salinities S=31 to S=33.5, demonstrating a Pacific/Chukchi sea influence. In the lower region of the halocline there continue to be

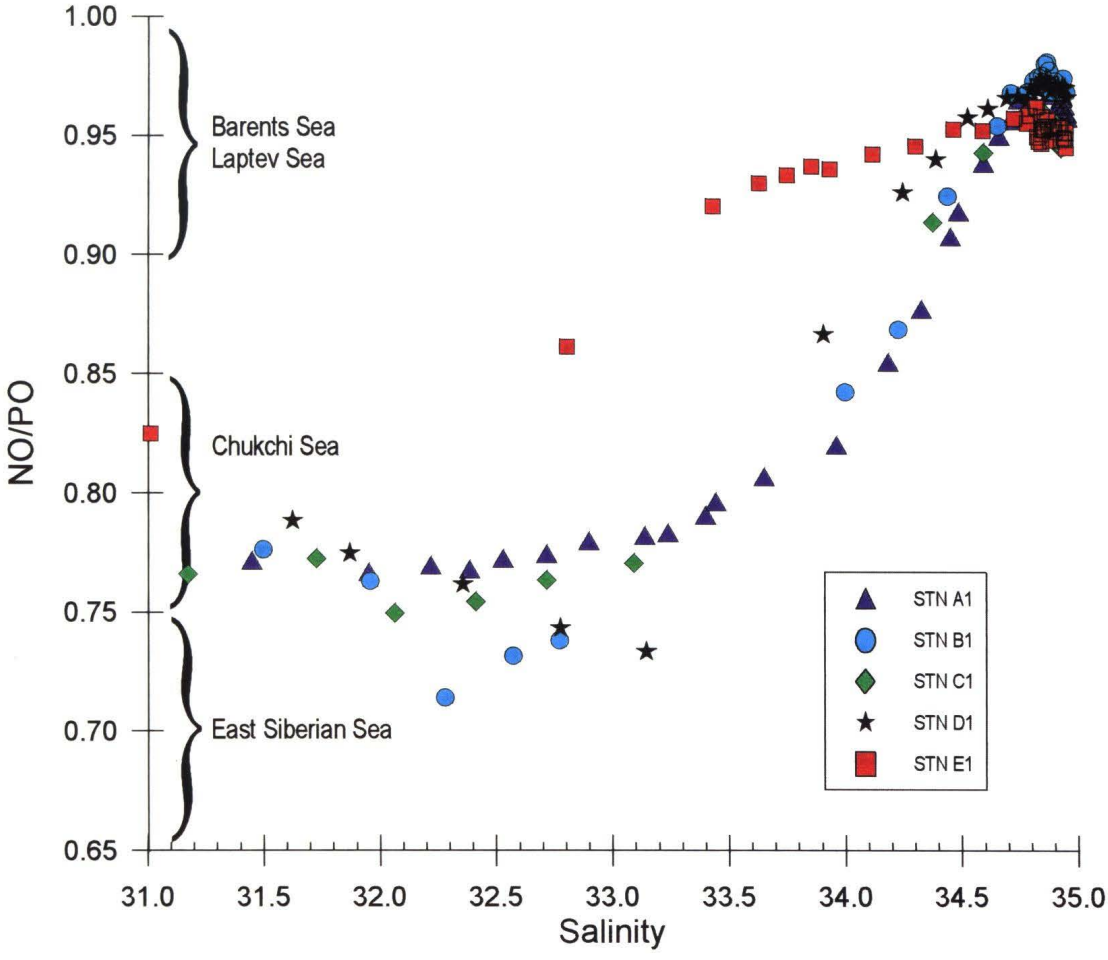
1.00
0.95
0.90
0.85
0.80
0.75
0.70
0.65
NO/PO
Barents Sea
Laptev Sea
Chukchi Sea
East Siberian Sea
STN A1
STN B1
STN C1
STN D1
STN E1
31.0
31.5
32.0
32.5
33.0
33.5
34.0
34.5
35.0
Salinity

Plate 5

differences in the NO/PO ratios of the EA and WA assemblies: at Station E1 at S=34.2 the ratio is 0.94; while at Station A1 at S=34.3 the ratio is 0.88. These ratios imply that these waters have related but different mixing histories. Although the lower region of the halocline in both EA and WA assemblies may originate in the Barents/Laptev seas, there must be further modification of the WA assembly water to account for the lower ratio and different geochemical properties. Mixing with waters from the Chukchi and East Siberian seas would reduce the NO/PO ratio and also contribute levels of silicate, both of which are consistent with **Larsen-93** measurements.

Property-property correlation diagrams further suggest that the Atlantic/Pacific front is not a vertical boundary, but is, instead, offset laterally with depth as seen by changes in the lower region of the halocline. For all water column properties within the halocline and Atlantic layers, Stations A1 and E1 represent "pure" assembly end-members. Stations C1 and D1, however, midway between the two, exhibit some properties of both end-members. Moving from Station A1 across the Atlantic/Pacific front toward Station E1, the Pacific influence is reduced to progressively shallower depths. For example, curves of $Si(OH)_4/S$, NO_3/S, and O_2/S from Station C1 follow those of Station A1 from the surface down to about S=33.8 (corresponding to a depth about 160 m). At this point, there is a break and, from S=34.4 onward (corresponding to a depth of 210 m), the curve then begins to mimic Station E1. Likewise, Station D1 follows Station A1 from the surface to about S=33.5 (about 100 m), and thereafter follows Station E1.

3.3.3 Vertical Sections

Vertical sections illustrate the lateral gradients of

the boundary between the two water mass assemblies. The salinity section (Figure 3) shows the presence of fresher surface water at Stations A1 and B1, a reflection of the Mackenzie River outflow. The isolines here show stratification throughout the water column. However, between Stations D1 and E1 the isolines in the salinity section are sloped, most strongly between S=34.8 and S=34.9 from 200 to 1200 m in the water column. This gradient region, beginning weakly at Station C1 suggests the presence of the Atlantic/Pacific boundary.

The potential temperature section (Figure 4) shows, on the Canada Basin side of the section, a warm surface mixed layer and a distinct upper halocline layer of cold (-1.4°C) water extending between Stations D1 to A1 from 70 to 175 m. This is Pacific origin water which enters via Herald Canyon. However, two different features are illustrated at Station E1; first, in the upper halocline waters, there is a layer of cold (-1.8°C) water between 30 and 80 m and second, there is a layer of warm (>1.0°C) Atlantic water between 200 and 600 m which extends toward but does not reach Station D1. The temperature maximum at Station E1 is shallower (near 220 m) than that at Station A1 (near 450 m); above the core of the Atlantic layer isotherms are strongly sloped as a result of this front.

The vertical section of silicate (Figure 5) shows Pacific origin water in the halocline of the WA assembly at Stations A1-D1. A silicate maximum is apparent from 50 to 150 m between Stations C1 and D1; these stations are downstream of the outflow of Pacific origin water. This core of high silicate extends beyond Station A1. At Station E1, in contrast, the silicate levels in the halocline of the EA assembly between 50 and 350 m are markedly lower (<5.5 mmol m^{-3}), with levels comparable to

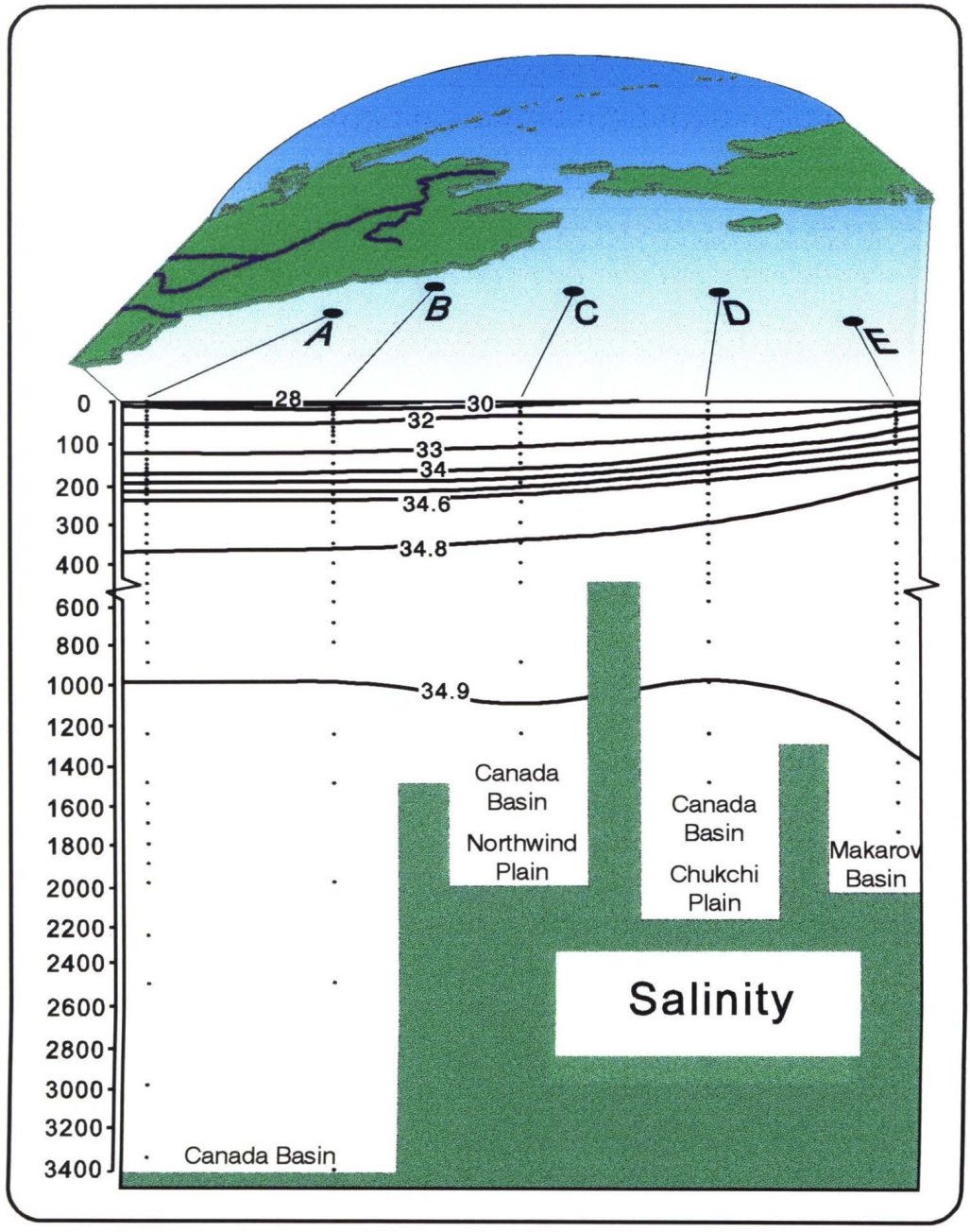
A
B
C
D
E
28
30
32
33
34
34.6
34.8
34.9
0
100
200
300
400
600
800
1000
1200
1400
1600
1800
2000
2200
2400
2600
2800
3000
3200
3400
Canada Basin
Northwind Plain
Canada Basin
Chukchi Plain
Makarov Basin
Salinity
Canada Basin

Figure 3

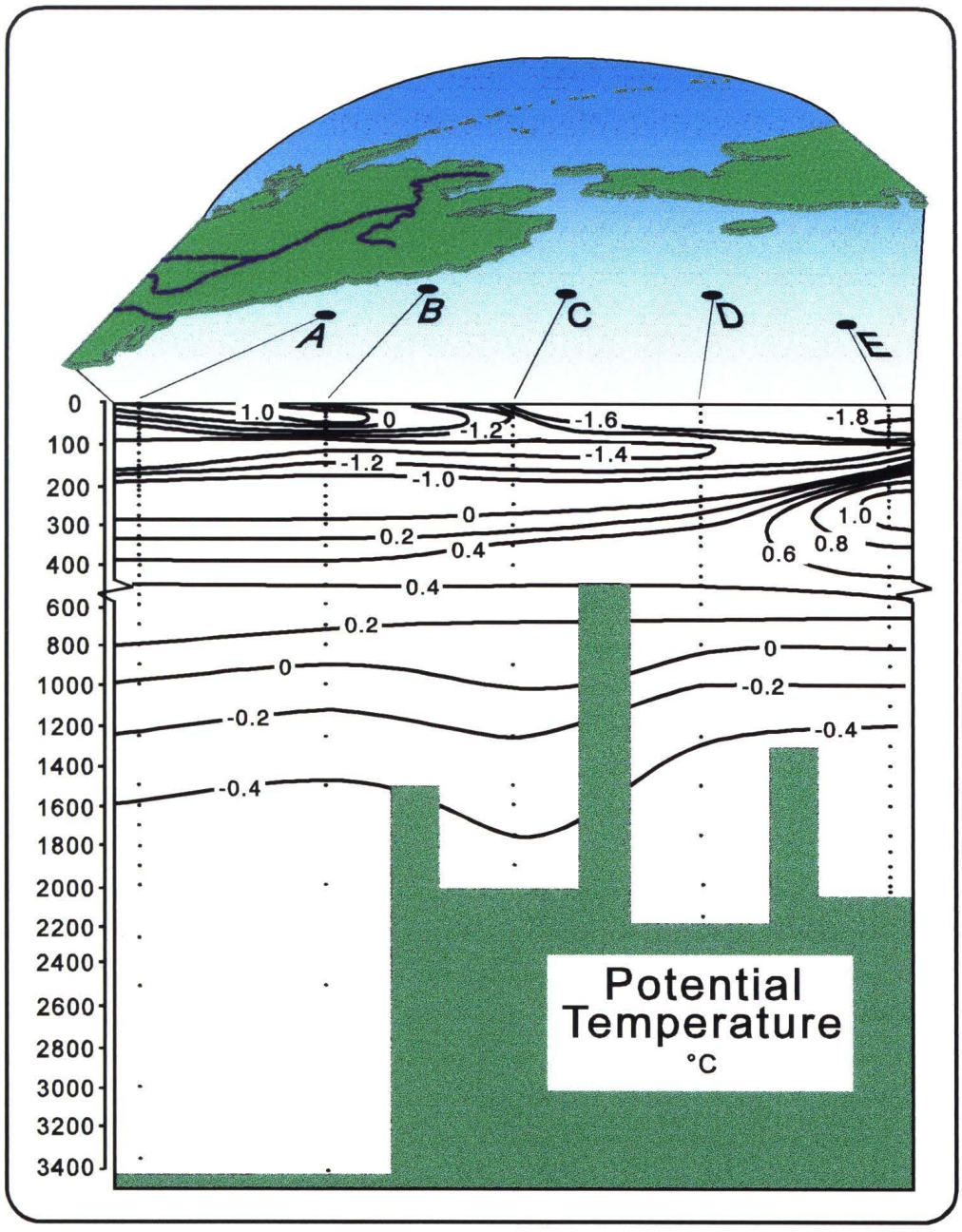
A
B
C
D
E
0
100
200
300
400
600
800
1000
1200
1400
1600
1800
2000
2200
2400
2600
2800
3000
3200
3400
1.0
0
-1.2
-1.6
-1.8
-1.4
-1.2
-1.0
0
0.2
0.4
0.4
0.2
0
-0.2
-0.4
1.0
0.8
0.6
0
-0.2
-0.4
Potential
Temperature
°C

Figure 4

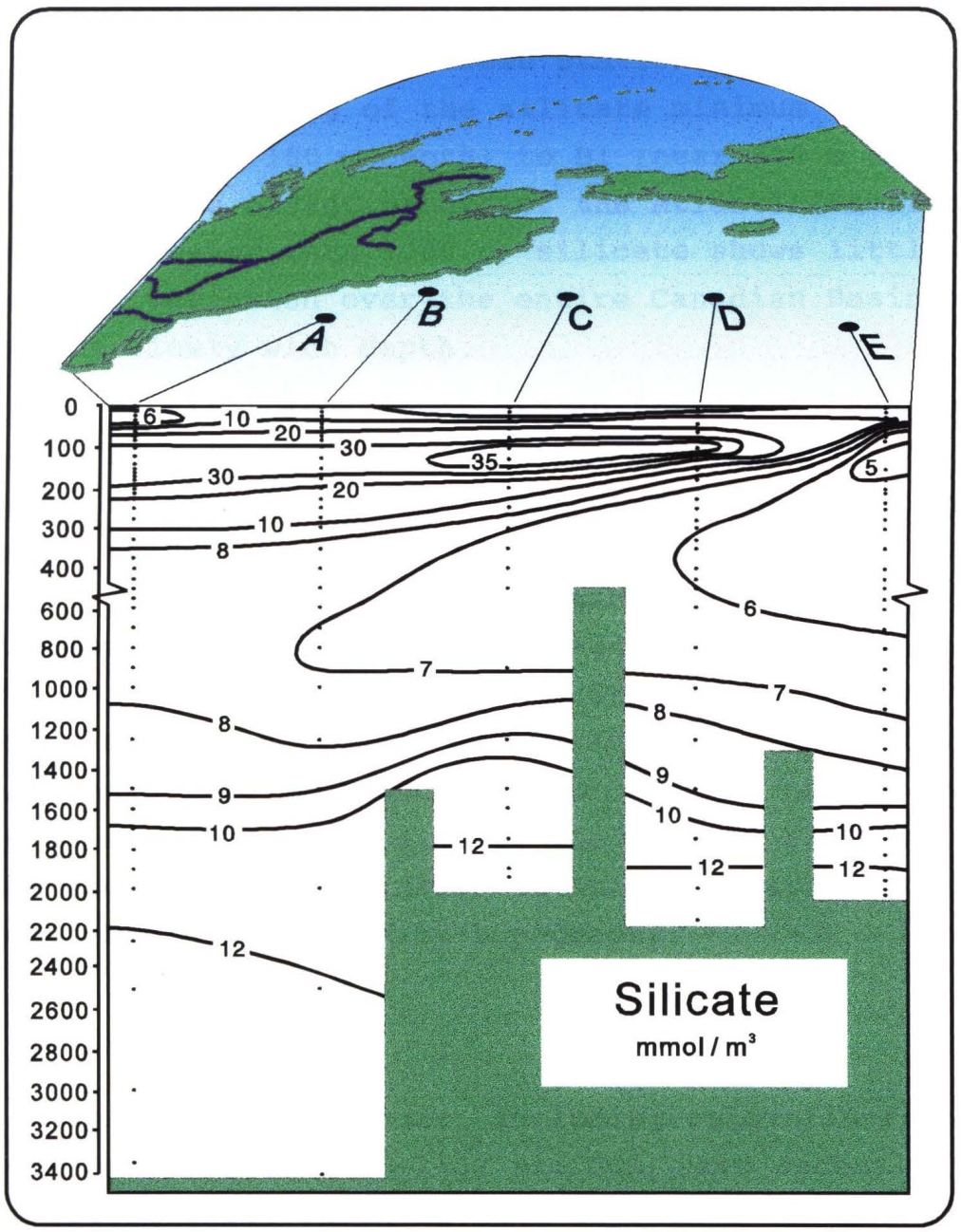
A
B
C
D
E
0
100
200
300
400
600
800
1000
1200
1400
1600
1800
2000
2200
2400
2600
2800
3000
3200
3400
6
10
20
30
35
5
Silicate
mmol / m³

Figure 5

those found in the Nansen Basin ($Si(OH)_4$=5.4 mmol m^{-3} at 190 m). Isolines at these depths between Stations E1 and D1 have significant lateral gradients, further confirmation of the presence of a front between Stations E1 and D1. The progressive deepening of the silicate minimum from Station E1 (near 160 m depth) to B1 (near 800 m depth) is evidence of the offset nature of the Atlantic/Pacific front. At depths greater than 1000 m, silicate shows little horizontal variation over the entire Canadian Basin and increases slowly with depth.

The vertical section of oxygen (Figure 6) confirms what has been seen in the other geochemical sections. At Station D1, from 50 to 150 m, low-oxygen Pacific origin water is evident extending eastward beyond Station A1. There is an oxygen minimum at Station A1 near 200 m (corresponding to salinity near S=34.4) in the lower region of the WA assembly halocline. At Station E1, a core of 310 mmol m^{-3} can be seen extending as far as Station D1 in the Atlantic layer between 300 and 1400 m. Oxygen levels are different on either side of the Chukchi Plateau, suggesting that the intrusion of Atlantic waters into the Canadian Basin is shaped by topography.

3.3.4 Ventilation

A suite of halocarbons, including chlorofluorocarbons (CFC-11, CFC-12, and CFC-113) and CCl_4 have recently demonstrated their value as time-dependent tracers of water mass circulation and processes that occur on decadal timescales (Gammon et al., 1982; Bullister and Weiss, 1983; Wisegarver and Gammon, 1988; Krysell and Wallace, 1988; Krysell, 1992). These compounds provide information spanning different timescales according to when these compounds first entered the atmosphere during this century.

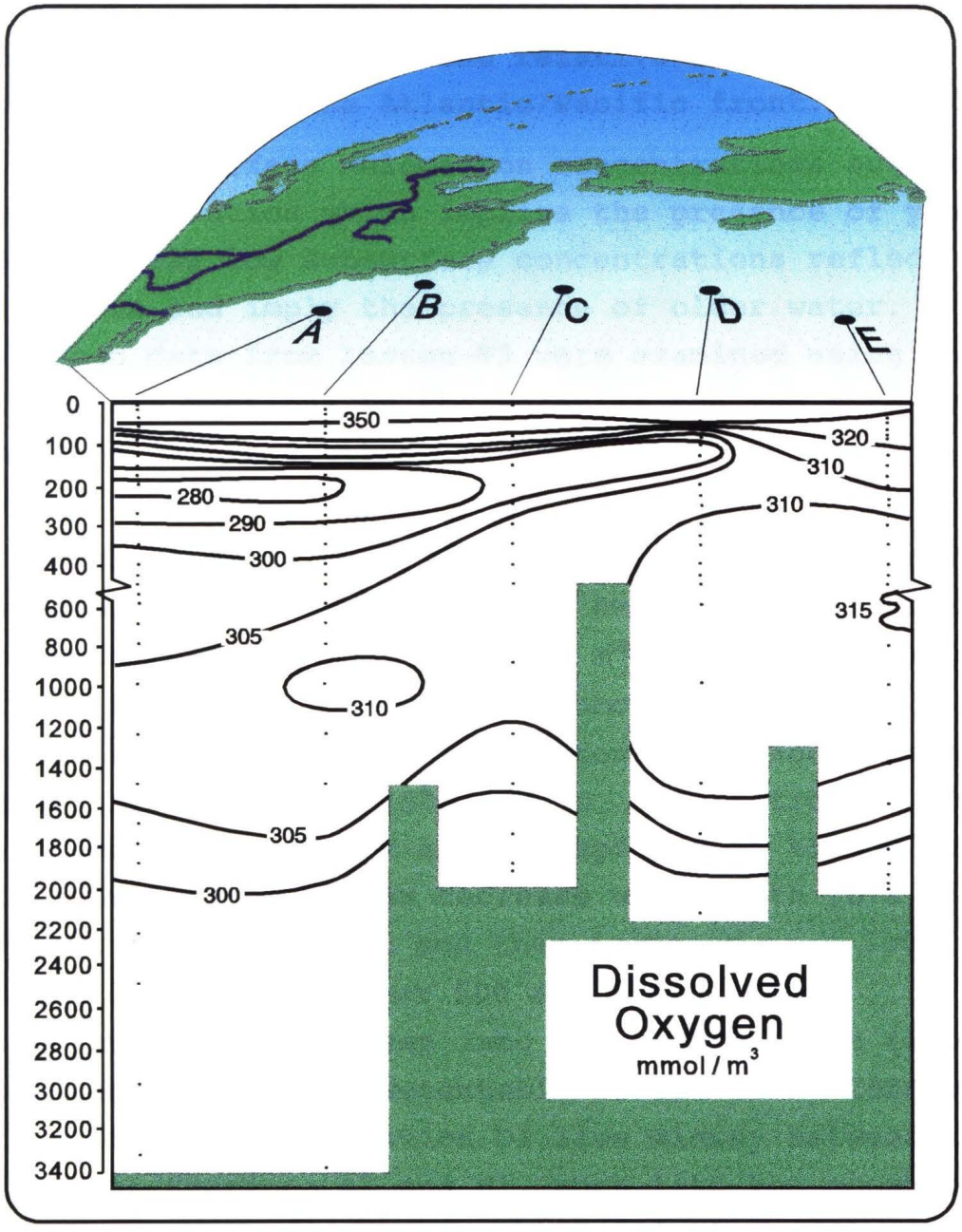
A
B
C
D
E
0
100
200
300
400
600
800
1000
1200
1400
1600
1800
2000
2200
2400
2600
2800
3000
3200
3400
350
320
310
280
290
310
300
315
305
310
305
300
Dissolved
Oxygen
mmol / m3

Figure 6

Although the quantitative interpretation of ventilation age is, in fact, model dependent (see Wallace et al. (1994), for discussion), we use the halocarbon distributions here to demonstrate qualitatively the relative difference in ventilation across the Atlantic/Pacific front.

High subsurface halocarbon concentrations suggest recent ventilation which implies the presence of young water, whereas low subsurface concentrations reflect slow ventilation and imply the presence of older water. Halocarbon data from **Larsen-93** were examined using vertical profiles and sections to characterize the two water mass assemblies in the southern Canadian Basin on this ventilation basis.

Vertical profiles of CFC-11 at Station A1 (Figure 7) show high surface levels (above 4 nmol m^{-3}) which decrease with depth to a minimum (1.7 nmol m^{-3}) near 200 m, and then increase to a local maximum (2.1 nmol m^{-3}) at 350 m. Below this depth, CFC-11 decreases monotonically and reaches undetectable levels at 1500-2000 m. At Station E1, however, CFC-11 levels are higher at all depths down to the detection limit. Subsurface values decrease with depth to a minimum (2.8 nmol m^{-3}) near 400 m and then increase to a local maximum (3.5 nmol m^{-3}) near 500 m. These higher concentrations extend deep into the water column (1600 m) before decreasing to undetectable levels below 2000 m. The profile of CFC-11 at Station D1 lies midway between the profiles at Stations A1 and E1, much like the geochemical property-property diagrams. The vertical profile of CCl_4 (not shown) illustrates the same features as those of CFC-11.

These measurements provide additional information about the two water mass assemblies characterized above. At Station A1 in the halocline at S=33.1 (near 140 m), the waters appear more ventilated than those at S=34.3 (near

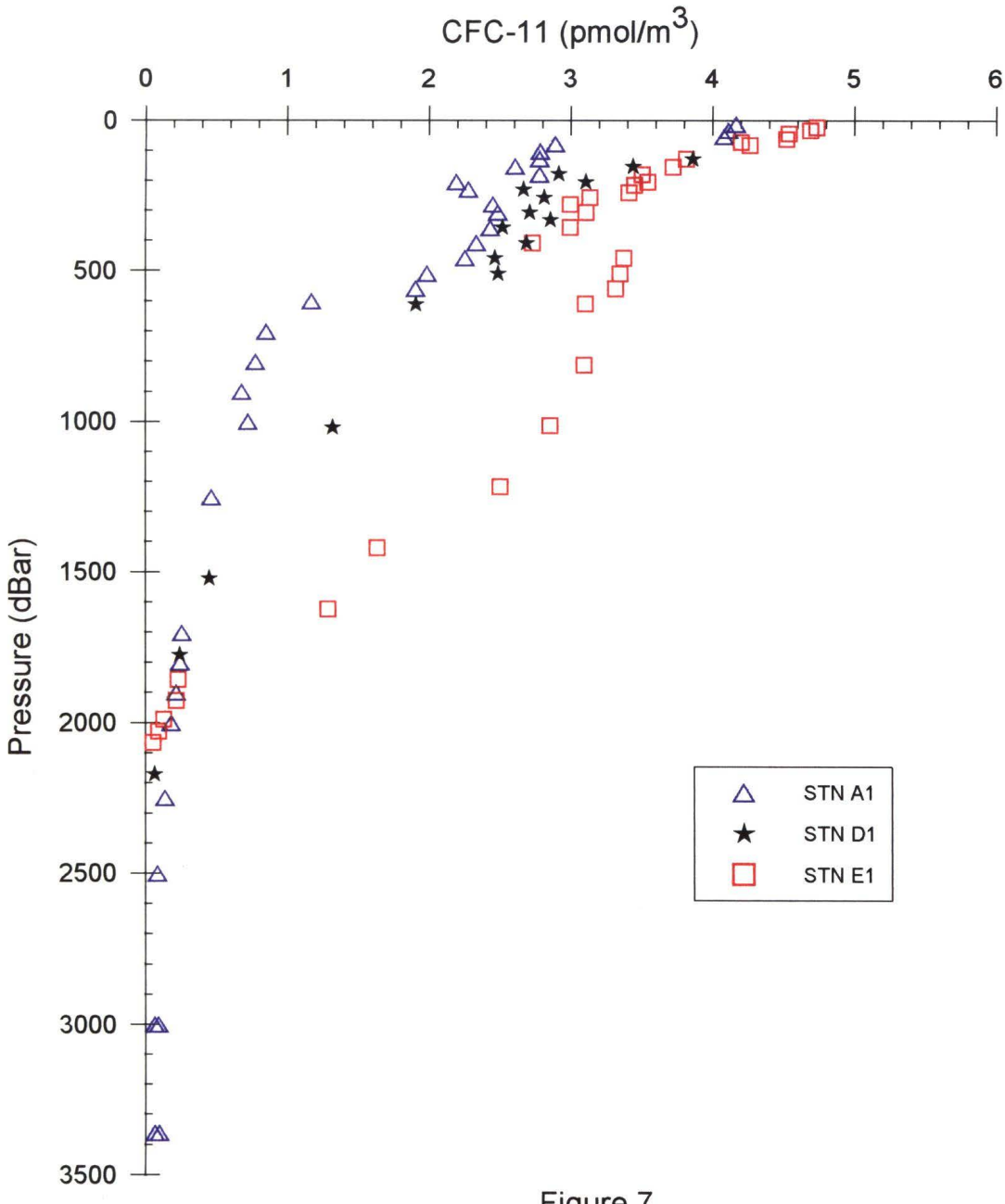
CFC-11 (pmol/m3)
0
1
2
3
4
5
6
0
500
1000
1500
2000
2500
3000
3500
Pressure (dBar)
STN A1
STN D1
STN E1

Figure 7

200 m). There is a subsurface maximum near 400 m at Station A1 corresponding to the Atlantic layer which indicates a ventilation age less than that of the overlying lower region of the WA assembly halocline. One explanation for this may be that the Atlantic layer here is renewed by relatively strong boundary currents. Note: the observed vertical CFC-11 structure (differences of order 0.6 nmol m^{-3}) cannot be accounted for by changes in the CFC-11 solubility of the initial source waters alone (of order 0.1 nmol m^{-3}).

The CFC-11 profiles illustrate two significant differences between Stations E1 and A1. First, CFC-11 levels are higher at the core of the Atlantic layer at Station E1 (3.4 nmol m^{-3} at about 250 m) than at Station A1 (2.1 nmol m^{-3} at 400 m), suggesting more recent ventilation. Second, the Station E1 local maximum at 500 m, and high values extending to about 1600 m, correspond to the lower transition zone between the Atlantic and deep layers. These higher CFC-11s, combined with the salinity and nutrient data discussed above, suggest the deep lateral transport of recently ventilated local shelf waters into the Makarov Basin. Altogether, waters of the EA assembly are more ventilated or younger than those of the WA. The midway character of the CFC-11s at Station D1 support the offset structure of the Atlantic/Pacific boundary described by the other geochemical data. In addition, the absence of CFC-11s at depths greater than 2000 m at Stations A1 and E1 suggest that these waters are older than a century and that the addition of ventilated waters to the deep layer has not occurred during this time.

The vertical section of CFC-11 (Figure 8) clearly illustrates the difference in penetration depth between Station E1 and Station A1. Following one isoline, at 2 nmol m^{-3} the penetration depth is 1200 m at Station E1 and 300 m at Station A1. CFC-11 appears to dome at Station C1,

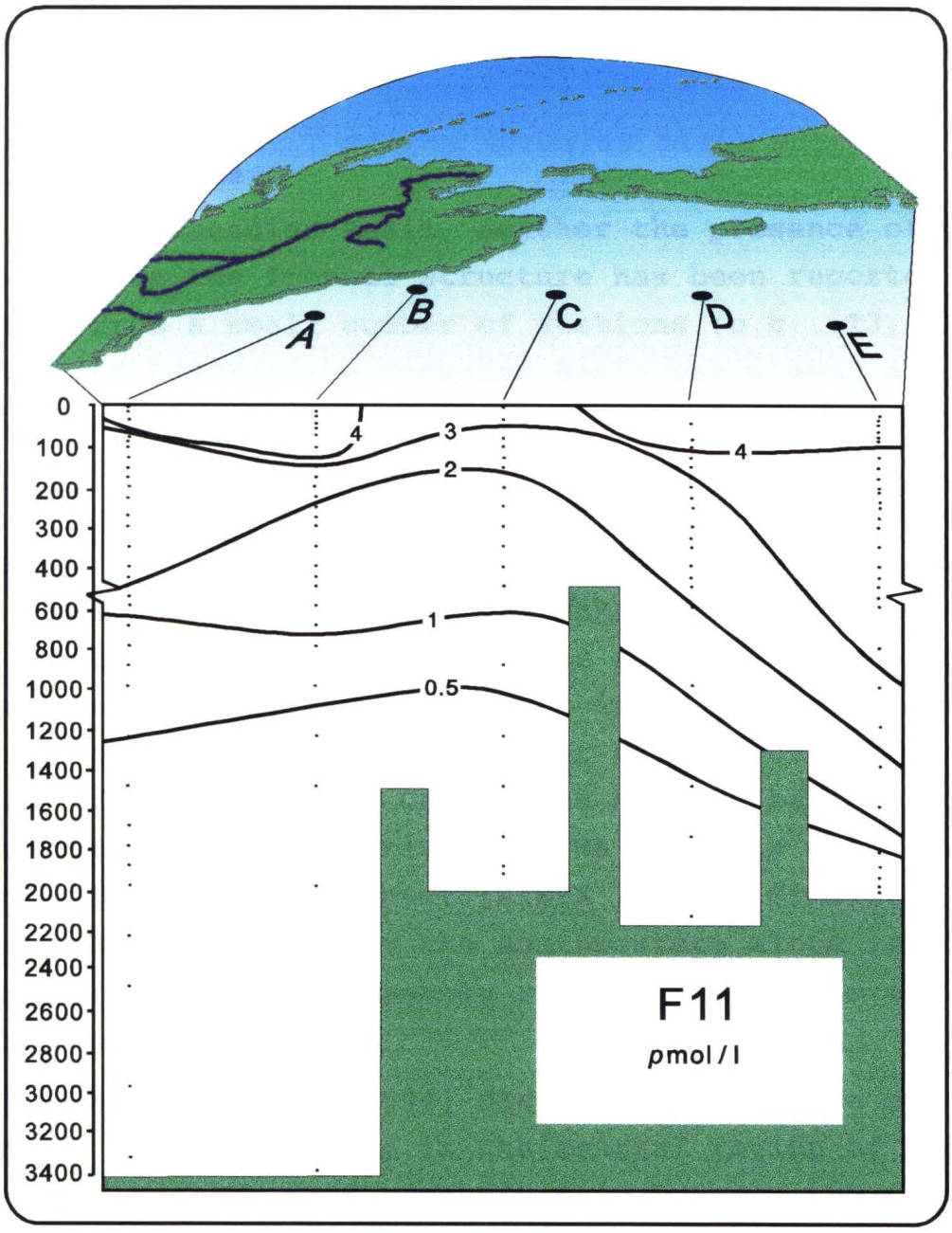
A
B
C
D
E
0
100
200
300
400
600
800
1000
1200
1400
1600
1800
2000
2200
2400
2600
2800
3000
3200
3400
4
3
2
1
0.5
4
F11
pmol / l

Figure 8

suggesting this water is not as well ventilated as water at adjacent stations. An explanation for this may be that waters here are isolated because of topographic influence on circulation, that is, flow around the Chukchi borderland.

3.4 Conclusions

In the Canadian Basin, neither the presence of the EA assembly nor the frontal structure has been reported. Based on data from a small number of stations (e.g., T3, AIWEX, CESAR, and LOREX), the Canadian Basin was viewed as a horizontally uniform domain, with no significant differences between the Canada and Makarov basins (Jones et al., 1990; A.F. Treshnikov, unpublished manuscript, 1959). Here, however, Θ/S plots from **Larsen-93** show a similarity between the waters at Station E1 in the Makarov Basin and those from the Nansen and Amundsen basins, as well as a difference between Station E1 and Station A1 in the Canada Basin. Using geochemical data, this paper demonstrates the distinct nature of waters in the Canada and Makarov basins. Canada Basin water is characteristic of WA assembly water, both now (**Larsen-93**) and in the past (AIWEX 1990). Similarly, Makarov Basin water from the southwestern slope is clearly characteristic of EA assembly water, at least to the depth of the deep layer.

Anderson et al. (1994) discuss the presence of a front over the Lomonosov Ridge in the central region of the Arctic Ocean and suggest that communication between the Canadian and Eurasian basins occurs near their southern boundaries. Here **Larsen-93** data provide confirmation of such communication along the perimeters. However, in 1993, the Atlantic/Pacific boundary was located well within the Canadian Basin, over the Mendeleyev Ridge between the Makarov and Canada basins. The position of the

Atlantic/Pacific front within the water column, marked by large lateral property gradients, is not vertical but rather is offset with depth in the lower region of the halocline. CFC-11 data illustrate the enhanced ventilation in the waters at Station E1 suggesting a rapid exchange has occurred with waters of the Eurasian Basin entering the Makarov Basin.

Larsen-93 data suggest that the Alpha-Mendeleyev Ridge may play a more significant role in the circulation of waters within the Canadian Basin than previously believed. One possible circulation scheme (Plate 6) is that EA water enters the Canadian Basin by crossing the Lomonosov Ridge north of the Laptev Sea, as Rudels et al. (1994) proposed. Then, near the Laptev and East Siberian Seas, colder and somewhat fresher waters, produced on the shelves, sinks and intrudes into the transition zone beneath the Atlantic layer. This may explain the colder and fresher characteristics found in the transition water at Station E1. The modified EA water continues until the Alpha-Mendeleyev Ridge, where the assembly again bifurcates. One branch, turned by the Alpha-Mendeleyev Ridge, flows into the Makarov Basin, while the other branch continues along the continental margin over the Mendeleyev Ridge carrying the top 1200-1400 m of the EA.

In summary, the Atlantic/Pacific front is found where the water of Atlantic origin (EA) intersects with water of Pacific origin (WA). Historical data indicated a front located near the Lomonosov Ridge, while **Larsen-93** data imply a front located near the Alpha-Mendeleyev Ridge. In both cases the Atlantic/Pacific front appears to favor a position over ridge topography. The reason for the breakdown of frontal structure over one ridge, its reestablishment over another, and the attendant change in interbasin circulation requires further investigation.

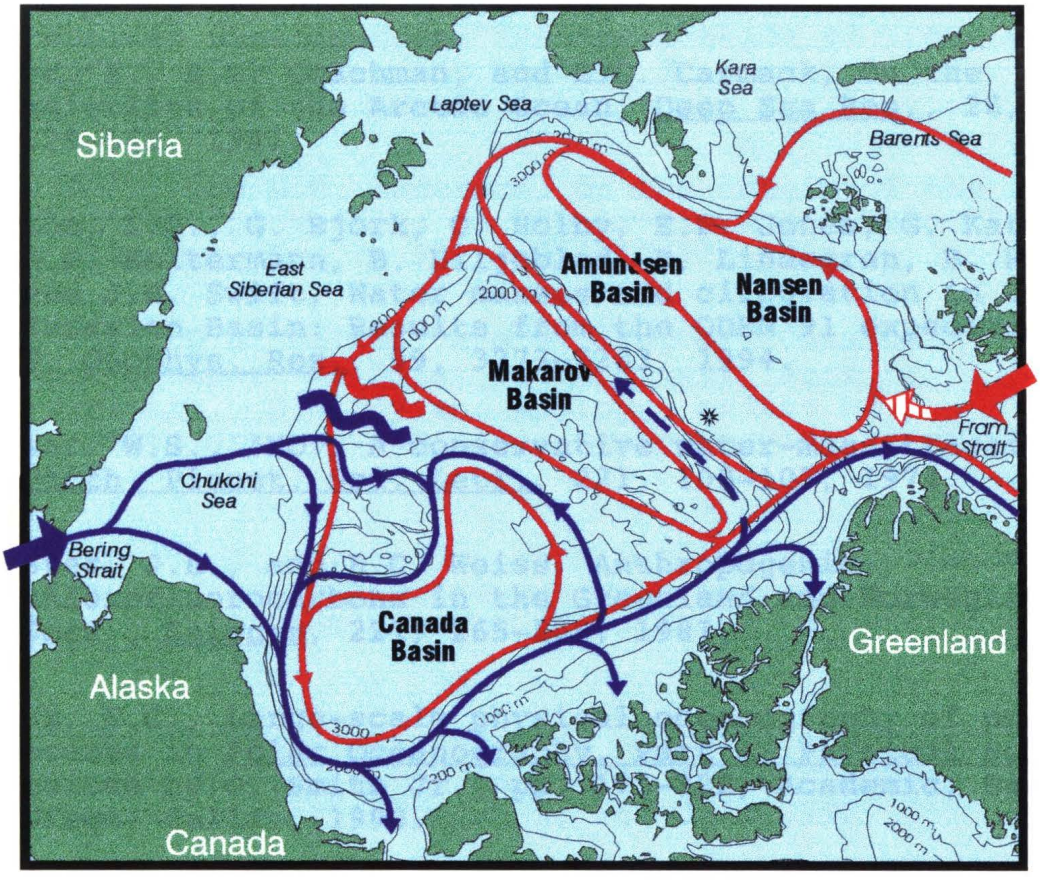
Siberia
Laptev Sea
Kara Sea
Barents Sea
East Siberian Sea
Amundsen Basin
Nansen Basin
Makarov Basin
Fram Strait
Chukchi Sea
Bering Strait
Canada Basin
Greenland
Alaska
Canada
3000 m
2000 m
1000 m
200 m

Plate 6

References:

Aagaard, K., A synthesis of the Arctic Ocean circulation, Rapp. P. V. Reun. Cons. Int. Explor. Mer Mediter., 188, 11-22, 1989.

Aagaard, K., and E.C. Carmack, The role of sea ice and other fresh water in the Arctic circulation, J. Geophys. Res., 94, 14485-14498, 1989.

Aagaard, K., L.K. Coachman, and E.C. Carmack, On the halocline of the Arctic Ocean, Deep Sea Res., 28, 529-545, 1981.

Anderson, L.G., G. Bjork, O. Holby, E.P. Jones, G. Kattner, K.P. Koltermann, B. Liljeblad, R. Lindegren, B. Rudels, and J.H. Swift, Water masses and circulation in the Eurasian Basin: Results from the ODEN 91 expedition, J. Geophys. Res., 99, 3273-3283, 1994.

Broecker, W.S., "NO", A conservative water-mass tracer, Earth Planet. Sci. Lett., 221, 100-107, 1974.

Bullister, J.L., and R.C. Weiss, Anthropogenic chlorofluorocarbons in the Greenland and Norwegian Seas, Science, 221, 265-268, 1983.

Carmack, E.C., Large-scale physical oceanography of polar oceans in Polar Oceanography, Part A: Physical Science, edited by O. Smith Jr., pp. 171-222, Academic, San Diego, Calif., 1990.

Cavalieri, D.J., and S. Martin, The contribution of Alaskan, Siberian, and Canadian coastal polynyas to the cold halocline layer of the Arctic Ocean, J. Geophys. Res., 99, 18343-18362, 1994.

Coachman, L.K., and K. Aagaard, Physical oceanography of Arctic and Subarctic seas in Marine Geology and Oceanography of the Arctic Seas, edited by Y. Herman, pp. 1-72, Springer-Verlag, New York, 1974.

Coachman, L.K., and C.A. Barnes, The contribution of Bering Sea water to the Arctic Ocean, Arctic, 14, 146-161, 1961.

Fofonoff, N.P., and R.C. Millard, Algorithms for computation of fundamental properties of seawater, UNESCO Tech. Pap. Mar. Sci., 44, 1983.

Foster, T.D., and E.C. Carmack, Temperature and salinity structure in the Weddell Sea, J. Phys. Oceanogr., 6, 36-44, 1976.

Gammon, R.H., J. Cline, and D. Wisegarver, Chlorofluoromethanes in the northeast Pacific Ocean: Measured vertical distributions and application as transient tracers of upper ocean mixing, J. Geophys. Res., 87, 9441-9454, 1982.

Jones, E.P., and L.G. Anderson, On the origin of the chemical properties of the Arctic Ocean halocline, J. Geophys. Res., 91, 10759-10767, 1986.

Jones, E.P., D.M. Nelson, and P. Treguer, Chemical oceanography, in Polar Oceanography, Part B: Chemistry, Biology and Geology, edited by O. Smith Jr., pp. 407-476, Academic, San Diego, Calif., 1990.

Jones, E.P., L.G. Anderson, and D.W.R. Wallace, Tracers of near-surface, halocline and deep waters in the Arctic Ocean: Implications for circulation, J. Mar. Syst., 2, 241-255, 1991.

Krysell, M., Carbon tetrachloride and methyl chloroform as tracers of deep water formation in the Weddell Sea, Antarctica, Mar. Chem., 39, 297-310, 1992.

Krysell, M., and D.W.R. Wallace, Arctic Ocean ventilation studied with a suite of anthropogenic halocarbon tracers, Science, 242, 746-749, 1988.

Macdonald, R.W., E.C. Carmack, and D.W.R. Wallace, Tritium and radiocarbon dating of Canada Basin deep waters, Science, 259, 103-104, 1993.

Macdonald, R.W., E.C. Carmack, R. Pearson, M. O'Brien, F.A. McLaughlin, J. Barwell-Clarke, D. Sieberg, D. Paton, and D. Tuele, NOGAP B.6, Physical and Chemical Data collected in the Beaufort, Chukchi and East Siberian Seas in August-September 1993, Can. Data Rep Hydrogr. and Ocean Sci., No. 139, Institute of Ocean Sciences, Sidney, B.C., Canada, 1995.

Melling, H., and E.L. Lewis, Shelf drainage flows in the Beaufort Sea and their effect on the Arctic Ocean pycnocline, Deep Sea Res., 29, 967-985, 1982.

Ostlund, H.G., The residence time of the fresh water component in the Arctic Ocean, J. Geophys. Res., 87, 2035-2043, 1982.

Rudels, B., A.M. Larsson, and P.I. Sehlstedt, Stratification and water mass formation in the Arctic Ocean: Some implications for the nutrient distribution, Polar Res., 10, 19-31, 1991.

Rudels, B., E.P. Jones, L.G. Anderson, and G. Kattner, On the intermediate depth waters of the Arctic Ocean, in The Polar Oceans and Their Role in Shaping the Global Environment: The Nansen Centennial Volume, Geophys. Monogr. Ser., 85, edited by O.M. Johannessen, R.D. Muench and J.E. Overland, pp. 33-46, AGU, washington, D.C., 1994.

Salmon, D.K., and C.P. McRoy, Nutrient-based tracers in the Western Arctic: A new lower halocline water defined, in The Polar Oceans and Their Role in Shaping the Global Environment: The Nansen Centennial Volume, Geophys. Monogr. Ser., 85, edited by O.M. Johannessen, R.D. Muench and J.E. Overland, pp. 47-61, AGU, Washington, D.C., 1994.

Schlosser, P., D. Bauch, R. Fairbanks, and G. Bonisch, Arctic river-runoff: Mean residence time on the shelves and in the halocline, Deep Sea Res., 41, 1053-1068, 1994.

Wallace, D.W.R., P. Beining, and A. Putzka, Carbon tetrachloride and chlorofluorocarbons in the south Atlantic Ocean, 19°S, J. Geophys. Res., 99, 7803-7819, 1994.

Wilson, C., and D.W.R. Wallace, Using the nutrient ratio NO/PO as a tracer of continental shelf waters in the central Arctic Ocean, J. Geophys. Res., 95, 22193-22208, 1990.

Wisegarver, D.P., and R.H. Gammon, A new transient tracer: Measured vertical distribution of CCl_2FCClF_2 (F-113) in the north Pacific subarctic gyre, Geophys. Res. Lett., 15, 188-191, 1988.

Chapter 4: Ventilation and Apparent Ages

This chapter first discusses how oceanographic halocarbon measurements have evolved, and describes the characteristics which qualify specific halocarbons as effective transient tracers. Following this, the method of determining apparent ages and dilution factors from water column measurements is presented, along with an examination of the uncertainties associated with these calculations. Finally, **Larsen-93** halocarbon data are presented and discussed to determine whether differences in ventilation exist between waters in the Canada and Makarov basins, waters shown in Chapter 3 to be situated on either side of the Atlantic/Pacific water mass boundary. Halocarbon profiles are analyzed to provide relative information about the ventilation of waters within the three main layers of both the WA and EA assemblies.

Apparent ages are calculated at five **Larsen-93** basin stations. Ages are first compared between and among the five stations and then compared to apparent age historical data from the Eurasian Basin. These comparisons are significant because apparent ages in the upper layer of the Canada and Makarov basins may yield information about shelf processes associated with halocline maintainance. Apparent ages of Atlantic and deep water layers may also suggest differences in ventilation between basins. Such information maybe used to verify ocean circulation models and in estimating rates of contaminant transport from shelves to basin interiors and between adjoining basins.

4.1 Halocarbon Histories

Since the early 1980s, chlorofluorocarbons (CFCs) CFC-11 and CFC-12 have been used to infer rates of subsurface circulation and mixing (Gammon et al., 1982; Bullister and Weiss, 1983; Wallace and Moore, 1985). Halocarbons enter the ocean via gas exchange at the surface where their equilibrium concentrations reflect their atmospheric concentration histories (Figure 1). When a parcel of water becomes isolated from the surface, it retains a halocarbon signature that is a function of both its partitioning according to Henry's Law and the atmospheric concentration present at the time it left the surface. Thus, when halocarbons are measured at depth, the halocarbon ratio reflects the year when the water parcel left the surface and, from this, its apparent age (or isolation age) can be determined.

With the recognition that CFCs threatened the ozone layer in the mid-1970s (Molina and Rowland, 1974), international regulations were introduced to limit CFC-11 and CFC-12 production (World Meteorological Organization (WMO), 1988). Consequently, the ratio between CFC-11 and CFC-12 in the atmosphere (Figure 2) has remained relatively constant since 1975, and the CFC-11/CFC-12 ratio cannot be used to resolve ages of waters younger than about 20 years old. This means that use of the CFC-11/CFC-12 ratio to estimate apparent ages is confined to a period from the mid-1940s, when their production began, to the mid-1970s, when their production was regulated.

To extend the range over which apparent ages can be determined, three additional halocarbons have been added recently as tracers; CFC-113, methyl chloroform (CH_3CCl_3) and carbon tetrachloride (CCl_4) (Wisegarver and Gammon, 1988; Krysell and Wallace, 1988). These halocarbons provide three additional time scales that correspond to their particular

4.1 Halocarbon Histories

Since the early 1980s, chlorofluorocarbons (CFCs) CFC-11 and CFC-12 have been used to infer rates of subsurface circulation and mixing (Gammon et al., 1982; Bullister and Weiss, 1983; Wallace and Moore, 1985). Halocarbons enter the ocean via gas exchange at the surface where their equilibrium concentrations reflect their atmospheric concentration histories (Figure 1). When a parcel of water becomes isolated from the surface, it retains a halocarbon signature that is a function of both its partitioning according to Henry's Law and the atmospheric concentration present at the time it left the surface. Thus, when halocarbons are measured at depth, the halocarbon ratio reflects the year when the water parcel left the surface and, from this, its apparent age (or isolation age) can be determined.

With the recognition that CFCs threatened the ozone layer in the mid-1970s (Molina and Rowland, 1974), international regulations were introduced to limit CFC-11 and CFC-12 production (World Meteorological Organization (WMO), 1988). Consequently, the ratio between CFC-11 and CFC-12 in the atmosphere (Figure 2) has remained relatively constant since 1975, and the CFC-11/CFC-12 ratio cannot be used to resolve ages of waters younger than about 20 years old. This means that use of the CFC-11/CFC-12 ratio to estimate apparent ages is confined to a period from the mid-1940s, when their production began, to the mid-1970s, when their production was regulated.

To extend the range over which apparent ages can be determined, three additional halocarbons have been added recently as tracers; CFC-113, methyl chloroform (CH_3CCl_3) and carbon tetrachloride (CCl_4) (Wisegarver and Gammon, 1988; Krysell and Wallace, 1988). These halocarbons provide three additional time scales that correspond to their particular

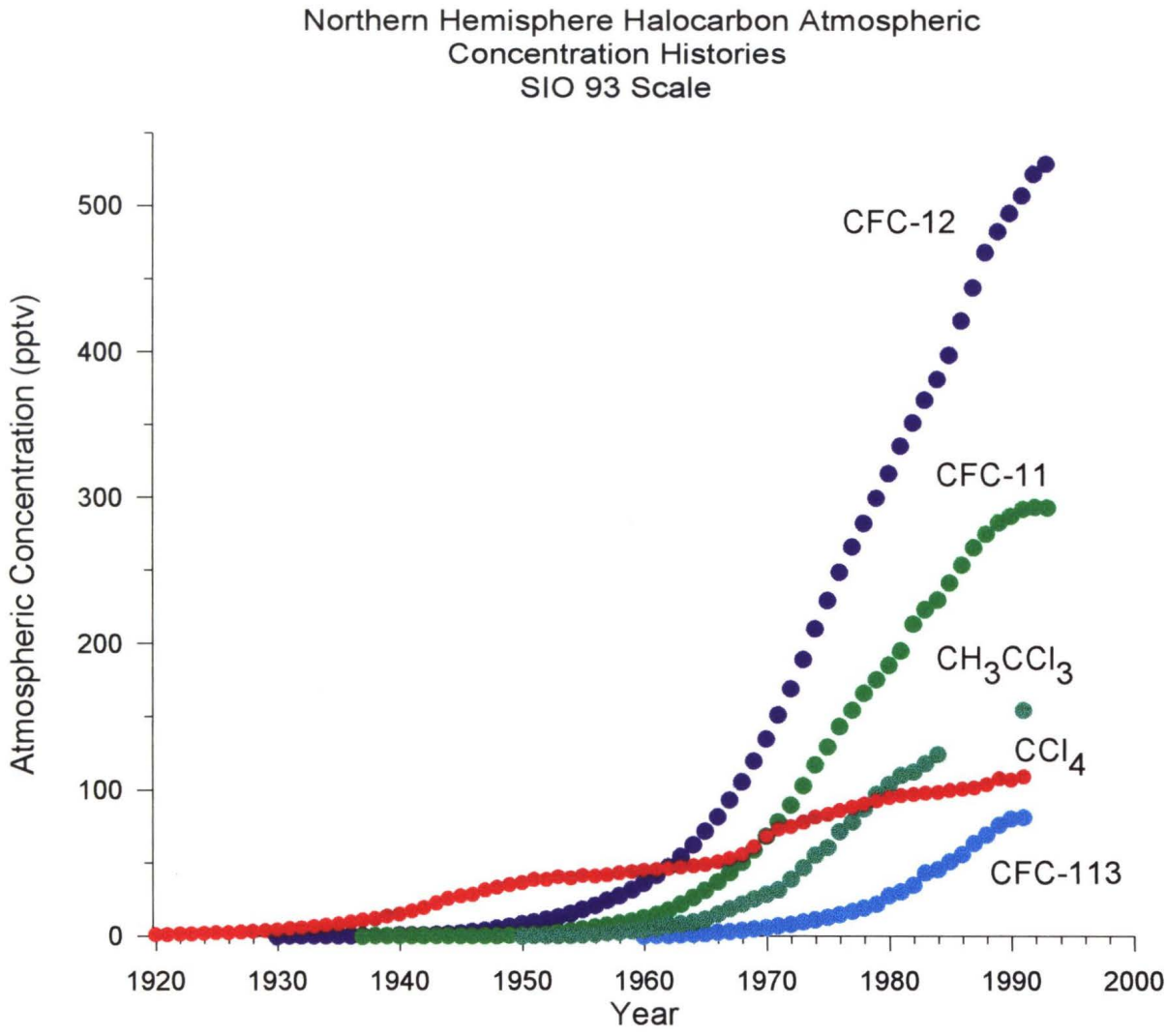
Northern Hemisphere Halocarbon Atmospheric
Concentration Histories
SIO 93 Scale
Atmospheric Concentration (pptv)
0
100
200
300
400
500
1920
1930
1940
1950
1960
1970
1980
1990
2000
Year
CFC-12
CFC-11
CH3CCl3
CCl4
CFC-113

Figure 1

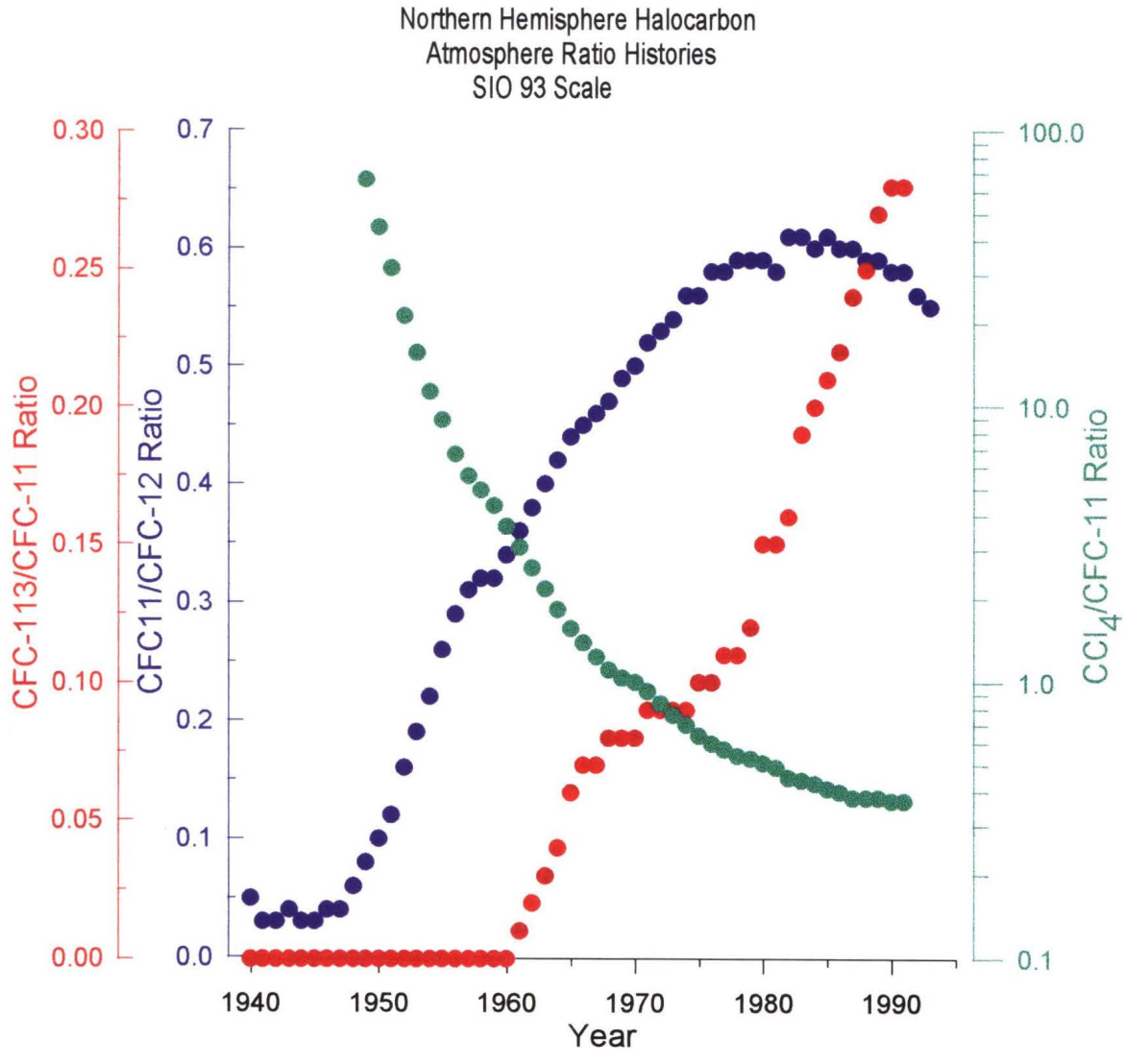
Northern Hemisphere Halocarbon
Atmosphere Ratio Histories
SIO 93 Scale
CFC-113/CFC-11 Ratio
CFC11/CFC-12 Ratio
CCl_4/CFC-11 Ratio
0.30
0.25
0.20
0.15
0.10
0.05
0.00
0.7
0.6
0.5
0.4
0.3
0.2
0.1
0.0
100.0
10.0
1.0
0.1
1940
1950
1960
1970
1980
1990
Year

Figure 2

production histories. CCl_4 production began in the 1920s, and broadens the timescale from the 1920s to the present. CCl_4/CFC-11 ratio provides timescale information from the 1940s to the present. Production of CH_3CCl_3 began in the 1940s, and provides timescale information similar to CFC-11 and CFC-12. CFC-113 production began in the mid-1970s, and, because of its relatively short production history, CFC-113/CFC-11 or CFC-113/CFC-12 ratios may be used to determine the apparent ages of waters isolated from the surface since 1975. In the ocean this usually means that ratios based on CFC-113 are used to estimate apparent ages of upper layer waters, and ratios based on CFC-11, CFC-12 and CCl_4 are used to estimate apparent ages of intermediate and deep layer waters.

4.2 Transient tracer characteristics

CFC-12, CFC-11, CFC-113, and CCl_4 exhibit characteristics which serve to make them effective tracers. First, all are man-made compounds with no natural sources. Although natural sources for CCl_4 have been postulated, researchers have concluded that pre-industrial concentrations were negligible (Wisegarver and Gammon, 1988). But, until further measurements of CCl_4 are made in isolated waters, the influence of a small natural background cannot be discounted.

Second, these halocarbons are stable and essentially conservative in the troposphere (rapid tropospheric mixing rate and half-lives of: CFC-12; 111 years, CFC-11; 74 years, CFC-113; 165 years and CCl_4; 40 years (Cunnold et al., 1994; Krysell and Wallace, 1988)). Upon entering ocean waters, these halocarbons are also assumed to behave conservatively and not subject to removal mechanisms such as particle scavenging, microbial attack or hydrolysis. Krysell and

Wallace (1988) examined whether the downward flux of particulate organic carbon would transport halocarbons to depth and concluded that, under open ocean conditions, halocarbons should not be affected by particulate transport. Hydrolysis is likewise believed negligible for CCl_4 over relevant timescales in cold arctic waters (7000 years, Wallace and Krysell, 1988; 2790 years, Jeffers and Wolfe, 1989). However, depletion of CCl_4 and CFC-11 in seawater has been recently reported under anoxic and low oxygen conditions (Krysell et al., 1994, Wallace et al., 1994, Bullister and Lee, 1995), suggesting that these two halocarbons may not behave conservatively under certain oceanic conditions. Such low oxygen conditions may exist in waters underlying the productive regions on the Arctic shelves.

Third, atmospheric concentrations of halocarbons vary independently with time. Atmospheric halocarbon concentrations have been reconstructed using both manufacture and release information, in addition to a program of global measurements begun in 1978 under the Atmospheric Lifetime Experiment/Global Atmospheric Gases Experiment (ALE/GAGE) (Cunnold et al., 1994).

Although CH_3CCl_3 is generally measured along with the other halocarbons, its value as a tracer is uncertain as it is biologically produced, has an atmospheric half-life of only 6.3 years, and may be removed through hydrolysis and dehydrohalogenation. For these reasons, CH_3CCl_3 data are not included in the following discussion.

4.3 Apparent Age and Dilution Factors

Halocarbon concentrations and their ratios in the water column are used to calculate apparent ages and dilution factors. To obtain apparent ages, seawater halocarbon

concentrations are first converted into equivalent atmospheric concentrations. This conversion assumes that surface seawater is at equilibrium with the atmosphere, and that seawater concentrations are proportional to atmospheric mole ratios according to the following relationship:

$$C^* = F(\Theta,S)x$$

where C^* = equilibrium seawater concentration, x = dry air mole fraction, and $F(\Theta,S)$ = solubility as a function of potential temperature and pressure (Weiss and Price, 1980) for the specific halocarbon at 1 atm pressure in moist air and for $x \ll 1$. Equivalent atmospheric concentrations or ratios are then compared with atmospheric concentration histories (see Figure 1), or with atmospheric ratio histories (see Figure 2), to estimate apparent ages.

Apparent ages are best estimated from halocarbon ratios (CFC-11/CFC-12, CCl_4/CFC-11, CFC-113/CFC-11) rather than from halocarbon concentrations because the ratio avoids bias introduced by undersaturation (see below). CFC-11 is selected for comparison because it is more soluble in seawater than CFC-12 and therefore has a larger dynamic range. The CCl_4/CFC-11 ratio offers a considerable advantage over the CFC-11/CFC-12 ratio in that it provides un-interrupted apparent age information from the mid-1940s to the present, although in the past few years its rate of change has slowed considerably. The CFC-113/CFC-11 ratio is still increasing and may be used to provide apparent age information from the early 1960s to the present. The time period for which each halocarbon ratio is most effective in determining apparent ages is represented in Figure 3.

The atmospheric ratio history for CCl_4/CFC-11, CFC-11/CFC-12 and CFC-113/CFC-11 (see Figure 2) shows that ratio-based ages are potentially more precise for older waters when halocarbon ratios changed more rapidly.

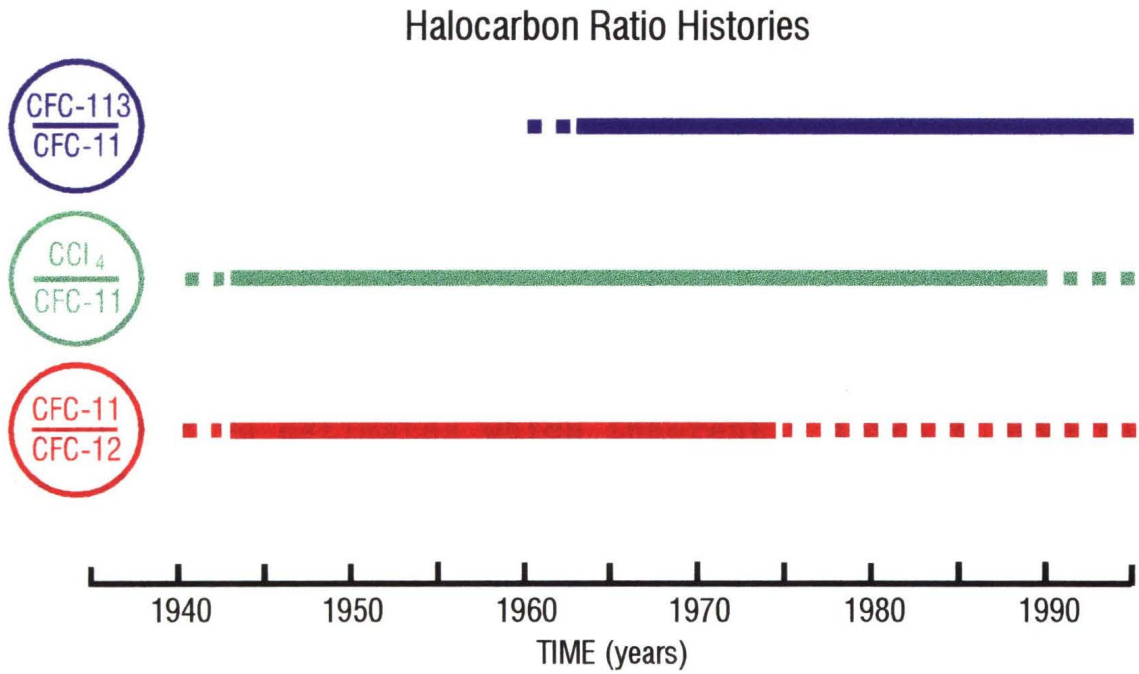
Halocarbon Ratio Histories
CFC-113
CFC-11
CCl4
CFC-11
CFC-11
CFC-12
1940
1950
1960
1970
1980
1990
TIME (years)

Figure 3

However, the apparent ages in older waters become difficult to determine due to the analytical uncertainty associated with measuring low concentrations. Accordingly, apparent age calculations in the following discussion are restricted to CFC-12, CFC-11, and CCl_4 concentrations greater than 0.08 nmol m^{-3}, 0.10 nmol m^{-3}, and 0.50 nmol m^{-3} respectively, where these values were determined by the analysis of spatial variability.

Apparent age calculations also allow estimates of dilution factors. Dilution factors are calculated by dividing the observed water concentration by the water concentration assumed to exist in the year of its apparent age, a calculation that assumes 100% saturation. This latter assumption is questionable in ice-covered waters and/or where rapid cooling of surface waters occurs.

4.4 Apparent age and dilution factor uncertainties:

Apparent ages and dilution factors are semi-quantitative estimates which inherently involve several uncertainties. First, uncertainties exist in the atmospheric concentration history (or source function) estimation and these uncertainties are difficult to assess. Virtually all CFCs produced are eventually released to the atmosphere, apart from material consumed in chemical reprocessing or that which is recycled and destroyed. For each halocarbon the source function estimation relies on: accurate reporting by manufacturers; knowledge of product application and rates of release; and, estimates of atmospheric lifetime derived from analysis of observed tropospheric trends. Source functions for CFC-12 and CFC-11 are likely more accurate because of efforts by the Chemical Manufacturers Association and others to collect historical production data and investigate release scenarios, and by

the ALE/GAGE program to measure atmospheric concentrations since 1978. These uncertainties have been estimated to be 6% to 8% for CFC-11 and 4% to 7% for CFC-12 (Cunnold et al., 1994). Uncertainties in CFC-113 and CCl_4 are difficult to assign but are generally assumed to be similar.

Second, uncertainties also exist in determining the solubility of halocarbons as a function of temperature and salinity. Warner and Weiss (1985) determined the solubility of CFC-12 and CFC-11, and Bu and Warner (1995) determined the solubility of CFC-113. Solubility measurements were made over a range in temperature (0 to 40 °C) in fresh, intermediate salinity (S=19) and high salinity (S=36) waters. The uncertainties reported for these measurements were 1.5% ± 0.7 for CFC-12 and CFC-11, and 1.5% ± 1.2 for CFC-113. The solubilities of CFC-11 and CCl_4 were also obtained over a similar range in temperature in fresh and saline (S=35) water by Hunter-Smith et al. (1983), and provide the only published data available for determining the solubility of CCl_4 in seawater. The Hunter-Smith et al. (1983) data however, have been reported to be at variance with recent measurements of CFC-11 (Warner and Weiss, 1985) and CCl_4 (Wallace et al., 1994). Use of the Hunter-Smith et al. (1983) solubility data may therefore introduce an uncertainty in CCl_4 equivalent atmospheric concentration calculations that is difficult to estimate, but may be from 10% to 20%. A CCl_4 solubility equation encompassing a broader range of temperature and salinity conditions will allow improved estimates to be made at a later date. The order of solubility, from most to least, is CCl_4, CFC-11, CFC-113 and CFC-12.

Here, halocarbon saturations were calculated for **Larsen-93** halocarbon data using Warner and Weiss' (1984) equations for CFC-12 and CFC-11, Bu and Warner's (1995) equation for CFC-113, and Hunter-Smith et al.'s (1983)

equation for CCl_4. These calculations show that a small difference exists in saturation among halocarbons; for example at Station B1 at 10m, CFC-11 and CFC-12 saturation is 60%, whereas CCl_4 saturation is 67%. This difference in saturation may be due to error in the CCl_4 solubility equation, or it may reflect a real difference in gas exchange rates.

Third, uncertainites also exist because of gas exchange rates. Seawater requires approximately one month to achieve equilibrium with the atmosphere (Broecker and Peng, 1974). However, in ice-covered regions such as the Arctic, gas exchange is suppressed which may lead to undersaturation. Such undersaturation (about 80%) has been reported in the Greenland Sea, due to ice cover suppressing gas exchange and/or rapid cooling of surface water (Rhein, 1991). Apparent ages calculated solely from concentrations will therefore appear "older" because of such undersaturation. Provided that the degree of undersaturation is similar for each halocarbon, calculation of apparent ages from ratios will give unbiased estimates. For these reasons, **Larsen-93** apparent age estimates are based on halocarbon ratios. Until a more precise solubility equation is available for CCl_4, calculations are based on the assumption that the degree of undersaturation of CFC-11, CFC-12, and CCl_4 is similar. Undersaturation does, however, affect the calculation of dilution factors.

Fourth, uncertainties result from the non-linear effects of mixing on ratio-based apparent age estimates. The apparent age estimates are not conserved on mixing because the both absolute concentrations as well as the ratio or age signature have changed with time. In a parcel of water that is a mixture of two components, each with a different age and halocarbon signature, the component with the higher concentration is more influential – or carries

more weight – in defining the apparent age. Since CFC concentrations increase with time, halocarbon ratio ages are therefore biased toward the younger component. In the extreme case of a mixture that consists of halocarbon-bearing water and water without halocarbons, the halocarbon ratio reflects the apparent age of the halocarbon-bearing water and does not provide information about the presence of the zero-halocarbon component. Such mixing effects also influence dilution factors.

In summary, when all quantifiable factors are combined, the total uncertainty in the CFC-11/CFC-12 apparent age calculation is estimated to be 9%. This corresponds to an age error of about three years for water that is 25 years old (isolated from the surface in 1968). The total uncertainty in the CCl_4/CFC-11 apparent age calculation is about 19%. However, the rate of change in the CCl_4/CFC-11 ratio has decreased significantly since the mid 1970s which accounts for the larger error reported for younger waters. For example the CCl_4/CFC-11 error is about five years for water six years old (1987), -6 years to +5 years for water 12 years old (1975-1986) and about two years for water 30 years old (1961-1965). The total uncertainty in the CFC-113/CFC-12 apparent age calculation is about 10%. This corresponds to an age error of -4 to +1 for water six years old (1983-1988) to about 2 years for water about 18 years (1973-1977). These estimates are similar to those calculated by Wallace et al. (1994) who reported the error to be about two years for waters older than 25 years, and about five years for more recently ventilated waters.

In the following **Larsen-93** apparent age figures, an age error is calculated and displayed for each apparent age. Age errors are calculated by applying the following propagation of error formula:

$$\sigma_{A/B}^2 = (A/B)^2 \, (\sigma_A^2/A^2 + \sigma_B^2/B^2)$$

to determine the age error for each ratio (i.e. CFC-11/CFC-12= ±9%, CCl_4/CFC-11=±16%, CFC-113/CFC-12=±11%). Two atmospheric ratios are calculated, the apparent age of each ratio is determined and then, by subtraction from the found age, the age errors are estimated. These errors include uncertainites due to analysis, solubility equations and source function but do not include uncertainties that arise due to mixing.

4.5 Larsen-93 Halocarbon Data

Larsen-93 CFC-11 data from Station A1, D1 and E1 were discussed in Chapter 3 to demonstrate, qualitatively, the relative differences in ventilation that exist across the Atlantic/Pacific water mass boundary. (As described in Chapter 3, high subsurface halocarbon concentrations suggest the presence of young waters and enhanced ventilation, whereas low subsurface concentrations suggest the presence of older waters and slow ventilation). From CFC-11 data, two significant differences were found. First, waters of the EA assembly in the Makarov Basin appeared more recently ventilated than WA assembly waters in the Canada Basin. Second, the presence of high halocarbon concentrations were found at Station E1, extending well below the core of the Atlantic layer to depths from 500 m to 1600 m. When considered together with salinity and nutrient measurements, these data suggested a deep lateral transport of recently ventilated shelf waters into the Makarov Basin.

The following discussion now examines halocarbon data collected at the five basin stations in greater detail (A1 and B1 in the Canada Basin, C1 on the Northwind Ridge, D1 on the Chukchi Plain, and E1 in the Makarov Basin). Concentration profiles of CFC-12, CFC-11, CFC-113 and CCl_4 at these stations are presented in Figures 4 to 8;

examination of these data reveals several common features.

In all five figures, the four halocarbons are marked by similar patterns in their vertical profiles. These distributions reflect the atmospheric concentrations when each layer of water was last in contact with the atmosphere and thereby denote similar levels of ventilation. This pattern of sub-surface ventilation is the result of spreading and mixing along constant density surfaces from regions where these densities intersect the ocean surface, and is not a result of simple vertical mixing and diffusion or a result of differences in solubility due to temperature and salinity.

Of the four halocarbons measured, CFC-11 and CCl_4 exhibit higher concentrations which reflect both their atmospheric burden and their greater solubility. In all five figures, CCl_4 is detected to greater depths in the water column than the other halocarbons in agreement with CCl_4's longer production history. Similarly, the limit of detection for CFC-113 occurs at a shallower depth than it does for the other halocarbons, consistent with CFC-113's shorter production history.

In addition to illustrating ventilation differences in waters on opposite sides of the Atlantic/Pacific front, Figures 4 to 8 also show the relative levels of ventilation found in the three main layers that constitute the two water mass assemblies. At Stations A1 and B1 (WA assembly), halocarbon concentrations are high in surface water, decrease to a subsurface minimum near 200 m (upper layer), increase to a subsurface maximum near 400 m (Atlantic layer), then, below about 1800 m, drop to detection levels (deep layer). Undetectable CCl_4 concentrations in the deep layer of the WA assembly suggests that these waters have not been in contact with the atmosphere for over 75 years, dating to before the 1920s when CCl_4 production began. This

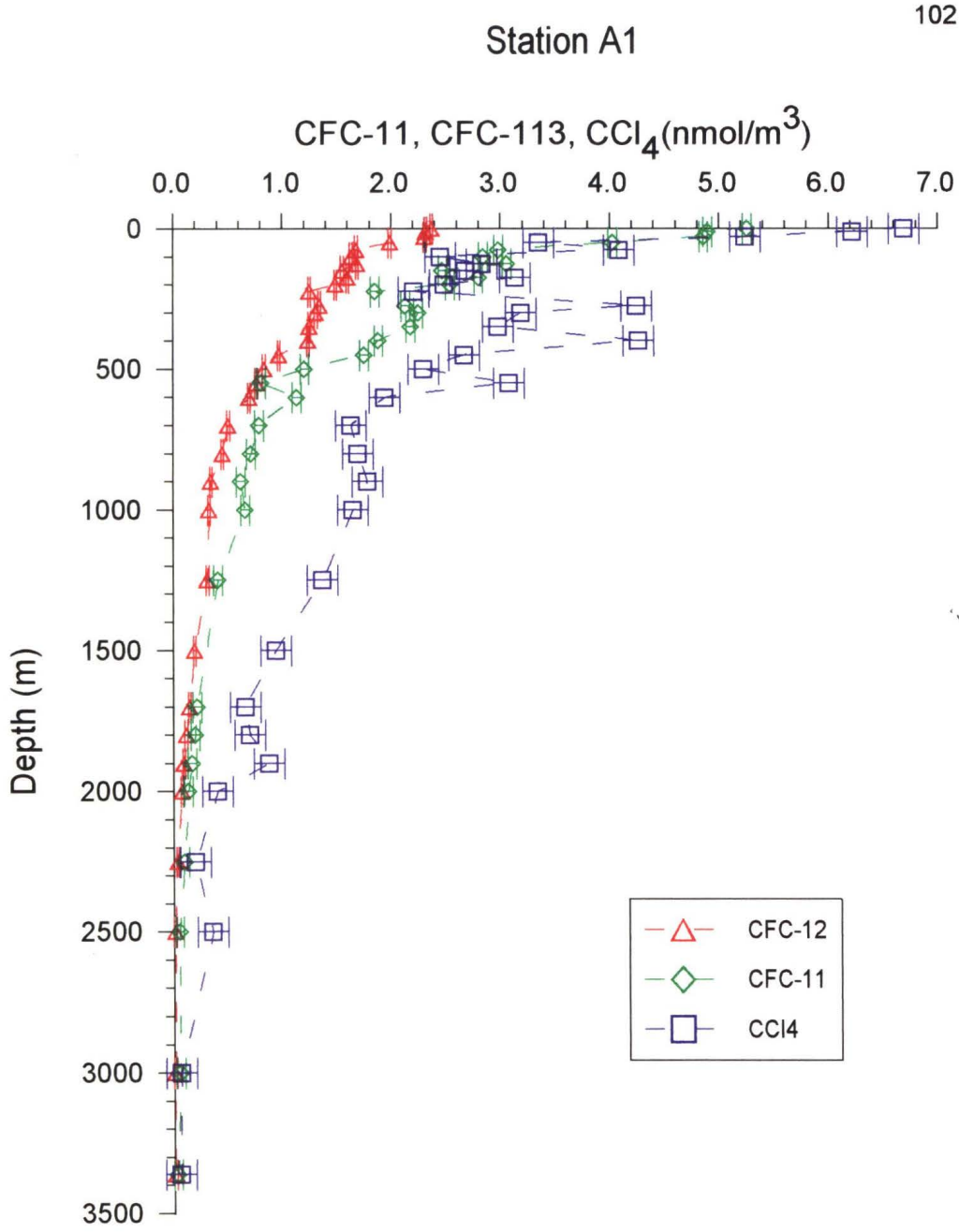
Station A1
CFC-11, CFC-113, CCl4(nmol/m3)
0.0
1.0
2.0
3.0
4.0
5.0
6.0
7.0
0
500
1000
1500
2000
2500
3000
3500
Depth (m)
CFC-12
CFC-11
CCl4

Figure 4

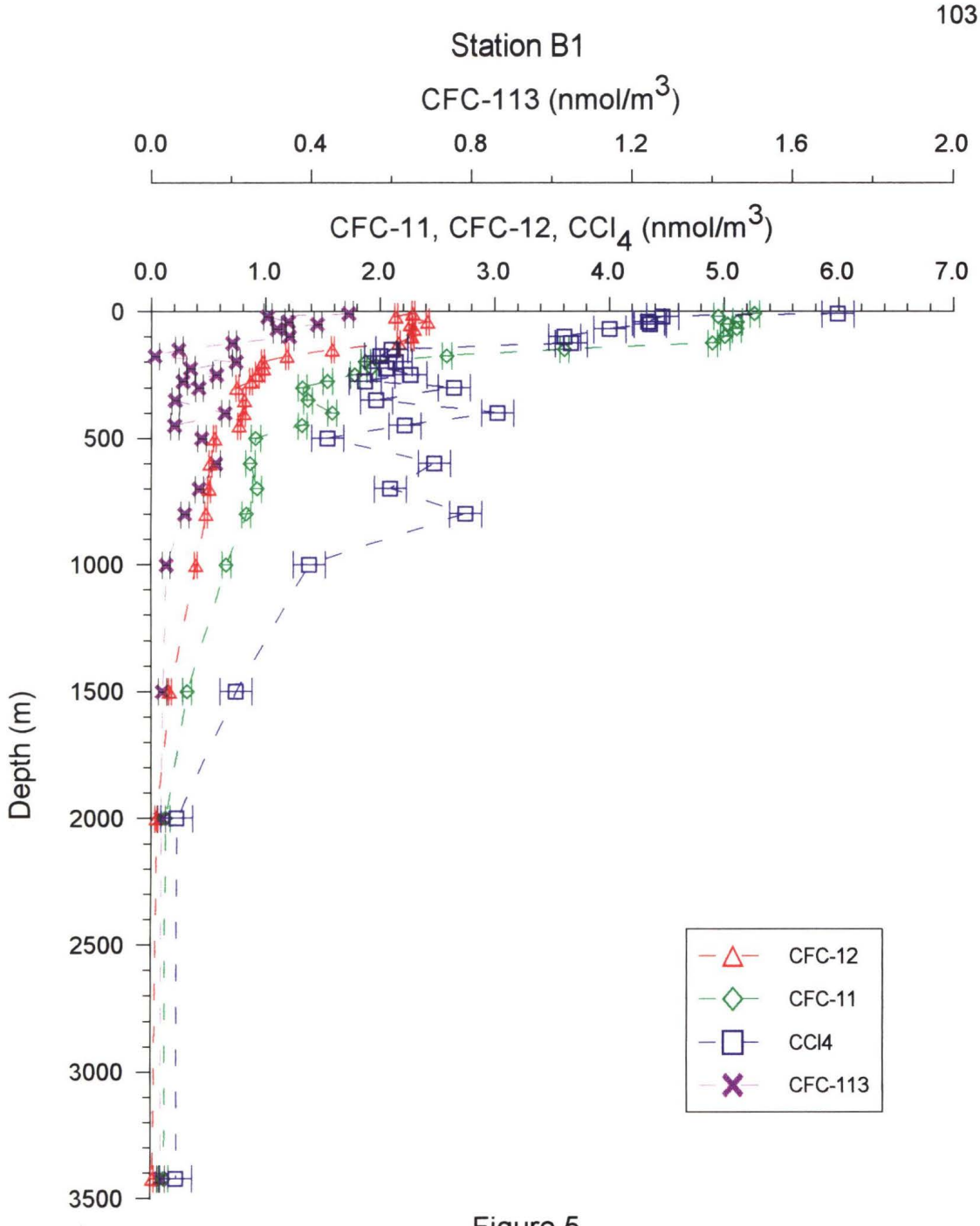
Station B1
CFC-113 (nmol/m3)
0.0
0.4
0.8
1.2
1.6
2.0
CFC-11, CFC-12, CCl4 (nmol/m3)
0.0
1.0
2.0
3.0
4.0
5.0
6.0
7.0
Depth (m)
0
500
1000
1500
2000
2500
3000
3500
CFC-12
CFC-11
CCl4
CFC-113

Figure 5

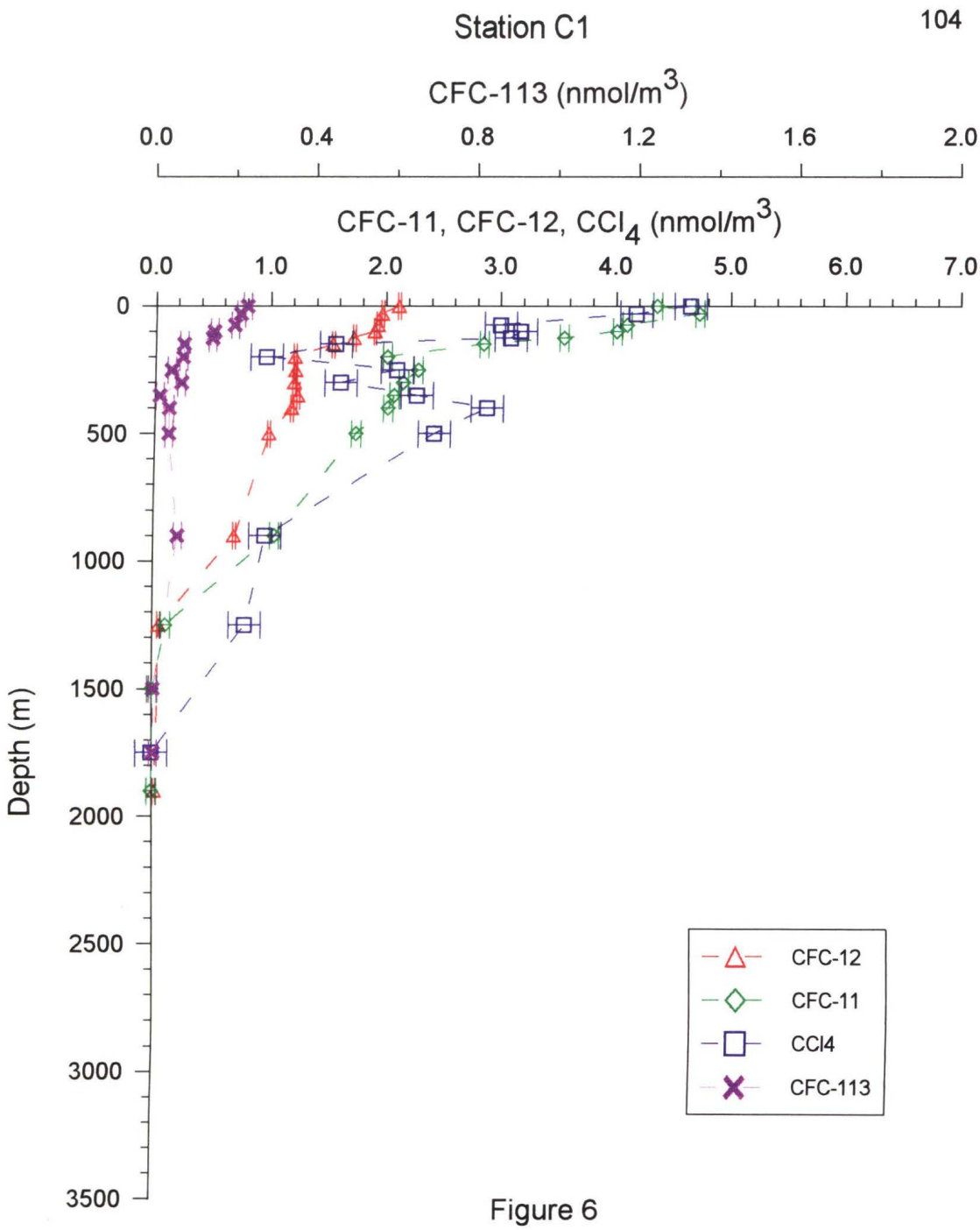
Station C1
CFC-113 (nmol/m3)
0.0
0.4
0.8
1.2
1.6
2.0
CFC-11, CFC-12, CCl4 (nmol/m3)
0.0
1.0
2.0
3.0
4.0
5.0
6.0
7.0
Depth (m)
0
500
1000
1500
2000
2500
3000
3500
CFC-12
CFC-11
CCl4
CFC-113

Figure 6

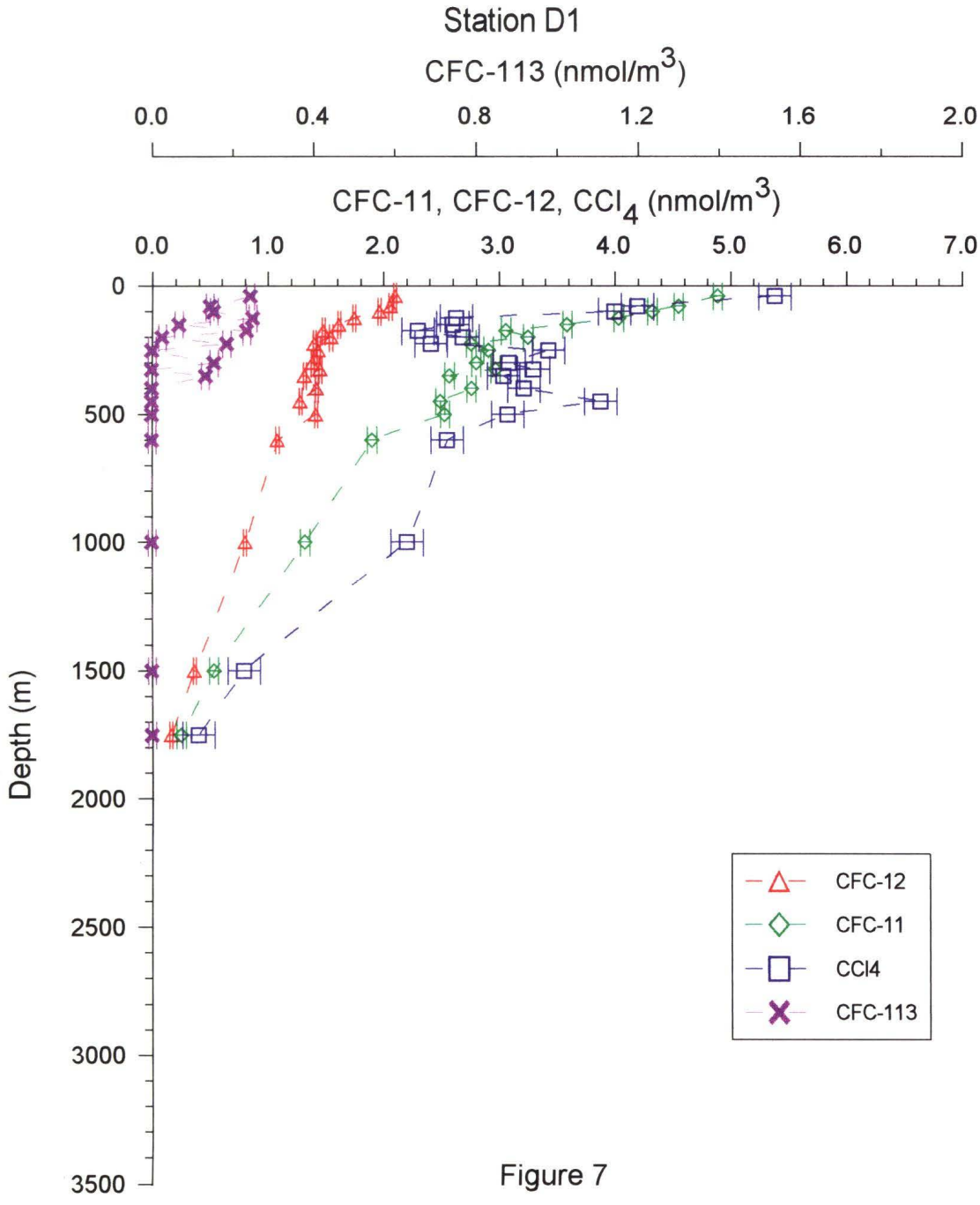
Station D1
CFC-113 (nmol/m3)
0.0
0.4
0.8
1.2
1.6
2.0
CFC-11, CFC-12, CCl4 (nmol/m3)
0.0
1.0
2.0
3.0
4.0
5.0
6.0
7.0
Depth (m)
0
500
1000
1500
2000
2500
3000
3500
CFC-12
CFC-11
CCl4
CFC-113

Figure 7

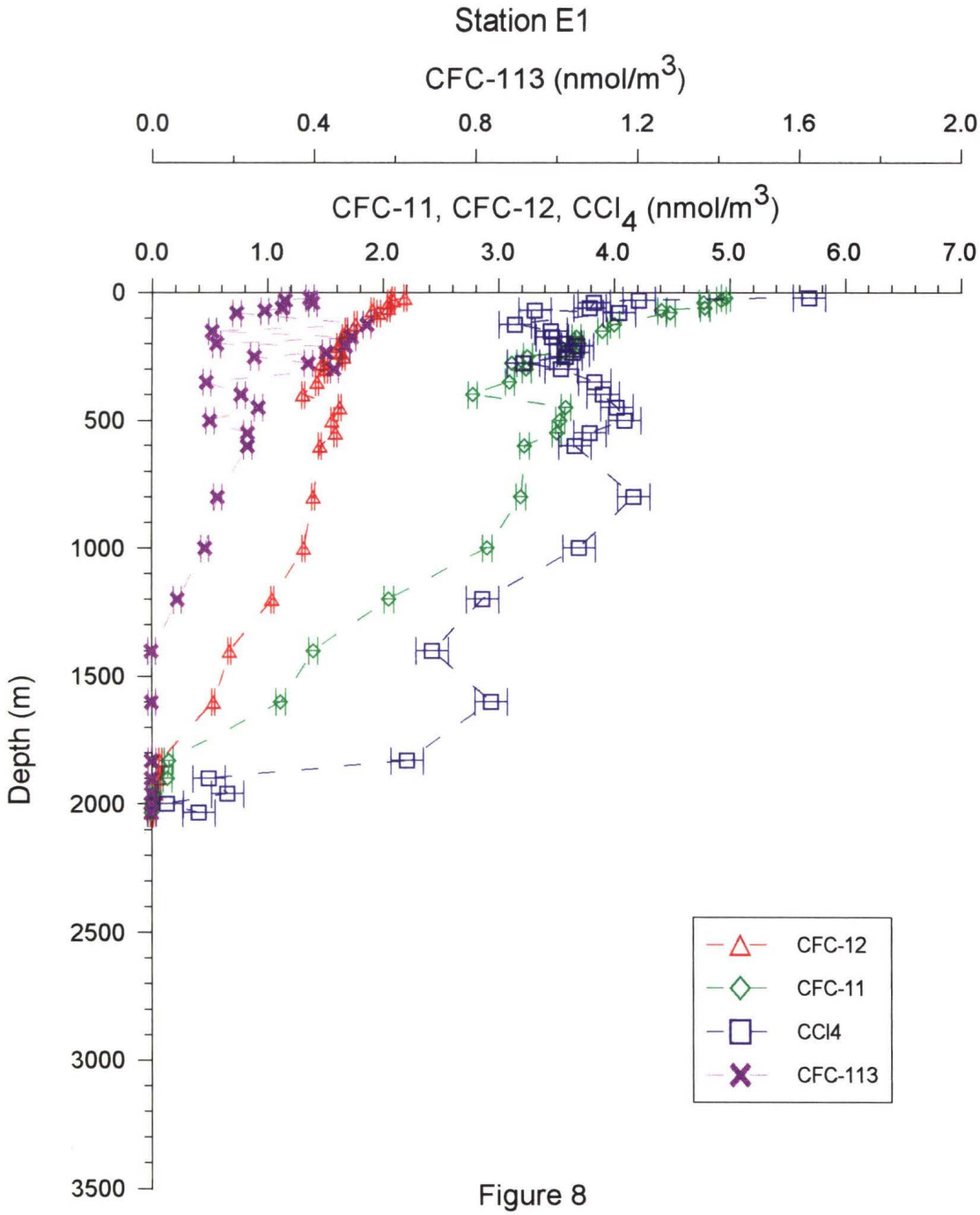
Station E1
CFC-113 (nmol/m3)
0.0
0.4
0.8
1.2
1.6
2.0
CFC-11, CFC-12, CCl4 (nmol/m3)
0.0
1.0
2.0
3.0
4.0
5.0
6.0
7.0
Depth (m)
0
500
1000
1500
2000
2500
3000
3500
CFC-12
CFC-11
CCl4
CFC-113

Figure 8

finding is consistent with deep Canada Basin water ventilation age estimates of 450-500 years, based on measurements of tritium and ^{14}C (Macdonald et al., 1993), as well as a mean residence age estimate of about 300 years (Schlosser et al.,1994).

At Stations A1 and B1, differences in halocarbon concentration are also apparent within the WA assembly upper layer (Figure 9). At Station A1, CFC-11 concentrations decrease from 4 nmol/m^3 between S=31.0 and S=32.0, to 3 nmol/m^3 at S=33.1, to 2 nmol/m^3 at S=34.4, salinities which, in order, characterize the upper, middle and lower halocline regions of the WA assembly upper layer. Concentration data suggest that upper halocline waters are more recently ventilated than middle halocline waters. One explanation is that Pacific origin waters with summer characteristics (low nutrients, S=31 to S=32) spend less time on the Chukchi shelf, and reach the Canada Basin interior faster, than waters with winter characteristics (high nutrients, S=33.1). This finding is consistent with reports of higher summer flow rates through Bering Strait (1.3 Sv in July compared to 0.3 Sv in December, Roach et al., 1995). However, mixing effects could also account for the decrease in CFC-11 concentration because the volume of the middle halocline (S=33.1, about 75-150 m) is greater than the volume of the upper halocline (S=31 to S=32, about 30-75 m). Thus, even with equal inflow rates, the concentration would appear lower because of greater dilution.

Figure 9 also illustrates that, at Station A1, halocarbon concentrations are lower in halocline waters (S=34.4) than waters in both the middle halocline region and the Atlantic layer. To explain the low halocarbon concentration, two possible origins of the lower halcline can be examined.

Jones and Anderson (1986) proposed that lower halocline

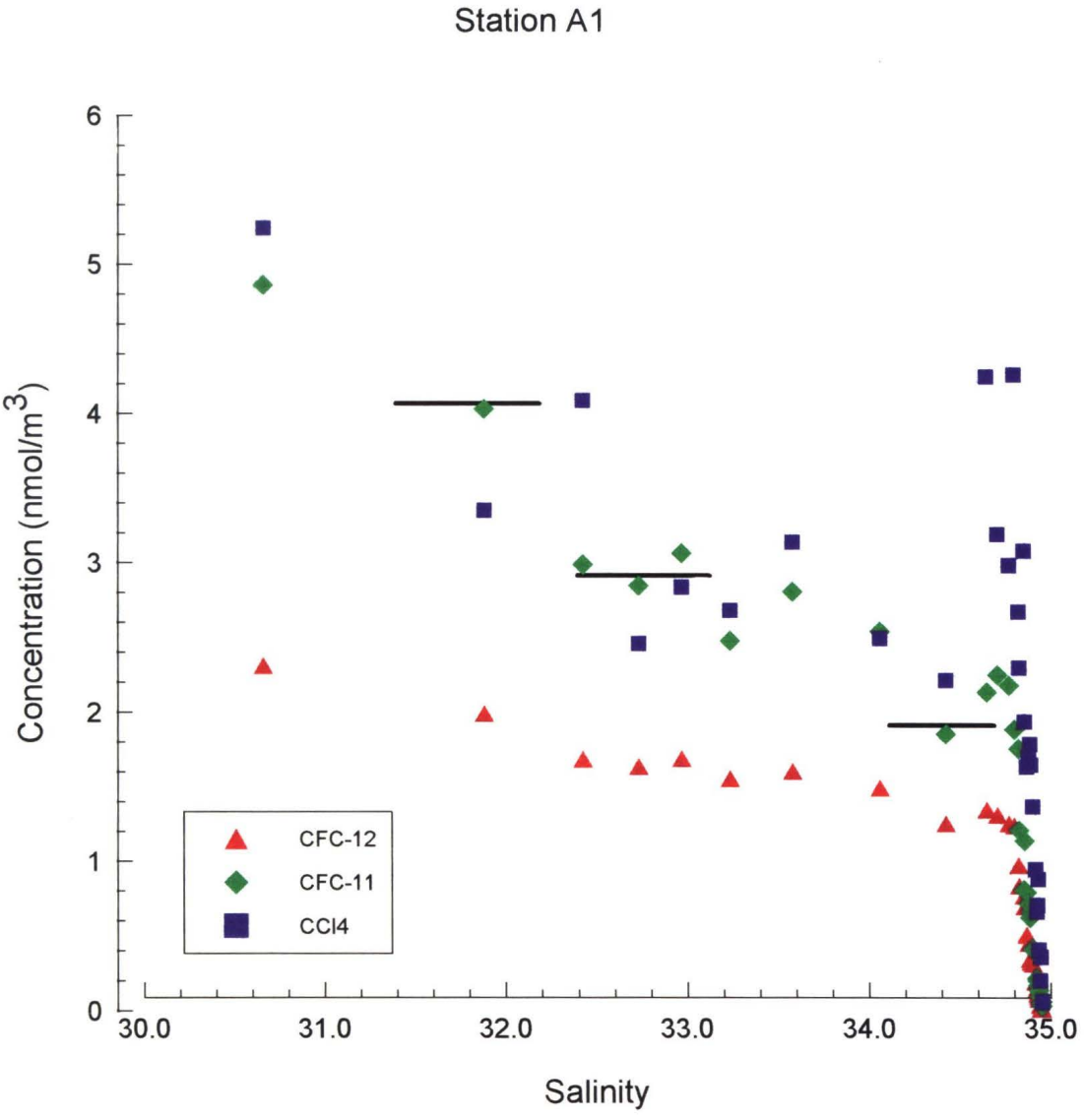
Station A1
Concentration (nmol/m3)
Salinity
CFC-12
CFC-11
CCl4
0
1
2
3
4
5
6
30.0
31.0
32.0
33.0
34.0
35.0

Figure 9

waters are waters of Atlantic origin that have been modified on the Barents and Kara Sea shelves. Convection resulting from ice formation on the shelves provides a mechanism for ventilation and, accordingly, waters modified on the Barents and other shelves should contain higher halocarbon concentrations. These waters would have been in contact more recently with the atmosphere than waters in the Atlantic layer and, therefore, would have higher concentrations. Lower concentrations in the lower halocline may be explained simply by different transport rates for each layer. If the core of the boundary current was located within the Atlantic layer, it may transport this layer more quickly than the overlying waters of the lower halocline. Lower concentrations also suggest either that there has been little addition of ventilated brine-drainage waters from other shelves, or that the degree of ventilation in brine-drainage waters is low due to ice-cover or short equilibration time before convection.

Alternatively, lower halocline waters found at Station A1 may be of Pacific origin, and have lower halocarbon concentrations because they have spent longer time on shelves in the Canadian Basin. The origins of lower halocline waters in the WA assembly may be difficult to establish, however. A shift of the Atlantic/Pacific water mass boundary from a location above the Lomonosov Ridge to a location above the Mendeleyev Ridge has altered the Makarov Basin water mass structure from one of the WA assembly to one of the EA assembly, down to depths of 1600-1800 m. Water mass characteristics once found throughout the Canadian Basin are now found solely in the Canada Basin. Although evidence of processes that modified Pacific origin waters within the Makarov Basin (for example, brine-drainage from the East Siberian Sea shelf) can still be found in the Canada Basin, these processes will now influence waters

within the Makarov Basin and will not likely influence halocline waters in the WA assembly as long as the Atlantic/Pacific front remains located above the Mendeleyev Ridge.

On the eastern side of the Atlantic/Pacific front, in the Makarov Basin at Station E1 (Figure 8), halocarbon concentrations are high in the surface water and decrease to a subsurface minimum near 120 m (upper layer), increase to a subsurface maximum near 200 m (Atlantic layer), remain high to a depth of about 1800 m, then decrease to detection levels below 1800 m (deep layer). The shallower depths at which these layers are found reflect the absence of Pacific origin water at Station E1. A comparison of Figures 9 and 10 show that Station E1 waters in the upper layer from S=30 to S=34 have higher halocarbon concentrations than Station A1 waters suggesting that waters in the EA assembly upper layer have been ventilated more recently than waters in the WA assembly upper layer. Also, the range in halocarbon concentrations is larger in the WA assembly halocline at Station A1 (CFC-11: 4.9 nmol m^{-3} to 2 nmol m^{-3}) than in the EA assembly halocline at Station E1 (CFC-11: 5 nmol m^{-3} to 4 nmol m^{-3}). A larger range was also found in oxygen concentrations in the WA assembly (discussed in Chapter 3), due to low oxygen concentrations in the lower halocline. Oxygen depletion due to regeneration is consistent with a Pacific origin and a longer shelf residence time for lower halocline waters of the WA assembly.

Ventilation of waters below the Atlantic layer from 600-1800 m is evident at Station E1 (Figure 8). Waters at these depths correspond to the fresher, cold thermocline transition zone between the Atlantic and deep water layers, and reflect a shelf influence that may arise from interleaving of brine enriched waters or outflow of modified Atlantic water from the Barents Sea (BSB). Below 1800 m,

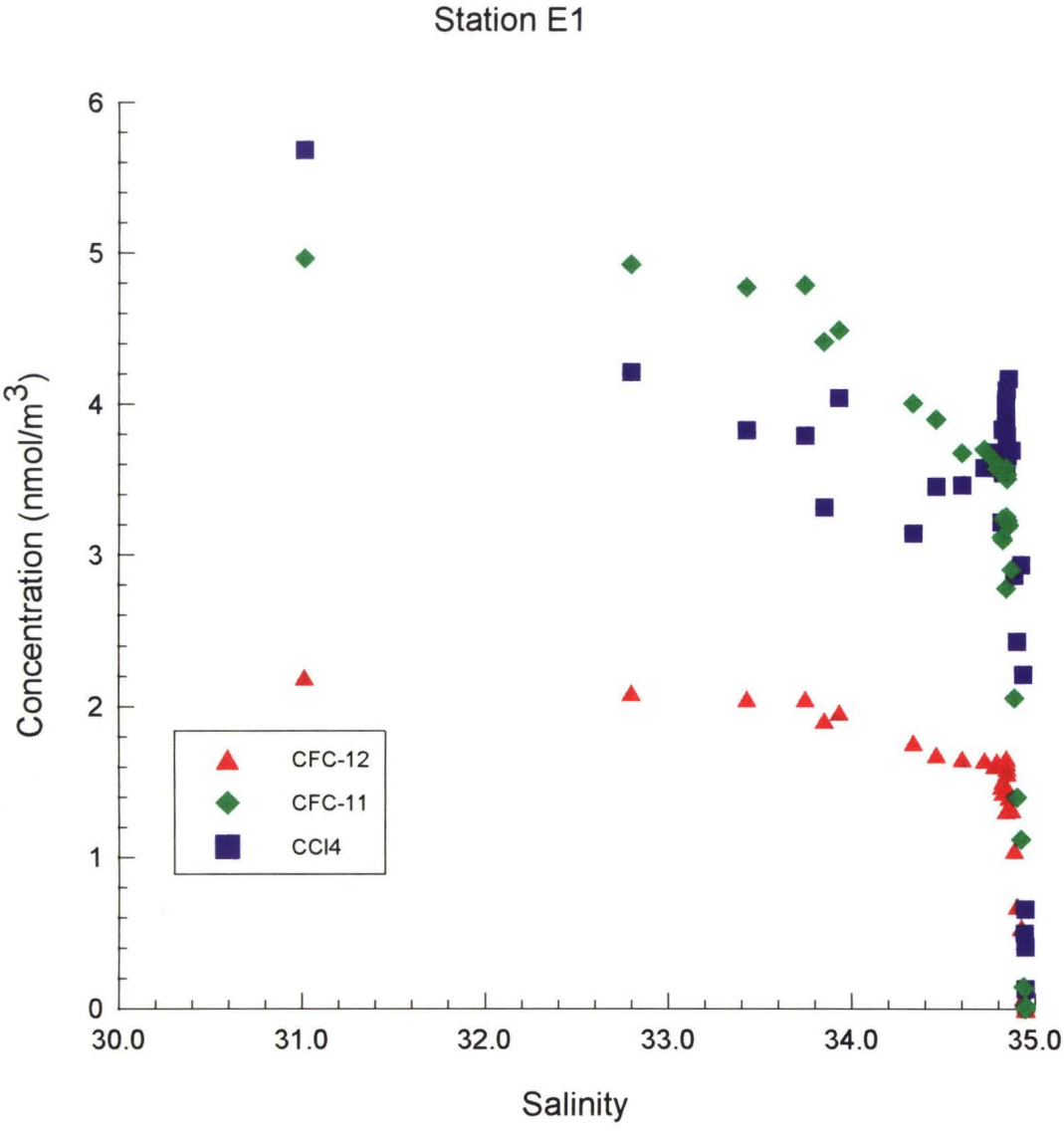
Station E1
Concentration (nmol/m3)
Salinity
CFC-12
CFC-11
CCl4
0
1
2
3
4
5
6
30.0
31.0
32.0
33.0
34.0
35.0

Figure 10

the concentration of all three CFCs are near the detection limit, and CCl_4 concentrations decrease rapidly. These findings are consistent with the discussion in Chapter 3, which identifies the deep layer at Station E1 as belonging to the WA assembly. The halocarbon concentrations in the deep layer at Stations A1 and B1 and in waters below 1800 m at Station E1 are near the detection limit, implying ventilation has not occurred for over 75 years.

Halocarbon profiles at Stations C1 and D1 (Figures 6 and 7) are similar to Station A1 in the upper layer to 200 m, and similar to Station E1 in and below the Atlantic layer deeper than 400 m. This observation illustrates the offset structure of the Atlantic/Pacific water mass boundary. Figures 11a, 11b, and 11c which plot Θ, CFC-11, and CCl_4 at Stations A1, D1, and E1 from 0 m to 1600 m, clearly identify that the core of the Atlantic layer (Θ_{max}) is found at increasing depths on going from Station E1 to Station D1, and similarly, on going from Station D1 to Station A1. Furthermore, CFC-11 and CCl_4 are found in higher concentrations at Station E1 than at Station D1 both in the core of the Atlantic layer and in the underlying water. Halocarbon concentrations are similarly higher in the Atlantic and underlying water layers at Station D1 than at Station A1. This pattern portrays the Atlantic/Pacific water mass boundary as an intrusion appearing first at depth in WA assembly waters. The structure of the front below the Atlantic layer was not apparent from analysis of geochemical properties in Chapter 3.

CFC-11 and CCl_4 profiles at Station E1 suggest that the core of Atlantic water (150-225 m) and deeper shelf-origin water (450-1600 m) were both ventilated recently. This suggests that these waters either outcrop at the surface in proximity to each other and the currents transporting them have similar flow rates, or the source of the ventilated

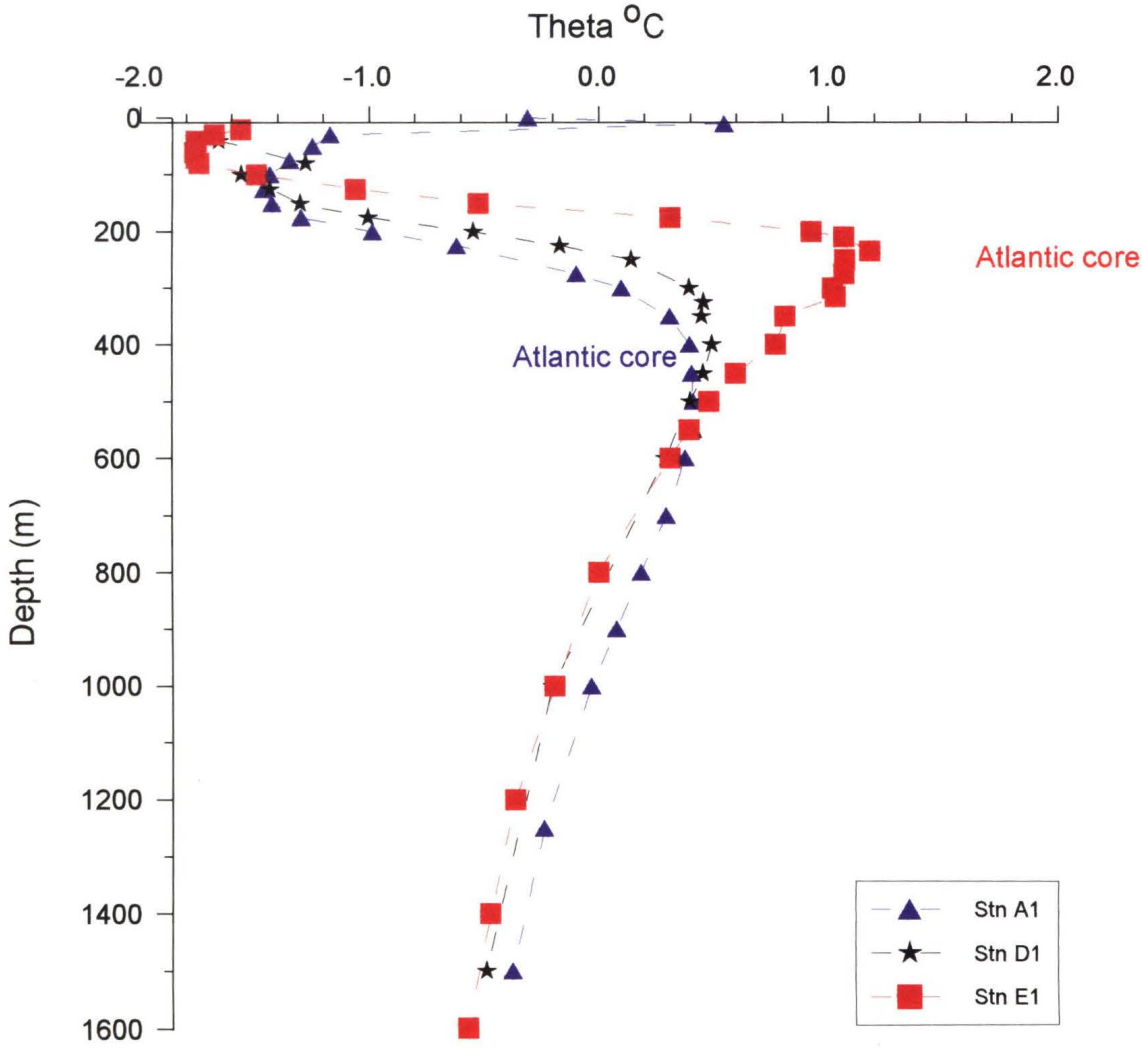
Theta °C
-2.0
-1.0
0.0
1.0
2.0
0
200
400
600
800
1000
1200
1400
1600
Depth (m)
Atlantic core
Atlantic core
Stn A1
Stn D1
Stn E1

Figure 11a

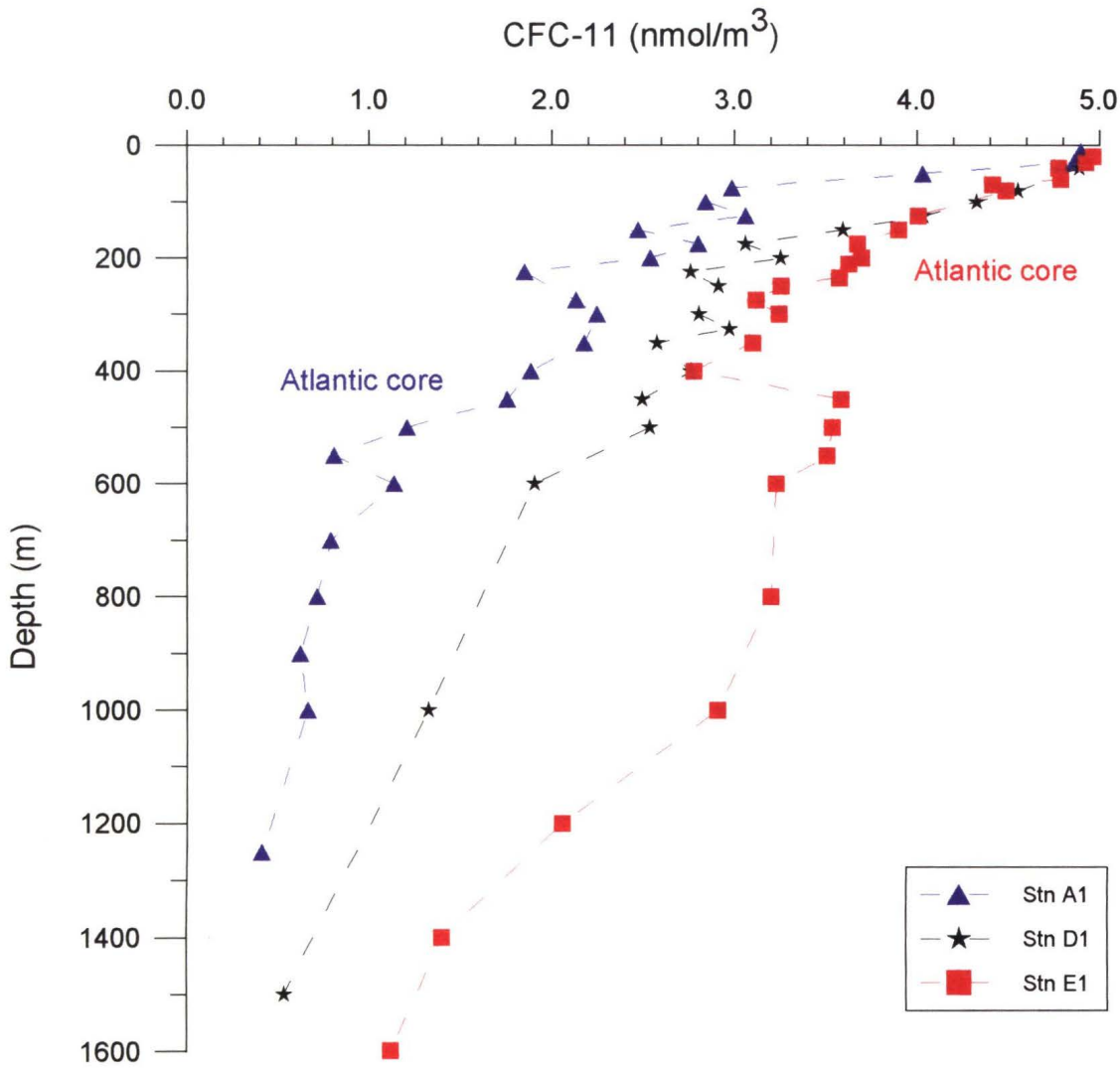
CFC-11 (nmol/m3)
0.0
1.0
2.0
3.0
4.0
5.0
0
200
400
600
800
1000
1200
1400
1600
Depth (m)
Atlantic core
Atlantic core
Stn A1
Stn D1
Stn E1

Figure 11b

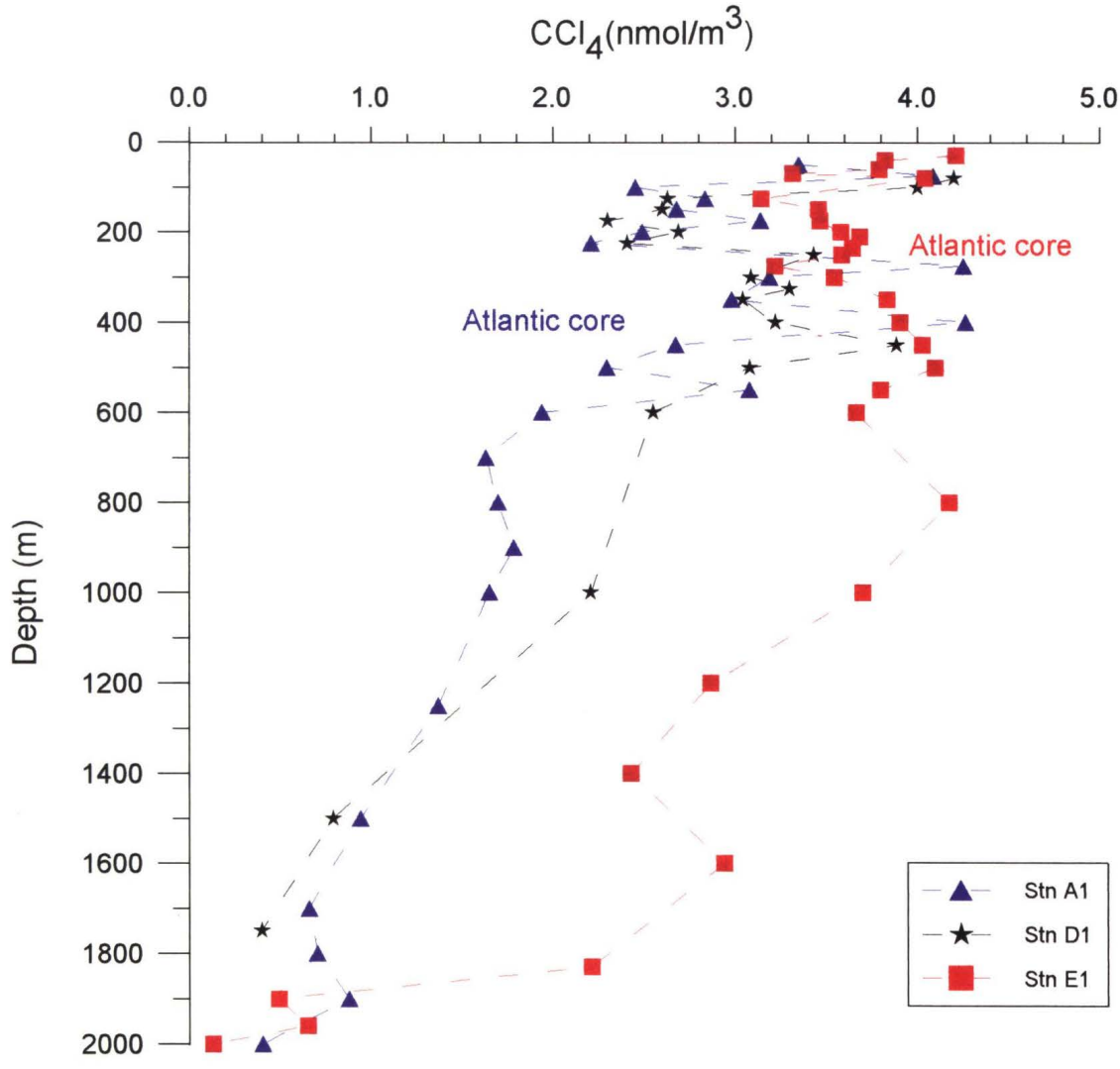
CCl4(nmol/m3)
0.0
1.0
2.0
3.0
4.0
5.0
0
200
400
600
800
1000
1200
1400
1600
1800
2000
Depth (m)
Atlantic core
Atlantic core
Stn A1
Stn D1
Stn E1

Figure 11c

shelf-origin water is closer to Station E1. If the Barents Sea is the source of the shelf-origin water, this suggests that the boundary current transporting the Atlantic layer extends from about 200 m to about 1700 m. Ventilation of the transition zone below the Atlantic layer is quite different between Station A1 and Station E1 (Figures 11b and 11c). CCl_4 concentrations at Station E1 are about 3.8 nmol m^{-3} in the Atlantic core and the same at 800 m. At Station D1, however, CCl_4 concentrations are 3.4 nmol m^{-3} in the Atlantic layer, and 2.4 nmol m^{-3} at 800 m. At Station A1 they are 3 nmol m^{-3} in the Atlantic layer, and 1.6 nmol m^{-3} at 800 m. These differences in concentration suggest that Makarov Basin waters are rapidly renewed by relatively strong boundary currents which transport both Atlantic and underlying waters.

In contrast, at Station A1 in the Canada Basin, only the Atlantic layer appears to be actively ventilated, and then by a still weaker current. Although halocarbons are found in the transition zone underlying the Atlantic layer at Station A1, halocarbon concentrations are significantly lower than those found at Station E1. Perhaps the change in water mass boundary location is linked to a change in the outflow from the Barents Sea.

4.6 Apparent Age Data

Using **Larsen-93** halocarbon concentration data, this discussion now examines saturation levels, apparent ages, and dilution factors. These semi-quantitative values are derived from halocarbon concentrations, solubility equations, and source function histories.

Surface waters in the Canada and Makarov basins were undersaturated in all four halocarbons due to ice-cover and/or rapid cooling of surface waters. Percent saturations

of surface waters were found to be similar between basins and are about 60% for CFC-12 and CFC-11, 40% to 60% for CFC-113 and 60% to 70% for CCl_4. The percent saturation values are lower than those found by Rhein (1991) in the Greenland Sea (80%), and may reflect the presence of a more permanent ice-cover.

Figures 12 to 16 (CFC-11/CFC-12, CCl_4/CFC-11 and CFC-113/CFC-12 apparent ages, and the dilution factor of CFC-11 derived from CCl_4/CFC-11 apparent ages at each station) reveal several common features. There are no apparent ages for waters below 2000 m because low halocarbon concentrations result in large uncertainties in the ratios. The CFC-11/CFC-12 ratio cannot be used to estimate apparent ages of waters in the upper layer at Stations A1 and B1, in waters shallower than 500 m at Station C1 and D1, and in waters shallower than 1000 m at Station E1 because the CFC-11/CFC-12 ratio is in the range (>0.56) of ambiguity. This signals that waters at these depths are younger than about 20 years, because the CFC-11/CFC-12 ratio has not changed since the mid-1970s. Where CFC-11/CFC-12 apparent age estimates are obtained they are older than CCl_4/CFC-11 ages, and do not increase with depth as expected. This appears to be caused by CFC-11 undersaturation relative to CFC-12 saturation.

Also CCl_4/CFC-11 apparent ages of one year are found in the halocline region of both assemblies. An apparent age of one is assigned when CCl_4/CFC-11 equivalent atmospheric ratios are lower than ratios found in the atmospheric ratio history record. Such a ratio suggests that CCl_4 is not conservative and that losses have occurred in this particular region of the water column. Even when CCl_4 concentrations are increased by 18%, (the upper limit of CCl_4 uncertainty), non-conservative behaviour is still implied. Also, where surface data is available, CCl_4 is

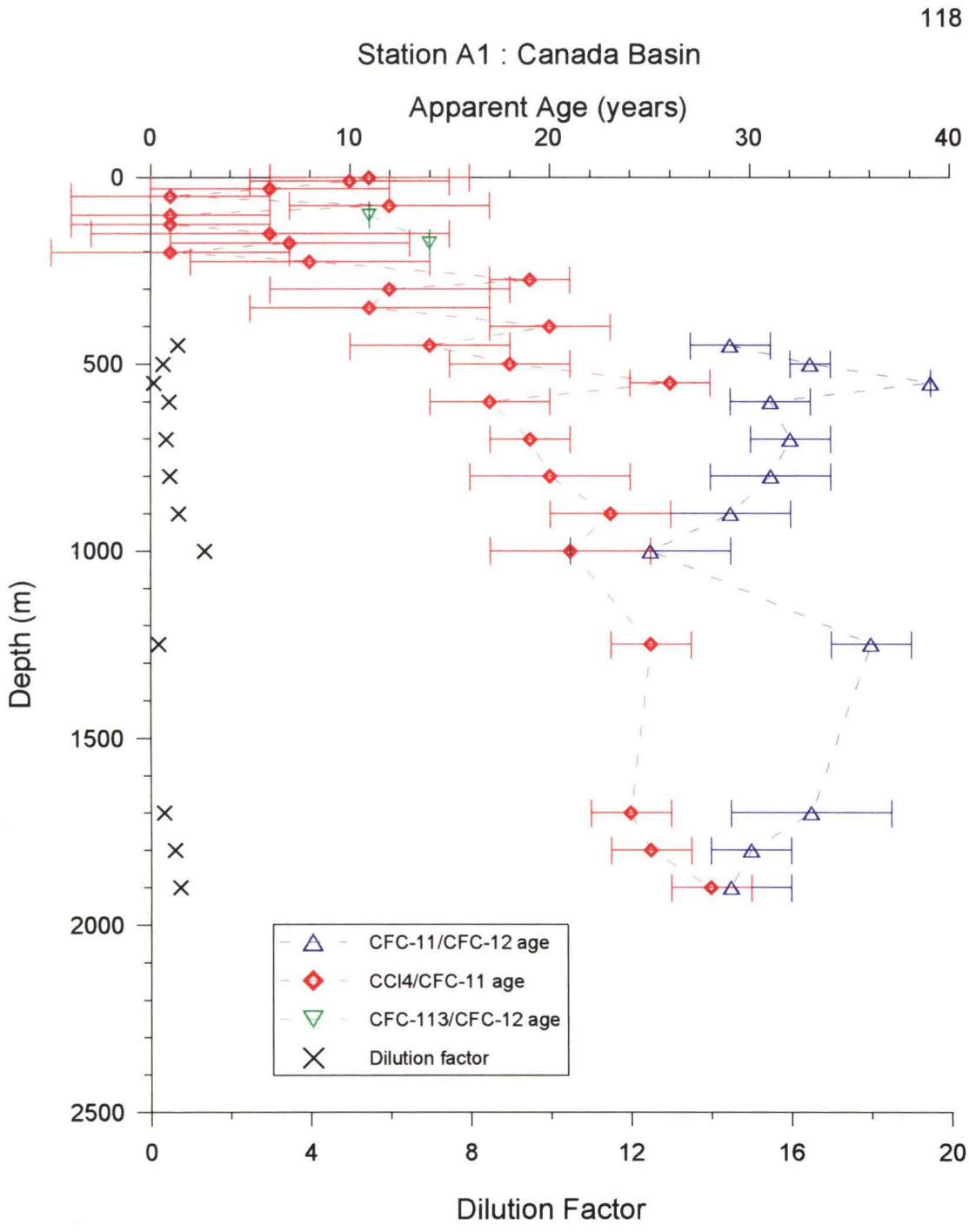
Station A1 : Canada Basin
Apparent Age (years)
0
10
20
30
40
Depth (m)
0
500
1000
1500
2000
2500
CFC-11/CFC-12 age
CCl4/CFC-11 age
CFC-113/CFC-12 age
Dilution factor
0
4
8
12
16
20
Dilution Factor

Figure 12

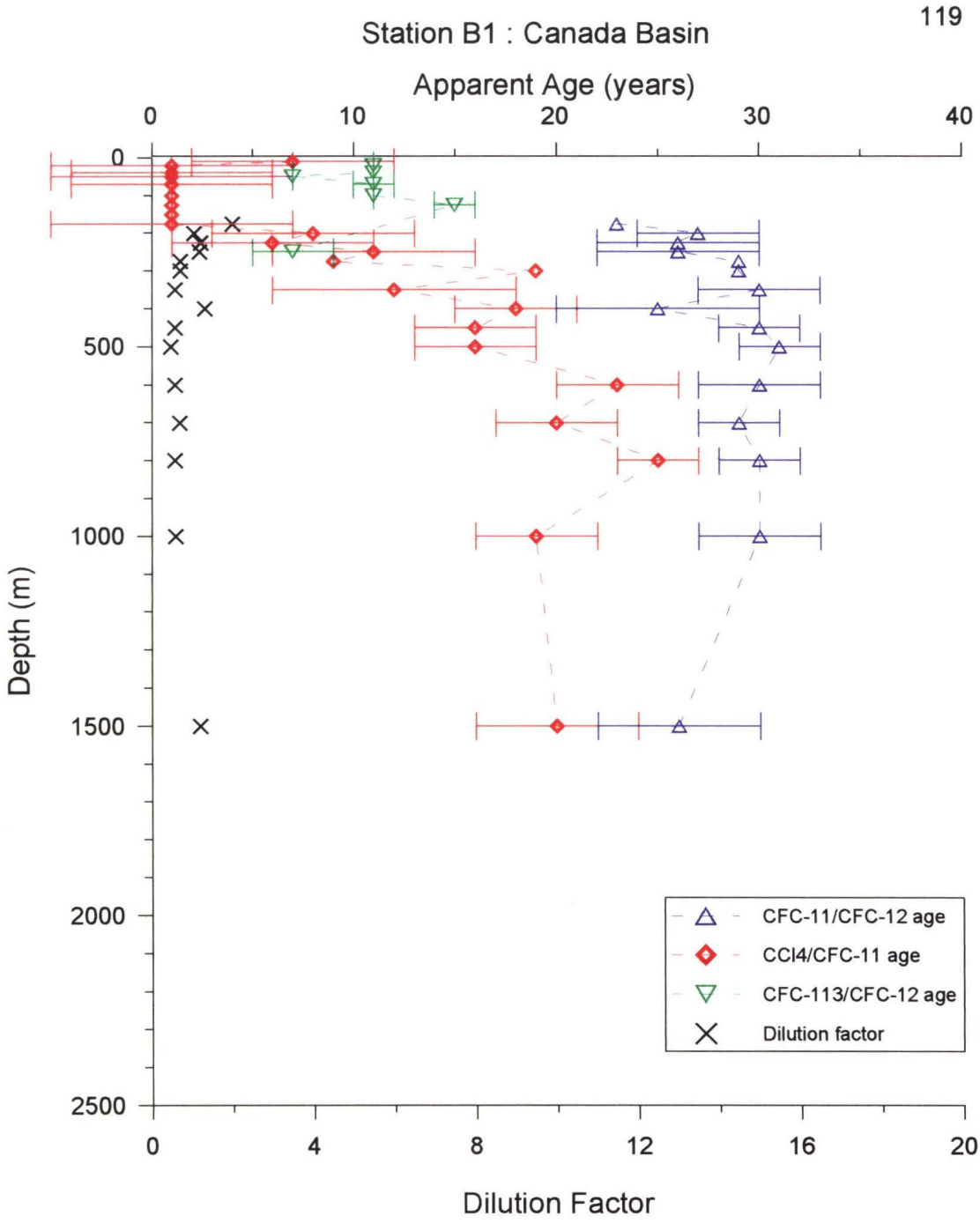
Station B1 : Canada Basin
Apparent Age (years)
0
10
20
30
40
Depth (m)
0
500
1000
1500
2000
2500
0
4
8
12
16
20
Dilution Factor
CFC-11/CFC-12 age
CCl4/CFC-11 age
CFC-113/CFC-12 age
Dilution factor

Figure 13

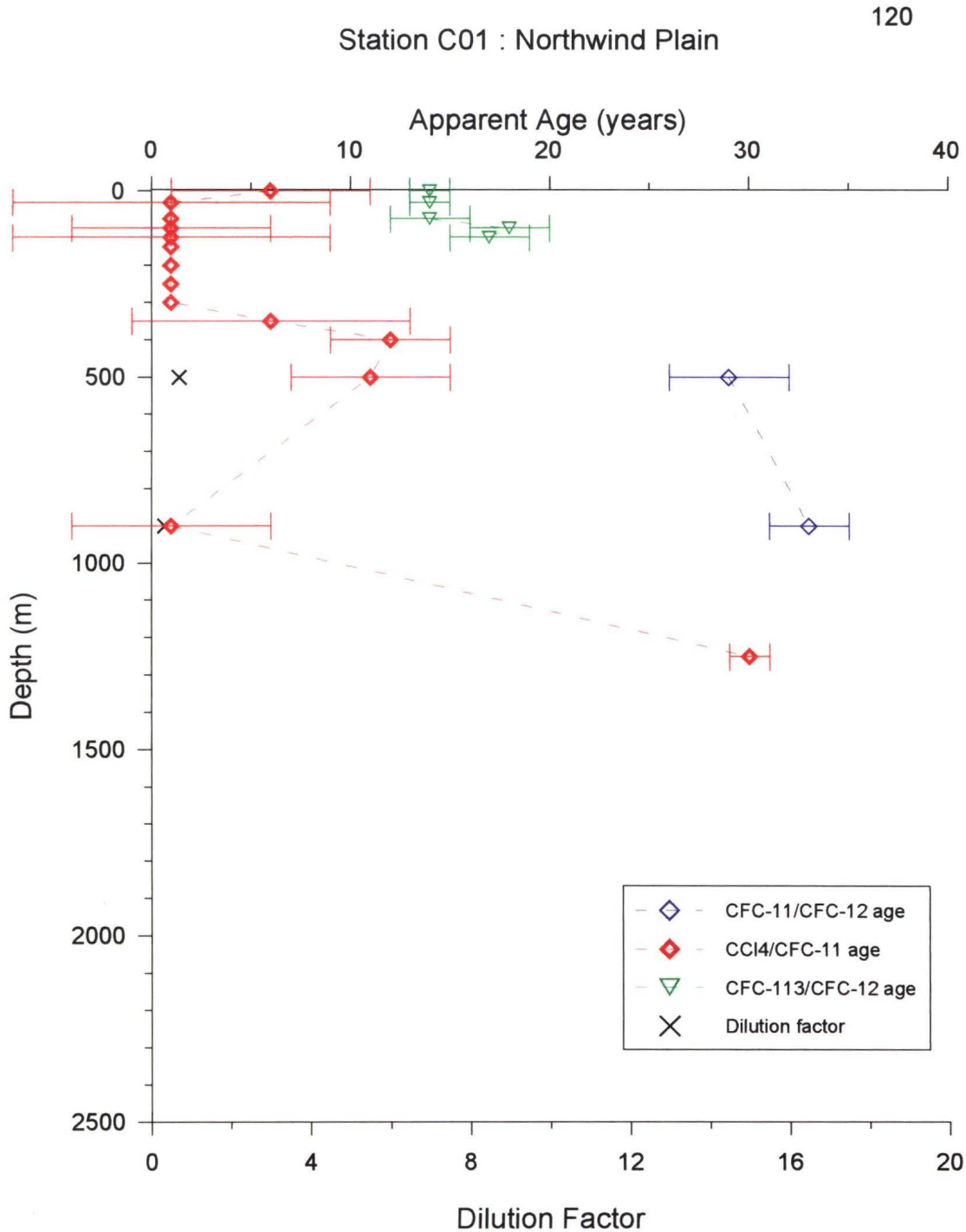
Station C01 : Northwind Plain
Apparent Age (years)
0
10
20
30
40
Depth (m)
0
500
1000
1500
2000
2500
0
4
8
12
16
20
Dilution Factor
CFC-11/CFC-12 age
CCl4/CFC-11 age
CFC-113/CFC-12 age
Dilution factor

Figure 14

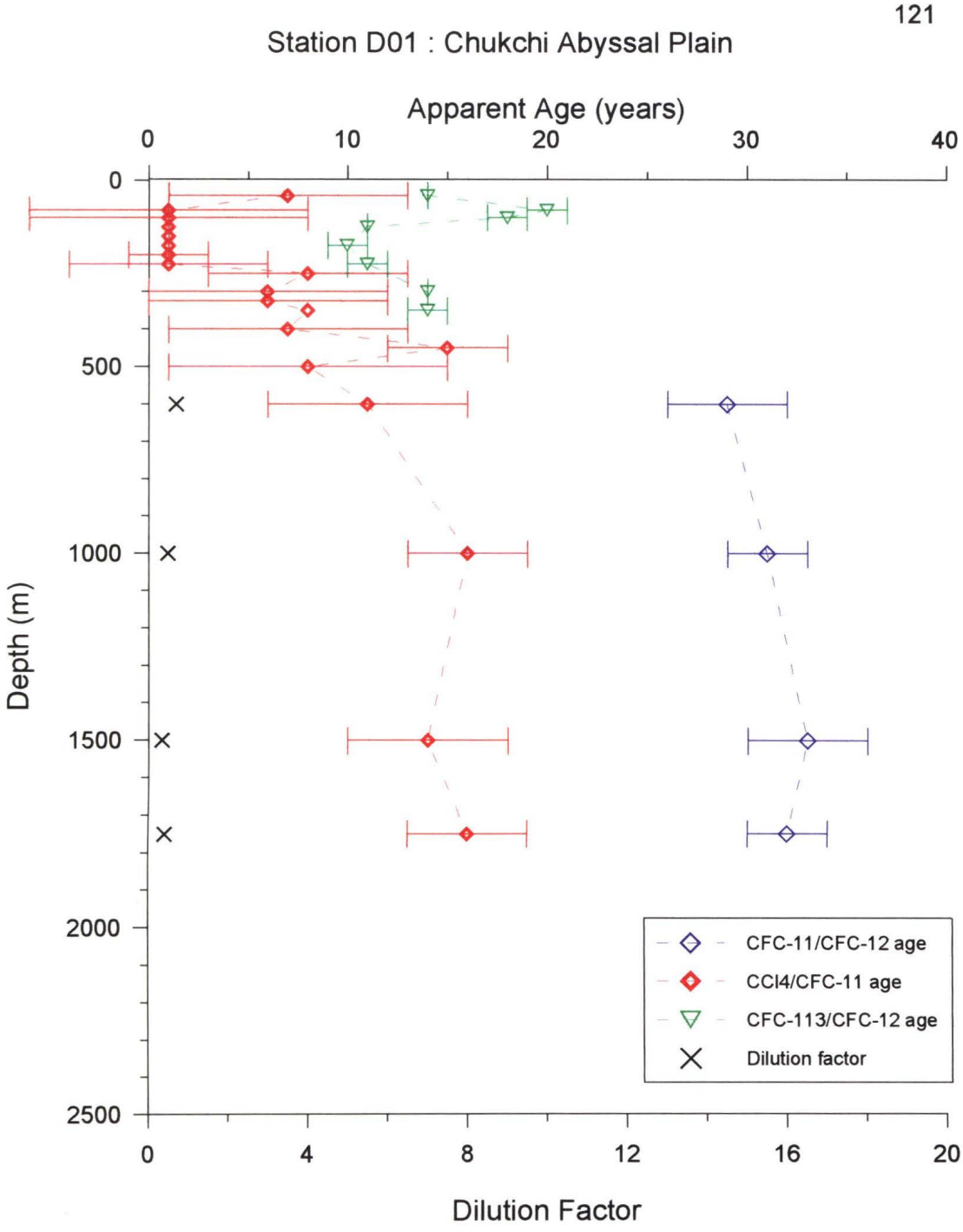
Station D01 : Chukchi Abyssal Plain
Apparent Age (years)
0
10
20
30
40
Depth (m)
0
500
1000
1500
2000
2500
0
4
8
12
16
20
Dilution Factor
CFC-11/CFC-12 age
CCl4/CFC-11 age
CFC-113/CFC-12 age
Dilution factor

Figure 15

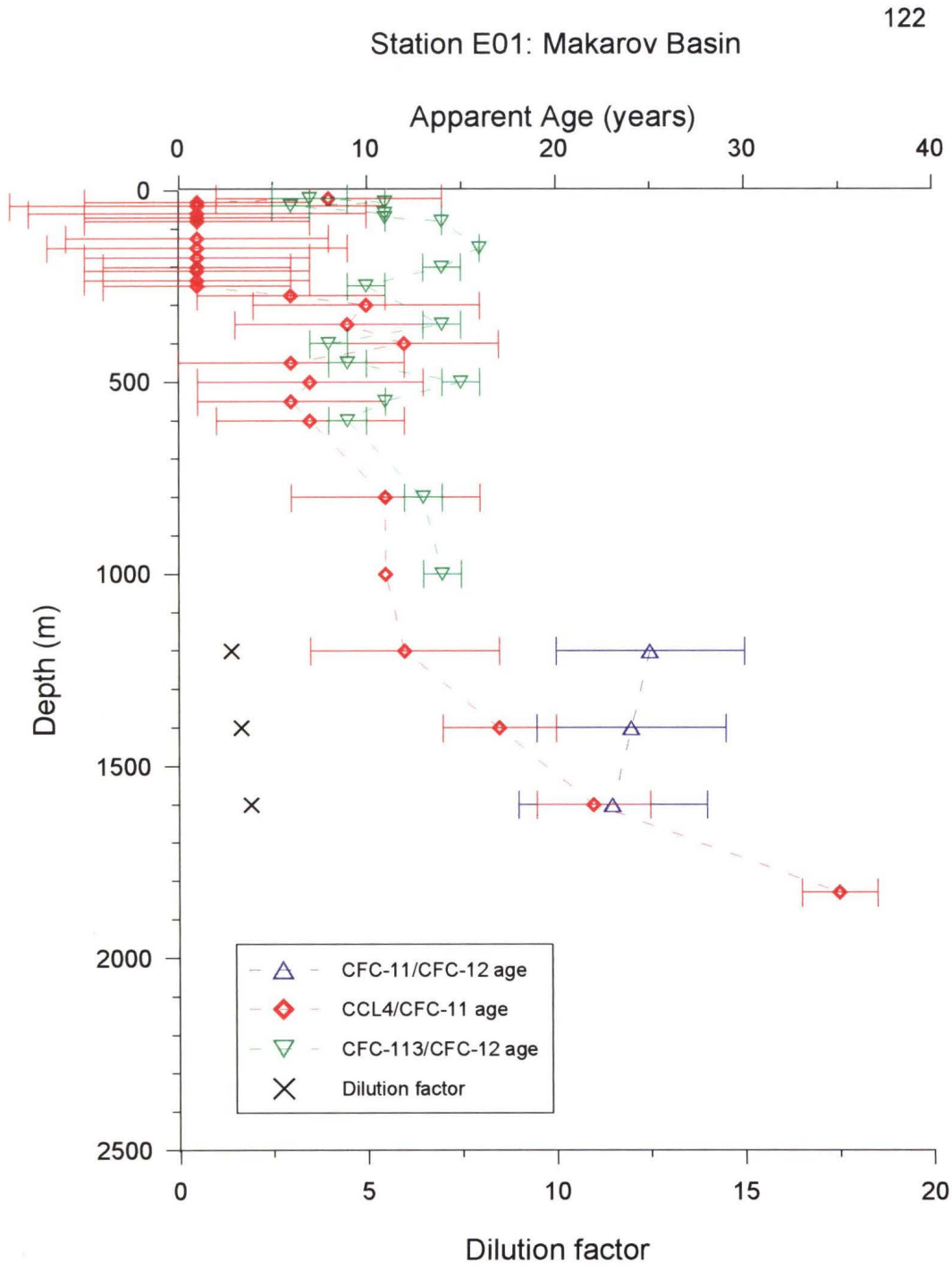
Station E01: Makarov Basin
Apparent Age (years)
0
10
20
30
40
Depth (m)
0
500
1000
1500
2000
2500
0
5
10
15
20
Dilution factor
CFC-11/CFC-12 age
CCL4/CFC-11 age
CFC-113/CFC-12 age
Dilution factor

Figure 16

conservative which suggests that the depletion is not the result of local undersaturation. Evidence of CCl_4 removal has been found in an anoxic fjord (Krysell et al., 1994) and in a low-oxygen region of the open ocean (Wallace et al., 1994). Although halocline waters in both WA and EA assemblies have depleted oxygen concentrations relative to the Atlantic layer, oxygen values are not as low (280 mmol m^{-3}) as those reported by Wallace et al. (1994) in the south Atlantic (<100 mmol m^{-3}). However, Wallace et al. (1994) also suggest that CCl_4 may also be removed by anaerobic bacterial degradation at the sediment-water interface underlying productive regions and this may explain the depletion of CCl_4 in the Arctic halocline region. Halocline waters of the WA assembly found in the Canada Basin spend time crossing the highly productive Chukchi shelf and halocline waters of the EA assembly spend time crossing the highly productive Barents Sea shelf. Perhaps depletion of CCl_4 in arctic waters can be used as a signature of shelf-origin waters.

Non-conservative behaviour of CFC-11 relative to CFC-12 has been found in anoxic and intermittently anoxic locations by Bullister and Lee (1995). They propose additional studies to look for evidence of slow CFC-11 removal in highly productive regions. To date, no study has examined the relative depletion of CCl_4 and CFC-11 halocarbons under low oxygen conditions or in waters underlying productive regions. The conservative behaviour of other halocarbons under such conditions should also be verified.

To determine whether CCl_4 is conservative at all depths in the water column, CFC-12 and CCl_4 calculated atmospheric concentrations are plotted and compared to the historical record (Figures 17 to 21). Data found in the region bound by a mixing line connecting 1940 and 1993 concentrations and the mixing curve of the historical atmospheric record show

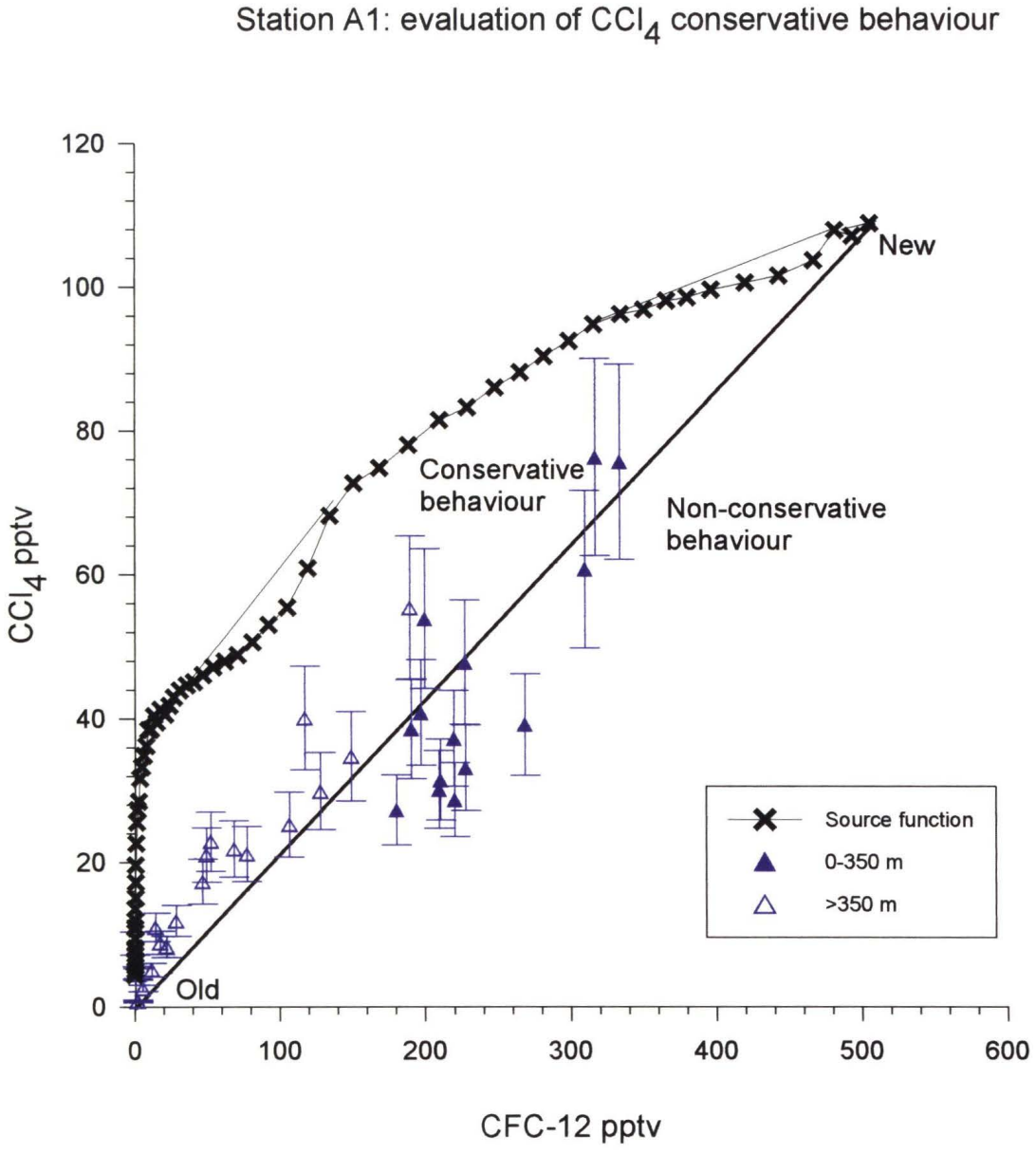
Station A1: evaluation of CCl_4 conservative behaviour
120
100
80
60
40
20
0
CCl_4 pptv
0
100
200
300
400
500
600
CFC-12 pptv
New
Old
Conservative behaviour
Non-conservative behaviour
Source function
0-350 m
>350 m

Figure 17

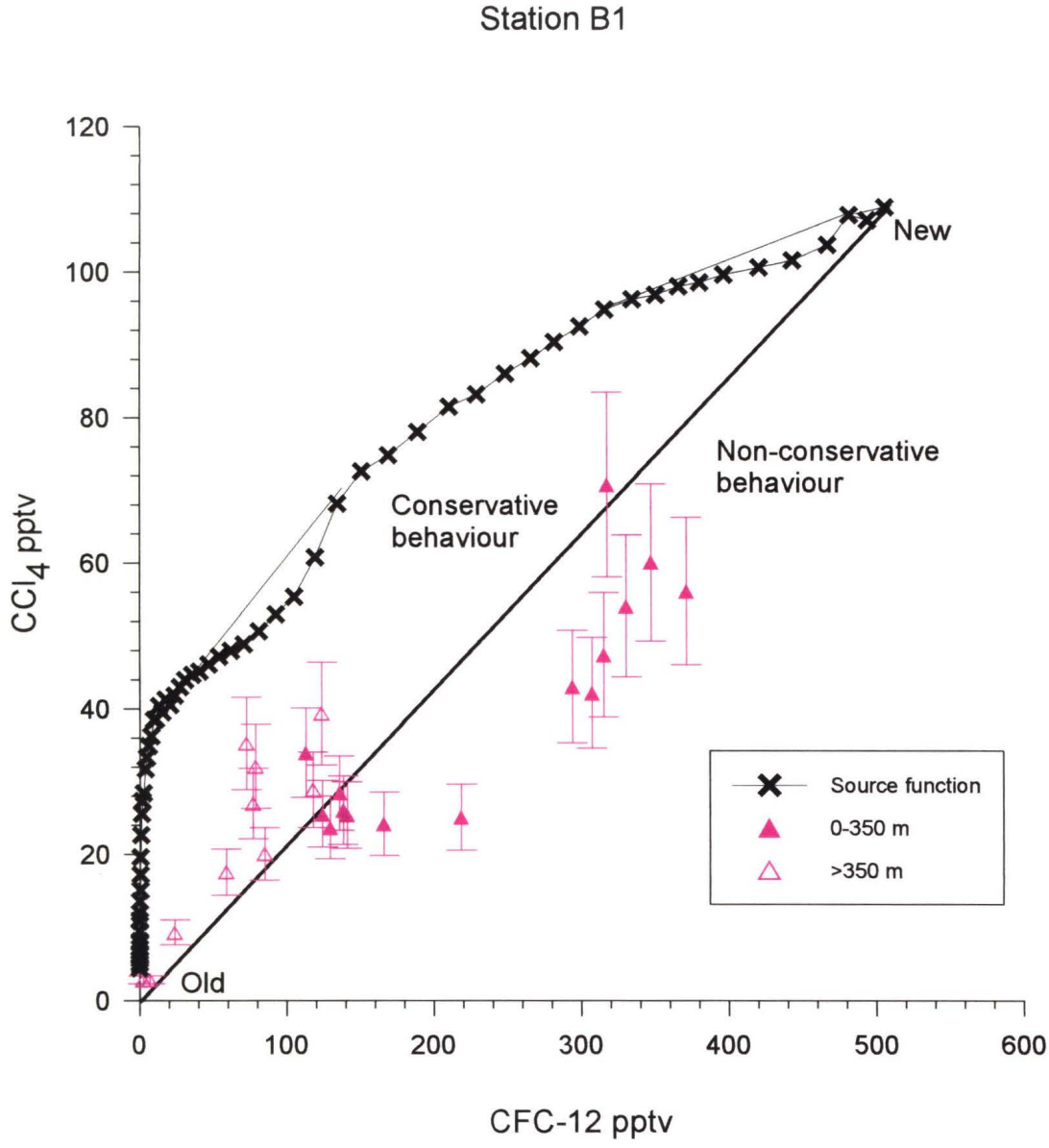
Station B1
120
100
80
60
40
20
0
CCl_4 pptv
0
100
200
300
400
500
600
CFC-12 pptv
New
Old
Conservative behaviour
Non-conservative behaviour
Source function
0-350 m
>350 m

Figure 18

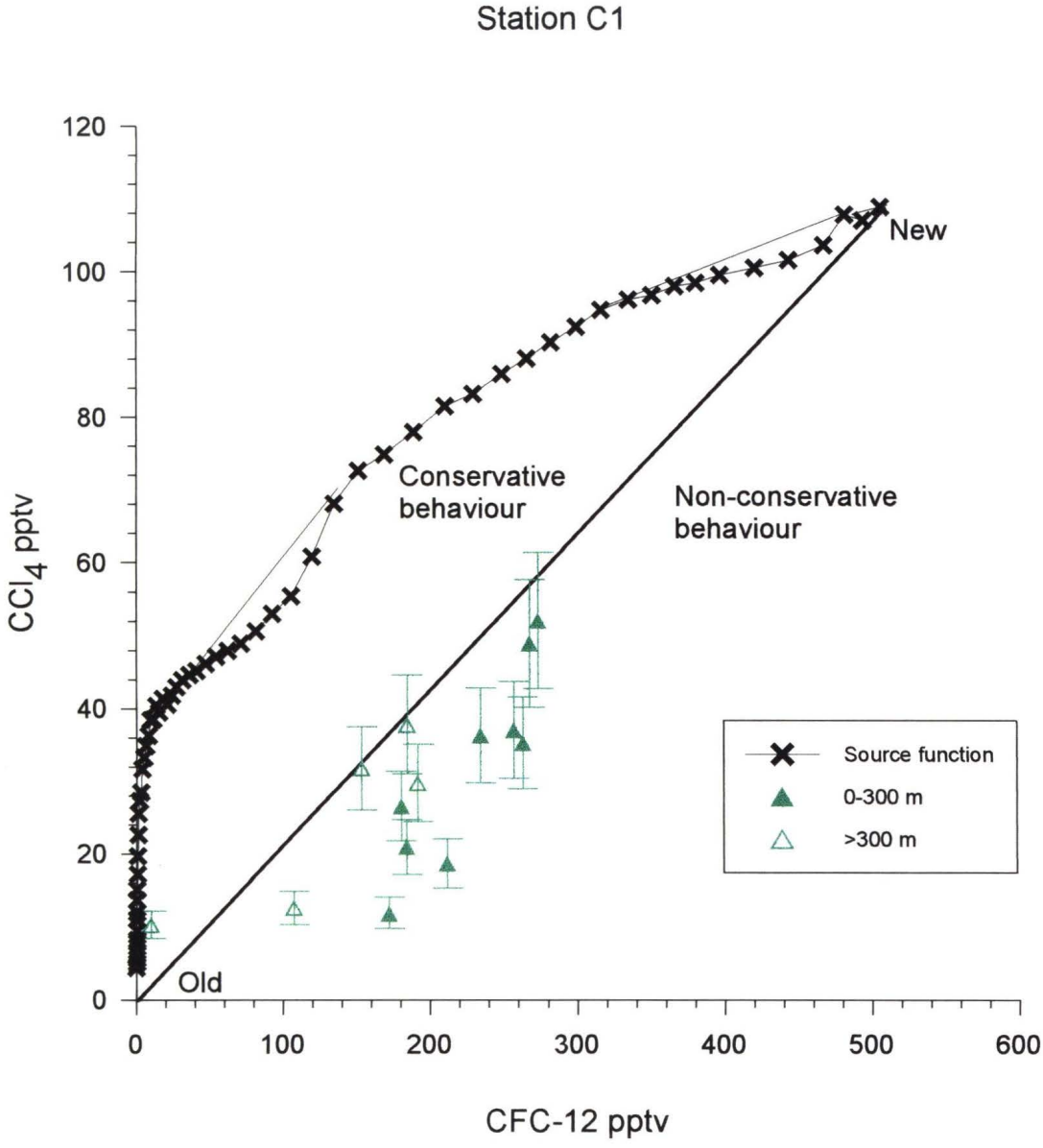
Station C1
120
100
80
60
40
20
0
CCl_4 pptv
0
100
200
300
400
500
600
CFC-12 pptv
New
Old
Conservative behaviour
Non-conservative behaviour
Source function
0-300 m
>300 m

Figure 19

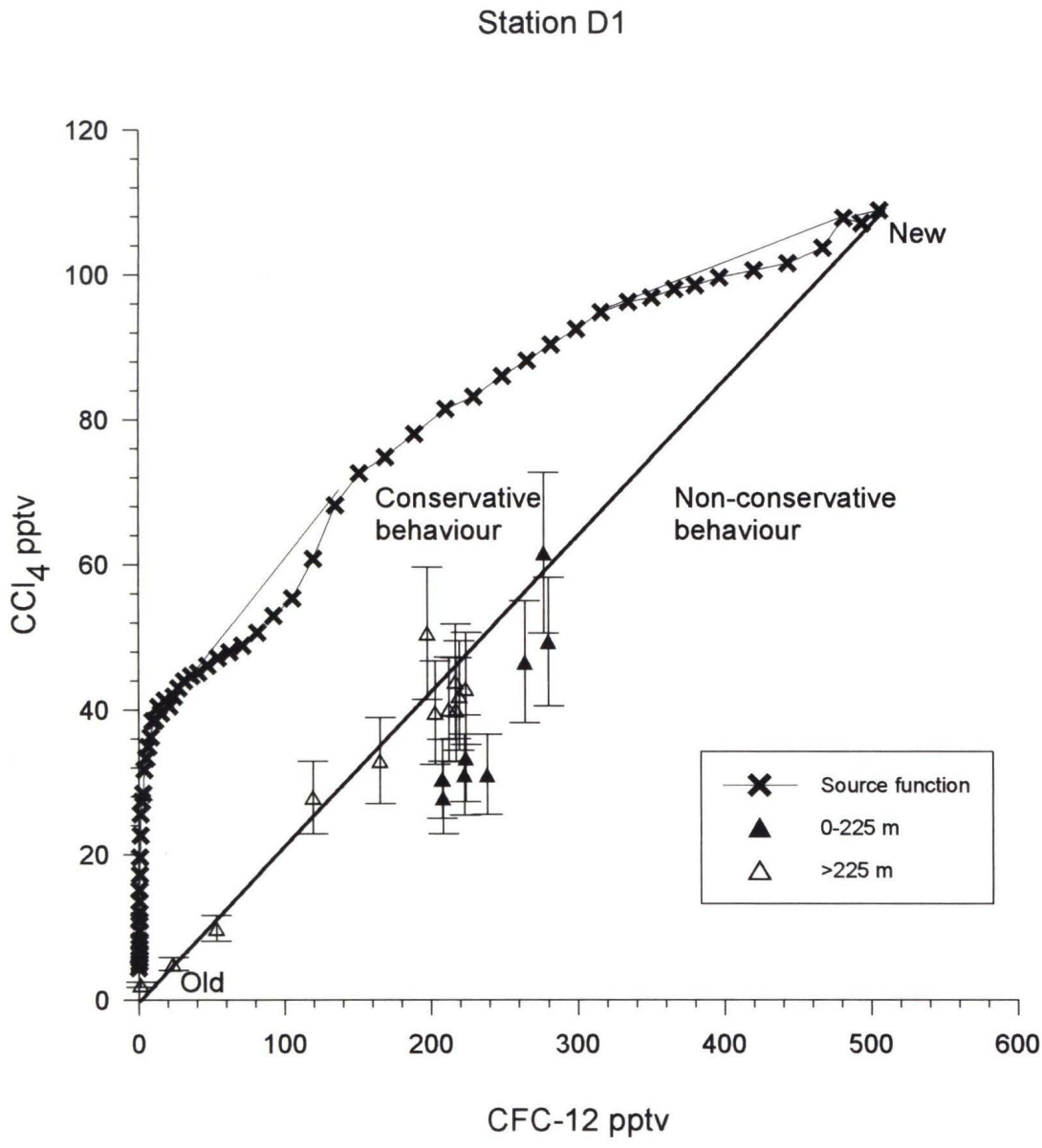
Station D1
120
100
80
60
40
20
0
CCl_4 pptv
0
100
200
300
400
500
600
CFC-12 pptv
New
Old
Conservative behaviour
Non-conservative behaviour
Source function
0-225 m
>225 m

Figure 20

Station E1

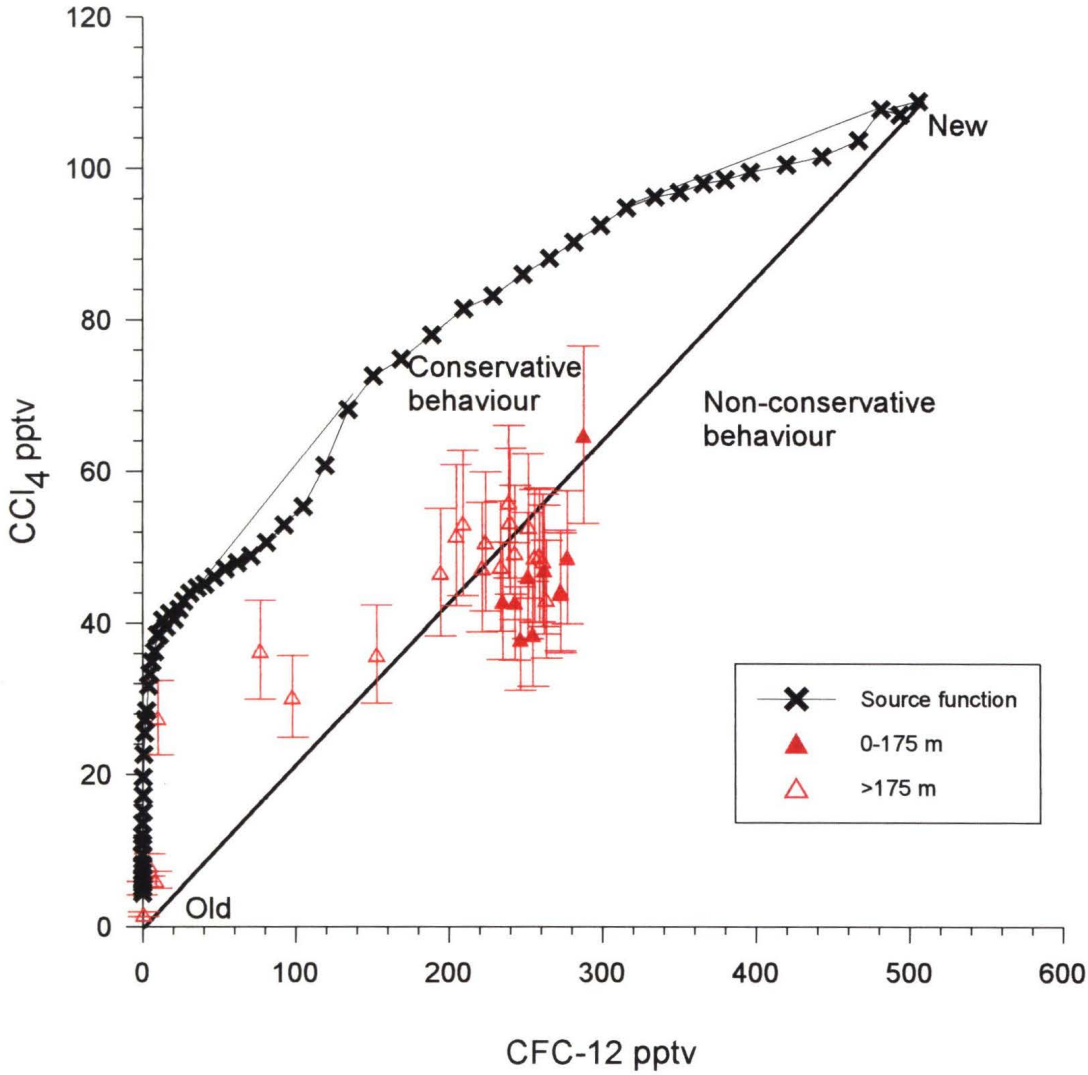

Figure 21

conservative behaviour. Data which lie outside this region, below the old-new mixing line, show non-conservative behaviour and suggest that depletion has occurred. As Figures 17 to 21 illustrate, CCl_4 appears to be non-conservative in the halocline region at all stations.

Figures 12-16 show CFC-113/CFC-12 apparent ages in the upper layer, including the halocline where CCl_4/CFC-11 is not conservative. CFC-12 was paired with CFC-113 to provide apparent age data because non-conservative behaviour of CFC-11 has been reported in the literature. CFC-113 measurements and therefore the ratio data exhibit variations however. CFC-113 elutes in a region that can be influenced by methyl iodide and/or DB-624 contamination. The DB-624 column is very sensitive to the presence of water (a result of breakthrough on the magnesium perchlorate trap) which can cause a shift in the baseline, whereas the methyl iodide peak may cause difficulties in quantitating a small peak on the shoulder of a large peak. Improving the accuracy of CFC-113 measurements is an important future priority because the CFC-113/CFC-12 ratio provides the best means to estimate the apparent age of young waters (< 20 years), particularly since the CCl_4/CFC-11 ratio is increasingly less discriminating in this age range. Nevertheless, in the **Larsen-93** data, where CFC-113/CFC-12 apparent ages were compared to CCl_4/CFC-11 apparent ages, reasonable agreement was found to exist (see Table 1).

Apparent age data for the three main layers in the WA and EA assemblies (Stations A1, B1, and E1) are summarized in Table 1. CCl_4/CFC-11 appparent ages are not reported in the upper layer because of non-conservative behaviour. This summary indicates that the apparent age of surface waters in both assemblies appears to be about 7-10 years, which reflects the isolation of surface waters from the atmosphere due to ice cover. The apparent age of the WA assembly upper

layer is about 7-14 years: in the Atlantic layer it is about 18 years; and at 1900 m, in the transition zone between the Atlantic and deep layers, the apparent age is about 28 years.

Table 1: Apparent Age Estimates

Stn	Depth	S	11/12	CCl_4/11	113/12
A1	0	25	-	11 (1-16)	-
B1	10	27.8	-	7 (1-12)	-
A1	75	32.4	-	-	-
B1	70	32.3	-	-	11 (9-12)
A1	175	33.6	-	-	14 (12-16)
B1	150	33.5	-	-	-
A1	225	34.4	-	-	-
B1	225	34.4	26 (22-28)	-	7 (5-9)
A1	500	34.83	33 (30-34)	18 (13-21)	-
B1	450	34.84	30 (26-32)	16 (11-19)	-
A1	1900	34.94	29 (25-32)	28 (26-30)	-
B1	1500	34.92	26 (23-30)	20 (18-24)	-
E1	20	33.1	-	8 (1-14)	7 (3-8)
E1	70	33.9	-	-	11 (8-12)
E1	275	34.82	-	6 (1-11)	10 (6-11)
E1	800	34.87	-	11 (2-16)	13 (13-14)
E1	1600	34.93	23 (14-28)	22 (19-25)	-

Within the upper, middle and lower regions of the halocline at Station A1, apparent ages of 11, 14 and 6 years appear to contradict earlier discussion about the halocarbon concentration differences in the halocline. However, this discrepancy in expected ages may be due to the effects of mixing, where the apparent age is biased toward the younger

component. In regions of mixing, apparent age data should be interpreted with caution and in conjunction with concentration profiles.

In contrast to apparent ages in the WA assembly, Table 1 shows that apparent ages in EA assembly waters are younger, above 1600 m. The apparent age in the upper layer is about 7 to 11 years: in the Atlantic layer core at 275 m it is about 6-10 years; and, in the transition zone from 800 to 1200 m, the apparent age is about 11-13 years. At Station E1, below 1600 m, the apparent age of 22 years is similar to the apparent age at Station A1 (24 years at 1700 m). This agreement confirms that waters below 1600 m at Station E1 belong to the WA assembly. Figure 22 illustrates how apparent age varies with depth at Stations A1 and E1, and shows that between 300 and 1600 m, waters at Station E1 are markedly younger than at Station A1.

The sparseness of arctic halocarbon data makes it difficult to compare the **Larsen-93** apparent age data with other similar data. Only one set of CFC measurements have been made in waters representative of the WA assembly; this was in 1983 at CESAR (a drifting ice station located above the Alpha Ridge in the Canadian Basin). Based on these measurements, Wallace and Moore (1985) estimated the ventilation age of the halocline at depths between 60-120 m as 5-15 years, and as 30 years for the Atlantic layer. These estimates were based not on calculations, as in the present analysis, but on results derived from two different mixing models. Despite these differences in approach, the two methods are in reasonable agreement with one another.

Since Station E1 features EA assembly characteristics, it can only be inter-compared to data from the Eurasian Basin. To date, the only apparent age data reported from this region was by Wallace et al. (1992) from samples collected aboard the **Polarstern** in the Nansen Basin in 1987.

Comparison of CCl4/CFC-11 Apparent Ages between the Canada Basin (A1) and Makarov Basin (E1)

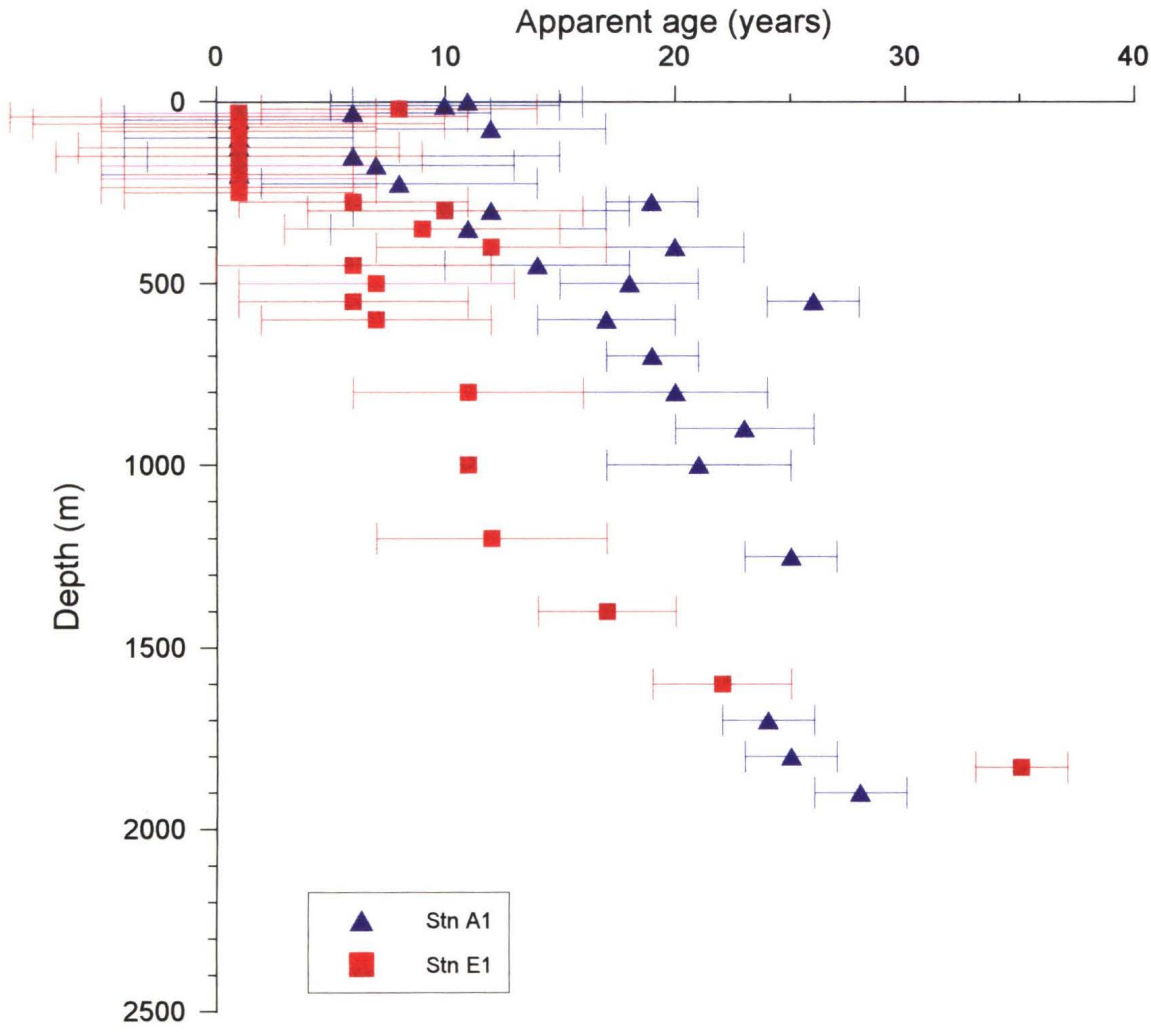

Figure 23

Stations were located in the Barents abyssal plain region of the Nansen Basin, close to the Atlantic Fram Strait Branch inflow. The apparent age of surface water in the middle of the Nansen Basin was reported at 7 years, from tritium/^{3}He measurements. CCl_4/CFC-11 apparent ages in the upper layer were estimated to be from about 5-7 years in the upper halocline to about 14 years at the lower boundary; and, in the Atlantic layer the apparent age was reported to be about 12 years. Given the time that has elapsed since 1987, the geographic separation of the stations, and the recent change in circulation, Nansen Basin apparent ages generally agree with apparent age estimates of waters at Station E1. However, the apparent age of the Atlantic layer in the Makarov Basin in 1993 is younger than that of the Atlantic layer in the Nansen Basin in 1987, which is closer to the region where this layer outcrops at the surface. Changes in arctic ocean circulation between 1987 and 1993, evidenced by the relocation of the Atlantic/Pacific front, may explain this difference in apparent ages.

Analysis of **Larsen-93** data underscore the differences that exist in ventilation and apparent ages between waters in the Canada and Makarov basins. Waters in the Makarov Basin are younger than those in the Canada Basin, and appear to be more rapidly transported from regions of outcropping, a fact of great importance to climate issues involving heat and salt transport within the Arctic Ocean. Further, the rapid transport of the ventilated shelf-origin waters underlying the Atlantic layer may have important implications for the transport of organochlorine and radionuclide contaminants from Eurasian Basin shelves into the Canadian Basin.

References:

Aagaard K. and L. K. Coachman, Toward an ice-free Arctic Ocean,EOS, 56, 484-486, 1975.

Anderson, L. G., E. P. Jones, K. P. Koltermann, P. Schlosser, J. H. Swift and D. R. W. Wallace, The first oceanographic section across the Nansen Basin in the Arctic Ocean, Deep-Sea Res., 36, 475-482, 1990.

Anderson, L. G., G. Bjork, O. Holby, E. P. Jones, G. Kattner, K. P. Koltermann, B. Liljeblad, R. Lindegren, B. Rudels and J. H. Swift, Water masses and circulation in the Eurasian Basin: Results from the ODEN 91 expedition, J. Geophys. Res., 99, 3273-3283, 1994.

Bu, X. and M. J. Warner, Solubility of chlorofluorocarbon 113 in water and seawater, Deep-Sea Res., 42, 1151-1161, 1995.

Bullister, J. L. and B.-S. Lee, Chlorofluorocarbon-11 Removal in Anoxic Marine Waters, Geophys. Res. Lett., 22, 1893-1896, 1995.

Bullister, J. L. and R. F. Weiss, Anthropogenic chlorofluoromethanes in the Greenland and Norwegian Seas, Science, 221, 265-268, 1983.

Cunnold, D. M., P. J. Fraser, R. F. Weiss, R. G. Prinn, P. G. Simmonds, B. R. Miller, F. N. Alyea and A. J. Crawford, Global trends and annual releases of CCl_3F and CCl_2F_2 estimated from ALE/GAGE and other measurements from July 1978 to June 1991, J. Geophys. Res., 99, 1107-1126, 1994.

Fisher, D. A. and P. A. Midgley, Uncertainties in the calculation of atmospheric releases of chlorofluorocarbons, J. Geophys. Res., 99, 16643-16650, 1994.

Gammon, R. H., J. Cline, D. Wisegarver, Chlorofluoromethanes in the Northeast Pacific Ocean: measured vertical distributions and application as transient tracers of upper ocean mixing, J. Geophys. Res., 87, 9441-9454, 1982.

Hunter-Smith, R. J., P. W. Balls, and P. S. Liss, Henry's Law constants and the air-sea exchange of various low molecular weight halocarbon gases, Tellus, 35B, 170-176, 1983.

Jeffers, P. M. and N. L. Wolfe, Hydrolysis of carbon tetrachloride, Science, 246, 1638-1639, 1989.

Krysell, M. and D. W. R. Wallace, Arctic Ocean ventilation studied with a suite of anthropogenic halocarbon tracers, Science, 242, 746-749, 1988.

Krysell, K., E. Fogelqvist and T. Tanhua, Apparent removal of the transient tracer carbon tetrachloride from anoxic seawater, Geopys. Res. Lett., 21, 2511-2514, 1994.

Macdonald, R. W. and E. C. Carmack, Age of Canada Basin deep water: a way to estimate primary production for the Arctic Ocean, Science, 254, 1348-1350, 1991.

Macdonald, R. W., E. C. Carmack and D. W. R. Wallace, Tritium and radiocarbon dating of Canada Basin deep waters, Science, 259, 103-104, 1993.

Molina, M. J. and F. S. Rowland, Stratospheric sink for chlorofluoromethanes: Chlorine atomic-catalysed destruction of ozone, Nature, 249, 810-812, 1974.

Rhein, M., Ventilation rates of the Greenland and Norwegian Sea derived from distributions of the chlorofluoromethanes F11 and F12, Deep-Sea Res., 38, 485-503, 1991.

Roach, A. T., K. Aagaard, C. H. Pease, S. A. Salo, T. Weingartner, V. Pavlov and M. Kulakov, Direct measurement of transport and water properties through Bering Strait, J. Geophys. Res., 100, 18443-18457, 1995.

Rudels, B., E. P. Jones, L. G. Anderson, G. Kattner, "On the intermediate waters of the Arctic Ocean" in The Polar Oceans and Their Role in Shaping the Global Environment: the Nansen Centennial Volume, O. M. Johannessen, R. D. Muench and J. E. Overland, eds., Geophysical Monograph 85, American Geophysical Union, 1994.

Schlosser, P. G. Bonisch, B. Kromer, K. O. Munnich and K. P. Koltermann, Ventilation rates of the waters in the Nansen Basin of the Arctic Ocean derived from a multitracer approach, J. Geophys. Res., 95, 3265-3272, 1990.

Schlosser, P., D. Bauch, R. Fairbanks and G. Bonisch, Arctic river-runoff: mean residence time on the shelves and in the halocline, Deep-Sea Res., 41, 1053-1068, 1994.

Schlosser, P., B. Kromer, H. G. Ostlund, B. Ekwurzel, G. Bonisch, H. H. Loosli and R. Purtschert, On the distribution of ^{14}C and ^{39}Ar in the Arctic Ocean: implications for deep water formation, Radiocarbon, 36, 327-343, 1994.

Wallace, D. W. R. and R. M. Moore, Vertical profiles of CCl_2F_2 (F-12) and CCl_3F (F-11) in the central Arctic Ocean Basin, J. Geophys. Res., 90, 1155-1166, 1985.

Wallace, D. W. R., P. Schlosser, M. Krysell and G. Bonisch, Halocarbon ratio and tritium/^3He dating of water masses in the Nansen Basin, Arctic Ocean, Deep-Sea Res., 39, S435-S458, 1992.

Wallace, D. W. R., P. Beining and A. Putzka, Carbon tetrachloride and chlorofluorocarbons in the South Atlantic Ocean, 19°S, J.Geophys. Res., 99, 7803-7819, 1994.

Warner, M. J. and R. F. Weiss, Solubilities of chlorofluorocarbons 11 and 12 in water and seawater, Deep-Sea Res., 12, 1485-1497, 1985.

Weiss, R. F. and B. A. Price, Nitrous oxide solubility in water and seawater, Mar. Chem.,8, 347-359, 1980.

Wisegarver, D. P. and R. H. Gammon, A new transient tracer; measure vertical distribution of CCl_2FCClF_2 (F-113) in the North Pacific subarctic gyre, Geophys. Res. Lett., 15, 188-191, 1988.

World Meteorological Organization (WMO), The Montreal Protocol on substances that deplete the ozone layer, WMO Bull., 37, 94-97, 1988.

Chapter 5: Shelf Processes

Samples were collected at three shelf/slope stations along a 400 km section from the Chukchi Shelf to the Makarov Slope on the **Larsen-93** cruise. Although these stations were selected primarily to collect sediment samples for contaminant analysis, they also provided an opportunity to look for evidence of shelf processes in a region previously unsampled by western investigators. Accordingly, temperature, salinity, nutrients, oxygen, and halocarbon samples were collected at one shelf station (F09), and two slope stations (TA/TC and E04). Station F09 is located on the Chukchi Shelf with a bottom depth of 90 m; Stations TA and TC are located on the Chukchi slope at 650 m; and Station E04 is located near the East Siberian Sea on the Makarov Basin slope at 800 m. Geographic locations, sampled during September 1993, as well as descriptions of sample collection and measurement techniques are reported in Chapter 2.

Discussion of these data is divided into three parts. Part one examines geochemical properties of the samples collected at the three stations for evidence of the Atlantic/Pacific front and provides further spatial definition of this boundary. Part two summarizes modification processes that take place on arctic shelves and are believed to contribute to the maintenance of the arctic halocline. Geochemical properties at each of the three stations are examined to determine if evidence of these shelf processes can be found. The final part focuses on halocarbon data from the three stations, and first, examines percent halocarbon saturation to determine conservative

behaviour and, then, reports apparent age estimates.

5.1 Evidence of the Atlantic/Pacific Water Mass Boundary

Based on analysis of data collected at five basin stations, Chapter 3 provided evidence that the Atlantic/Pacific water mass boundary had shifted from a location above the Lomonosov Ridge, observed in 1979 during **LOREX**, to a location above the Mendeleyev Ridge, observed in 1993. It is reasonable to ask if this water mass boundary extended to shelf and slope waters in the Chukchi and East Siberian Seas in 1993. The spatial extent of the boundary has implications for the nature of circulation in the Arctic Ocean as well as for biological activity in the region. Whether the waters of the East Siberian shelf are of Atlantic (EA assembly - low nutrient) rather than Pacific (WA assembly - high nutrient) origin determines their potential productivity.

Chapter 3 established that silicate and potential temperature are the tracers most useful in delineating the Atlantic/Pacific water mass boundary. In the WA assembly, high concentrations of silicate are found at depths between 100 and 175 m and the temperature maximum of the Atlantic layer is found near 400 m; in the EA assembly, there are no high silicate concentrations and the temperature maximum is found near 200 m. Figure 1a presents a vertical section of silicate data collected at the three shelf stations. From the low concentrations of silicate present, this figure clearly illustrates that EA assembly waters are found at Station E04. Similarly, from the high concentrations of silicate present, WA assembly waters are equally evident at Stations F09. Station TA/TC is located within the water mass front, a transition zone where both assemblies are present. At Station TC from the surface to 75 m (and also

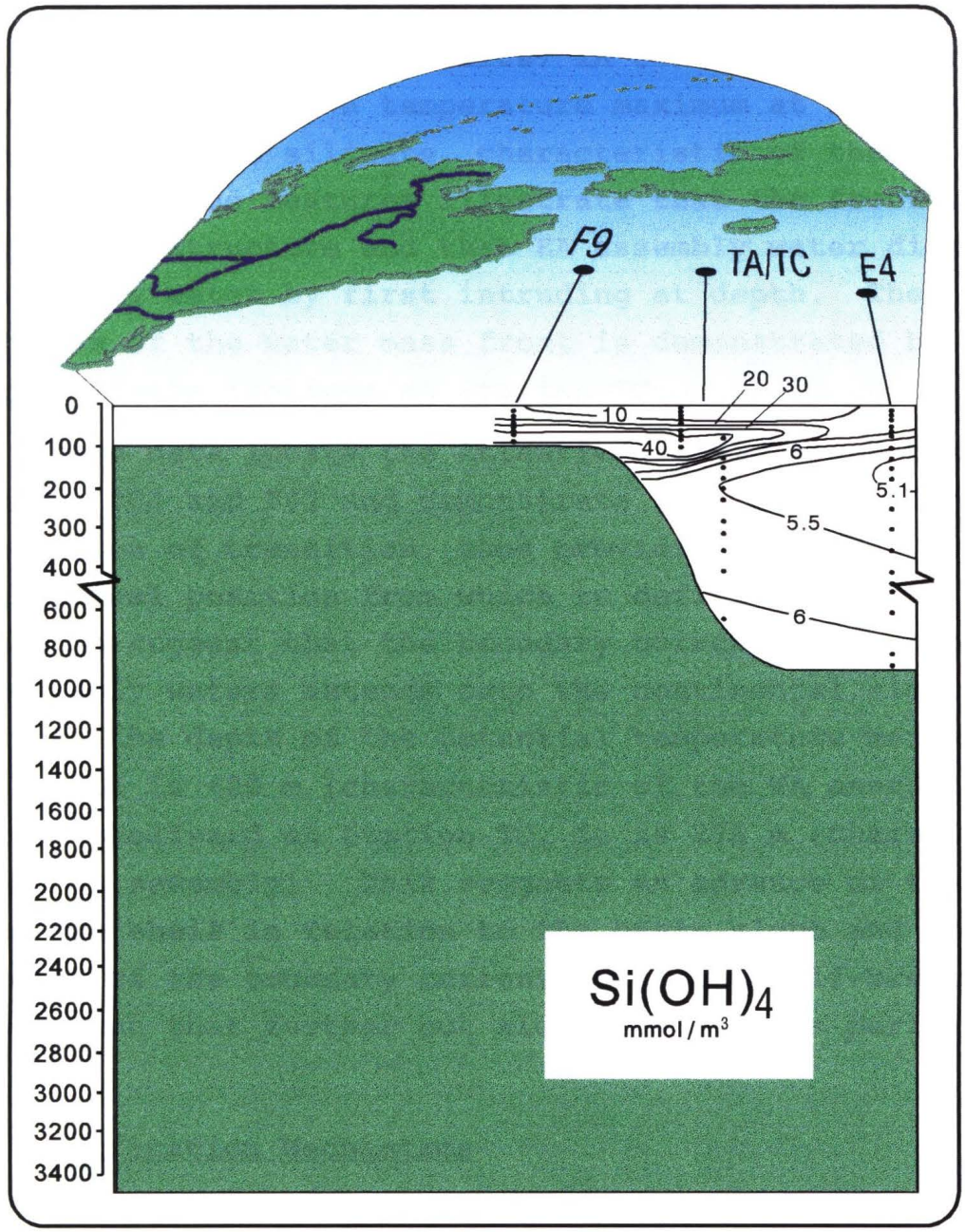
F9
TA/TC
E4
20
30
10
40
6
5.1
5.5
6
0
100
200
300
400
600
800
1000
1200
1400
1600
1800
2000
2200
2400
2600
2800
3000
3200
3400
Si(OH)4
mmol / m3

Figure 1(a)

0-100 m at Station TA), the waters are cold, exhibit a local temperature maximum near 70 m (Figure 1b) and are silicate rich, all features that reflect a Pacific origin influence and WA assembly characteristics. In contrast, at Station TC below 75 m, there is a temperature maximum at 275 m and the waters are low in silicate, characteristic of the EA assembly. These features illustrate that the front is not vertical in structure and that EA assembly water displaces WA assembly water by first intruding at depth. The sharpness of the water mass front is demonstrated by the steep silicate isolines at Station TC.

These data locate the Atlantic/Pacific front between Stations E04 and F09 and demonstrate that Station TA/TC is in a region of transition, thus providing a second geographical position from which to define the front. The data also suggest that the boundary current which transports EA assembly waters extends onto the continental slope. Further, the depth of the potential temperature maximum at Station D1 is 400 m (characteristic of the WA assembly), whereas shelfward at Station TC, it is 275 m (characteristic of the EA assembly). This suggests an advance of the front along the shelf in relation to the basin slope and that the velocity of the boundary current near the shelf-break may be higher than that further out along the basin's perimeter.

5.2 Modification Mechanisms

Two main seasonal processes influence shelf water mass characteristics in the Arctic Ocean: ice formation in winter, and biological activity in summer. Although riverine inputs are a significant contributor of fresh water onto Arctic shelves, it is not a significant component of the upper layer at the three stations (about 7-8%; S=29.8 to S=32).

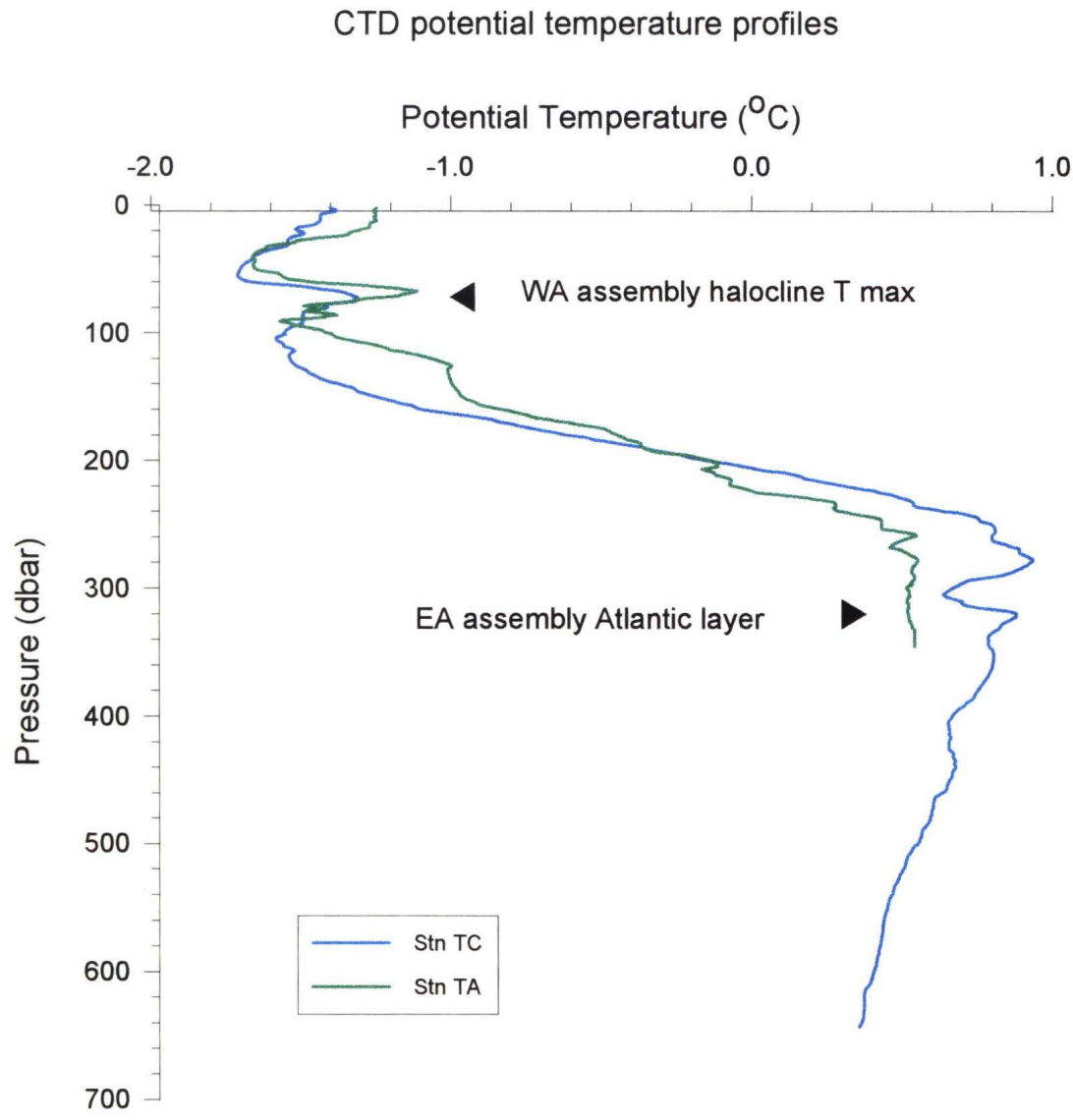
CTD potential temperature profiles
Potential Temperature (°C)
-2.0
-1.0
0.0
1.0
0
100
200
300
400
500
600
700
Pressure (dbar)
WA assembly halocline T max
EA assembly Atlantic layer
Stn TC
Stn TA

Figure 1b

5.2.1 Ice and Dense Water Formation

Ice and brine are formed most rapidly in regions of open water (polynyas) during cold northern winters. Ice formed in polynyas can be easily exported by offshore winds, thus enabling further production of ice. Polynyas are believed to contribute relatively large amounts of brine to the arctic halocline because of repeated freezing and export cycles. They form primarily above shallow coastal shelves, and one such polynya site observed in the Chukchi Sea in the Canadian Basin (Cavalieri and Martin, 1994) is where Stations F09 and TA/TC are located .

When ice forms from seawater, dissolved salts (brine) are excluded from the ice crystal structure. This exclusion produces ice with a lower salinity (from S<1 to S=9) than is found in the surrounding seawater. Enriched by brine, the cold underlying seawater is denser than the surrounding water and therefore sinks, sometimes to the bottom of the shelf. With the formation of every metre of ice, salinity in the top 50 m is estimated to increase by S=0.6: in a region of ice export, the salinity could increase by S=1.2 (Melling and Lewis, 1982).

Recently convected water as a result of brine fomation can be identified by the concurrence of elevated salinities, near freezing point temperatures and surface dissolved gas concentrations at depth. Although nutrients are excluded along with salts during ice formation, nutrient levels are too variable to be used to unambiguously identify brine induced convection. For example, ice can form from water depleted in nutrients by summer productivity or from winter water replenished by inflowing nutrient-rich waters and/or regeneration.

Although brine enriched waters have been observed by several investigators (Aagaard et al., 1981; Melling and

processes as well as in-situ processes.

5.3 Evidence of Modification at Larsen-93 Shelf Stations

Station F09, located on the Chukchi Shelf near Herald Canyon, illustrates water mass properties characteristic of the WA assembly. Salinity is low (S<30) in the top 12 m, due to freshwater inputs from ice melt and/or river runoff (Figure 2). From 12-20 m, salinity increases rapidly to S=32, before gradually increasing to S=32.75 at 75 m. A sharp break occurs between 75 m and 85 m where salinity increases from S=32.75 to S=34.2. In contrast, temperature decreases from the surface to a minimum at 60 m then, at 75 m, increases rapidly from about -1.6 °C to -0.65 °C at 85 m. Halocarbon data in Figure 3 shows high concentrations from the surface to 75 m, and a break to low concentrations at 85 m. For example, the CFC-11 concentrations are high (4.6 to 4.9 nmol m^{-3}) from the surface to 75 m then decrease abruptly to 2.2 nmol m^{-3} at 85 m.

A temperature minimum at 60 m, and the well-oxygenated overlying waters, point to 60 m as the depth of the previous winter mixed layer. In spring, assuming that 60 m was the depth of the winter mixed layer, the water column from the surface to 60 m would be homogeneously mixed and the water column from 0-60 m would have oxygen concentrations of 300 mmol m^{-3}, and nutrient concentrations (Figure 4) of NO_3=14.6 mmol m^{-3}, PO_4=2.12 mmol m^{-3} and $Si(OH)_4$=46 mmol m^{-3}. These concentrations, however, are not observed from 0-60 m. Above 60 m, oxygen increases from 300 to 380 mmol m^{-3} at 25 m and to 410 mmol m^{-3} at the surface (Figure 2). This increase in oxygen is related to biological productivity. Below 75 m, however, oxygen decreases markedly to 250 mmol m^{-3} at 85 m. The three nutrient profiles show depletion from the surface to about 50-60 m, which suggests biological uptake

Lewis, 1982; Midttun, 1985; Melling and Moore, 1995), rates of formation and spatial influence of these waters are unknown. Sampling at different times of the year may also influence interpretations. For example, sampling in late summer in the Chukchi Sea may not provide evidence of dense water formed during the previous winter if the dense water has already flowed off the shelf. Such evidence, however, has been observed in the Barents Sea in August (Middtun,1985).

5.2.2 Biological activity

In the Arctic Ocean, biological activity increases significantly during spring and summer when daylight returns. River breakup and the resulting freshwater flow, combined with warmer temperatures, causes ice to melt along the ocean shoreline. This frees the ice to move offshore, and allows light to penetrate the surface layers. In addition to light, the presence of nutrients is also required for biological activity. Nutrients are found in surface waters as a result of inflow of Pacific origin waters through Bering Strait and river water, as well as from the regeneration and mixing that occurs within the upper layer of the water column during winter.

During the summer, nutrients are consumed by biological activity. When phytoplankton and zooplankton complete their life cycles, nutrients are regenerated in the presence of oxygen. Regeneration consumes oxygen and releases nutrients throughout the water column but at depth the rate of nutrient release exceeds that of uptake. Accordingly, low nutrients and high oxygen in the photic zone constitute evidence of biological activity and, deeper in the water column, a nutrient maximum and oxygen minimum denote regeneration. These features may be the result of advective

to these depths. In the top 12 m, nitrate is completely depleted whereas phosphate and silicate concentrations are low. This implies that nitrate is the nutrient that limits production at this station.

Figures 2, 3, and 4 illustrate a difference in the water properties between waters from the surface to 75 m and waters at 85 m. An increase in salinity between 75 and 85 m cannot be interpreted as the product of brine drainage because it is not accompanied by high (surface) concentrations of either oxygen or halocarbons. The presence of water with these characteristics might be explained by upwelling (caused by offshore winds) which transports deeper offshore waters up onto the shelf. Accordingly, to determine whether upwelling has occurred, water mass properties from Station F09 at 85 m were compared with water mass properties from Stations A1 and B1 (Table 1).

Table 1: Water column properties at Stations A1, B1 and F09

	A01	A01	A01	B01	B01	F09
Salinity	33.9	34.1	34.3	34.0	34.2	34.3
Theta °C	-1.1	-0.9	-0.7	-1.0	-0.8	-0.7
Oxygen mmol m^{-3}	279	270	268	275	273	244
CFC-11 nmol m^{-3}	-	2.54	-	2.58	1.87	2.1
NO_3 mmol m^{-3}	15.2	14.8	14.4	15.3	13.6	14.4
PO_4 mmol m^{-3}	1.69	1.49	1.37	1.59	1.35	1.8
$Si(OH)_4$ mmol m^{-3}	28.4	24.6	22.2	27.6	19.8	33.6
Depth m	192	202	212	180	205	87

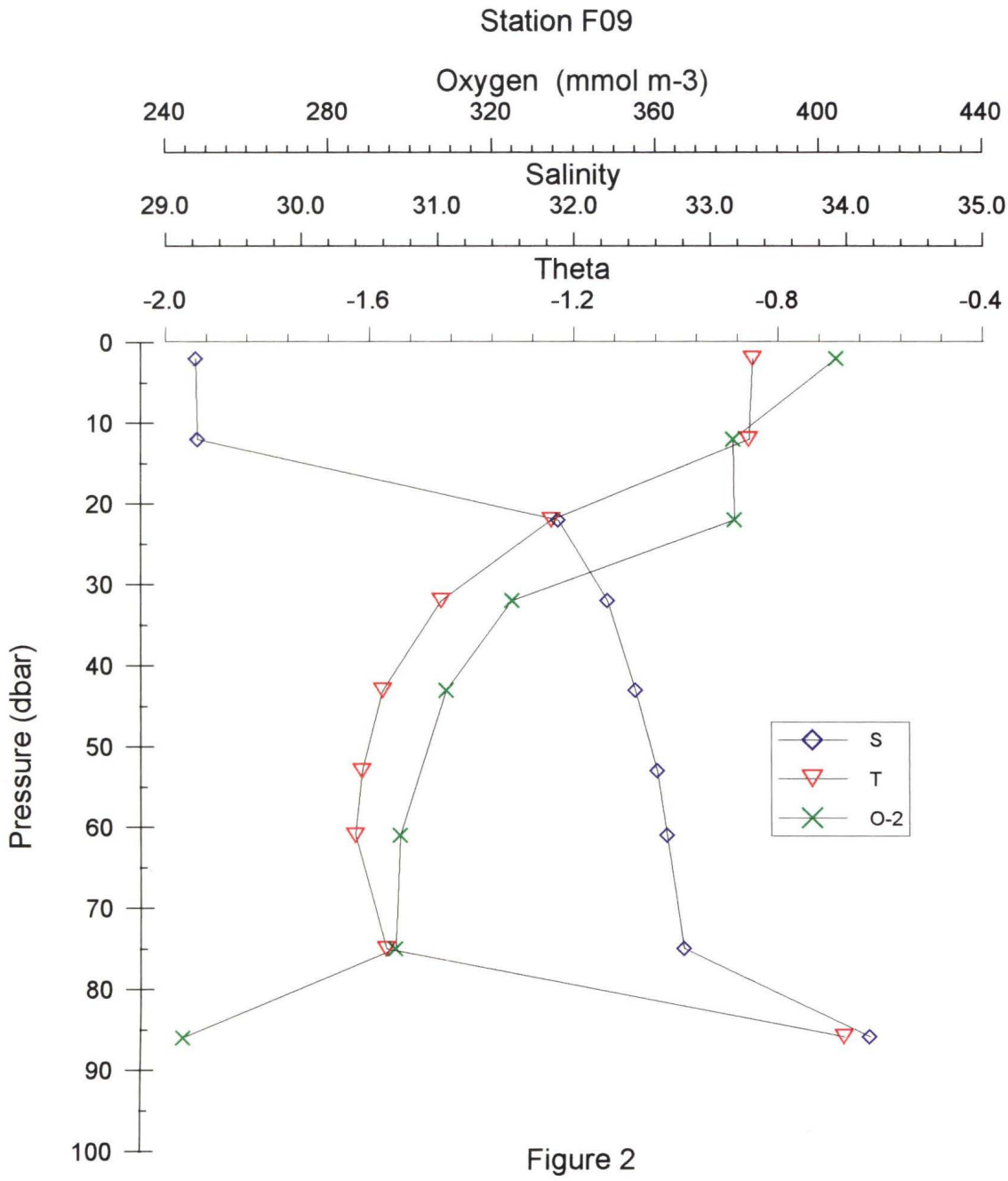
Station F09
Oxygen (mmol m-3)
240
280
320
360
400
440
Salinity
29.0
30.0
31.0
32.0
33.0
34.0
35.0
Theta
-2.0
-1.6
-1.2
-0.8
-0.4
Pressure (dbar)
0
10
20
30
40
50
60
70
80
90
100
S
T
O-2

Figure 2

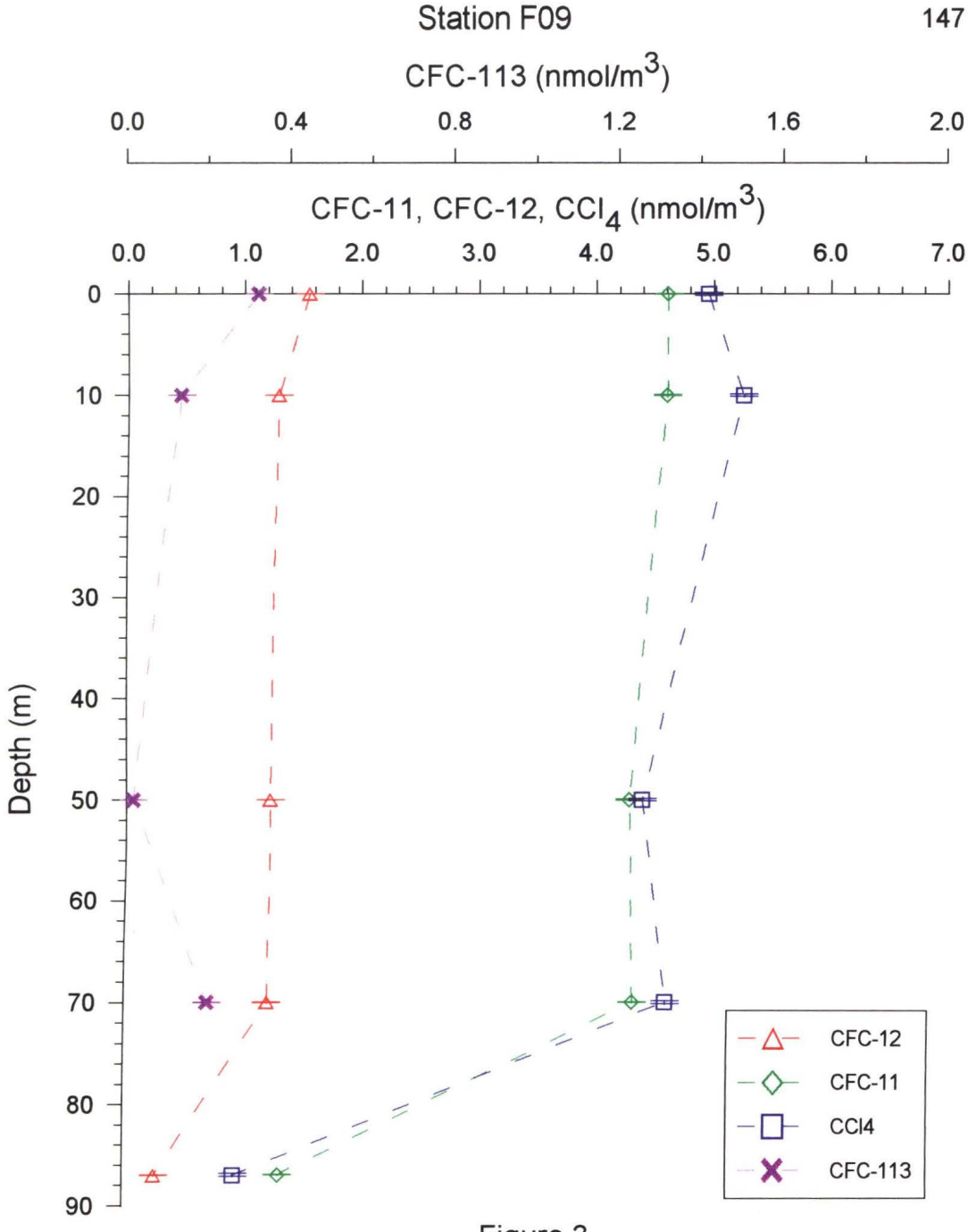
Station F09
CFC-113 (nmol/m3)
0.0
0.4
0.8
1.2
1.6
2.0
CFC-11, CFC-12, CCl4 (nmol/m3)
0.0
1.0
2.0
3.0
4.0
5.0
6.0
7.0
Depth (m)
0
10
20
30
40
50
60
70
80
90
CFC-12
CFC-11
CCl4
CFC-113

Figure 3

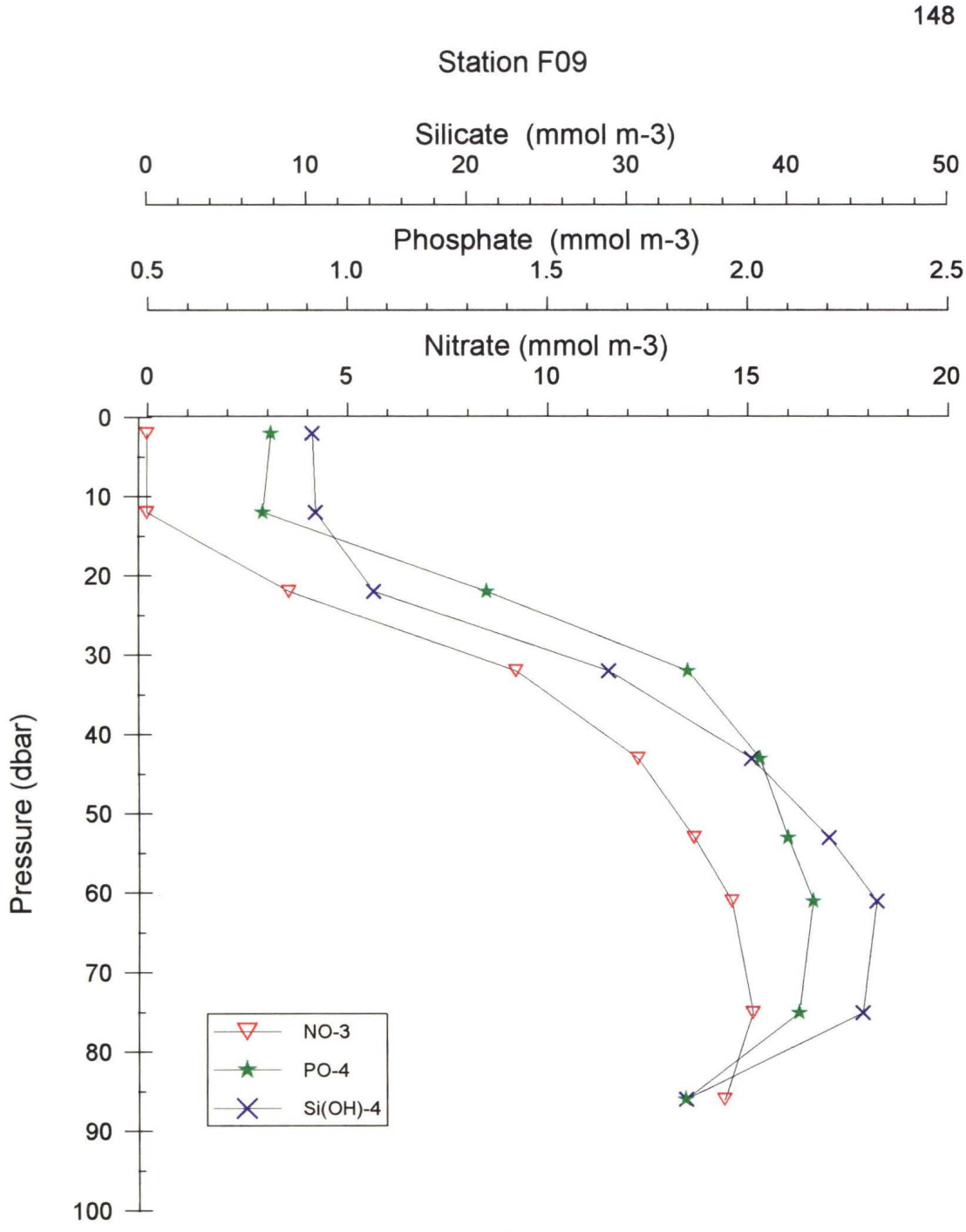
Station F09
Silicate (mmol m-3)
0
10
20
30
40
50
Phosphate (mmol m-3)
0.5
1.0
1.5
2.0
2.5
Nitrate (mmol m-3)
0
5
10
15
20
Pressure (dbar)
0
10
20
30
40
50
60
70
80
90
100
NO-3
PO-4
Si(OH)-4

Figure 4

This comparison demonstrates that waters with properties found at 85 m depth at Station F09 are similar to those between 180 and 200 m at Stations A1 and B1 and suggests that water at 85 m at Station F09 has upwelled from the lower halocline region of the WA assembly (S=34.2). (Note that data from Station C01, located closer to Station F09, could not be compared with data from Station F09, because the Atlantic/Pacific water mass front is evident at 200 m at Station C1). In summary, Station F09 provides evidence of biological processes and upwelling but no evidence of dense water formation. This suggests that if dense water did form during the previous winter, it had flowed off the shelf prior to the sampling in September.

The second station to be examined is a slope station, Station TA/TC, situated on the slope between the Chukchi Shelf and the Chukchi abyssal plain. This is a composite station located within the water mass front: at Station TA samples were collected from the surface to 100 m and, at Station TC 30 km away, from 75 m to 630 m. Station TA exhibits WA assembly characteristics (high nutrient concentrations) at least down to 100 m, whereas below 75 m, Station TC exhibits EA assembly characteristics (low nutrient concentrations).

Salinity at Station TA is low in surface waters (to 10 m), then increases from S=32 at 20 m to S=33.4 at 80 m (Figure 5). Temperature decreases from the surface to a minimum at 30 m, increases to a maximum at 50 m and, then, decreases to 80 m. The maximum reflects the advection of warm water. Oxygen decreases from the surface to depth, with a local oxygen minimum present at 50 m, the depth of the temperature maximum. Representative of the four halocarbon profiles (Figure 6), CFC-11 decreases from about 5 nmmol m^{-3} at the surface to 4.6 nmolm^{-3} at 80 m, concentrations which denote recent ventilation.

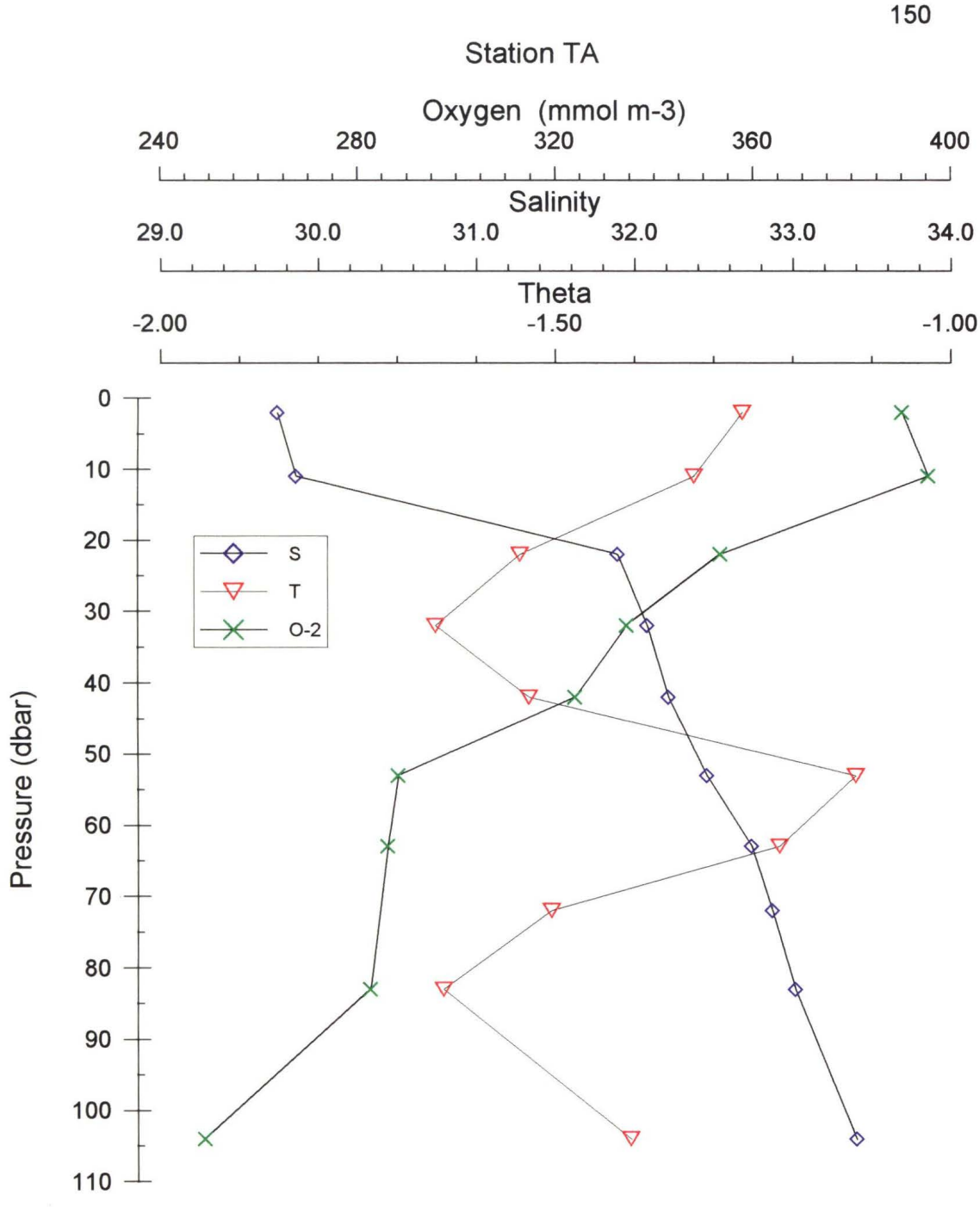
Station TA
Oxygen (mmol m-3)
240
280
320
360
400
Salinity
29.0
30.0
31.0
32.0
33.0
34.0
Theta
-2.00
-1.50
-1.00
Pressure (dbar)
0
10
20
30
40
50
60
70
80
90
100
110
S
T
O-2

Figure 5

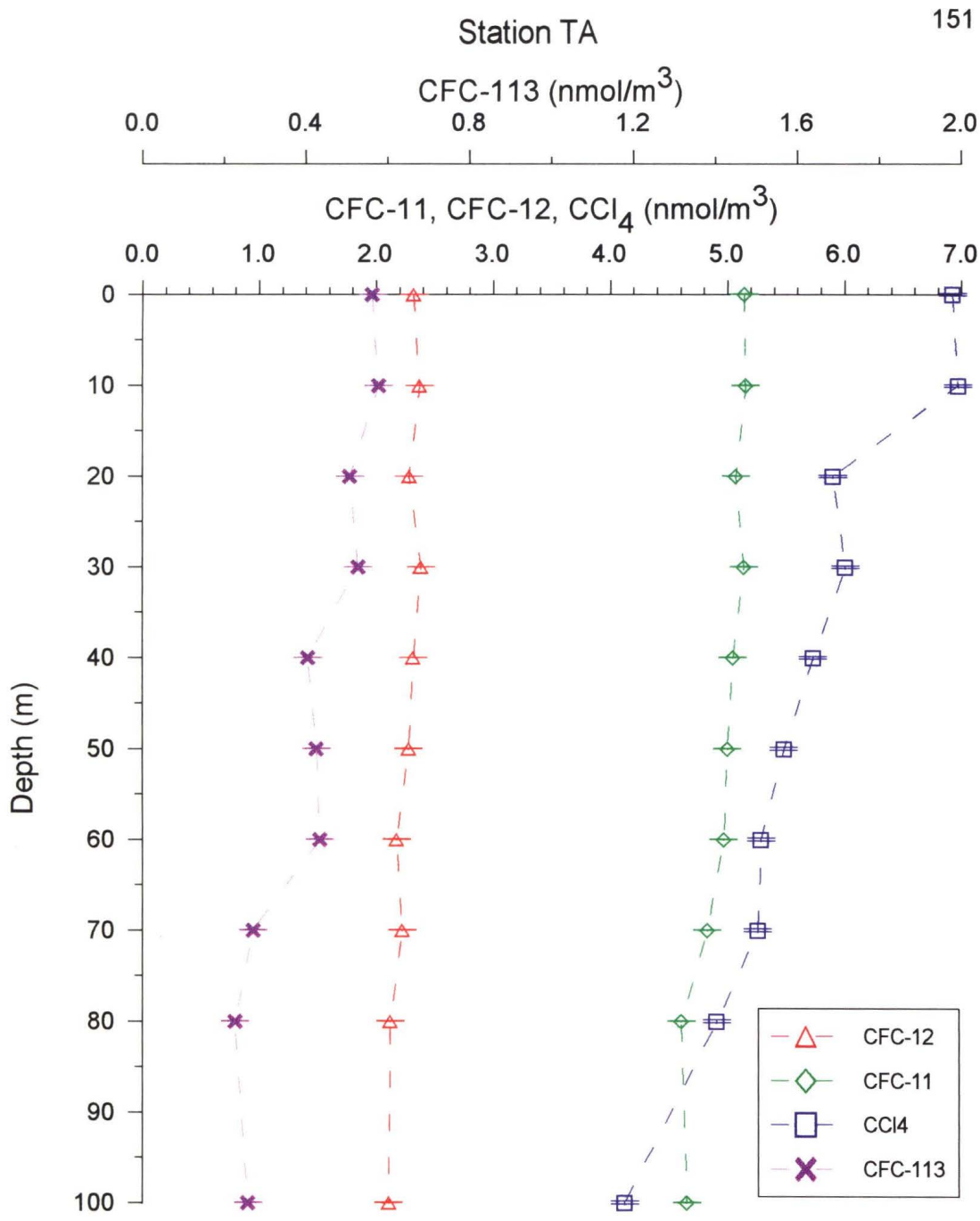
Station TA
CFC-113 (nmol/m3)
0.0
0.4
0.8
1.2
1.6
2.0
CFC-11, CFC-12, CCl4 (nmol/m3)
0.0
1.0
2.0
3.0
4.0
5.0
6.0
7.0
Depth (m)
0
10
20
30
40
50
60
70
80
90
100
CFC-12
CFC-11
CCl4
CFC-113

Figure 6

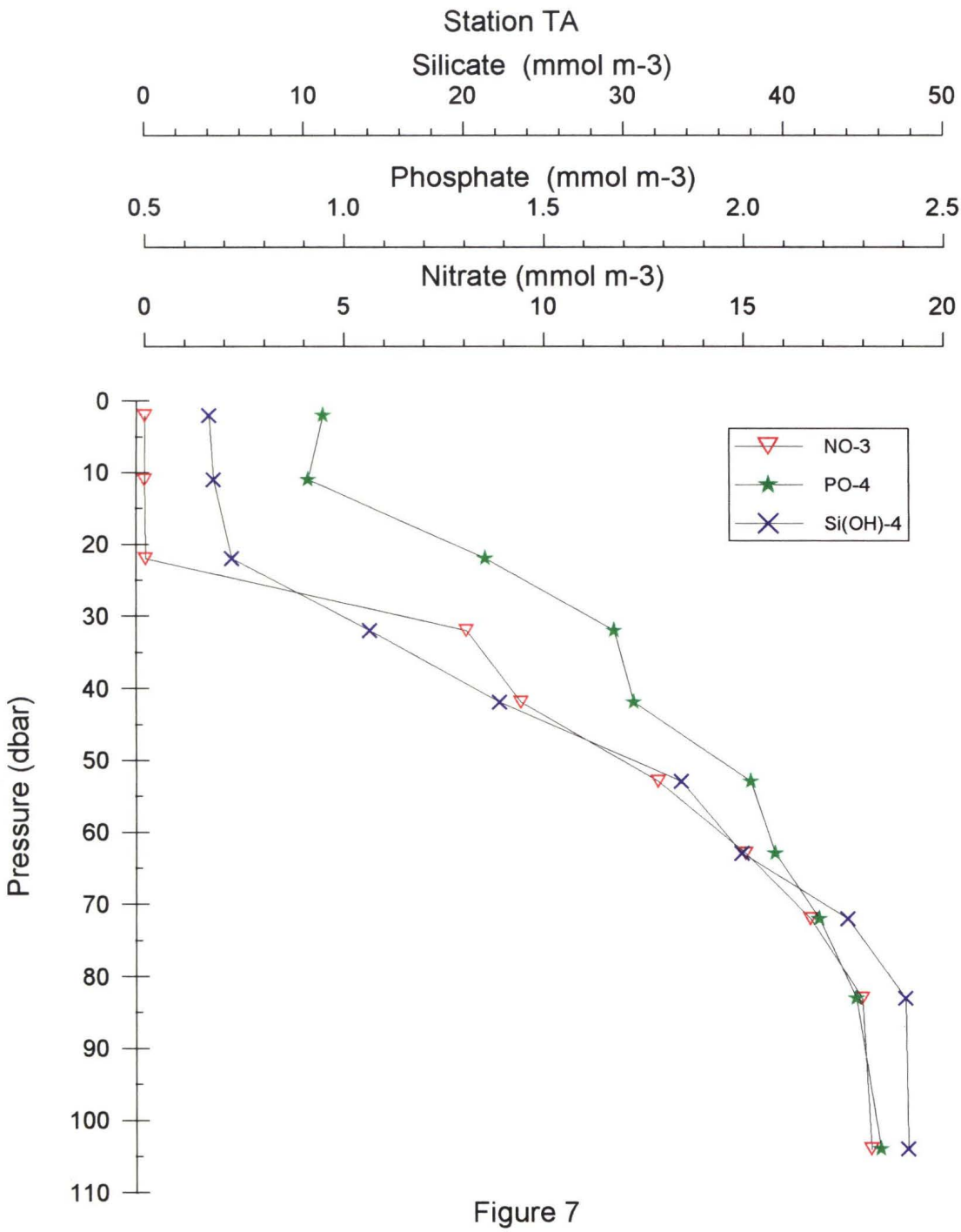
Station TA
Silicate (mmol m-3)
0
10
20
30
40
50
Phosphate (mmol m-3)
0.5
1.0
1.5
2.0
2.5
Nitrate (mmol m-3)
0
5
10
15
20
NO-3
PO-4
Si(OH)-4
Pressure (dbar)
0
10
20
30
40
50
60
70
80
90
100
110

Figure 7

Nutrients are zero (nitrate) to low (phosphate and silicate) at the surface, and increase with depth to a maximum at 80 m (Figure 7). Geochemical properties found in Station TA waters at 50 m characterize the upper halocline region of the WA assembly (Bering Sea summer water). Similarly, at 80 m, geochemical properties are characteristic of the middle halocline region of the WA assembly (Bering Sea winter water). Evidence of biological activity at Station TA is marked by the depletion of nutrients, as well as by an increase in oxygen between the surface and 30 m, the depth of the previous winter mixed layer (signalled by the shallow temperature minimum).

The second half of this composite station, Station TC, exhibits water mass characteristics of the WA assembly at 75m and of the EA assembly below 100 m. Salinity increases with depth, and temperature increases to a maximum of almost 1°C near 275 m (Figure 8). The temperature maximum signals the presence of the Atlantic layer and waters of the EA assembly.

Profiles of the four halocarbons illustrate that waters to 630 m are well ventilated (Figure 9). CFC-11 exhibits two sub-surface maxima; one (4.2 nmol m^{-3}) between 150 m and 275 m, and the other (3.2 nmol m^{-3}) at about 500 m, maxima which denote, respectively, the Atlantic layer and the underlying shelf-origin waters of the transition zone. Halocarbon concentrations are similar to those found to 700 m at Station E1 and provide further confirmation of the presence of EA assembly waters below 100m at Station TC.

The vertical profiles of oxygen and nutrients primarily illustrate the characteristics of the water mass boundary. For example, oxygen is lowest at 75 m, then increases to a maximum near 125 m then decreases with depth, with a low core centered about 225 m (Figure 8). Silicate also is highest at 75 m then decreases between 75 m and 125 m, and

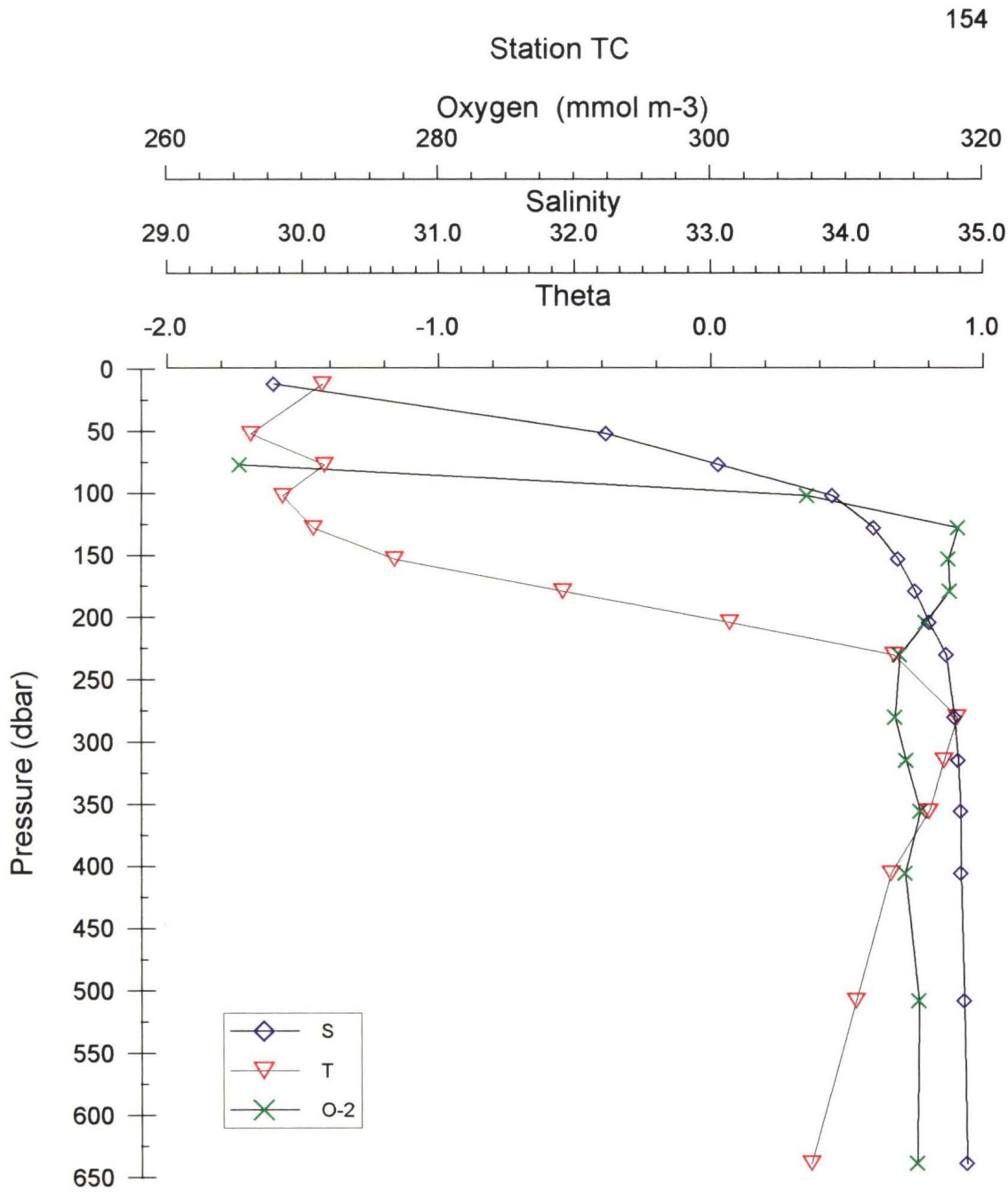
Station TC
Oxygen (mmol m-3)
260
280
300
320
Salinity
29.0
30.0
31.0
32.0
33.0
34.0
35.0
Theta
-2.0
-1.0
0.0
1.0
Pressure (dbar)
0
50
100
150
200
250
300
350
400
450
500
550
600
650
S
T
O-2

Figure 8

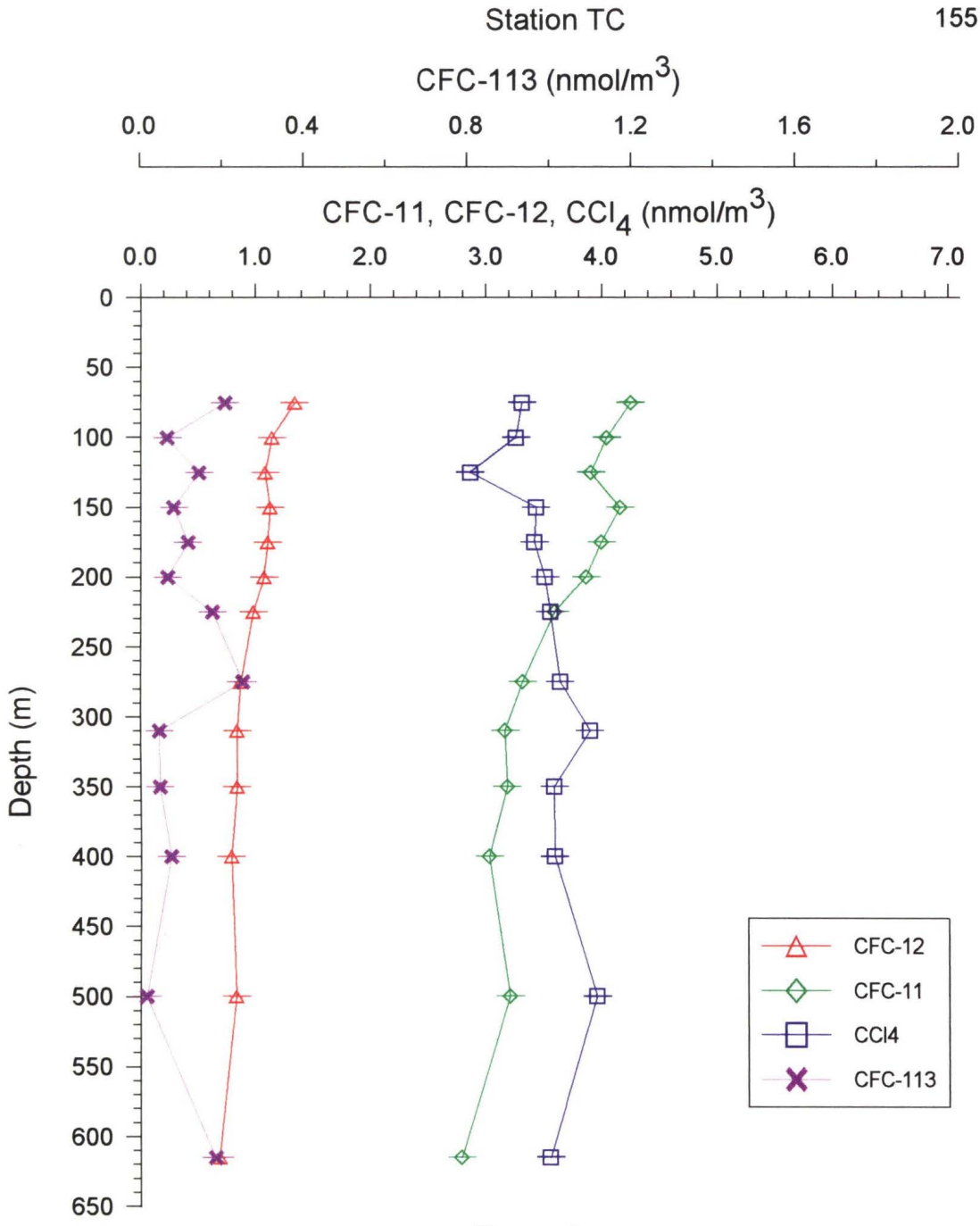
Station TC
CFC-113 (nmol/m3)
0.0
0.4
0.8
1.2
1.6
2.0
CFC-11, CFC-12, CCl4 (nmol/m3)
0.0
1.0
2.0
3.0
4.0
5.0
6.0
7.0
Depth (m)
0
50
100
150
200
250
300
350
400
450
500
550
600
650
CFC-12
CFC-11
CCl4
CFC-113

Figure 9

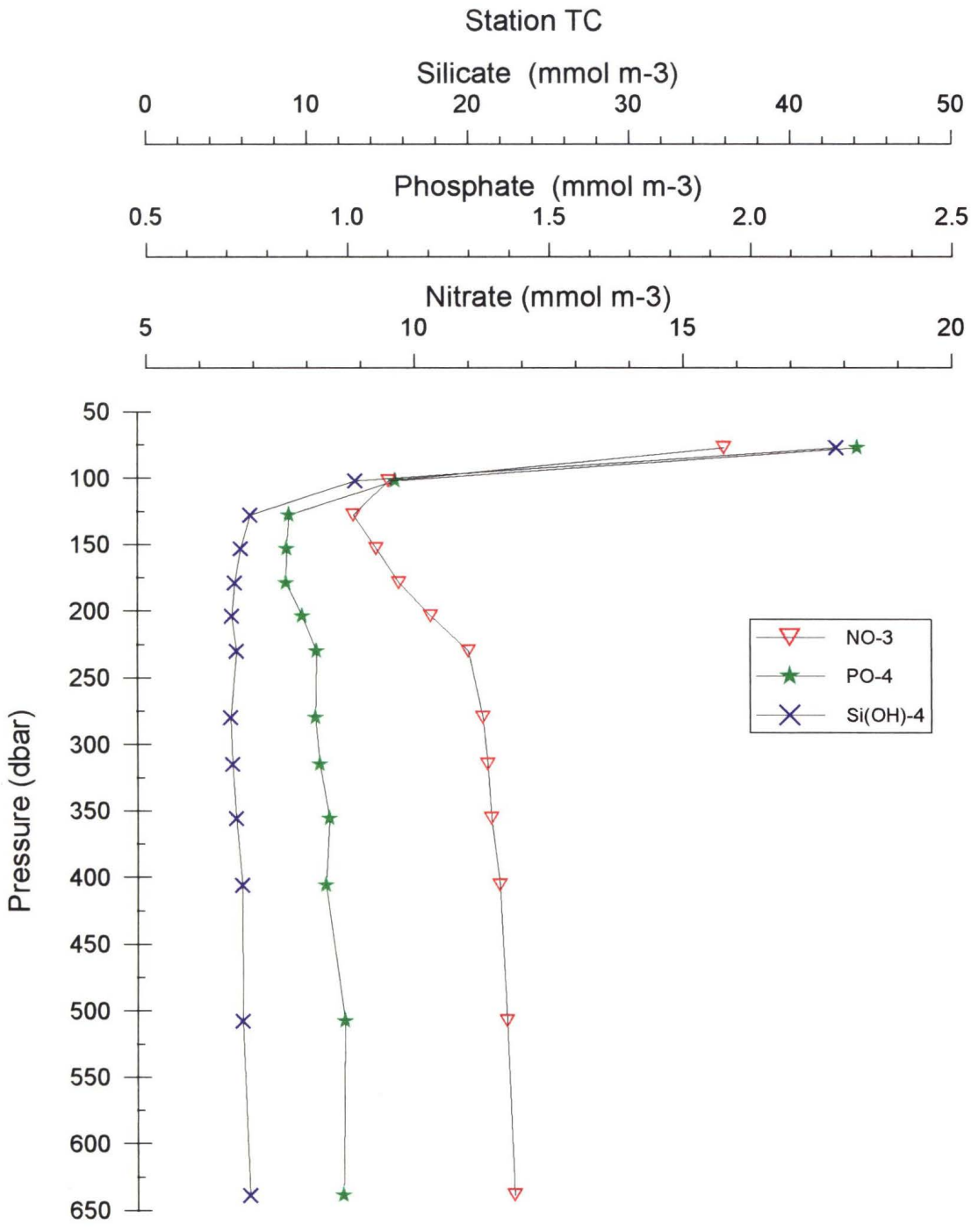
Station TC
Silicate (mmol m-3)
0
10
20
30
40
50
Phosphate (mmol m-3)
0.5
1.0
1.5
2.0
2.5
Nitrate (mmol m-3)
5
10
15
20
Pressure (dbar)
50
100
150
200
250
300
350
400
450
500
550
600
650
NO-3
PO-4
Si(OH)-4

Figure 10

remains constant between 150 m and 650 m (Figure 10). Similarly, nitrate and phosphate are highest at 75 m then decrease from 75 m to 125 m, and increase between 125 m and 225 m. Below 225 m, the concentrations do not change. These profiles refelect the high nutrient levels and low oxygen levels found in the WA assembly at 75 m, then the sharp transition to low nutrient levels and higher oxygen levels characteristic of the EA assembly below 100 m. Productivity at this station cannot be qualitatively described because no oxygen and nutrient samples were collected in the top 50 m, the depth shown by the temperature minimum to be the depth of the winter mixed layer. In summary, at Station TA/TC evidence of biological activity is observed but no evidence can be found of dense waters flowing off the shelf. Given the large lateral gradients associated with the Atlantic/Pacific front at this composite station, this is not surprising.

The third and final station, Station E04, is situated on the Makarov slope at a depth of 880 m. Although this station is predominantly comprised of waters with EA assembly characteristics, there is evidence of dilute Pacific origin water at 40 m where silicate concentrations are near 20 mmol m^{-3} (Figure 13). In addition, high silicate (15 mmol m^{-3}) and phosphate (1.2 mmol m^{-3}) levels in the surface waters may be influenced by Siberian river inflow. However, by 75 m silicate has decreased to 6 mmol m^{-3}, characteristic of Atlantic-origin EA assembly waters. Salinity is low from the surface to 30 m, increases rapidly between 30 m and 50 m to S=33.7, continues to increase with depth to S=34.76 at 200 m, then slowly increases to 34.96 at 800 m (Figure 11). Between 800 m and 850 m, salinity decreases by 0.1. Temperature remains near constant to 50 m, decreases to a minimum at 60 m, increases to a maximum of 1.4°C at 250 m, then decreases with depth. The temperature

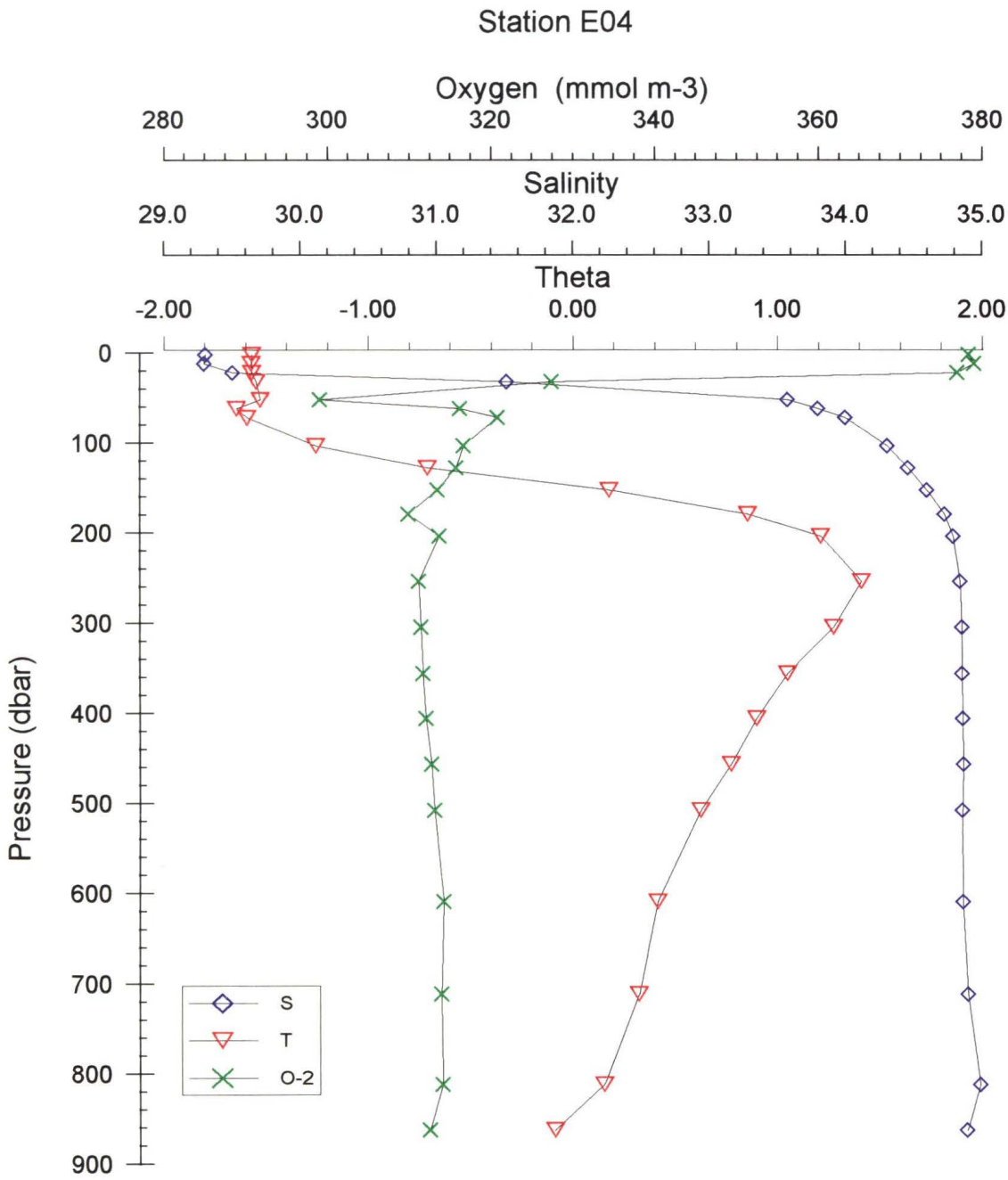
Station E04
Oxygen (mmol m-3)
280
300
320
340
360
380
Salinity
29.0
30.0
31.0
32.0
33.0
34.0
35.0
Theta
-2.00
-1.00
0.00
1.00
2.00
Pressure (dbar)
0
100
200
300
400
500
600
700
800
900
S
T
O-2

Figure 11

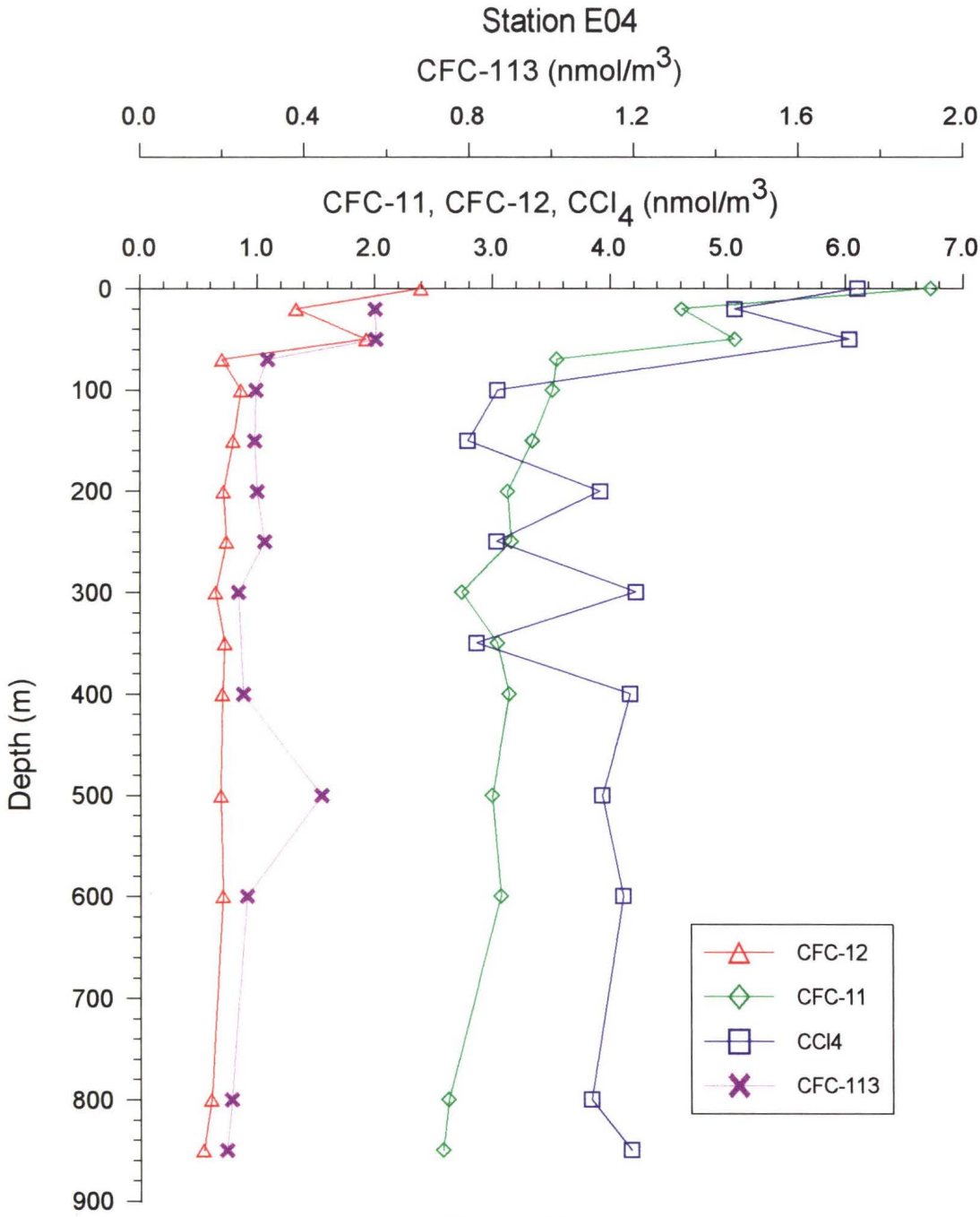
Station E04
CFC-113 (nmol/m3)
0.0
0.4
0.8
1.2
1.6
2.0
CFC-11, CFC-12, CCl4 (nmol/m3)
0.0
1.0
2.0
3.0
4.0
5.0
6.0
7.0
Depth (m)
0
100
200
300
400
500
600
700
800
900
CFC-12
CFC-11
CCl4
CFC-113

Figure 12

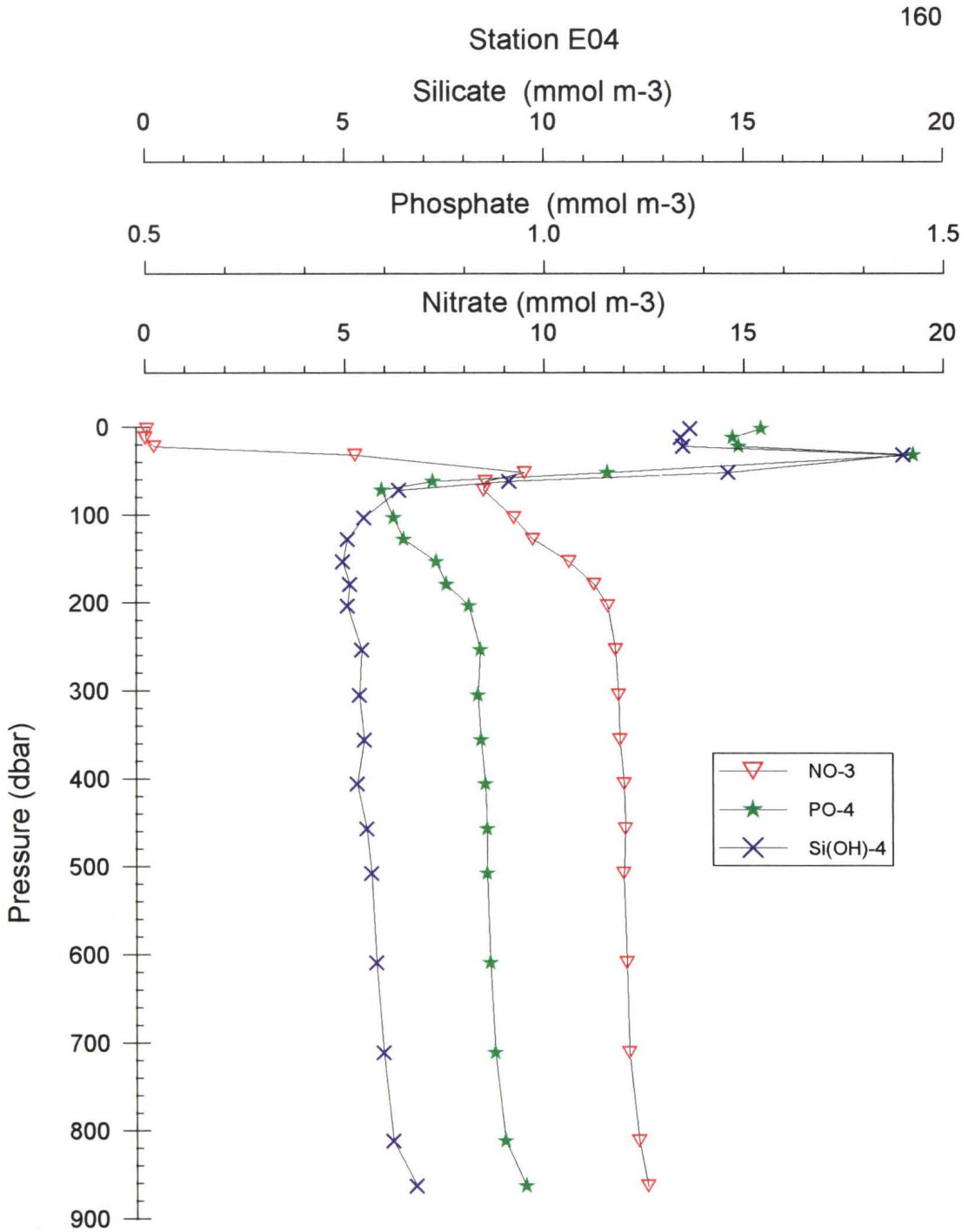
Station E04
Silicate (mmol m-3)
0
5
10
15
20
Phosphate (mmol m-3)
0.5
1.0
1.5
Nitrate (mmol m-3)
0
5
10
15
20
Pressure (dbar)
0
100
200
300
400
500
600
700
800
900
NO-3
PO-4
Si(OH)-4

Figure 13

maximum found at 250 m is representative of EA assembly waters.

Halocarbon concentrations at Station E04 are highest at the surface, decrease to about 75 m, and remain relatively constant to 850 m (Figure 12). Halocarbon profiles illustrate the enhanced ventilation of both the Atlantic layer and the underlying transition zone. The absence of high near-surface halocarbon concentrations at depth suggests that convection has not occurred recently.

Evidence of biological activity is shown in the vertical profiles of oxygen and nutrients. For example, oxygen is high in the surface water to 40 m then decreases to a minimum at 50 m, increases to a sub-surface maximum at 70 m, then decreases to near constant below 200 m (Figure 11). Nitrate is depleted in surface waters to 20 m, increases to a local maximum at 50 m, decreases to a sub-surface minimum at 70 m and then increases to 200 m, where, below this depth, it remains relatively constant (Figure 13). Silicate and phosphate are low in surface waters, and increase to a maximum at 50 m. Phosphate then resembles nitrate in behaviour, decreasing to a minimum at 70 m, increasing to 200 m and remaining constant to depth. Silicate decreases to a minimum at 150 m, then increase slightly to 800 m.

The depth of the winter mixed layer, denoted by the temperature minimum, is 60 m. Biological productivity from the surface to a depth of 30 m is evidenced by the depletion of nutrients, and by the high oxygen concentrations found in these waters. The three nutrient profiles illustrate primarily the vertically offset structure of the Atlantic/Pacific water mass boundary. The nutrient maximum at 50 m at Station E04 reflects the presence of Pacific origin nutrient-rich water, whereas the nutrient minimum at 70 m reflects nutrient-poor Atlantic origin water. Silicate

and phosphate profiles increase between 800 m and 850 m, depths at which salinity and temperature decrease. Most likely, this near-bottom layer of cold, relatively fresh water originated on a shelf, perhaps the East Siberian Shelf, and flowed off the shelf to this depth. The concentrations of dissolved gases do not increase between 800 and 850 m however, which implies that these waters are not the product of recent convection of surface equilibrated waters.

5.4 Ventilation

Chapter 4 presented evidence of CCl_4 non-conservative behaviour in the halocline of both the WA and EA assemblies. This halocarbon depletion is believed to occur in waters underlying productive regions. From the discussion earlier in this chapter, it is apparent that the three shelf/slope stations are situated in regions of productivity and, therefore, provide additional opportunities to examine whether such a correlation exists between productivity and non-conservative behaviour. Halocarbon depletion can be estimated at the three shelf/slope stations by examining the relationship between CFC-12 and CCl_4 atmospheric concentrations to determine whether the data lie within the region expected from the source histories and mixing. Data which lie outside this region exhibit non-conservative behaviour of CCl_4.

Beginning with the shelf station, Station F09, the calculated atmospheric concentrations show no evidence of depletion of either CCl_4 in the top 75 m of the water column (Figure 14). Non-conservative behaviour of CCl_4 is evident only at 85 m, where upwelling of halocline water from the slope region has likely occurred. The profile of apparent age of waters at Station F09 indicates that the age of the

top 75 m is about 5 years, and older at 85 m (Figure 15). The CFC-113/CFC-11 age estimates (about 10 years) compare well to those found at appropriate depths at Stations A1 and B1.

Slope Stations TA and TC calculated atmospheric concentrations (Figures 16 and 17) illustrate non-conservative behaviour of CCl_4 from 80 m to 100 m at Station TA, and from 75m to 200 m at Station TC. The CCl_4 depletion at Station TA (below 40 m) is found in waters of Pacific origin water that have crossed the Chukchi Sea shelf. The depletion evident at Station TC is found in lower halocline waters of Atlantic origin that have crossed the Barents and other Eurasian shelves. Depletion evident at both assemblies demonstrate that depletion of CCl_4 is a shelf process that takes place on both the Chukchi and Barents seas shelves. Apparent ages, presented in Figure 18, show that CCl_4/CFC-11 ages are available at depths below 300 m and that the apparent age of these waters is about 8-12 years. The estimates based on CFC-113/CFC-12 in the halocline show apparent ages of about 5 years at 75 m and about 10-14 below 100 m. These age estimates are similar to those found at Station D1.

Calculated atmospheric concentrations for slope Station E04 show non-conservative behaviour of CCl_4 in EA assembly halocline waters from 100 m to 125 m (Figure 19). The CCl_4/CFC-11 apparent age estimate of water between 300 and 600 m is about 8 years, and at 850 m, is about 11 years (Figure 20). The CFC-113/CFC-12 estimate for waters from 75-100 m is about 8 years. These apparent age estimates agree with those observed at Station E1.

In summary, the preceding discussion has examined three shelf/slope stations for evidence of modification processes. Evidence of productivity was found at all three stations. No evidence of convection due to ice formation

Station F09

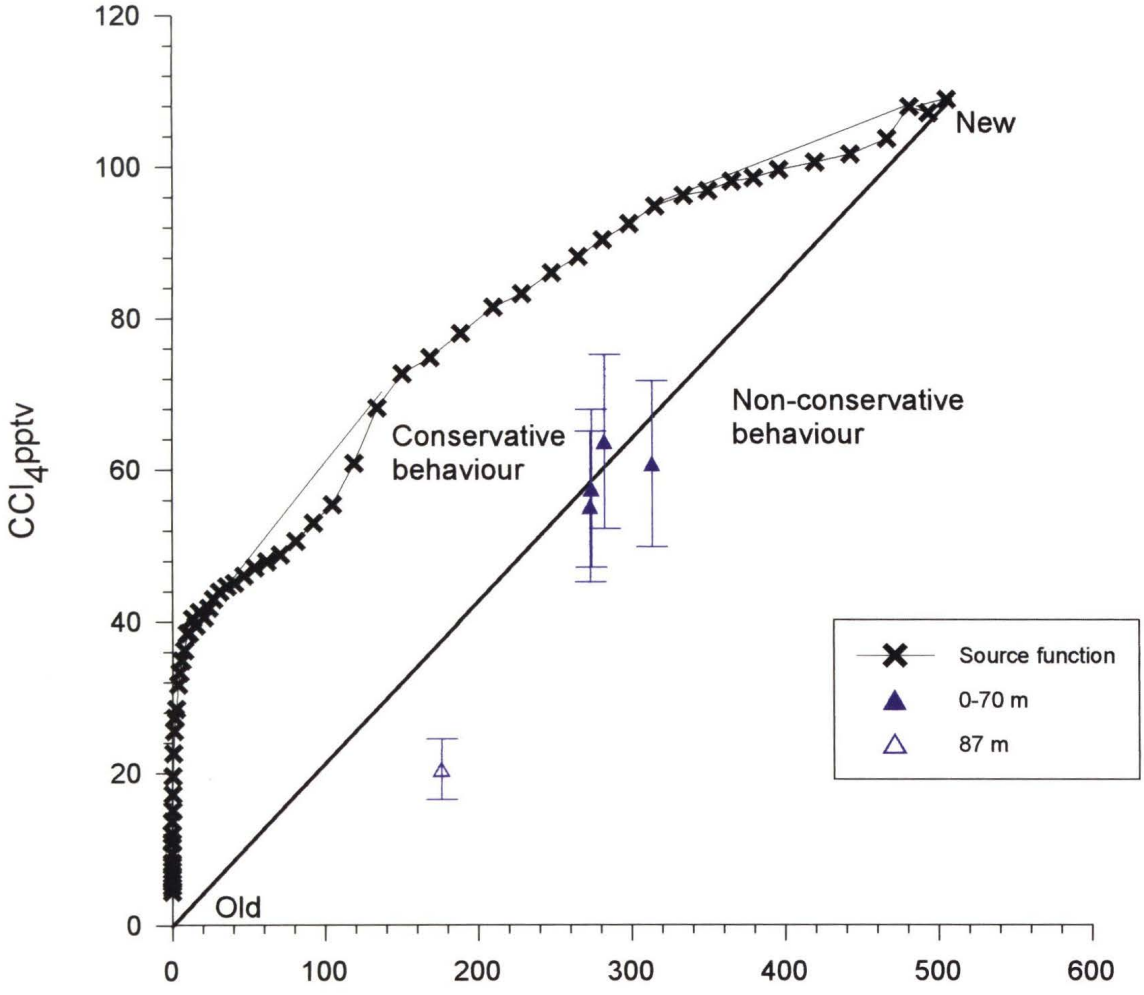

Figure 14

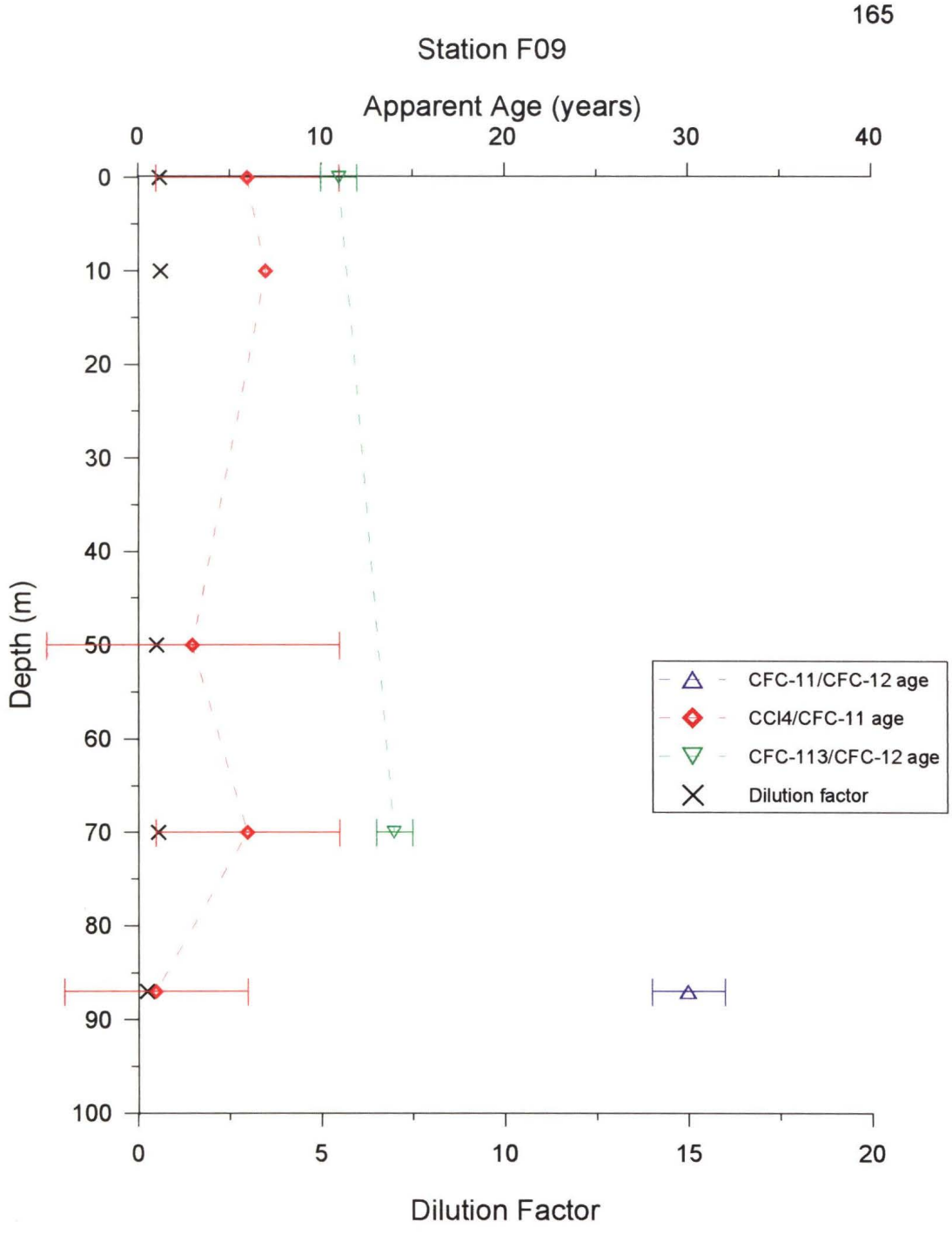
Station F09
Apparent Age (years)
0
10
20
30
40
Depth (m)
0
10
20
30
40
50
60
70
80
90
100
0
5
10
15
20
Dilution Factor
CFC-11/CFC-12 age
CCl4/CFC-11 age
CFC-113/CFC-12 age
Dilution factor

Figure 15

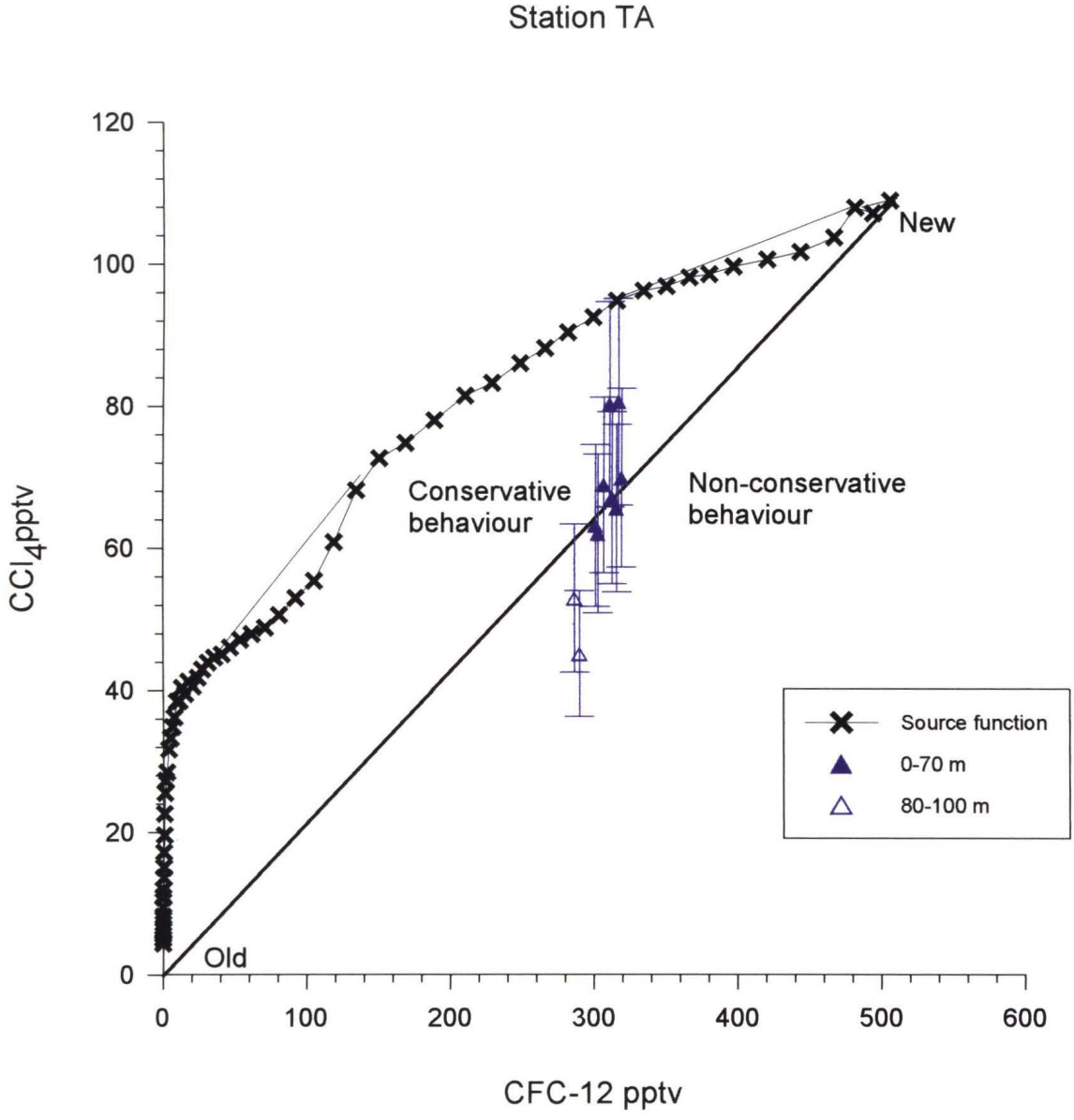
Station TA
120
100
80
60
40
20
0
0
100
200
300
400
500
600
CCl_4pptv
CFC-12 pptv
New
Old
Conservative behaviour
Non-conservative behaviour
Source function
0-70 m
80-100 m

Figure 16

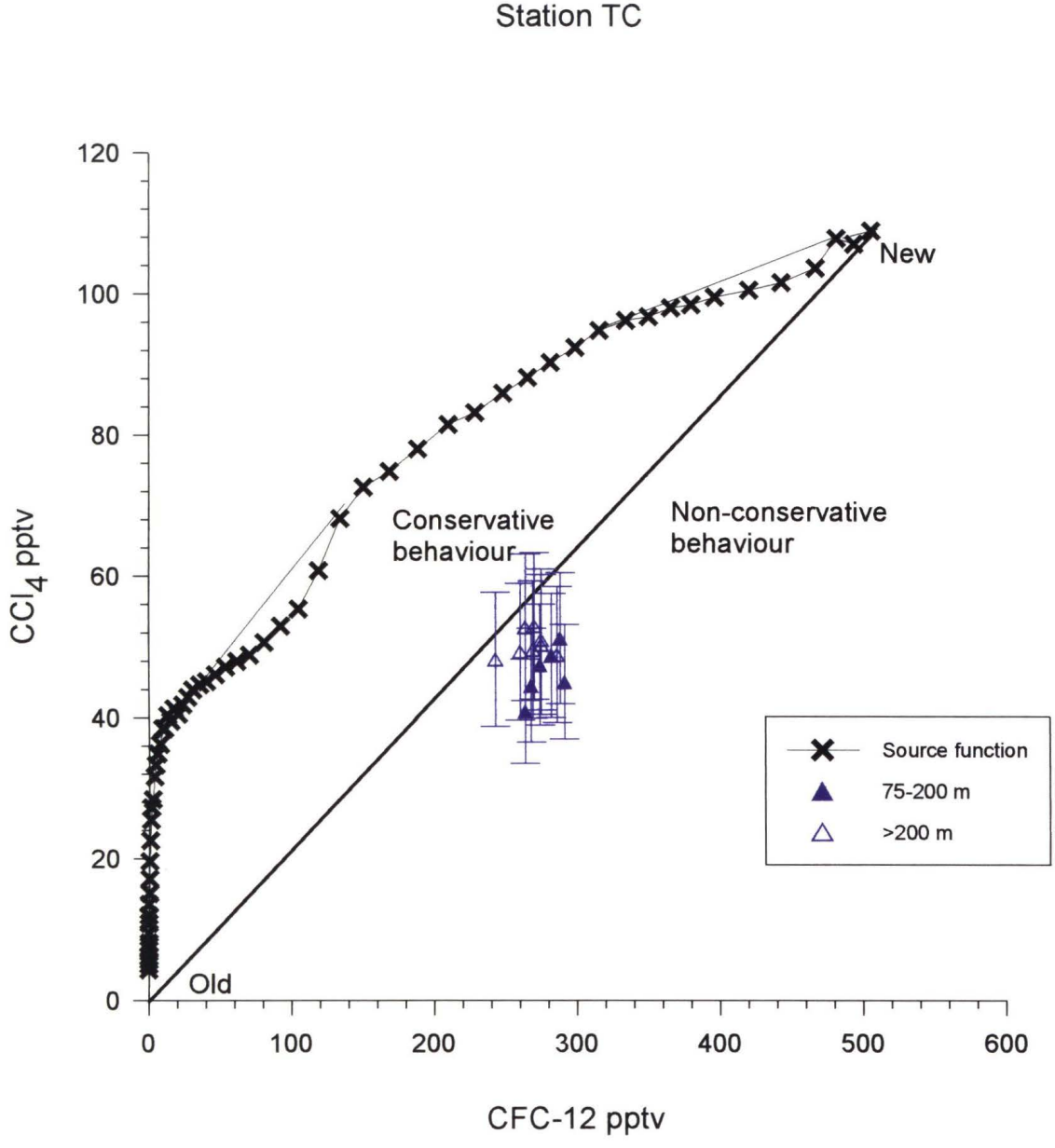
Station TC
120
100
80
60
40
20
0
CCl_4 pptv
0
100
200
300
400
500
600
CFC-12 pptv
New
Old
Conservative behaviour
Non-conservative behaviour
Source function
75-200 m
>200 m

Figure 17

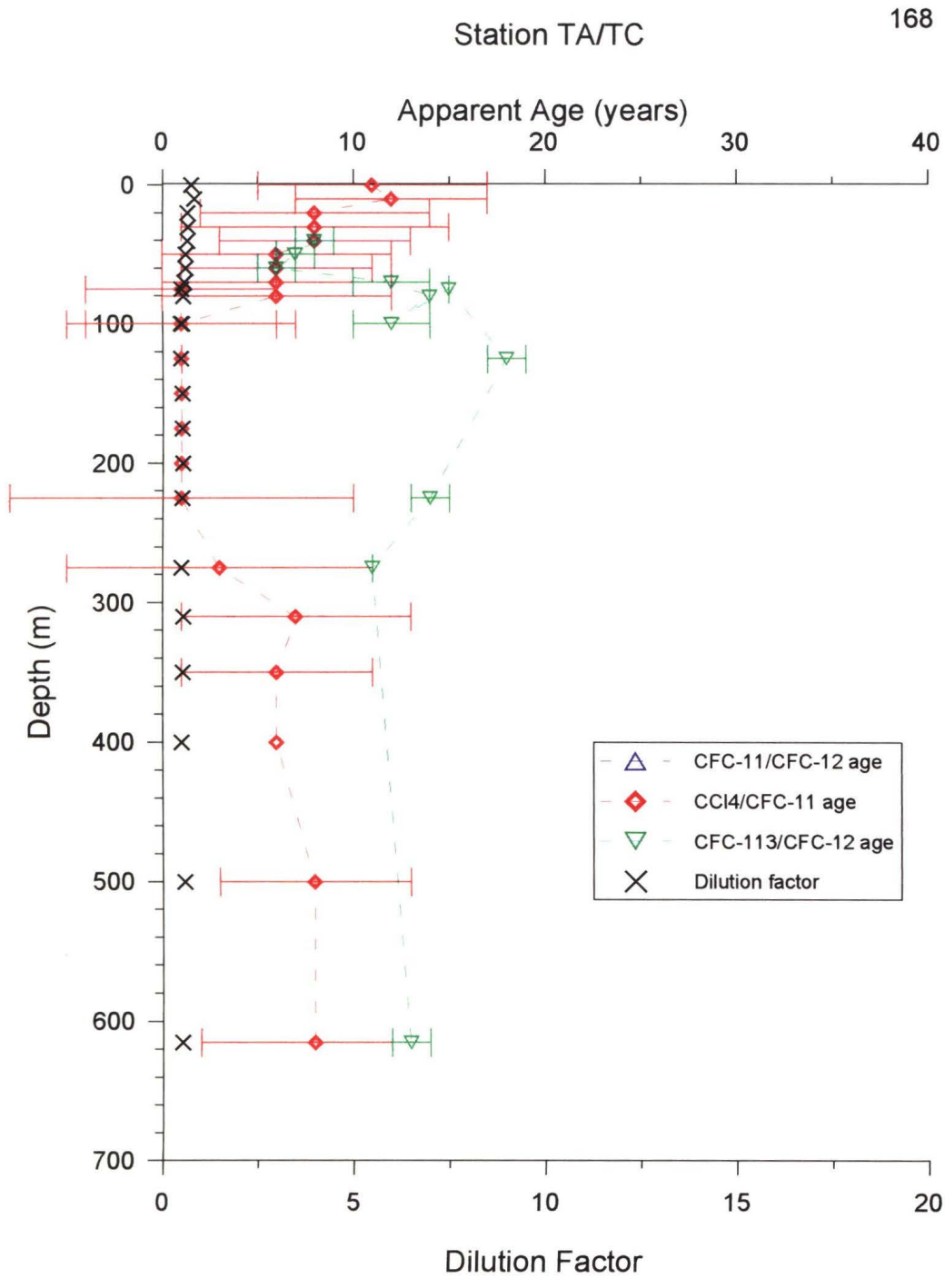
Station TA/TC
Apparent Age (years)
0
10
20
30
40
Depth (m)
0
100
200
300
400
500
600
700
0
5
10
15
20
Dilution Factor
CFC-11/CFC-12 age
CCl4/CFC-11 age
CFC-113/CFC-12 age
Dilution factor

Figure 18

Station E04

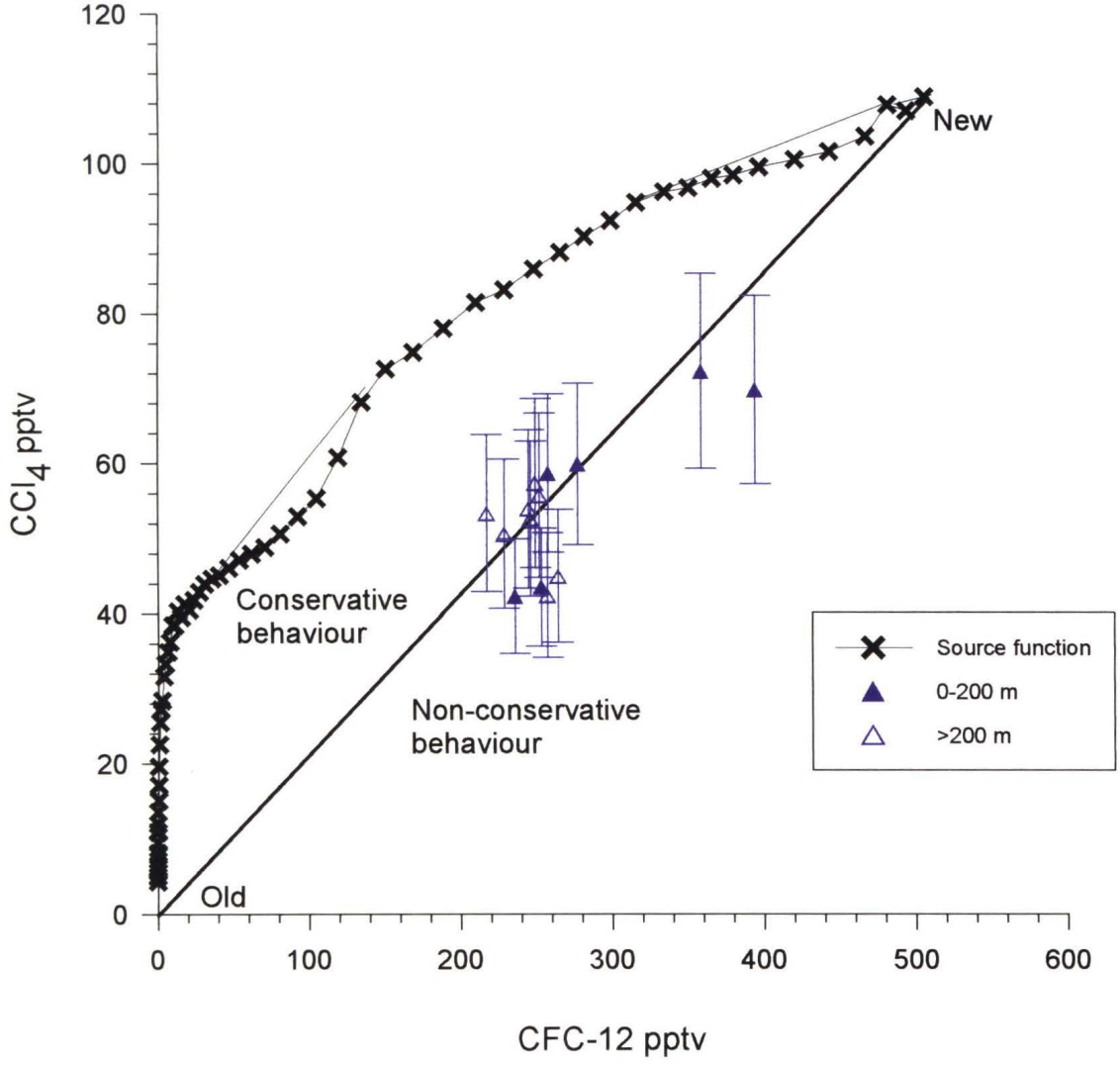

Figure 19

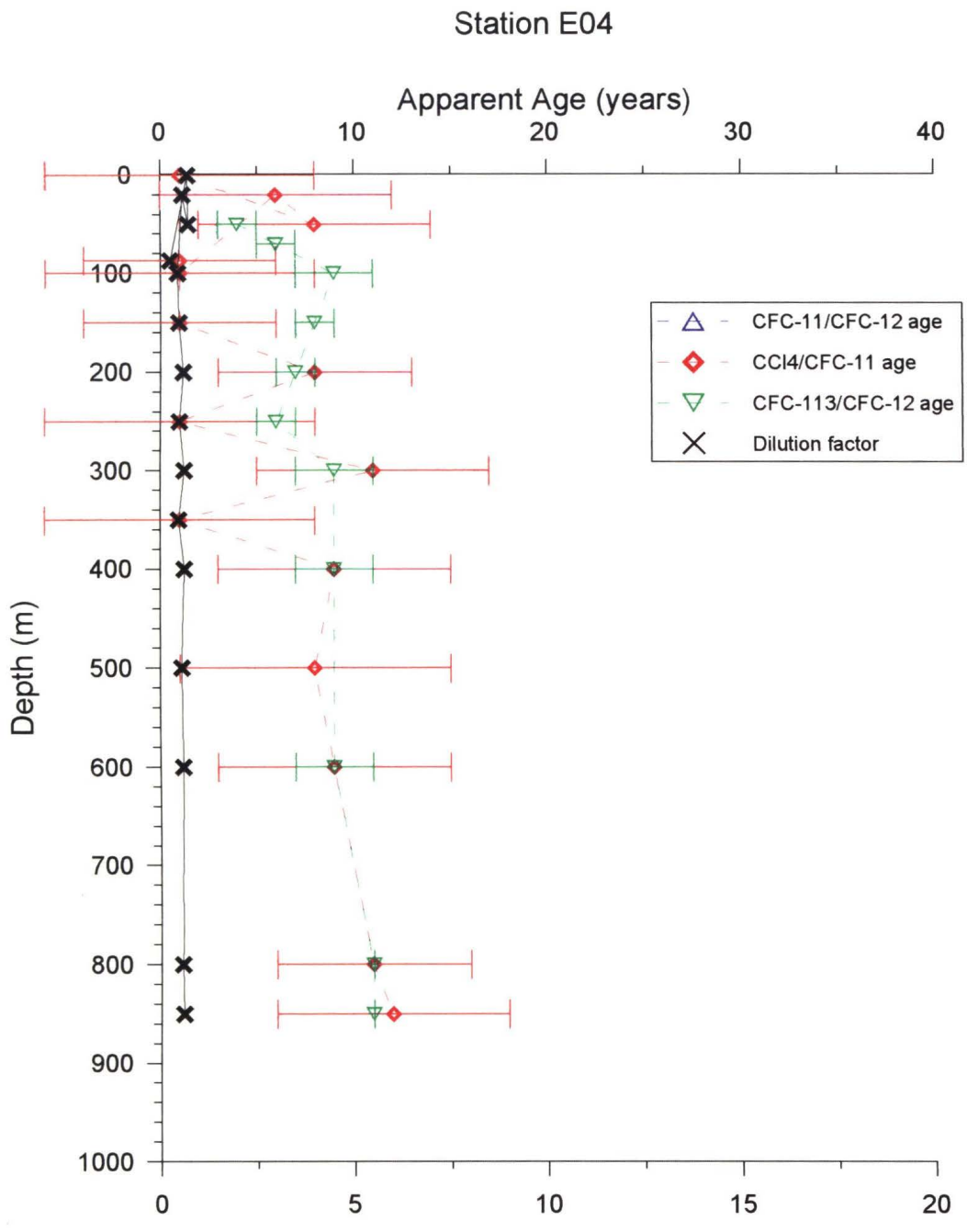
Station E04
Apparent Age (years)
0
10
20
30
40
Depth (m)
0
100
200
300
400
500
600
700
800
900
1000
CFC-11/CFC-12 age
CCl4/CFC-11 age
CFC-113/CFC-12 age
Dilution factor
0
5
10
15
20
Dilution Factor

Figure 20

processes could be detected, perhaps because of the time when sampling took place. However upwelling, a process that may precondition shelf waters for convection, was observed at Station F09 on the Chukchi Sea shelf. Finally, evidence of non-conservative behaviour of CCl_4 (CCl_4 depletion) was observed at the two slope stations. That CCl_4 depletion was not observed at the shelf station, where waters have been recently ventilated, suggests that CCl_4 depletion occurs over several years in waters underlying a biologically productive region. An opportunity for such depletion is provided during the decade that waters spend crossing the broad and productive Chukchi Shelf.

References:

Aagaard, K., L. K. Coachman, and E. C. Carmack, On the halocline of the Arctic Ocean, Deep-Sea Res., 28, 529-545, 1981.

Aagaard, K. and E. C. Carmack, The role of sea ice and other fresh water in the Arctic circulation, J. Geophys. Res., 94, 14485-14498, 1989.

Cavalieri, D. J. and S. Martin, The contribution of Alaskan, Siberian, and Canadian coastal polynyas to the cold halocline layer of the Arctic Ocean, J. Geophys. Res., 99, 18343-18362, 1994.

Coachman, L. K., K. Aagaard and R. B. Tripp, Bering Strait: The Regional Physical Oceanography, University of Washington Press, Seattle, 1975.

Kinney, P., M. E. Arhelger and D. C. Burrell. Chemical characteristics of water masses in the Amerasian basin of the Arctic Ocean, J. Geophys. Res., 75, 4097-4104, 1970.

Macdonald, R. W., C. S. Wong and P. E. Erickson. The distribution of nutrients in the southeastern Beaufort Sea: implications for water circulation and primary production, J. Geophys. Res., 92, C3, 2939-2952, 1987.

McRoy, C. P. ISHTAR, the project: an overview of Inner Shelf Transfer And Recycling in the Bering and Chukchi Seas, Cont. Shelf Res., 13, 5/6, 473-479, 1993.

Melling, H. The formation of a halocline shelf front in wintertime in an ice-covered arctic sea, Cont. Shelf Res., 13, 1123-1147, 1993.

Melling, H. and R. M. Moore, Modification of halocline source waters during freezing on the Beaufort Sea shelf: evidence from oxygen isotopes and dissolved nutrients, Cont. Shelf Res., 15, 89-113, 1995.

Melling, H. and E. L. Lewis, Shelf drainage flows in the Beaufort Sea and their effect on the Arctic Ocean pycnocline, Deep-Sea Res., 29, 967-985, 1982.

Midttun, L., Formation of dense bottom water in the Barents Sea, Deep-Sea Res., 32, 1233-1241, 1985.

Redfield, A. C., B. H. Ketchum, and F. A. Richards. "The influence of organisms on the composition of seawater," in The Sea, vol. 2, edited by M. N. Hill, pp. 26-77, Interscience, New York, 1963.

Springer, A. M. and C. P. McRoy. The paradox of pelagic food webs in the northern Bering Sea-III. Patterns of primary production. Cont. Shelf Res., 13, 5/6, 575-599, 1993.

Weeks, W. F. and S. F. Ackley. The growth, structure, and properties of sea ice, CRREL Monograph 82-1, US Army Corps of Engineers, Cold Regions Research and Engineering Laboratory, Hanover, New Hampshire, USA, 1982.

Chapter 6: Summary of Findings

Prior to **Larsen-93**, the oceanography of the Canadian Basin was defined primarily by sample analyses from four ice-camps, two in the Canada Basin, one in the Makarov Basin, and one above the Alpha Ridge. Data from these stations led oceanographers to conclude that the Canadian Basin was laterally homogeneous, with no apparent distinctions drawn between waters in the Canada and Makarov basins.

This thesis has focused on physical and geochemical data collected during the **Larsen-93** expedition in late summer 1993. It has concluded that waters in the Canada Basin (represented by Station A1, B1, C1 and D1) are relatively homogeneous along constant density surfaces, a finding that concurs with historical views of Canada Basin waters. Likewise, this thesis has further shown that processes which influence ventilation of subsurface waters below 1500 m have not changed between 1993 and 1995. In these respects, this thesis confirms historical views.

Where this thesis differs most appreciably with long-standing views of arctic oceanography is in its identification of a frontal structure previously unrecognized in the hydrography of the Canadian Basin. Analysis of **Larsen-93** physical and geochemical data collected at eight stations, from the Beaufort Sea in the Canada Basin to the Makarov Slope, point to the relocation of the Atlantic/Pacific boundary from a position above the Lomonosov Ridge to a position above the Mendeleyev Ridge. Earlier measurements (**LOREX**, 1979) suggest that this shift occurred sometime after 1980 and probably since 1990 (Loeng,

personal communication). **Larsen-93** data suggests that the Alpha-Mendeleyev Ridge may play a more significant role in the circulation of waters within the Canadian Basin than previously believed. The Atlantic/Pacific front appears to favor a position over ridge topography. Why the frontal structure breaks down over one ridge, and reestablishes itself over another remains unknown.

The Atlantic/Pacific front was identified through the understanding that two basic water mass assemblies are present in the Arctic Ocean--the Western Arctic (WA) assembly and the Eastern Arctic (EA) assembly. The primary distinctions between these two assemblies are the presence, or absence, of Pacific origin water, and the relative amounts of Atlantic origin water. The term water mass assembly was introduced in this thesis to describe the basic arrangement of Arctic Ocean water masses. This description recognizes that water masses often occur in distinct groupings, and that components within each grouping may be different as a result of different source waters and mixing histories.

This paper argues that the front separating these two assemblies is marked by large lateral gradients in all measured properties. Canada Basin water is characteristic of WA assembly water, both now (**Larsen-93**) and in the past (**AIWEX**, 1990). Similarly, water from the southwestern slope of the Makarov Basin is clearly characteristic of EA assembly water, at least down to the deep layer. The Atlantic/Pacific front within the water column is not vertical, but is, instead, offset with depth above and below the Atlantic layer.

In addition, anthropogenic halocarbon concentrations are found two to three times deeper in the Makarov Basin than in the Canada Basin, which implies enhanced rates of ventilation in these waters. These halocarbon measurements

suggest that rapid exchange has occurred where waters of the Eurasian Basin have entered the Makarov Basin, and that physical and geochemical properties, including contaminants, may be transported by boundary currents more quickly from one basin to another than previously estimated. Analysis of **Larsen-93** data also shows that, in addition to enhanced ventilation, the transition region between the Atlantic and deep layers is fresher in the Makarov Basin than corresponding water in either the Canada or Eurasian basins. The source of this cold, low-salinity, well-ventilated water is likely of shelf origin, perhaps from shelves in the Barents, Laptev, and East Siberian seas.

Although the use of halocarbons as tracers of water mass circulation has assumed that halocarbons behave conservatively, this examination of **Larsen-93** data suggests that CCl_4 measurements in waters of the Arctic halocline appear to exhibit non-conservative behaviour. This difference in behaviour, although the subject of some speculation in the literature, is now documented in **Larsen-93** measurements of halocarbons collected at basin and slope stations. This research suggests that CCl_4 depletion appears to be a function of the time that waters spend in transit across productive shelves. Analysis of nutrients sampled in late summer at shelf/slope stations in the Chukchi Shelf region demonstrated the biological productivity of Arctic shelves.

Analysis of **Larsen-93** data has added to understandings of Arctic Ocean circulation. Anderson et al. (1994) suggested that communication between the Canadian and Eurasian basins occurred mostly around basin perimeters and, in addition, suggested that circulation around the Canadian Basin perimeter appeared weaker than around the Eurasian Basin. This thesis supported Anderson's view that circulation within the Canada Basin is weak by demonstrating

that these waters are less ventilated and, therefore, more isolated than waters found in other Arctic basins. However, in contrast to Anderson's view, analysis of **Larsen-93** data illustrated that this weak circulation appears exclusively confined to the Canada Basin. Moreover, this weak circulation is not generally descriptive of circulation within the larger Canadian Basin due to the relocation of the Atlantic/Pacific water mass boundary. The enhanced ventilation of Marakov Basin waters suggests that the boundary current, reported by Rudels et al. (1994), in the Eurasian Basin is now also evident in the Makarov Basin. Analysis of **Larsen-93** data shows that this change in circulation extends down to a depth of 1600 m.

One important question raised by this research concerns the relocation of the Atlantic/Pacific front. EA assembly waters have moved eastward into the Canadian Basin, at least to a depth of 1800 m, an event which has caused the displacement of Pacific water. This leads to the question: "Where has the Pacific water gone?" Given that two possible routes allow for the export of Pacific-origin water, one through Fram Strait and the other via the Canadian Archipelago, it is possible to speculate that the Atlantic/Pacific front relocation has prompted a change in the relative amounts of outflow through these two exits. Figure 1 shows the influence of the Atlantic/Pacific water mass boundary on the export of Pacific-origin water. When the Atlantic/Pacific front is located above the Lomonosov Ridge, export may be predominantly through Fram Strait (Figure 2). When the Atlantic/Pacific front is located above the Alpha-Mendeleyev Ridge, export may increase through the Canadian Archipelago (Figure 3). The route of the cold freshwater export thus has important climate implications. Freshwater export from the Arctic Ocean via Fram Strait is believed to condition northern latitude

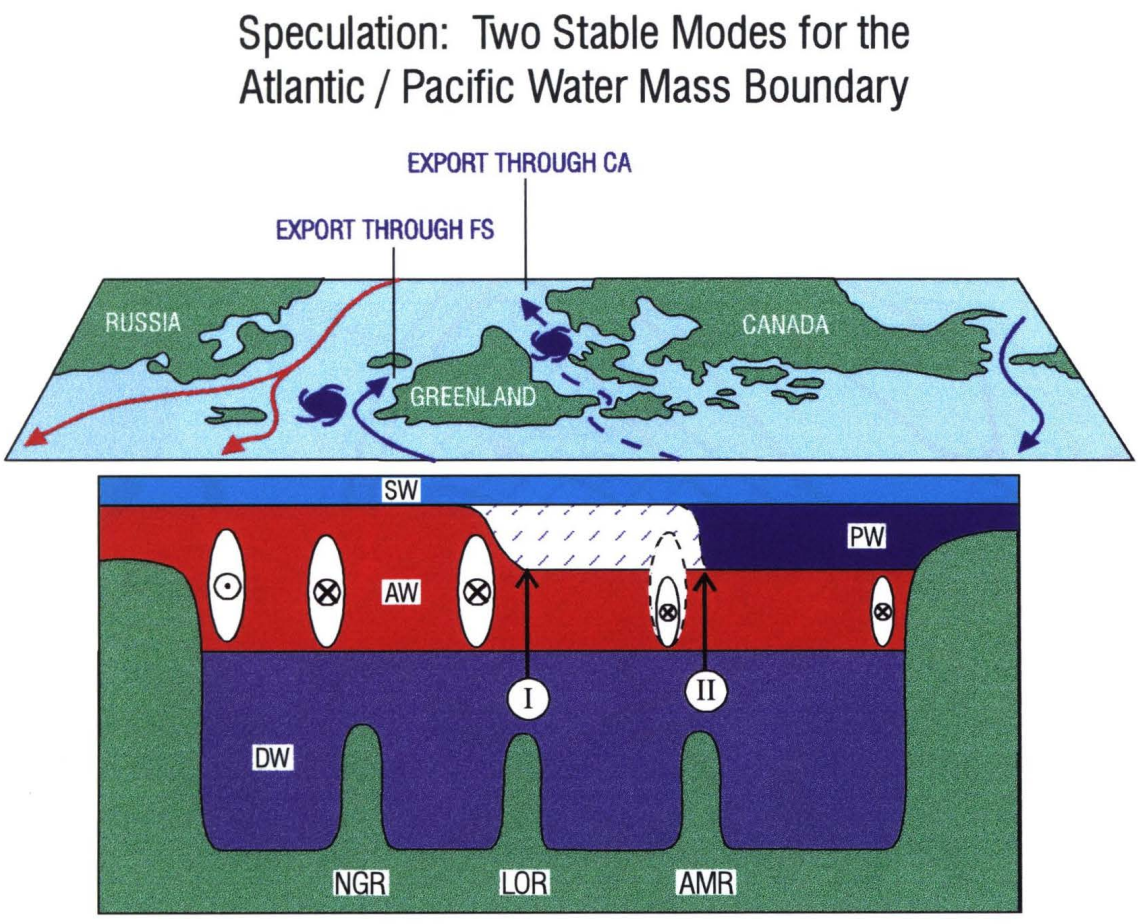
Speculation: Two Stable Modes for the
Atlantic / Pacific Water Mass Boundary
EXPORT THROUGH CA
EXPORT THROUGH FS
RUSSIA
CANADA
GREENLAND
SW
PW
AW
I
II
DW
NGR
LOR
AMR
MODE I FW (FS) > FW (CA)
MODE II FW (FS) < FW (CA)

Figure 1

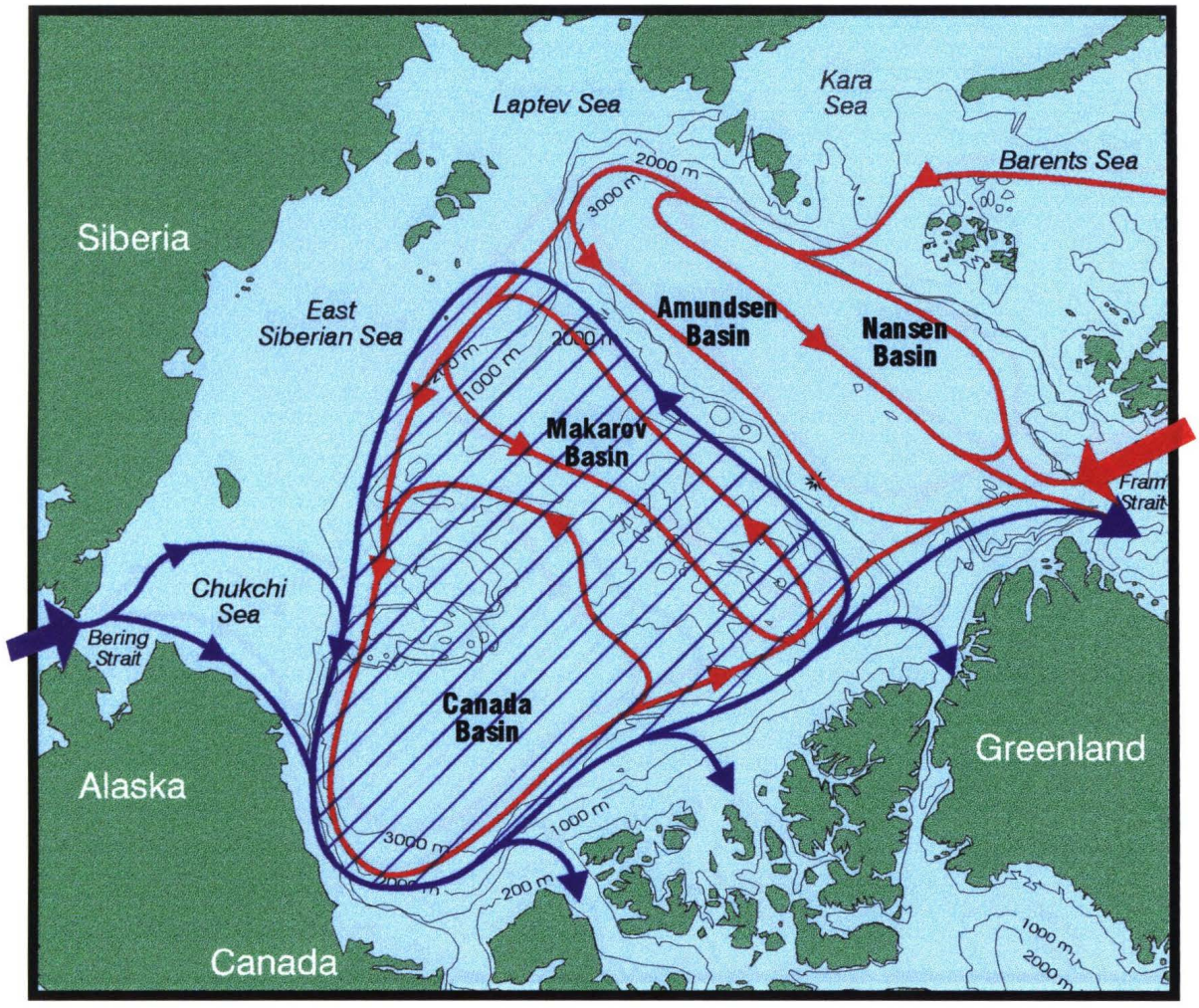

MODE I

Figure 2

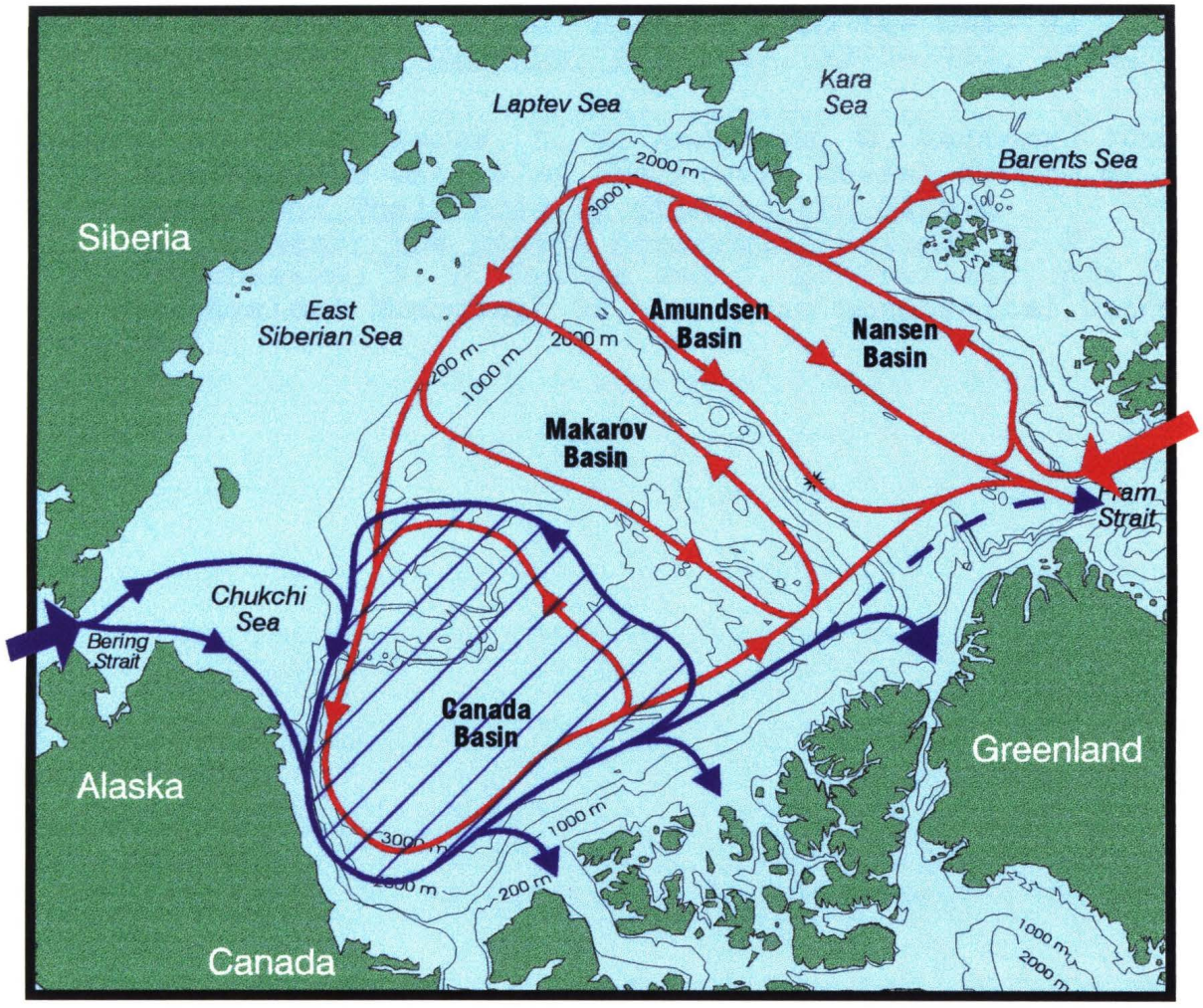

MODE II

Figure 3

convection and the water mass transformation that drives global overturning in the ocean (Aagaard and Carmack, 1989).

References:

Anderson, L. G., G. Bjork, O. Holby, E. P. Jones, G. Kattner, K. P. Koltermann, B. Liljeblad, R. Lindegren, B. Rudels and J. H. Swift, Water masses and circulation in the Eurasian Basin: Results from the ODEN 91 expedition, J. Geophys. Res., 99, 3273-3283, 1994.

Rudels, B., E. P. Jones, L. G. Anderson, G. Kattner, "On the intermediate waters of the Arctic Ocean" in The Polar Oceans and Their Role in Shaping the Global Environment: the Nansen Centennial Volume, O. M. Johannessen, R. D. Muench and J. E. Overland, eds., Geophysical Monograph 85, American Geophysical Union, 1994.

Appendix

1. Solubility equations:

a. CFC-11, CFC-12 and CFC-113 take the form:

$$C^* = F(\Theta,S)x$$

where C* = equilibrium seawater concentration, x = dry air mole fraction, and F(Θ,S) = solubility as a function of potential temperature and pressure (Weiss and Price, 1980) for the specific halocarbon at 1 atm pressure in moist air and for x<<1

where $\ln F = a_1 + a_2(100/T) + a_3\ln(T/100) + a_4(T/100)^2 + S(b_1 + b_2(T/100) + b_3(T/100)^2)$

and

	CFC-11	CFC-12	CFC-113
a_1	-232.0411	-220.2120	-230.016
a_2	322.5546	301.8695	320.338
a_3	120.4956	114.8533	118.173
a_4	-1.39165	-1.39165	-1.3917
b_1	-0.146531	-0.147718	-0.02425
b_2	0.093621	0.093175	0.004381
b_3	-0.0160693	-0.0157340	0.0002708

b. For CCl_4 the Hunter-Smith solubility equation takes the form:

At S=0 $\ln H = -2918T^{-1} + 9.77$

and at S = 35 $\ln H = -3230T^{-1} + 11.27$

To add a salinity term by applying the logarithmic Setchenow salinity dependence which takes the form:

$\ln B = b_1 + b_2S$

so the final equation will take the form:

$\ln H = m_1T^{-1} + m_2S + b$

we know

$-2918T^{-1} + 35m_2 + 9.77 = -3230T^{-1} + 11.27$

$m_2 = -8.914T^{-1} + 0.0428$

so

$\text{Ln } H = m_1T^{-1} + (-8.914T^{-1} + 0.0428)S + b$

$= m_1T^{-1} - 8.914T^{-1}S + 0.0428S + b$

or

$\text{Ln } H = m_1T^{-1} + m_2T^{-1}S + m_3S + b$

where

$m_1 = -2918$
$m_2 = -8.914$
$m_3 = 0.0428$
$b = 9.77$

2. Data Tables:

Pages 185 to 212 report physical and geochemical data as well as apparent age estimates. Blank corrections were applied to halocarbon data obtained at Station C1, due to a small leak in the extraction system.

3. CFC Standard Curves:

Typical halocarbon satndard curves are illustrated from pages 213-217 to demonstrate the GC-EC detector response for each halocarbon.

Stn	Date	Latitude	Longitude	Sample	Pressure	Temp	Salinity	Theta	Oxygen	Nitrate	Phosphate	Silicate
		deg/min	deg/min	#	dbar	deg C		deg C	mmol/m3	mmol/m3	mmol/m3	mmol/m3
A01	29-Aug-93	72 32 N	143 54W	118501	2	2.7	25.910	2.700	351.85	0.1	0.52	6.9
A01	29-Aug-93	72 32 N	143 54W	118502	13	0.751	29.382	0.751		0.0	0.74	5.1
A01	29-Aug-93	72 32 N	143 54W	118503	23	0.07	30.638	0.069	401.40			
A01	29-Aug-93	72 32 N	143 54W	118503	23	0.07	30.612	0.069		0.0	0.82	4.6
A01	29-Aug-93	72 32 N	143 54W	118504	33	-0.781	30.882	-0.782	404.79	0.0	0.84	5.3
A01	29-Aug-93	72 32 N	143 54W	118505	43	-1.226	31.449	-1.227	397.61	1.5	1.00	8.8
A01	29-Aug-93	72 32 N	143 54W	118506	53	-1.2	31.955	-1.201	360.81	5.6	1.30	13.3
A01	29-Aug-93	72 32 N	143 54W	118507	63	-1.297	32.220	-1.298	332.31	9.1	1.53	19.2
A01	29-Aug-93	72 32 N	143 54W	118508	73	-1.355	32.387	-1.356	317.28	10.9	1.66	23.6
A01	29-Aug-93	72 32 N	143 54W	118509	83	-1.404	32.531	-1.406	309.52	12.4	1.75	26.7
A01	29-Aug-93	72 32 N	143 54W	118510	103	-1.483	32.717	-1.485	300.92	14.0	1.85	32.4
A01	29-Aug-93	72 32 N	143 54W	118511	123	-1.502	32.900	-1.504	298.69	14.6	1.87	33.0
A01	29-Aug-93	72 32 N	143 54W	118512	143	-1.49	33.140	-1.493	295.52	15.4	1.92	35.1
A01	29-Aug-93	72 32 N	143 54W	118513	153	-1.471	33.240	-1.474	292.49	15.7	1.93	34.6
A01	29-Aug-93	72 32 N	143 54W	118514	163	-1.441	33.400	-1.445	287.00	16.2	1.93	34.3
A01	29-Aug-93	72 32 N	143 54W	118515	173	-1.358	33.444	-1.362	289.01	15.7	1.86	33.0
A01	29-Aug-93	72 32 N	143 54W	118516	182	-1.298	33.653	-1.302	287.67	15.9	1.82	34.1
A01	30-Aug-93	72 32 N	143 54W	118517	192	-1.101	33.962	-1.106	278.77	15.2	1.69	28.4
A01	30-Aug-93	72 32 N	143 54W	118518	202	-0.888	34.187	-0.894	270.01	14.8	1.49	24.6
A01	30-Aug-93	72 32 N	143 54W	118519	212	-0.667	34.330	-0.674	268.36	14.4	1.37	22.2
A01	30-Aug-93	72 32 N	143 54W	118520	227	-0.583	34.454	-0.590	281.56	13.0	1.17	16.6
A01	30-Aug-93	72 32 N	143 54W	118521	232	-0.524	34.490	-0.532	280.18	12.9	1.12	15.7
A01	30-Aug-93	72 32 N	143 54W	118522	252	-0.301	34.599	-0.310	284.41	12.6	1.03	12.9
A01	30-Aug-93	72 32 N	143 54W	118523	277	-0.046	34.666	-0.056	286.73	12.7	1.00	11.9
A01	30-Aug-93	72 32 N	143 54W	118524	302	0.0975	34.717	0.086	292.93	12.4	0.97	9.8
A01	30-Aug-93	72 32 N	143 54W	118525	327	0.2445	34.751	0.231	297.71	12.3	0.93	8.6
A01	30-Aug-93	72 32 N	143 54W	118526	352	0.339	34.778	0.324	299.94	12.3	0.92	7.9
A01	30-Aug-93	72 32 N	143 54W	118527	377	0.398	34.797	0.382	301.07	12.3	0.91	7.8
A01	30-Aug-93	72 32 N	143 54W	118528	402	0.422	34.810	0.405	299.89	12.4	0.92	7.6
A01	30-Aug-93	72 32 N	143 54W	118529	452	0.424	34.827	0.405	299.73	12.5	0.92	7.3
A01	30-Aug-93	72 32 N	143 54W	118530	502	0.421	34.841	0.399	301.81	12.6	0.91	7.3
A01	30-Aug-93	72 32 N	143 54W	118531	551	0.405	34.855	0.381	301.76	12.6	0.93	7.2

Stn	Date	Latitude	Longitude	Sample	Pressure	Temp	Salinity	Theta	Oxygen	Nitrate	Phosphate	Silicate
		deg/min	deg/min	#	dbar	deg C		deg C	mmol/m3	mmol/m3	mmol/m3	mmol/m3
A01	30-Aug-93	72 32 N	143 54W	118532	602	0.3865	34.860	0.360	303.41	12.6	0.92	8.2
A01	30-Aug-93	72 32 N	143 54W	118533	701	0.33	34.874	0.299	303.01	12.7	0.94	7.2
A01	30-Aug-93	72 32 N	143 54W	118534	801	0.224	34.882	0.188	304.31	12.7	0.95	7.5
A01	30-Aug-93	72 32 N	143 54W	118535	901	0.109	34.888	0.069	305.60	12.7	0.95	8.1
A01	30-Aug-93	72 32 N	143 54W	118536	1001	0.0285	34.896	-0.016	305.55	12.8	0.95	7.7
A01	30-Aug-93	72 32 N	143 54W	118537	1251	-0.179	34.906	-0.236	307.58	13.0	0.97	8.5
A01	30-Aug-93	72 32 N	143 54W	118538	1501	-0.308	34.917	-0.378		13.4	1.00	8.8
A01	31-Aug-93	72 32 N	143 54W	118552	601	0.4	34.861	0.373				
A01	31-Aug-93	72 32 N	143 54W	118553	701	0.323	34.873	0.292				
A01	31-Aug-93	72 32 N	143 54W	118554	801	0.217	34.881	0.181				
A01	31-Aug-93	72 32 N	143 54W	118555	901	0.1165	34.889	0.076				
A01	31-Aug-93	72 32 N	143 54W	118556	1001	0.0115	34.895	-0.033				
A01	31-Aug-93	72 32 N	143 54W	118557	1251	-0.1845	34.904	-0.241				
A01	31-Aug-93	72 32 N	143 54W	118540	1501	-0.3075	34.920	-0.377	305.29	13.1	1.00	8.8
A01	31-Aug-93	72 32 N	143 54W	118540	1501	-0.3065	34.919	-0.376				
A01	31-Aug-93	72 32 N	143 54W	118541	1601	-0.347	34.932	-0.423	305.06	13.3	1.02	9.4
A01	31-Aug-93	72 32 N	143 54W	118542	1701	-0.3705	34.927	-0.452	303.61	13.6	1.03	10.1
A01	31-Aug-93	72 32 N	143 54W	118543	1800	-0.392	34.930	-0.479	302.14	13.8	1.06	10.6
A01	31-Aug-93	72 32 N	143 54W	118544	1900	-0.402	34.936	-0.496	301.01	13.9	1.04	10.8
A01	31-Aug-93	72 32 N	143 54W	118545	2000	-0.405	34.938	-0.506	299.04	14.1	1.10	11.4
A01	31-Aug-93	72 32 N	143 54W	118546	2250	-0.3995	34.946	-0.517	295.79	14.2	1.07	12.1
A01	31-Aug-93	72 32 N	143 54W	118547	2500	-0.3825	34.950	-0.519	293.82	14.5	1.10	12.8
A01	31-Aug-93	72 32 N	143 54W	118548	3000	-0.3315	34.956	-0.508	289.54	14.3	1.09	13.6
A01	31-Aug-93	72 32 N	143 54W	118548	3000	-0.3315	34.956	-0.509				
A01	31-Aug-93	72 32 N	143 54W	118549	3360	-0.299	34.958	-0.508	290.03	14.6	1.11	13.7
A01	31-Aug-93	72 32 N	143 54W	118549	3360	-0.299	34.956	-0.508				
A01	02-Sep-93	72 32 N	143 54W	F1	2	-0.3055	25.170	-0.306				6.9
A01	02-Sep-93	72 32 N	143 54W	F2	12	0.5495	27.589	0.549				5.1
A01	02-Sep-93	72 32 N	143 54W	F3	32	-1.17	30.660	-1.171				5.3
A01	02-Sep-93	72 32 N	143 54W	F4	52	-1.245	31.884	-1.246				13.3
A01	02-Sep-93	72 32 N	143 54W	F5	77	-1.3445	32.428	-1.346				25
A01	02-Sep-93	72 32 N	143 54W	F6	103	-1.431	32.734	-1.433				32.4

Stn	Date	Latitude	Longitude	Sample	Pressure	Temp	Salinity	Theta	Oxygen	Nitrate	Phosphate	Silicate
		deg/min	deg/min	#	dbar	deg C		deg C	mmol/m3	mmol/m3	mmol/m3	mmol/m3
A01	02-Sep-93	72 32 N	143 54W	F7	128	-1.4575	32.974	-1.460				33.5
A01	02-Sep-93	72 32 N	143 54W	F8	153	-1.419	33.239	-1.422				34.6
A01	02-Sep-93	72 32 N	143 54W	F9	179	-1.292	33.585	-1.296				33.5
A01	02-Sep-93	72 32 N	143 54W	F10	204	-0.979	34.066	-0.985				24.6
A01	02-Sep-93	72 32 N	143 54W	F11	229	-0.612	34.428	-0.619				16.6
A01	02-Sep-93	72 32 N	143 54W	F13	279	-0.085	34.652	-0.095				11.9
A01	02-Sep-93	72 32 N	143 54W	F14	305	0.11	34.712	0.098				9.8
A01	02-Sep-93	72 32 N	143 54W	F15	357	0.325	34.775	0.310				7.9
A01	02-Sep-93	72 32 N	143 54W	F16	407	0.413	34.807	0.396				7.6
A01	02-Sep-93	72 32 N	143 54W	F17	457	0.4235	34.828	0.404				7.3
A01	02-Sep-93	72 32 N	143 54W	F18	508	0.4325	34.830	0.410				7.3
A01	02-Sep-93	72 32 N	143 54W	F19	559	0.4315	34.855	0.407				7.3
B01	09-Sep-93	72 32 N	152 27 W	118572	2	-0.6955	27.285	-0.696	381.24	0.0	0.61	6.8
B01	09-Sep-93	72 32 N	152 27 W	118573	12	-0.132	27.807	-0.132	377.49	0.0	0.61	7.8
B01	09-Sep-93	72 32 N	152 27 W	118574	22	2.3595	29.411	2.358	376.18	0.0	0.60	9.3
B01	09-Sep-93	72 32 N	152 27 W	118575	32	2.5485	30.425	2.547	389.67			
B01	09-Sep-93	72 32 N	152 27 W	118575	32	2.5675	30.408	2.566		0.0	0.66	9.5
B01	09-Sep-93	72 32 N	152 27 W	118576	42	1.0155	31.500	1.014	390.63	0.6	0.88	12.5
B01	09-Sep-93	72 32 N	152 27 W	118577	52	0.04	31.960	0.038	358.23	2.5	1.21	17.8
B01	09-Sep-93	72 32 N	152 27 W	118578	62	-0.7575	32.153	-0.759		4.4	1.40	20.5
B01	09-Sep-93	72 32 N	152 27 W	118579	72	-1.058	32.283	-1.060	336.69	5.7	1.53	23.3
B01	09-Sep-93	72 32 N	152 27 W	118580	82	-1.2945	32.433	-1.296	319.31			
B01	09-Sep-93	72 32 N	152 27 W	118580	82	-1.2895	32.428	-1.291		7.8	1.69	26.9
B01	09-Sep-93	72 32 N	152 27 W	118581	103	-1.4045	32.574	-1.407	317.73	10.4	1.81	32.8
B01	09-Sep-93	72 32 N	152 27 W	118582	128	-1.3185	32.775	-1.321	306.51	10.7	1.77	32.9
B01	09-Sep-93	72 32 N	152 27 W	118583	153	-1.193	33.521	-1.197	292.17			
B01	09-Sep-93	72 32 N	152 27 W	118583	153	-1.1845	33.510	-1.188		14.0	1.72	31.1
B01	09-Sep-93	72 32 N	152 27 W	118584	180	-1.038	34.000	-1.043	275.41	15.3	1.59	27.6
B01	08-Sep-93	72 32 N	152 27 W	118585	205	-0.843	34.229	-0.849	273.09	13.6	1.35	19.8
B01	08-Sep-93	72 32 N	152 27 W	118586	229	-0.626	34.445	-0.633	280.22	12.7	1.08	14.3
B01	08-Sep-93	72 32 N	152 27 W	118587	254	-0.301	34.579		283.70			
B01	08-Sep-93	72 32 N	152 27 W	118587	254	-0.301	34.579	-0.310		12.6	1.03	12.1

Stn	Date	Latitude	Longitude	Sample	Pressure	Temp	Salinity	Theta	Oxygen	Nitrate	Phosphate	Silicate
		deg/min	deg/min	#	dbar	deg C		deg C	mmol/m3	mmol/m3	mmol/m3	mmol/m3
B01	08-Sep-93	72 32 N	152 27 W	118588	279	-0.092	34.659	-0.102	286.82	12.6	0.98	10.5
B01	08-Sep-93	72 32 N	152 27 W	118589	305	0.138	34.718	0.126	291.42	12.6	0.94	9.5
B01	08-Sep-93	72 32 N	152 27 W	118590	355	0.364	34.789	0.349	296.28	12.4	0.93	7.5
B01	08-Sep-93	72 32 N	152 27 W	118559	406	0.422	34.814	0.405	300.87	12.5	0.91	7.4
B01	08-Sep-93	72 32 N	152 27 W	118560	457	0.438	34.836	0.418	302.34	12.5	0.92	7.0
B01	08-Sep-93	72 32 N	152 27 W	118561	508	0.435	34.853	0.413	300.78	12.6	0.92	7.3
B01	08-Sep-93	72 32 N	152 27 W	118562	602	0.38	34.866	0.353	304.66	12.6	0.90	7.1
B01	08-Sep-93	72 32 N	152 27 W	118563	704	0.262	34.875	0.231	306.36	12.7	0.91	7.0
B01	08-Sep-93	72 32 N	152 27 W	118564	808	0.135	34.882	0.099	309.30	12.5	0.91	6.9
B01	08-Sep-93	72 32 N	152 27 W	118566	1014	-0.0845	34.893	-0.129	310.73	12.6	0.94	7.1
B01	08-Sep-93	72 32 N	152 27 W	118567	1267	-0.236	34.908	-0.293	309.39	13.0	0.95	7.9
B01	08-Sep-93	72 32 N	152 27 W	118568	1523	-0.354	34.923	-0.425	308.86	13.4	1.00	9.0
B01	08-Sep-93	72 32 N	152 27 W	118569	2029	-0.411	34.943	-0.513	300.47	14.4	1.04	11.4
B01	08-Sep-93	72 32 N	152 27 W	118570	2537	-0.375	34.956		308.45			
B01	08-Sep-93	72 32 N	152 27 W	118571	3482	-0.289	34.956	-0.510	293.18	14.6	1.08	13.3
TA	11-Sep-93	75 1 N	173 1 W	118591	2	-1.264	29.739	-1.264	389.94	0.0	0.95	4.0
TA	11-Sep-93	75 1 N	173 1 W	118592	11	-1.326	29.858	-1.326	395.11	0.0	0.91	4.3
TA	11-Sep-93	75 1 N	173 1 W	118593	22	-1.5455	31.886	-1.546	353.10	0.0	1.35	5.5
TA	11-Sep-93	75 1 N	173 1 W	118594	32	-1.652	32.070	-1.653	334.10	8.0	1.67	14.1
TA	11-Sep-93	75 1 N	173 1 W	118595	42	-1.5335	32.203	-1.534	323.66	9.4	1.72	22.2
TA	11-Sep-93	75 1 N	173 1 W	118596	53	-1.122	32.445	-1.123	287.98	12.8	2.02	33.5
TA	11-Sep-93	75 1 N	173 1 W	118597	63	-1.2175	32.727	-1.219	285.84	15.0	2.08	37.3
TA	11-Sep-93	75 1 N	173 1 W	118598	72	-1.505	32.856	-1.506		16.6	2.18	43.9
TA	11-Sep-93	75 1 N	173 1 W	118599	83	-1.641	33.002	-1.643	282.27	17.9	2.28	47.5
TA	11-Sep-93	75 1 N	173 1 W	118600	104	-1.405	33.386	-1.407	248.87	18.1	2.34	47.6
TC	13-Sep-93	75 19 N	174 0 W	118601	12	-1.427	29.786	-1.427				
TC	13-Sep-93	75 19 N	174 0 W	118602	52	-1.69	32.230	-1.691				
TC	13-Sep-93	75 19 N	174 0 W	118603	77	-1.418	33.052	-1.420	265.35	15.7	2.26	42.8
TC	13-Sep-93	75 19 N	174 0 W	118604	102	-1.572	33.888	-1.574	307.03	9.5	1.12	13.0
TC	13-Sep-93	75 19 N	174 0 W	118605	128	-1.457	34.189	-1.460	318.09	8.9	0.85	6.4
TC	13-Sep-93	75 19 N	174 0 W	118606	153	-1.158	34.369	-1.162	317.37	9.3	0.85	5.8
TC	13-Sep-93	75 19 N	174 0 W	118607	179	-0.539	34.491	-0.545	317.46	9.7	0.85	5.5

Stn	Date	Latitude	Longitude	Sample	Pressure	Temp	Salinity	Theta	Oxygen	Nitrate	Phosphate	Silicate
		deg/min	deg/min	#	dbar	deg C		deg C	mmol/m3	mmol/m3	mmol/m3	mmol/m3
TC	13-Sep-93	75 19 N	174 0 W	118608	204	0.075	34.593	0.067	315.68	10.3	0.89	5.3
TC	13-Sep-93	75 19 N	174 0 W	118609	230	0.679	34.719	0.669	313.76	11.0	0.92	5.6
TC	13-Sep-93	75 19 N	174 0 W	118610	280	0.913	34.777	0.900	313.40	11.3	0.92	5.2
TC	13-Sep-93	75 19 N	174 0 W		280		34.777					
TC	13-Sep-93	75 19 N	174 0 W	118611	315	0.864	34.804	0.850	314.21	11.3	0.93	5.3
TC	13-Sep-93	75 19 N	174 0 W	118611	315	0.864	34.804	0.850				
TC	13-Sep-93	75 19 N	174 0 W	118612	356	0.812	34.819	0.796	315.23	11.4	0.95	5.6
TC	13-Sep-93	75 19 N	174 0 W	118613	406	0.673	34.822	0.655	314.12	11.6	0.94	5.9
TC	13-Sep-93	75 19 N	174 0 W	118614	508	0.549	34.845	0.526	315.10	11.7	0.99	6.0
TC	13-Sep-93	75 19 N	174 0 W	118615	639	0.39	34.861	0.362	314.97	11.8	0.99	6.4
D01	15-Sep-93	76 35 N	174 3 W	118641		-1.572	30.187		401.13	0.1	0.83	3.1
D01	15-Sep-93	76 35 N	174 3 W	118642		-1.587	31.625		373.30	4.9	1.16	12.7
D01	15-Sep-93	76 35 N	174 3 W	118643		-1.657	31.873		360.19	6.7	1.35	15.7
D01	15-Sep-93	76 35 N	174 3 W	118644		-1.65	32.358		330.75	10.5	1.69	25.4
D01	15-Sep-93	76 35 N	174 3 W	118645		-1.276	32.776		290.97	15.2	2.10	37.3
D01	15-Sep-93	76 35 N	174 3 W	118646		-1.558	33.146		269.74	17.1	2.28	45.0
D01	14-Sep-93	76 35 N	174 3 W	118620	128	-1.433	33.908	-1.436	286.44	11.5	1.21	18.6
D01	14-Sep-93	76 35 N	174 3 W	118621	152	-1.298	34.251	-1.302	305.55	10.4	0.93	9.2
D01	14-Sep-93	76 35 N	174 3 W	118622	177	-1	34.393	-1.005	305.33	10.6	0.89	7.9
D01	14-Sep-93	76 35 N	174 3 W	118623	204	-0.541	34.532	-0.548	306.58	11.0	0.87	7.0
D01	14-Sep-93	76 35 N	174 3 W	118624	229	-0.163	34.620	-0.171	306.58	11.4	0.88	6.8
D01	14-Sep-93	76 35 N	174 3 W	118625	255	0.1495	34.701	0.140	307.83	11.6	0.88	6.3
D01	14-Sep-93	76 35 N	174 3 W	118626	279	0.2845	34.747	0.273	309.79	11.8	0.89	6.1
D01	14-Sep-93	76 35 N	174 3 W	118627	306	0.406	34.789	0.393	310.06	11.9	0.91	6.1
D01	14-Sep-93	76 35 N	174 3 W	118628	330	0.4685	34.803	0.455	311.26	11.9	0.89	5.9
D01	14-Sep-93	76 35 N	174 3 W	118629	355	0.4615	34.823	0.446	310.51	12.2	0.90	5.8
D01	14-Sep-93	76 35 N	174 3 W	118630	407	0.5075	34.832	0.490	312.33	12.1	0.90	6.0
D01	14-Sep-93	76 35 N	174 3 W	118631	458	0.471	34.841	0.451	311.91	12.3	0.91	6.0
D01	14-Sep-93	76 35 N	174 3 W	118632	509	0.418	34.855	0.396	313.09	12.3	0.91	6.0
D01	14-Sep-93	76 35 N	174 3 W	118633	611	0.3125	34.885	0.286	310.64	12.5	0.93	7.1
D01	14-Sep-93	76 35 N	174 3 W	118634	819	0.0315	34.872	-0.004	309.75	12.6	0.92	6.6
D01	14-Sep-93	76 35 N	174 3 W	118635	1019	-0.161	34.890	-0.205	312.87	12.9	0.96	7.1

Stn	Date	Latitude	Longitude	Sample	Pressure	Temp	Salinity	Theta	Oxygen	Nitrate	Phosphate	Silicate
		deg/min	deg/min	#	dbar	deg C		deg C	mmol/m3	mmol/m3	mmol/m3	mmol/m3
D01	14-Sep-93	76 35 N	174 3 W	118636	1270	-0.316	34.906	-0.372	313.45	13.2	0.98	8.2
D01	14-Sep-93	76 35 N	174 3 W	118637	1522	-0.425	34.920	-0.495	311.09	13.6	1.01	9.1
D01	14-Sep-93	76 35 N	174 3 W	118638	1775	-0.4545	34.937	-0.539	305.11	14.2	1.05	10.6
D01	14-Sep-93	76 35 N	174 3 W	118639	2030	-0.4205	34.949	-0.523	298.20	14.6	1.07	12.3
D01	14-Sep-93	76 35 N	174 3 W	118640	2171	-0.3925	34.956	-0.505	294.67	15.0	1.11	14.2
E01	17-Sep-93	78 47 N	176 3 E	118652	2	-1.64	30.526	-1.640	382.85	0.3	0.62	8.3
E01	17-Sep-93	78 47 N	176 3 E	118653	11	-1.6505	30.594		378.34			
E01	17-Sep-93	78 47 N	176 3 E	118654	21	-1.5585	31.013	-1.559	372.45	1.0	0.67	9.3
E01	17-Sep-93	78 47 N	176 3 E	118655	31	-1.675	32.805	-1.676	336.26	6.2	0.88	10.9
E01	17-Sep-93	78 47 N	176 3 E	118656	42	-1.7545	33.434	-1.755	344.09	6.3	0.68	6.1
E01	17-Sep-93	78 47 N	176 3 E	118657	51	-1.7915	33.632	-1.792	344.58	6.4	0.65	5.1
E01	17-Sep-93	78 47 N	176 3 E	118658	62	-1.7615	33.753	-1.763	338.07	6.9	0.67	5.4
E01	17-Sep-93	78 47 N	176 3 E	118659	72	-1.753	33.858	-1.754	335.97	7.2	0.68	5.3
E01	17-Sep-93	78 47 N	176 3 E	118660	82	-1.7405	33.937	-1.742	333.25	7.5	0.70	5.2
E01	17-Sep-93	78 47 N	176 3 E	118661	103	-1.4905	34.121	-1.493	323.13	8.4	0.74	4.8
E01	17-Sep-93	78 47 N	176 3 E	118662	127	-1.12	34.305	-1.123	318.33	9.2	0.78	4.9
E01	17-Sep-93	78 47 N	176 3 E	118663	154	-0.518	34.469	-0.523	315.14	10.0	0.82	4.8
E01	17-Sep-93	78 47 N	176 3 E	118664	178	0.2435	34.595	0.237	313.54	10.3	0.84	5.4
E01	17-Sep-93	78 47 N	176 3 E	118665	205	0.936	34.731	0.927	310.10	11.3	0.89	5.1
E01	18-Sep-93	78 47 N	176 3 E	118668	12	-1.629	30.728	-1.629		0.6	0.68	9.1
E01	18-Sep-93	78 47 N	176 3 E	118669	32	-1.6945	33.016	-1.695				
E01	18-Sep-93	78 47 N	176 3 E	118670	52	-1.772	33.603	-1.773				
E01	18-Sep-93	78 47 N	176 3 E	118672	103	-1.504	34.136	-1.506				
E01	18-Sep-93	78 47 N	176 3 E	118673	128	-1.057	34.342	-1.060				
E01	18-Sep-93	78 47 N	176 3 E	118675	179	0.3185	34.608	0.311				
E01	18-Sep-93	78 47 N	176 3 E	118676	214	1.079	34.786	1.069	310.19	11.4	0.90	5.2
E01	18-Sep-93	78 47 N	176 3 E	118677	239	1.191	34.799	1.180	304.04	11.6	0.90	5.2
E01	18-Sep-93	78 47 N	176 3 E	118678	255	1.0825	34.848	1.071	309.03	11.7	0.91	5.3
E01	18-Sep-93	78 47 N	176 3 E	118679	280	1.08	34.823	1.067	309.75	11.8	0.91	5.2
E01	18-Sep-93	78 47 N	176 3 E	118680	305	1.0325	34.831	1.018	310.95	12.0	0.92	5.4
E01	18-Sep-93	78 47 N	176 3 E	118681	407	0.77	34.846	0.751				
E01	18-Sep-93	78 47 N	176 3 E	118683	320	1.046	34.837	1.031	310.82	11.7	0.95	5.5

Stn	Date	Latitude	Longitude	Sample	Pressure	Temp	Salinity	Theta	Oxygen	Nitrate	Phosphate	Silicate
		deg/min	deg/min	#	dbar	deg C		deg C	mmol/m3	mmol/m3	mmol/m3	mmol/m3
E01	18-Sep-93	78 47 N	176 3 E	118684	356	0.825	34.830	0.809	310.42	11.9	0.96	5.6
E01	18-Sep-93	78 47 N	176 3 E	118685	407	0.789	34.848	0.770	311.80	12.0	0.96	5.5
E01	18-Sep-93	78 47 N	176 3 E	118686	457	0.614	34.848	0.594	312.38	12.0	0.97	5.7
E01	18-Sep-93	78 47 N	176 3 E	118687	508	0.5005	34.852	0.478	313.40	12.0	0.95	5.8
E01	18-Sep-93	78 47 N	176 3 E	118688	559	0.417	34.852	0.392	314.83	12.1	0.96	5.7
E01	18-Sep-93	78 47 N	176 3 E	118689	609	0.336	34.857	0.309	313.05	12.1	0.96	5.8
E01	18-Sep-93	78 47 N	176 3 E	118690	711	0.159	34.860	0.128	314.92	12.2	0.97	6.0
E01	18-Sep-93	78 47 N	176 3 E	118691	811	0.0335	34.865	-0.002	313.54	12.2	0.97	6.4
E01	18-Sep-93	78 47 N	176 3 E	118692	913	-0.064	34.873	-0.104	313.27	12.4	0.97	7.1
E01	18-Sep-93	78 47 N	176 3 E	118693	1014	-0.149	34.880	-0.193	312.87	12.5	0.98	6.7
E01	18-Sep-93	78 47 N	176 3 E	118694	1116	-0.2455	34.886	-0.294	312.36	12.7	1.02	7.0
E01	18-Sep-93	78 47 N	176 3 E	118695	1217	-0.3125	34.893	-0.366	311.93	12.6	1.00	7.1
E01	18-Sep-93	78 47 N	176 3 E	118696	1319	-0.3635	34.901	-0.422	311.20	12.9	1.01	7.5
E01	18-Sep-93	78 47 N	176 3 E	118697	1420	-0.4105	34.907	-0.474	309.03	13.1	1.03	8.1
E01	18-Sep-93	78 47 N	176 3 E	118698	1521	-0.458	34.920	-0.527	307.70	13.5	1.05	8.7
E01	18-Sep-93	78 47 N	176 3 E	118699	1623	-0.5	34.930	-0.575	306.09	13.8	1.08	9.5
E01	18-Sep-93	78 47 N	176 3 E	118700	1748	-0.4635	34.934	-0.547	300.92	14.1	1.11	10.6
E01	18-Sep-93	78 47 N	176 3 E	118701	1855	-0.444	34.944	-0.534	296.72	14.6	1.14	11.7
E01	18-Sep-93	78 47 N	176 3 E	118702	1926	-0.4395	34.949	-0.534	294.72	14.6	1.15	12.2
E01	18-Sep-93	78 47 N	176 3 E	118703	1988	-0.419	34.952	-0.518	293.96	14.9	1.16	13.2
E01	18-Sep-93	78 47 N	176 3 E	118704	2028	-0.407	34.954	-0.509	290.35	14.9	1.18	13.5
E01	18-Sep-93	78 47 N	176 3 E	118705	2065	-0.403	34.953	-0.508	292.78	15.0	1.17	13.6
E01	18-Sep-93	78 47 N	176 3 E	118705	2065	-0.403	34.954	-0.508				
E04	19-Sep-93	76 58 N	174 9 E	123102	2	-1.571	29.305	-1.571	378.30	0.0	1.27	13.6
E04	19-Sep-93	76 58 N	174 9 E	123103	12	-1.5725	29.295	-1.573	378.97	0.0	1.24	13.4
E04	19-Sep-93	76 58 N	174 9 E	123104	22	-1.5685	29.502	-1.569	376.91	0.2	1.24	13.5
E04	19-Sep-93	76 58 N	174 9 E	123105	32	-1.548	31.510	-1.549	327.36	5.3	1.46	19.0
E04	19-Sep-93	76 58 N	174 9 E	123106	52	-1.527	33.569	-1.528	299.04	9.5	1.08	14.6
E04	19-Sep-93	76 58 N	174 9 E	123107	62	-1.644	33.790	-1.645	316.12	8.5	0.86	9.1
E04	19-Sep-93	76 58 N	174 9 E	123108	72	-1.592	33.990	-1.593	320.72	8.5	0.80	6.4
E04	19-Sep-93	76 58 N	174 9 E	123109	103	-1.255	34.299	-1.257	316.57	9.2	0.81	5.5
E04	19-Sep-93	76 58 N	174 9 E	123110	128	-0.706	34.448	-0.710	315.68	9.7	0.82	5.1

Stn	Date	Latitude	Longitude	Sample	Pressure	Temp	Salinity	Theta	Oxygen	Nitrate	Phosphate	Silicate
		deg/min	deg/min	#	dbar	deg C		deg C	mmol/m3	mmol/m3	mmol/m3	mmol/m3
E04	19-Sep-93	76 58 N	174 9 E	123111	153	0.183	34.588	0.177	313.45	10.6	0.86	5.0
E04	19-Sep-93	76 58 N	174 9 E	123112	179	0.8575	34.714	0.850	309.88	11.2	0.88	5.1
E04	19-Sep-93	76 58 N	174 9 E	123113	204	1.2145	34.780	1.205	313.60	11.6	0.90	5.1
E04	19-Sep-93	76 58 N	174 9 E	123114	254	1.418	34.828	1.405	311.09	11.8	0.92	5.4
E04	19-Sep-93	76 58 N	174 9 E	123115	305	1.283	34.842	1.268	311.44	11.8	0.92	5.4
E04	19-Sep-93	76 58 N	174 9 E	123116	356	1.059	34.843	1.042	311.62	11.9	0.92	5.5
E04	19-Sep-93	76 58 N	174 9 E	123117	406	0.9105	34.845	0.891	312.02	12.0	0.93	5.3
E04	19-Sep-93	76 58 N	174 9 E	123118	457	0.789	34.848	0.768	312.69	12.0	0.93	5.5
E04	19-Sep-93	76 58 N	174 9 E	123119	508	0.643	34.843	0.620	313.05	12.0	0.93	5.7
E04	19-Sep-93	76 58 N	174 9 E	123120	609	0.4385	34.844	0.411	314.12	12.0	0.93	5.8
E04	19-Sep-93	76 58 N	174 9 E	123121	711	0.3505	34.880	0.319	313.89	12.1	0.94	6.0
E04	19-Sep-93	76 58 N	174 9 E	123122	812	0.1845	34.967	0.148	313.98	12.3	0.95	6.2
F09	22-Sep-93	73 30 N	166 2 W	123127	2	-0.85	29.222	-0.850	404.17	0.0	0.81	10.3
F09	22-Sep-93	73 30 N	166 2 W	123128	12	-0.8575	29.234	-0.858	378.88	0.0	0.79	10.5
F09	22-Sep-93	73 30 N	166 2 W	123129	22	-1.2445	31.882	-1.245	379.23	3.5	1.35	14.2
F09	22-Sep-93	73 30 N	166 2 W	123130	32	-1.46	32.243	-1.461	324.82	9.2	1.85	28.8
F09	22-Sep-93	73 30 N	166 2 W	123131	43	-1.574	32.444	-1.575	308.68	12.3	2.03	37.7
F09	22-Sep-93	73 30 N	166 2 W	123132	53	-1.6145	32.608	-1.615		13.6	2.10	42.5
F09	22-Sep-93	73 30 N	166 2 W	123133	61	-1.627	32.676	-1.628	297.37	14.6	2.16	45.5
F09	22-Sep-93	73 30 N	166 2 W	123134	75	-1.5665	32.803	-1.568	296.23	15.1	2.12	44.6
F09	22-Sep-93	73 30 N	166 2 W	123135	86	-0.67	34.167	-0.673	244.23	14.4	1.84	33.6
C01	23-Sep-93	75 0 N	162 1 W	123136	2	-1.569	29.052	-1.569	386.55	0.0	0.81	3.2
C01	23-Sep-93	75 0 N	162 1 W	123137	12	-1.577	29.080	-1.577	387.40	0.0	0.76	2.9
C01	23-Sep-93	75 0 N	162 1 W	123138	22	-1.178	31.176	-1.178	377.00	1.8	1.01	6.7
C01	23-Sep-93	75 0 N	162 1 W	123139	32	-1.1745	31.727	-1.175	362.46	4.1	1.14	9.0
C01	23-Sep-93	75 0 N	162 1 W	123140	52	-1.3505	32.064	-1.351	325.67	8.5	1.57	21.4
C01	23-Sep-93	75 0 N	162 1 W	123141	77	-1.252	32.414	-1.254	313.54	11.7	1.79	29.2
C01	23-Sep-93	75 0 N	162 1 W	123142	103	-1.499	32.717	-1.501	308.01	13.3	1.87	36.4
C01	23-Sep-93	75 0 N	162 1 W	123143	127	-1.416	33.094	-1.419	290.97	15.6	1.99	34.7
C01	23-Sep-93	75 0 N	162 1 W	123144	153	-1.3455	33.557	-1.349		18.1	2.10	40.3
C01	23-Sep-93	75 0 N	162 1 W	123145	204	-0.942	34.380	-0.948	292.84	11.3	1.03	12.0
C01	23-Sep-93	75 0 N	162 1 W	123146	255	-0.258	34.598	-0.267	300.51	11.3	0.94	8.1

Stn	Date	Latitude	Longitude	Sample	Pressure	Temp	Salinity	Theta	Oxygen	Nitrate	Phosphate	Silicate
		deg/min	deg/min	#	dbar	deg C		deg C	mmol/m3	mmol/m3	mmol/m3	mmol/m3
C01	23-Sep-93	75 0 N	162 1 W	123147	305	0.256	34.760	0.244	327.63	11.7	0.92	6.9
C01	23-Sep-93	75 0 N	162 1 W	123148	356	0.4645	34.798	0.449	307.18	11.9	0.92	6.5
C01	23-Sep-93	75 0 N	162 1 W	123149	407	0.4845	34.819	0.467	307.92	12.0	0.93	6.7
C01	23-Sep-93	75 0 N	162 1 W	123150	508	0.423	34.845	0.401	307.87	12.2	0.94	6.7
C01	23-Sep-93	75 0 N	162 1 W	123151	913	0.0655	34.877	0.025	308.50	12.5	0.97	7.0
C01	23-Sep-93	75 0 N	162 1 W	123152	1267	-0.147	34.911	-0.205	303.37	13.2	1.03	9.4
C01	23-Sep-93	75 0 N	162 1 W	123153	1521	-0.2785	34.924	-0.350	299.51	13.9	1.08	11.6
C01	23-Sep-93	75 0 N	162 1 W	123154	1623	-0.303	34.929	-0.380	297.71	13.9	1.10	12.6
C01	23-Sep-93	75 0 N	162 1 W	123155	1776	-0.311	34.931	-0.398	297.75	14.0	1.12	11.9
C01	23-Sep-93	75 0 N	162 1 W	123156	1929	-0.3085	34.932	-0.406	295.43	14.1	1.11	12.7
C01	23-Sep-93	75 0 N	162 1 W	123157	1971	-0.305	34.931	-0.405	296.01	14.2	1.13	13.1

Station	Depth	Sample#	Salinity	Theta	CFC-12	CFC-11	CFC-113	CH3CCl3	CCl4	Comments
				Deg C	nmol/m3	nmol/m3	nmol/m3	nmol/m3	nmol/m3	
A01	0	wf1	25.170	-0.306	2.37	5.26		14.15	6.69	conc >measured in air
A01	10	wf2	27.589	0.549	2.32	4.90		13.71	6.23	conc >measured in air
A01	30	wf3	30.660	-1.171	2.31	4.86	0.61	14.04	5.25	
A01	50	wf4	31.884	-1.246	1.99	4.03	0.69	11.66	3.35	
A01	75	wf5	32.428	-1.346	1.68	2.99	0.41	9.45	4.09	
A01	100	wf6	32.734	-1.433	1.64	2.85	0.25	7.64	2.46	
A01	125	wf7	32.974	-1.460	1.69	3.07	0.57	10.02	2.84	
A01	150	wf8	33.239	-1.422	1.56	2.48	0.34	8.55	2.68	
A01	175	wf9	33.585	-1.296	1.60	2.80	0.18	9.30	3.14	
A01	200	wf10	34.066	-0.985	1.49	2.54	0.50	7.79	2.49	
A01	225	wf11	34.428	-0.619	1.25	1.85	0.31	6.04	2.21	
A01	275	wf13	34.652	-0.095	1.35	2.13	0.11	6.76	4.25	
A01	300	wf14	34.712	0.098	1.31	2.25	0.29	7.51	3.19	
A01	350	wf15	34.775	0.310	1.25	2.18	0.43	5.95	2.98	
A01	400	wf16	34.807	0.396	1.24	1.89	0.05	6.43	4.26	
A01	450	wf17	34.828	0.404	0.98	1.76	0.44	4.59	2.67	
A01	500	wf181	34.830	0.410	0.84	1.21	0.37	3.44	2.30	
A01	550	wf192	34.855	0.407	0.77	0.81	0.02	3.19	3.08	
A01	600	w118552	34.861	0.373	0.70	1.14	0.02	2.73	1.94	bubbles in from V3
A01	700	w118553	34.873	0.292	0.51	0.79	0.17	2.89	1.63	
A01	800	w118554	34.881	0.181	0.45	0.72	0.13	2.27	1.70	113 shift
A01	900	w118555	34.889	0.076	0.35	0.62	0.16	2.64	1.79	
A01	1000	w118556	34.895	-0.033	0.33	0.66	0.26	2.06	1.65	
A01	1250	w118557	34.904	-0.241	0.32	0.41	0.31	1.42	1.37	113 shift
A01	1500	w118540a	34.920	-0.377	0.20		0.22	1.34	0.95	water peak, 113 shift
A01	1700	w118542	34.927	-0.452	0.15	0.22	0.27	0.83	0.66	113 shift
A01	1800	w117543	34.930	-0.479	0.12	0.21	0.01	0.61	0.71	
A01	1900	w118544	34.936	-0.496	0.10	0.17	0.13	1.32	0.88	
A01	2000	w118545	34.938	-0.506	0.08	0.14	0.04	1.09	0.41	
A01	2250	w118546	34.946	-0.517	0.04	0.10	0.02	0.56	0.21	
A01	2500	w118547	34.950	-0.519	0.02	0.05	0.14	1.81	0.36	
A01	3000	w118548	34.956	-0.508	0.01	0.06	0.00	0.68	0.07	

Station	Depth	Sample#	Salinity	Theta	CFC-12	CFC-11	CFC-113	CH3CCl3	CCl4	Comments
				Deg C	nmol/m3	nmol/m3	nmol/m3	nmol/m3	nmol/m3	
A01	3360	w118549	34.958	-0.508	0.02	0.04	0.00	0.00	0.06	bubbles in from V3
B01	10	w118573	27.807	-0.132	2.29	5.27	0.49	12.88	6.00	113 shift
B01	20	w118574	29.411	2.358	2.14	4.96	0.29	12.51	4.47	
B01	40	w118576	31.500	1.014	2.42	5.12	0.34	13.50	4.34	113 shift
B01	50	w118577	31.960	0.038	2.27	5.04	0.42	12.80	4.36	
B01	70	w118579	32.283	-1.060	2.30	5.11	0.31	13.34	4.01	113 shift
B01	100	w118581	32.574	-1.407	2.28	5.01	0.35	13.86	3.61	
B01	125	w118582	32.775	-1.321	2.17	4.90	0.20	12.69	3.67	113 shift
B01	150	w118583	33.521	-1.197	1.59	3.61	0.07	9.81	2.11	
B01	175	w118584	34.000	-1.043	1.19	2.58	0.01	7.46	2.01	113 shift
B01	200	118585	34.229	-0.849	0.98	1.87	0.21	5.69	2.14	113 shift
B01	225	118586	34.445	-0.633	0.98	1.93	0.10	5.68	2.06	113 shift
B01	250	118587	34.579	-0.310	0.93	1.78	0.16	5.13	2.27	
B01	275	118588	34.659	-0.102	0.87	1.54	0.08	4.01	1.87	
B01	300	118589	34.718	0.126	0.75	1.32	0.12	3.26	2.65	
B01	350	118590	34.789	0.349	0.82	1.37	0.06	3.48	1.97	
B01	400	118559	34.814	0.405	0.81	1.58	0.19	5.01	3.03	
B01	450	118560	34.836	0.418	0.77	1.32	0.06	2.73	2.22	
B01	500	118561	34.853	0.413	0.56	0.92	0.13	1.16	1.54	
B01	600	118562	34.866	0.353	0.52	0.87	0.16	1.42	2.48	
B01	700	118563	34.875	0.231	0.51	0.93	0.12	2.46	2.09	
B01	800	118564	34.882	0.099	0.48	0.84	0.09	1.82	2.75	
B01	1000	118566	34.893	-0.129	0.40	0.66	0.04	0.95	1.39	
B01	1250	118567	34.908	-0.293						Don't use comment in log
B01	1500	118568	34.923	-0.425	0.17	0.32	0.03	0.00	0.75	
B01	2000	118569	34.943	-0.513	0.05	0.13	0.03	0.00	0.23	
B01	2500	118570q	34.956							Bottle leaking - ? depth
B01	3423	118571	34.956	-0.510	0.02	0.12	0.03	0.20	0.23	
E01	20	w118654	31.013	-1.559	2.19	4.97	0.39	13.33	5.69	
E01	30	w118655	32.805	-1.676	2.09	4.93	0.33	14.13	4.22	
E01	40	w118656	33.434	-1.755	2.05	4.78	0.40	13.62	3.83	
E01	60	w118658	33.753	-1.763	2.05	4.79	0.32	13.45	3.79	

Station	Depth	Sample#	Salinity	Theta	CFC-12	CFC-11	CFC-113	CH3CCl3	CCl4	Comments
				Deg C	nmol/m3	nmol/m3	nmol/m3	nmol/m3	nmol/m3	
E01	70	w118659	33.858	-1.754	1.91	4.42	0.28	12.19	3.32	
E01	80	w118660	33.937	-1.742	1.96	4.49	0.21	12.02	4.04	
E01	100	w118661	34.121	-1.493						Elastic
E01	125	w118673	34.342	-1.060	1.76	4.01	0.53	11.01	3.14	
E01	150	w118663	34.469	-0.523	1.68	3.90	0.15	11.38	3.46	Same syringe repeat inj
E01	175	w118675	34.608	0.311	1.66	3.68	0.49	11.00	3.47	
E01	200	w118665	34.731	0.927	1.65	3.70	0.16	10.40	3.58	
E01	210	w118676	34.786	1.069	1.61	3.63	0.48	10.33	3.68	
E01	235	w118677	34.799	1.180	1.64	3.58	0.43	9.57	3.65	
E01	250	w118678	34.848	1.071	1.66	3.26	0.25	9.70	3.58	
E01	275	w118679	34.823	1.067	1.47	3.12	0.39	8.15	3.22	
E01	300	w118680	34.831	1.018	1.51	3.24	0.45	8.77	3.55	
E01	315	w118683	34.837	1.031						elastic
E01	350	w118684	34.830	0.809	1.43	3.10	0.14	8.28	3.83	
E01	400	w118685	34.848	0.770	1.31	2.78	0.22	7.31	3.90	
E01	450	w118686t	34.848	0.594	1.63	3.58	0.26	9.71	4.03	
E01	500	w118687	34.852	0.478	1.56	3.53	0.14	9.66	4.10	
E01	550	w118688	34.852	0.392	1.59	3.51	0.24	8.25	3.80	
E01	600	w118689	34.857	0.309	1.46	3.23	0.24	7.46	3.66	
E01	800	w118691	34.865	-0.002	1.40	3.20	0.16	8.18	4.17	tail on CCl4
E01	1000	w118693	34.880	-0.193	1.32	2.90	0.13	7.64	3.70	
E01	1200	w118695	34.893	-0.366	1.05	2.05	0.06	5.25	2.86	
E01	1400	w118697	34.907	-0.474	0.68	1.40	0.00	4.35	2.43	
E01	1600	w118699	34.930	-0.575	0.53	1.12	0.00	3.99	2.94	
E01	1830	w118701	34.944	-0.534	0.07	0.15	0.00	1.90	2.21	
E01	1900	w118702	34.949	-0.534	0.06	0.13	0.00	1.26	0.49	
E01	1960	w118703	34.952	-0.518	0.03	0.02	0.00	1.70	0.65	
E01	2000	w118704	34.954	-0.509	0.01	0.00	0.00	0.41	0.13	
E01	2035	w118705a	34.953	-0.508	0.00	0.00	0.00	1.52	0.41	MC/CCl4 unresolved
blank correction for C					0.16	0.09	0.09	1.34	0.36	
C01	0	w123136	29.052	-1.569	2.12	4.37	0.23	10.20	4.66	
C01	30	w123139	31.727	-1.175	1.98	4.73	0.21	13.20	4.18	

Station	Depth	Sample#	Salinity	Theta	CFC-12	CFC-11	CFC-113	CH3CCl3	CCl4	Comments
				Deg C	nmol/m3	nmol/m3	nmol/m3	nmol/m3	nmol/m3	
C01	75	w123141	32.414	-1.254	1.94	4.10	0.20	10.80	3.00	
C01	100	w123142	32.717	-1.501	1.91	4.02	0.15	10.22	3.18	
C01	125	w123143	33.094	-1.419	1.73	3.56	0.14	10.75	3.10	
C01	150	w123144	33.557	-1.349	1.55	2.86	0.07	7.20	1.58	
C01	200	w123145	34.380	-0.948	1.22	2.02	0.07	5.92	0.97	
C01	250	w123146	34.598	-0.267	1.23	2.29	0.04	6.05	2.11	
C01	300	w123147	34.760	0.244	1.21	2.17	0.07	7.32	1.62	
C01	350	w123148	34.798	0.449	1.25	2.09	0.01	5.08	2.28	
C01	400	w123149	34.819	0.467	1.20	2.04	0.04	5.62	2.90	
C01	500	w123150	34.845	0.401	1.00	1.76	0.04	4.98	2.44	
C01	900	w123151	34.877	0.025	0.72	1.06	0.06	3.61	0.98	
C01	1250	w123152	34.911	-0.205	0.07	0.12	-0.01	0.28	0.81	
C01	1500	w123153	34.924	-0.350	0.00	0.01	0.00		-0.36	poor resolution,leak?
C01	1750	w123155	34.931	-0.398	-0.02	-0.01	0.00	0.00	0.00	
C01	1900	w123156	34.932	-0.406	0.03	0.00	0.00		-0.36	poor resolution,leak?
C01	1940	w123157	34.931	-0.405	0.00	0.00	-0.03		-0.36	poor resolution,leak?
D01	40	w118643	31.873	-1.658	2.10	4.89	0.24	14.26	5.38	
D01	80	w118645	32.776	-1.278	2.06	4.55	0.14	13.04	4.20	
D01	100	w118646	33.146	-1.560	1.96	4.33	0.15	12.45	4.00	
D01	125	w118620	33.908	-1.436	1.75	4.04	0.25	11.78	2.63	
D01	150	w118621	34.251	-1.302	1.62	3.59	0.07	10.72	2.60	
D01	175	w118622	34.393	-1.005	1.48	3.06	0.23	8.81	2.30	
D01	200	w118623	34.532	-0.548	1.55	3.25	0.02	8.83	2.69	
D01	225	w118624	34.620	-0.171	1.40	2.76	0.18	7.56	2.41	
D01	250	w118625	34.701	0.140	1.44	2.91	0.00	7.69	3.43	
D01	300	w118627	34.789	0.393	1.39	2.80	0.15	8.26	3.09	
D01	325	w118628	34.803	0.455	1.46	2.97	0.00	7.87	3.30	
D01	350	w118629	34.823	0.446	1.32	2.57	0.13	7.63	3.04	
D01	400	w118630	34.832	0.490	1.42	2.76	0.00	7.37	3.22	
D01	450	w118631	34.841	0.451	1.28	2.49	0.00	7.25	3.88	
D01	500	w118632	34.855	0.396	1.42	2.53	0.00	7.56	3.08	
D01	600	w118633	34.885	0.286	1.09	1.90	0.00	5.69	2.55	

Station	Depth	Sample#	Salinity	Theta	CFC-12	CFC-11	CFC-113	CH3CCl3	CCl4	Comments
				Deg C	nmol/m3	nmol/m3	nmol/m3	nmol/m3	nmol/m3	
D01	1000	w118635	34.890	-0.205	0.80	1.32	0.00	4.13	2.21	Elastic on
D01	1500	w118637	34.920	-0.495	0.36	0.53	0.00	1.17	0.79	
D01	1750	w118638	34.937	-0.539	0.16	0.25	0.00	0.26	0.40	
D01	2150	w118640	34.956	-0.505	0.01	0.01	0.00	0.00	0.17	
TA	0	w118591	29.739	-1.264	2.36	5.22	0.56	15.22	7.03	
TA	10	w118592	29.858	-1.326	2.41	5.23	0.58	15.67	7.07	
TA	20	w118593	31.886	-1.546	2.31	5.14	0.51	16.51	5.98	
TA	30	w118594	32.070	-1.653	2.42	5.21	0.53	16.81	6.09	
TA	40	w118595	32.203	-1.534	2.35	5.11	0.41	15.15	5.81	
TA	50	w118596	32.445	-1.123	2.31	5.07	0.43	15.89	5.56	
TA	60	w118597	32.727	-1.219	2.21	5.04	0.43	15.62	5.36	
TA	70	w118598	32.856	-1.506	2.26	4.89	0.27	15.71	5.33	
TA	80	w118599	33.002	-1.643	2.15	4.67	0.23	14.59	4.98	
TA	100	w118600	33.386	-1.407	2.14	4.72	0.26	14.00	4.18	
TC	75	w118603	33.052	-1.420	2.16	4.65	0.21	13.49	3.85	
TC	100	w118604	33.888	-1.574	1.99	4.48	0.07	14.12	3.80	
TC	125	w118605	34.189	-1.460	1.94	4.36	0.15	12.36	3.46	
TC	150	w118606	34.369	-1.162	1.97	4.57	0.08	13.56	3.95	
TC	175	w118607	34.491	-0.545	1.95	4.44	0.12	12.74	3.94	
TC	200	w118608	34.593	0.067	1.93	4.32	0.07	12.15	4.01	
TC	225	w118609	34.719	0.669	1.85	4.09	0.18	11.22	4.05	
TC	275	w118610 r	34.777	0.900	1.75	3.85	0.25	11.37	4.13	coelution? water pk with 12
TC	310	w118611	34.804	0.850	1.72	3.72	0.05	11.17	4.35	F11 too big- water,trap chnged
TC	350	w118612	34.819	0.796	1.72	3.73	0.05	11.07	4.08	
TC	400	w118613	34.822	0.655	1.68	3.60	0.08	10.28	4.09	
TC	500	w118614	34.845	0.526	1.72	3.75	0.02	10.79	4.40	
TC	615	w118615	34.861	0.362	1.59	3.39	0.19	10.27	4.05	
F09	0	w123127	29.222	-0.850	2.33	4.95	0.32	11.45	5.25	
F09	10	w123128	29.234	-0.858	2.10	4.95	0.13	12.84	5.50	
F09	50	w123132	32.608	-1.615	2.06	4.68	0.02	12.61	4.77	
F09	70	w123134	32.803	-1.568	2.05	4.72	0.20	13.16	4.96	
F09	87	w1231305	34.167	-0.673	1.23	2.14	0.01	6.89	1.82	

Station	Depth	Sample#	Salinity	Theta	CFC-12	CFC-11	CFC-113	CH3CCl3	CCl4	Comments
				Deg C	nmol/m3	nmol/m3	nmol/m3	nmol/m3	nmol/m3	
E04	0	w123102	29.305	-1.571	3.05	6.77		16.08	6.24	conc > measured in air
E04	20	w123104	29.502	-1.569	2.14	4.95	0.57	16.31	5.34	
E04	50	w123106	33.569	-1.528	2.66	5.34	0.58	14.75	6.17	
E04	70	w123108	33.990	-1.593	1.60	4.04	0.31	14.74		File lost, can't verify low CCl4
E04	100	w123109	32.299	-1.257	1.74	4.01	0.28	11.83	3.61	ice in syringe
E04	150	w123111	34.588	0.177	1.68	3.86	0.28	11.32	3.39	
E04	200	w123113	34.780	1.205	1.61	3.68	0.29	11.14	4.36	
E04	250	w123114	34.828	1.405	1.63	3.71	0.30	11.60	3.60	
E04	300	w123115	34.842	1.268	1.55	3.35	0.24	9.96	4.62	ice in syringe
E04	350	w123116	34.843	1.042	1.62	3.61		11.43	3.45	conc > measured in air
E04	400	w123117	34.845	0.891	1.60	3.69	0.25	11.09	4.57	
E04	500	w123119	34.843	0.620	1.59	3.57	0.44	10.85	4.37	
E04	600	w123120	34.844	0.411	1.60	3.63	0.26	10.55	4.52	
E04	800	w123122	34.967	0.148	1.52	3.24	0.22	9.00	4.29	
E04	850	w123123	34.871	-0.091	1.46	3.20	0.21	9.63	4.58	

Station	Depth	CFC-12 (air	F-11(air)	F-113(air)	MET(air)	CCl4 (air)
	m	pptv	pptv	pptv	pptv	pptv
A01	0	317.58	168.46		79.56	76.30
A01	10	334.33	169.92		80.81	75.64
A01	30	310.31	155.25	61.49	75.17	60.70
A01	50	269.37	129.67	69.62	62.14	39.14
A01	75	227.55	96.01	41.05	50.08	47.78
A01	100	220.74	91.13	25.45	40.27	28.67
A01	125	228.26	98.22	57.44	52.76	33.13
A01	150	211.03	79.73	34.88	45.11	31.47
A01	175	220.04	91.41	18.37	49.46	37.21
A01	200	209.79	85.00	52.51	42.12	30.12
A01	225	180.51	63.72	34.07	33.37	27.28
A01	275	200.38	76.10	12.84	38.46	53.85
A01	300	197.56	81.30	33.09	43.19	40.81
A01	350	190.87	79.92	49.84	34.64	38.57
A01	400	190.15	69.54	5.80	37.59	55.36
A01	450	149.48	64.85	51.48	26.85	34.73
A01	500	128.28	44.65	43.36	20.12	29.85
A01	550	117.64	29.86	2.18	18.67	40.03
A01	600	106.90	41.91	1.89	15.93	25.18
A01	700	77.49	28.99	20.38	16.77	21.14
A01	800	68.59	26.07	14.54	13.09	21.86
A01	900	52.52	22.53	18.75	15.15	22.87
A01	1000	49.51	23.85	30.04	11.75	21.02
A01	1250	46.95	14.60	35.21	8.00	17.28
A01	1500	28.87		24.61	7.53	11.85
A01	1700	21.95	7.68	29.81	4.62	8.29
A01	1800	17.38	7.15	1.08	3.38	8.83
A01	1900	14.32	6.07	14.60	7.33	11.00
A01	2000	11.61	4.86	4.67	6.05	5.09
A01	2250	5.64	3.62	2.45	3.12	2.55
A01	2500	2.25	1.90	15.66	10.07	4.52
A01	3000	2.01	2.14	0.00	3.79	0.84
A01	3000	0.04	1.31	13.04	8.19	8.77
A01	3360	2.20	1.29	0.00	0.00	0.76
A01	3360	1.72	2.28	16.76	7.36	4.73
B01	10	317.74	175.22	51.99	73.13	70.75
B01	20	347.64	196.41	37.05	81.53	60.08
B01	40	371.43	190.21	40.73	81.70	56.12
B01	50	330.93	176.50	46.29	73.36	54.08
B01	70	315.61	167.16	32.44	71.87	47.37
B01	100	307.65	160.58	34.97	73.19	42.15
B01	125	294.15	158.24	20.67	67.34	43.05
B01	150	218.84	118.43	7.24	52.46	25.04
B01	175	166.39	86.03	1.05	40.25	24.15
B01	200	138.53	63.35	22.67	31.03	26.03
B01	225	141.36	66.20	10.69	31.35	25.37
B01	250	135.94	62.65	18.20	28.84	28.42
B01	275	129.61	55.03	9.00	22.81	23.68
B01	300	113.26	47.90	13.82	18.75	33.94

Station	Depth	CFC-12 (air	F-11(air)	F-113(air)	MET(air)	CCl4 (air)
	m	pptv	pptv	pptv	pptv	pptv
B01	350	124.59	50.38	7.10	20.31	25.52
B01	400	124.22	58.45	21.74	29.32	39.33
B01	450	118.21	48.82	6.88	15.96	28.85
B01	500	85.29	33.82	14.93	6.79	20.06
B01	600	79.29	32.04	19.02	8.27	32.11
B01	700	77.43	33.92	14.06	14.23	26.99
B01	800	72.98	30.30	9.84	10.44	35.25
B01	1000	59.04	23.66	4.45	5.42	17.56
B01	1250					
B01	1500	24.17	11.13	3.27	0.00	9.34
B01	2000	7.22	4.45	2.88	0.00	2.85
B01	2500					
B01	3423	2.73	4.14	2.95	1.13	2.81
E01	20	288.47	155.03	38.31	69.80	64.86
E01	30	278.03	155.36	32.64	73.53	48.67
E01	40	273.33	150.78	39.37	70.52	44.29
E01	60	273.69	151.50	32.03	69.65	44.02
E01	70	255.29	139.97	27.73	63.14	38.56
E01	80	262.85	142.51	20.89	62.28	47.06
E01	100					
E01	125	247.01	133.68	55.98	59.28	37.94
E01	150	243.53	135.03	16.36	63.21	42.86
E01	150	235.52	123.78	7.62	54.09	42.96
E01	175	251.95	134.58	57.43	63.98	46.23
E01	200	259.77	141.04	19.50	62.65	49.01
E01	210	256.59	139.69	58.93	62.69	48.84
E01	235	261.93	138.68	53.43	58.45	48.28
E01	250	264.30	125.45	31.26	58.88	43.17
E01	275	234.28	120.09	47.59	49.48	47.51
E01	300	239.78	124.59	55.35	53.10	56.01
E01	315					
E01	350	224.58	117.46	16.40	49.53	50.76
E01	400	205.28	105.02	26.65	43.62	51.61
E01	450	252.36	133.93	31.45	57.39	52.79
E01	500	240.65	131.11	17.00	56.72	53.42
E01	550	243.81	129.32	27.82	48.19	49.29
E01	600	222.12	118.40	27.72	43.38	47.38
E01	800	209.81	114.92	18.69	46.77	53.21
E01	1000	195.04	103.17	14.85	43.20	46.74
E01	1200	153.48	72.16	7.12	29.42	35.93
E01	1400	98.49	48.81	0.00	24.25	30.30
E01	1600	77.44	38.74	0.00	22.08	36.47
E01	1830	10.48	5.05	0.00	10.53	27.52
E01	1900	9.27	4.67	0.00	7.02	6.16
E01	1960	4.79	0.71	0.00	9.45	8.14
E01	2000	0.97	0.00	0.00	2.29	1.65
E01	2035	0.00	0.00	0.00	8.43	5.08
E01	2035	0.27	0.00	0.00		
C01	0	273.62	133.55	21.96	53.38	52.03

Station	Depth	CFC-12 (air	F-11(air)	F-113(air)	MET(air)	CCl4 (air)
	m	pptv	pptv	pptv	pptv	pptv
C01	30	267.86	152.71	21.54	70.66	48.89
C01	75	263.11	132.59	20.12	57.56	35.25
C01	100	256.82	128.13	14.65	53.67	37.02
C01	125	234.53	114.49	14.37	56.77	36.28
C01	150	211.78	92.94	7.30	38.17	18.62
C01	200	172.33	68.07	7.46	32.08	11.82
C01	250	180.40	80.82	4.69	34.09	26.51
C01	300	184.36	79.08	7.70	42.46	20.88
C01	350	191.91	77.23	1.53	29.80	29.73
C01	400	184.44	75.47	4.36	33.00	37.74
C01	500	153.65	65.00	4.30	29.09	31.73
C01	900	107.47	38.36	7.13	20.68	12.56
C01	1250	9.82	4.37	0.00	1.59	10.25
C01	1500	-0.39	0.36	0.56		
C01	1750	-2.22	0.00	0.45	-0.03	0.03
C01	1900	4.38	0.13	0.00		
C01	1940	-0.06	0.00	0.00		
D01	40	277.12	152.88	23.81	74.24	61.63
D01	80	280.47	147.36	14.53	69.38	49.37
D01	100	264.07	137.94	15.30	65.20	46.58
D01	125	238.32	130.72	25.35	62.13	31.06
D01	150	222.96	117.82	6.80	56.98	31.00
D01	175	208.28	102.54	24.72	47.58	27.85
D01	200	223.64	112.50	2.72	48.94	33.30
D01	225	207.59	97.91	20.76	42.82	30.41
D01	250	216.84	105.46	0.00	44.31	43.93
D01	300	212.22	103.38	18.01	48.29	40.08
D01	325	223.75	109.99	0.00	46.17	42.94
D01	350	202.75	95.23	15.52	44.72	39.60
D01	400	219.26	102.51	0.00	43.31	41.97
D01	450	197.33	92.32	0.00	42.53	50.53
D01	500	217.18	93.44	0.00	44.20	39.99
D01	600	165.29	69.76	0.00	33.08	32.96
D01	1000	119.12	46.97	0.00	23.33	27.87
D01	1500	53.07	18.58	0.00	6.53	9.89
D01	1750	23.42	8.68	0.00	1.42	4.99
D01	2150	1.31	0.29	0.00	0.00	2.11
TA	0	311.66	164.05	55.69	81.06	80.22
TA	10	317.68	163.91	57.03	83.17	80.57
TA	20	307.61	162.08	50.35	86.55	68.87
TA	30	319.91	163.36	51.98	87.59	69.87
TA	40	313.35	161.78	40.33	79.42	67.09
TA	50	316.54	165.18	43.87	85.29	65.59
TA	60	301.75	163.59	44.46	83.41	63.16
TA	70	303.43	156.12	27.30	82.52	62.08
TA	80	287.26	147.89	22.64	76.05	57.66
TA	100	290.63	152.31	26.35	73.96	49.16
TC	75	292.08	149.62	21.12	71.22	45.07
TC	100	268.63	143.61	6.74	73.86	44.58

Station	Depth	CFC-12 (air	F-11(air)	F-113(air)	MET(air)	CCl4 (air)
	m	pptv	pptv	pptv	pptv	pptv
TC	125	264.55	141.33	14.83	65.11	40.91
TC	150	274.96	151.64	8.75	72.64	47.45
TC	175	282.70	153.34	12.89	70.63	48.77
TC	200	289.02	155.69	7.72	69.75	51.22
TC	225	286.86	153.26	21.23	66.58	53.28
TC	275	275.87	146.57	30.51	68.36	54.83
TC	275				63.47	54.52
TC	310	270.92	141.16	5.73	67.00	57.65
TC	310	275.81		6.18	69.02	55.59
TC	350	269.79	141.23	5.89	66.15	54.02
TC	400	260.80	134.94	9.04	60.98	53.70
TC	500	264.79	139.62	2.00	63.54	57.49
TC	615	243.40	124.83	21.70	59.94	52.56
F09	0	314.32	159.25	32.37	62.40	60.78
F09	10	283.43	158.96	13.15	69.94	63.70
F09	50	274.02	147.83	1.68	65.83	55.13
F09	70	274.65	149.83	20.40	68.87	57.53
F09	87	176.64	73.25	1.16	37.91	22.31
E04	0	394.95	207.54		84.17	69.85
E04	50	359.12	171.34	58.12	77.36	72.33
E04	20	277.96	152.23	55.37	85.37	59.93
E04	70	216.80	129.70	31.45	77.03	
E04	100	236.37	129.45	28.88	62.99	42.31
E04	150	253.68	140.13	32.39	65.39	43.52
E04	200	258.48	142.97	35.60	68.12	58.74
E04	250	264.86	146.04	38.34	71.71	49.03
E04	300	249.86	130.70	30.01	61.14	62.46
E04	350	257.83	138.64		69.30	46.23
E04	400	252.57	140.57	30.77	66.68	60.75
E04	500	246.85	133.51	52.67	64.25	57.31
E04	600	245.49	133.94	30.50	61.76	58.73
E04	800	229.38	117.94	25.66	51.86	55.13
E04	850	217.65	114.56	23.92	54.79	58.11

		Air ratios:					Ages:				
Station	Depth	F11/F12	CCl4/F11	F113/F11	CCl4/F12	F113/F12	F11/F12	CCl4/F1	F113/F11	CCl4/F12	F113/F12
	m						years	years	years	years	years
A01	0	0.53	0.45		0.24			11		7	
A01	10	0.51	0.45		0.23			10		4	
A01	30	0.50	0.39	0.40	0.20	0.20		6		1	
A01	50	0.48	0.30	0.54	0.15	0.26		1		1	
A01	75	0.42	0.50	0.43	0.21	0.18		12		1	
A01	100	0.41	0.31	0.28	0.13	0.12		1	4	1	11
A01	125	0.43	0.34	0.58	0.15	0.25		1		1	
A01	150	0.38	0.39	0.44	0.15	0.17		6		1	
A01	175	0.42	0.41	0.20	0.17	0.08		7	9	1	14
A01	200	0.41	0.35	0.62	0.14	0.25		1		1	
A01	225	0.35	0.43	0.53	0.15	0.19		8		1	
A01	275	0.38	0.71	0.17	0.27	0.06		19		10	
A01	300	0.41	0.50	0.41	0.21	0.17		12		1	
A01	350	0.42	0.48	0.62	0.20	0.26		11		1	
A01	400	0.37	0.80	0.08	0.29			20		12	
A01	450	0.43	0.54	0.79	0.23	0.34	29	14		6	
A01	500	0.35	0.67	0.97	0.23	0.34	33	18		6	
A01	550	0.25	1.34	0.07	0.34	0.02	39	26		16	
A01	600	0.39	0.60	0.05	0.24	0.02	31	17		6	
A01	700	0.37	0.73	0.70	0.27	0.26	32	19		10	
A01	800	0.38	0.84	0.56	0.32	0.21	31	20		14	
A01	900	0.43	1.02	0.83	0.44	0.36	29	23		20	
A01	1000	0.48	0.88	1.26	0.42	0.61	25	21		20	
A01	1250	0.31	1.18	2.41	0.37	0.75	36	25		18	
A01	1500				0.41	0.85				19	
A01	1700	0.35	1.08	3.88	0.38	1.36	33	23		18	
A01	1800	0.41	1.24		0.51		30	25		23	
A01	1900	0.42	1.81		0.77		29	28		28	
A01	2000										
A01	2250										
A01	2500										

		Air ratios:					Ages:				
Station	Depth	F11/F12	CCl4/F11	F113/F11	CCl4/F12	F113/F12	F11/F12	CCl4/F1	F113/F11	CCl4/F12	F113/F12
	m						years	years	years	years	years
A01	3000										
A01	3000										
A01	3360										
A01	3360										
B01	10	0.55	0.40	0.30	0.22	0.16		7		3	
B01	20	0.56	0.31	0.19	0.17	0.11		1	11	1	11
B01	40	0.51	0.30	0.21	0.15	0.11		1	8	1	11
B01	50	0.53	0.31	0.26	0.16	0.14		1	5	1	7
B01	70	0.53	0.28	0.19	0.15	0.10		1	10	1	11
B01	100	0.52	0.26	0.22	0.14	0.11		1	8	1	11
B01	125	0.54	0.27	0.13	0.15	0.07		1	14	1	15
B01	150	0.54	0.21	0.06	0.11	0.03		1		1	
B01	175	0.52	0.28		0.15		23	1		1	
B01	200	0.46	0.41	0.36	0.19	0.16	27	8		1	
B01	225	0.47	0.38	0.16	0.18	0.08	26	6		1	
B01	250	0.46	0.45	0.29	0.21	0.13	26	11		1	7
B01	275	0.42	0.43	0.16	0.18	0.07	29	9		1	
B01	300	0.42	0.71	0.29	0.30	0.12	29	19		13	
B01	350	0.40	0.51	0.14	0.20	0.06	30	12		1	
B01	400	0.47	0.67	0.37	0.32	0.18	25	18		14	
B01	450	0.41	0.59	0.14	0.24	0.06	30	16		7	
B01	500	0.40	0.59	0.44	0.24	0.18	31	16		6	
B01	600	0.40	1.00	0.59	0.40	0.24	30	23		19	
B01	700	0.44	0.80	0.41	0.35	0.18	29	20		17	
B01	800	0.42	1.16	0.32	0.48	0.13	30	25		22	
B01	1000	0.40	0.74		0.30		30	19		12	
B01	1250										
B01	1500	0.46	0.84		0.39		26	20		18	
B01	2000										
B01	2500										
B01	3423										

		Air ratios:					Ages:				
Station	Depth	F11/F12	CCl4/F11	F113/F11	CCl4/F12	F113/F12	F11/F12	CCl4/F1	F113/F11	CCl4/F12	F113/F12
	m						years	years	years	years	years
E01	20		0.42	0.25	0.22	0.13		8	6	4	7
E01	30		0.31	0.21	0.18	0.12		1	8	1	11
E01	40		0.29	0.26	0.16	0.14		1	5	1	6
E01	60		0.29	0.21	0.16	0.12		1	8	1	11
E01	70		0.28	0.20	0.15	0.11		1	10	1	11
E01	80		0.33	0.15	0.18	0.08		1	14	1	14
E01	100										
E01	125	0.54	0.28	0.42	0.15	0.23		1		1	
E01	150	0.55	0.32	0.12	0.18	0.07		1	14	1	16
E01	150	0.53	0.35	0.06	0.18	0.03		1		1	
E01	175	0.53	0.34	0.43	0.18	0.23		1		1	
E01	200	0.54	0.35	0.14	0.19	0.08		1	14	1	14
E01	210	0.54	0.35	0.42	0.19	0.23		1		1	
E01	235	0.53	0.35	0.39	0.18	0.20		1		1	
E01	250	0.47	0.34	0.25	0.16	0.12		1	6	1	10
E01	275	0.51	0.40	0.40	0.20	0.20		6		1	
E01	300	0.52	0.45	0.44	0.23	0.23		10		6	
E01	315										
E01	350	0.52	0.43	0.14	0.23	0.07		9	14	4	14
E01	400	0.51	0.49	0.25	0.25	0.13		12	5	8	8
E01	450	0.53	0.39	0.23	0.21	0.12		6	7	1	9
E01	500	0.54	0.41	0.13	0.22	0.07		7	14	3	15
E01	550	0.53	0.38	0.22	0.20	0.11		6	8	1	11
E01	600	0.53	0.40	0.23	0.21	0.12		7	7	1	9
E01	800	0.55	0.46	0.16	0.25	0.09		11	11	8	13
E01	1000	0.53	0.45	0.14	0.24	0.08		11	14	7	14
E01	1200	0.47	0.50	0.10	0.23	0.05	25	12		6	
E01	1400	0.50	0.62		0.31		24	17		13	
E01	1600	0.50	0.94		0.47		23	22		21	
E01	1830		5.45					35			
E01	1900										

		Air ratios:					Ages:				
Station	Depth	F11/F12	CCl4/F11	F113/F11	CCl4/F12	F113/F12	F11/F12	CCl4/F1	F113/F11	CCl4/F12	F113/F12
	m						years	years	years	years	years
E01	1960										
E01	2000										
E01	2035										
E01	2035										
C01	0	0.49	0.39	0.16	0.19	0.08		6	11	1	14
C01	30	0.57	0.32	0.14	0.18	0.08		1	14	1	14
C01	75	0.50	0.27	0.15	0.13	0.08		1	12	1	14
C01	100	0.50	0.29	0.11	0.14	0.06		1	15	1	18
C01	125	0.49	0.32	0.13	0.15	0.06		1	14	1	17
C01	150	0.44	0.20	0.08	0.09	0.03		1		1	
C01	200	0.40	0.17	0.11	0.07	0.04		1		1	
C01	250	0.45	0.33	0.06	0.15	0.03		1		1	
C01	300	0.43	0.26	0.10	0.11	0.04		1		1	
C01	350	0.40	0.38		0.15			6		1	
C01	400	0.41	0.50		0.20			12		1	
C01	500	0.42	0.49		0.21		29	11		1	
C01	900	0.36	0.33		0.12		33	1		1	
C01	1250		2.35					30			
C01	1500										
C01	1750										
C01	1900										
C01	1940										
D01	40	0.55	0.40	0.16	0.22	0.09		7	12	3	14
D01	80	0.53	0.34	0.10	0.18	0.05		1	19	1	20
D01	100	0.52	0.34	0.11	0.18	0.06		1	15	1	18
D01	125	0.55	0.24	0.19	0.13	0.11		1	10	1	11
D01	150	0.53	0.26	0.06	0.14	0.03		1		1	
D01	175	0.49	0.27	0.24	0.13	0.12		1	6	1	10
D01	200	0.50	0.30		0.15			1		1	
D01	225	0.47	0.31	0.21	0.15	0.10		1	8	1	11
D01	250	0.49	0.42	0.00	0.20	0.00		8		1	

		Air ratios:					Ages:				
Station	Depth	F11/F12	CCl4/F11	F113/F11	CCl4/F12	F113/F12	F11/F12	CCl4/F1	F113/F11	CCl4/F12	F113/F12
	m						years	years	years	years	years
D01	300	0.49	0.39	0.17	0.19	0.08		6	11	1	14
D01	325	0.49	0.39	0.00	0.19			6		1	
D01	350	0.47	0.42	0.16	0.20	0.08		8	11	1	14
D01	400	0.47	0.41		0.19			7		1	
D01	450	0.47	0.55		0.26			15		8	
D01	500	0.43	0.43		0.18			8		1	
D01	600	0.42	0.47		0.20		29	11		1	
D01	1000	0.39	0.59		0.23		31	16		6	
D01	1500	0.35	0.53		0.19		33	14		1	
D01	1750	0.37	0.57		0.21		32	16		1	
D01	2150										
TA	0	0.53	0.49	0.34	0.26	0.18		11		8	
TA	10	0.52	0.49	0.35	0.25	0.18		12		8	
TA	20	0.53	0.42	0.31	0.22	0.16		8		4	
TA	30	0.51	0.43	0.32	0.22	0.16		8		3	
TA	40	0.52	0.41	0.25	0.21	0.13		8	6	1	8
TA	50	0.52	0.40	0.27	0.21	0.14		6	5	1	7
TA	60	0.54	0.39	0.27	0.21	0.15		6	4	1	6
TA	70	0.51	0.40	0.17	0.20	0.09		6	11	1	12
TA	80	0.51	0.39	0.15	0.20	0.08		6	12	1	14
TA	100	0.52	0.32	0.17	0.17	0.09		1	11	1	12
TC	75	0.51	0.30	0.14	0.15	0.07		1	14	1	15
TC	100	0.53	0.31	0.05	0.17	0.03		1		1	
TC	125	0.53	0.29	0.10	0.15	0.06		1	17	1	18
TC	150	0.55	0.31	0.06	0.17	0.03		1		1	
TC	175	0.54	0.32	0.08	0.17	0.05		1		1	
TC	200	0.54	0.33	0.05	0.18	0.03		1		1	
TC	225	0.53	0.35	0.14	0.19	0.07		1	14	1	14
TC	275	0.53	0.37	0.21	0.20	0.11		3	9	1	11
TC	275										
TC	310	0.52	0.41		0.21			7		1	

		Air ratios:					Ages:				
Station	Depth	F11/F12	CCl4/F11	F113/F11	CCl4/F12	F113/F12	F11/F12	CCl4/F1	F113/F11	CCl4/F12	F113/F12
	m						years	years	years	years	years
TC	310	0.00			0.20					1	
TC	350	0.52	0.38		0.20			6		1	
TC	400	0.52	0.40	0.07	0.21	0.03		6		1	
TC	500	0.53	0.41		0.22			8		3	
TC	615	0.51	0.42	0.17	0.22	0.09		8	11	2	13
F09	0	0.51	0.38	0.20	0.19	0.10		6	9	1	11
F09	10	0.56	0.40	0.08	0.22	0.05		7		4	
F09	50	0.54	0.37		0.20			3		1	
F09	70	0.55	0.38	0.14	0.21	0.07		6	14	1	14
F09	87	0.41	0.30		0.13		30	1		1	
E04	0	0.53	0.34		0.18			1		1	
E04	50	0.48	0.42	0.34	0.20	0.16		8		1	4
E04	20	0.55	0.39	0.36	0.22	0.20		6		2	
E04	70	0.60		0.24		0.15			6		6
E04	100	0.55	0.33	0.22	0.18	0.12		1	7	1	9
E04	150	0.55	0.31	0.23	0.17	0.13		1	7	1	8
E04	200	0.55	0.41	0.25	0.23	0.14		8	6	4	7
E04	250	0.55	0.34	0.26	0.19	0.14		1	5	1	6
E04	300	0.52	0.48	0.23	0.25	0.12		11	7	7	9
E04	350	0.54	0.33		0.18			1		1	
E04	400	0.56	0.43	0.22	0.24	0.12		9	8	7	9
E04	500	0.54	0.43	0.39	0.23	0.21		8		6	
E04	600	0.55	0.44	0.23	0.24	0.12		9	7	7	9
E04	800	0.51	0.47	0.22	0.24	0.11		11	8	7	11
E04	850	0.53	0.51	0.21	0.27	0.11		12	9	9	11

Station A1, 1995:Preliminary										
SAMPLE	Pressure	Temp	Theta	Bottle	CFC-12	CFC-11	CFC-11 cor	F-113	CH3CCl3	CCl4
#	CTD	CTD		Salinity						
	dbar	deg C	deg C		nmol/m3	nmol/m3	nmol/m3	nmol/m3	nmol/m3	nmol/m3
129141	0	-0.705	-0.705	24.974	2.72	5.94	5.75	0.85	17.31	7.59
129140	10	-0.505	-0.505	29.548	2.84	5.90	5.71	1.45	19.28	6.50
129139	19	-1.088	-1.089	29.966	3.01	5.92	5.73	1.00	18.38	6.74
129138	29	-1.352	-1.352	30.368	2.68	5.91	5.72	0.81	17.18	6.05
129137	39	-1.525	-1.526	30.819	2.66	5.86	5.67	0.92	18.83	6.04
129136	49	-1.459	-1.459	31.368	2.49	5.32	5.13	0.90	16.91	4.66
129135	59	-1.366	-1.367	31.901	2.21	4.79	4.60	0.50	15.38	4.07
129134	69	-1.341	-1.342	32.167	2.13	4.48	4.29	1.26	15.55	3.68
129133	80	-1.357	-1.358	32.344	2.10	4.27	4.08	0.48	13.23	3.38
129133	80	-1.357	-1.358	32.344	2.19	4.35	4.16	0.37	15.43	3.72
129164	100	-1.394	-1.396	32.969	2.10	3.75	3.56	0.34	11.61	3.00
129122	110	-1.433	-1.435	32.722	1.81	3.56	3.37	0.54	13.50	3.13
129119	121	-1.461	-1.464	32.831	1.77	3.56	3.37	1.74	13.60	3.13
129159	140	-1.471	-1.474	33.023	1.70	3.36	3.17	0.31	11.02	2.80
129159	140	-1.471	-1.474	33.023	1.70	3.52	3.33	0.35	12.40	3.62
129151	149	-1.445	-1.448	33.156	1.84	3.18	2.99	0.31	10.34	2.94
129150	159	-1.389	-1.392	33.298	1.40	3.11	2.92	0.26	9.87	2.73
129149	169	-1.316	-1.320	33.463	1.45	2.95	2.76	0.24	9.48	2.63
129148	179	-1.218	-1.222	33.714	1.41	2.71	2.52	0.22	8.72	2.43
129156	179	-1.237	-1.242	33.633	1.40	2.91	2.72	0.29	8.85	3.29
129147	189	-1.083	-1.088	33.853	1.29	2.54	2.35	0.21	8.25	2.37
129146	200	-0.918	-0.923	34.055	1.19	2.42	2.23	0.22	8.12	2.37
129145	210	-0.775	-0.781	34.184	1.27	2.50	2.31	0.28	8.23	2.43
129144	220	-0.677	-0.684	34.337	1.34	2.38	2.19	0.19	7.54	2.40
129143	230	-0.568	-0.576	34.488	1.27	2.32	2.13	0.20	7.38	2.36
129142	241	-0.456	-0.464	34.486	1.10	2.32	2.13	0.19	7.39	2.46
129142	241	-0.456	-0.464	34.486	1.16	2.43	2.24	0.23	9.18	3.05
129174	250	-0.347	-0.355	34.547	1.15	2.47	2.28	0.26	7.60	2.55
129173	259	-0.222	-0.231	34.590	1.17	2.41	2.22	0.16	7.67	2.73
129173	259	-0.222	-0.231	34.590	1.27	2.51	2.32	0.20	8.14	2.69

Station A1, 1995:Preliminary										
SAMPLE	Pressure	Temp	Theta	Bottle	CFC-12	CFC-11	CFC-11 cor	F-113	CH3CCl3	CCl4
#	CTD	CTD		Salinity						
	dbar	deg C	deg C		nmol/m3	nmol/m3	nmol/m3	nmol/m3	nmol/m3	nmol/m3
129172	269	-0.164	-0.174	34.620	1.19	2.54	2.35	0.24	8.65	2.80
129171	280	-0.118	-0.128	34.643	1.28	2.52	2.33	0.23	8.32	2.71
129170	290	-0.048	-0.059	34.665	1.24	2.63	2.44	0.26	10.45	3.02
129167	300	0.040	0.028	34.682	1.30	2.74	2.55	0.34	9.70	3.26
129166	325	0.220	0.207	34.727	1.52	2.78	2.59	0.19	8.99	3.20
129166	325	0.220	0.207	34.727	1.36	2.89	2.70	0.26	9.73	3.44
129165	352	0.321	0.307	34.759	1.40	2.91	2.72	0.29	9.66	3.29
129210	400	0.406	0.389	34.794	1.19	2.66	2.47	0.18	8.62	3.27
129209	449	0.431	0.411	34.813	1.26	2.56	2.37	0.16	7.99	3.26
129209	449	0.431	0.411	34.813	1.33	2.75	2.56	0.17	8.02	3.27
129195	499	0.437	0.416	34.826	1.26	2.40	2.21	0.17	7.84	3.25
129194	550	0.421	0.396	34.839	1.12	2.17	1.98	0.15	6.96	2.88
129193	600	0.400	0.373	34.849	0.99	1.91	1.72	0.13	6.18	2.84
129192	700	0.329	0.298	34.861	0.91	1.70	1.51	0.13	5.47	2.69
129191	800	0.230	0.194	34.870	0.75	1.54	1.35	0.14	4.83	2.42
129190	898	0.126	0.086	34.877	0.63	1.36	1.17	0.10	4.17	2.46
129190	898	0.126	0.086	34.877	0.72	1.54	1.35	0.06	4.83	2.70
129189	1000	0.023	-0.022	34.884	0.57	1.23	1.04	0.15	3.83	2.16
129296	1199	-0.135	-0.189	34.896	0.50	1.04	0.85	0.09	3.63	1.86
129297	1200	-0.135	-0.189	34.896	0.47	1.00	0.81	0.18	3.12	1.89
129297	1200	-0.135	-0.189	34.896	0.45	0.96	0.77	0.14	2.76	1.91
129294	1399	-0.251	-0.315	34.907	0.36	0.79	0.60	0.18	2.76	1.47
129295	1399	-0.251	-0.315	34.908	0.31	0.79	0.60	0.13	2.32	1.63
129284	1499	-0.295	-0.365	34.912	0.24	0.59	0.40	0.15	1.79	1.33
129285	1499	-0.295	-0.365	34.912	0.32	0.68	0.49	0.12	2.89	1.66
129285	1499	-0.295	-0.365	34.912	0.31	0.67	0.48	0.10	2.31	1.71
129282	1598	-0.333	-0.408	34.921	0.25	0.59	0.40	0.48	1.81	1.59
129283	1598	-0.333	-0.408	34.917	0.26	0.51	0.32	0.18	1.44	1.34
129280	1701	-0.362	-0.444	34.923	0.20	0.48	0.29	0.09	3.50	0.99
129281	1701	-0.362	-0.444	34.924	0.24	0.40	0.21	0.18	0.99	1.12

Station A1, 1995:Preliminary										
SAMPLE	Pressure	Temp	Theta	Bottle	CFC-12	CFC-11	CFC-11 cor	F-113	CH3CCl3	CCl4
#	CTD	CTD		Salinity						
	dbar	deg C	deg C		nmol/m3	nmol/m3	nmol/m3	nmol/m3	nmol/m3	nmol/m3
129233	1798	-0.378	-0.465	34.925	0.20	0.51	0.32	0.00	0.00	1.32
129232	1898	-0.395	-0.488	34.930	0.09	0.32	0.13	0.00	0.00	0.52
129231	1998	-0.405	-0.505	34.936	0.13	0.33	0.14	0.00	0.00	0.96
129230	2097	-0.408	-0.514	34.938	0.08	0.28	0.09	0.00	0.00	0.35
129229	2196	-0.406	-0.520	34.939	0.08	0.24	0.05	0.00	0.29	1.14
129228	2298	-0.401	-0.522	34.943	0.07	0.23	0.04	0.00	0.00	0.36
129227	2399	-0.395	-0.523	34.946	0.01	0.21	0.02	0.00	0.00	0.08
129224	2497	-0.388	-0.524	34.941	0.06	0.23	0.04	0.00	0.00	0.27
129223	2642	-0.376	-0.524	34.948	0.05	0.21	0.02	0.00	0.72	0.30
129222	2743	-0.364	-0.520	34.951	0.08	0.27	0.08	2.56	0.00	0.11
129221	2843	-0.350	-0.514	34.952	0.09	0.13	-0.06	0.00	0.00	0.09
129221	2843	-0.350	-0.514	34.952	0.00	0.19	0.00	0.00	0.00	0.00
129220	2947	-0.341	-0.513	34.953	0.24	0.60	0.41	0.00	0.49	0.52
129219	3049	-0.332	-0.514	34.953	0.03	0.23	0.04	0.00	0.64	0.20
129218	3152	-0.323	-0.514	34.953	0.02	0.20	0.01	0.00	0.00	0.00
129217	3202	-0.319	-0.514	34.946	0.06	0.32	0.13	0.00	0.00	0.01
129216	3254	-0.314	-0.514	34.954	0.00	0.19	0.00	0.00	0.00	0.08
129214	3355	-0.305	-0.514	34.956	0.07	0.23	0.04	0.00	0.00	0.00
129213	3406	-0.301	-0.514	34.956	0.00	0.19	0.00	0.00	0.86	0.00
129212	3465	-0.295	-0.514	34.954	0.08	0.17	-0.02		0.64	0.08
129212	3465	-0.295	-0.514	34.954	0.00	0.18	-0.01	0.00	2.62	0.25
129235	3467	-0.294	-0.513	34.953	0.00	0.18	-0.01	0.00	0.00	0.00
129236	3467	-0.294	-0.513	34.953	0.00	0.19	0.00	0.00	0.00	0.00

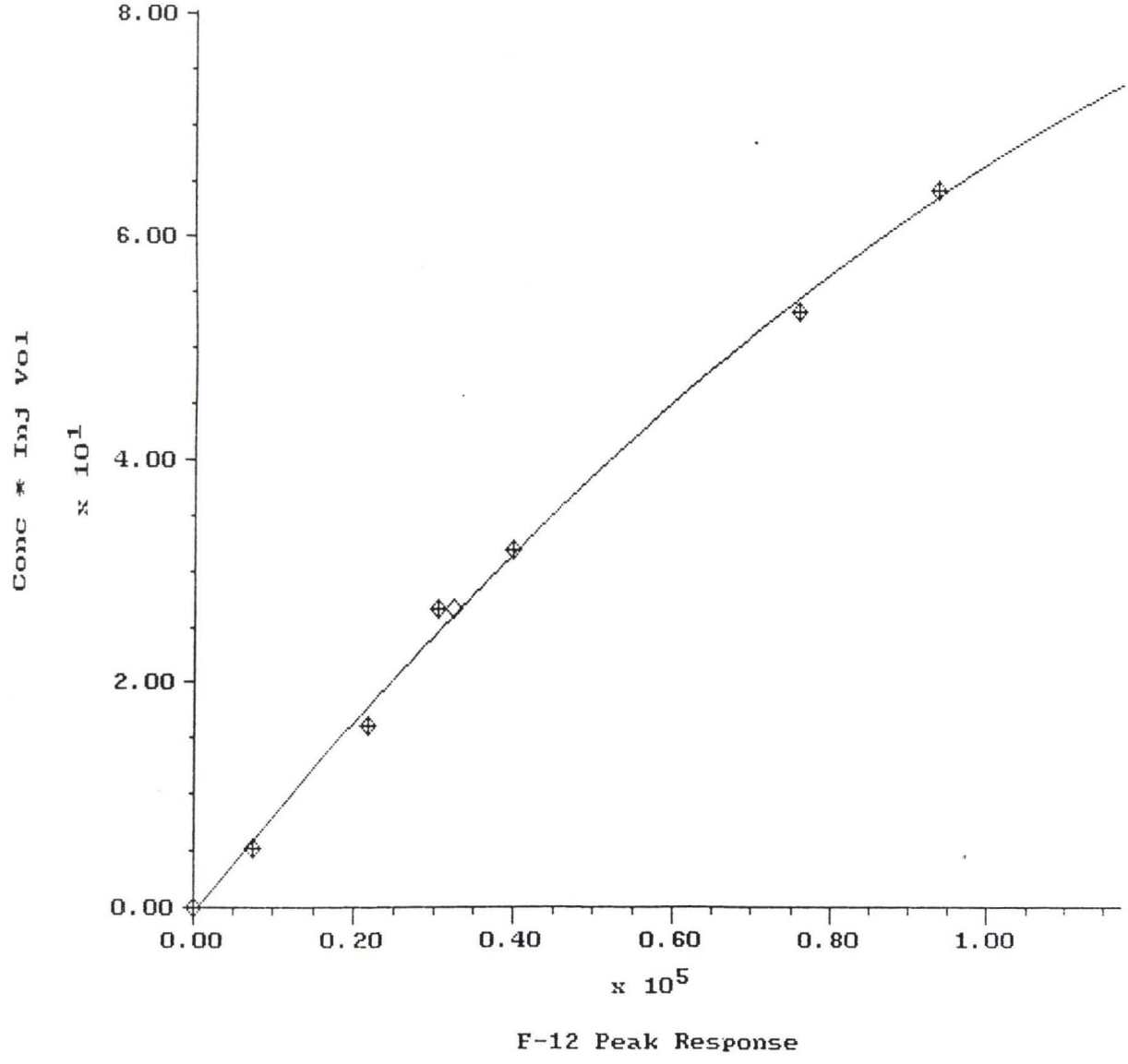
8.00
6.00
4.00
2.00
0.00
Conc * Inj Vol
x 10^1
0.00
0.20
0.40
0.60
0.80
1.00
x 10^5
F-12 Peak Response

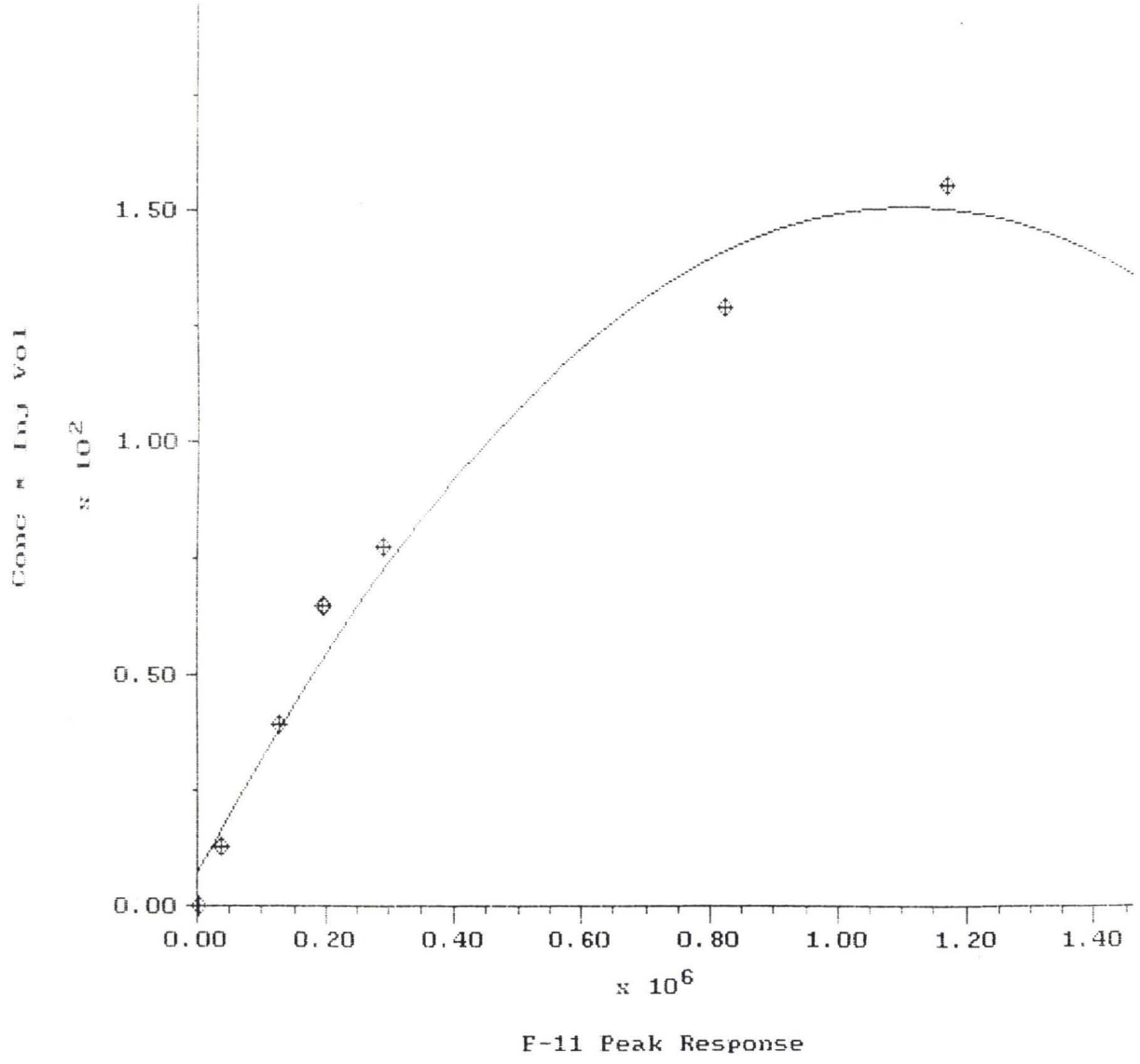
1.50
1.00
0.50
0.00
x 10^2
0.00
0.20
0.40
0.60
0.80
1.00
1.20
1.40
x 10^6
F-11 Peak Response

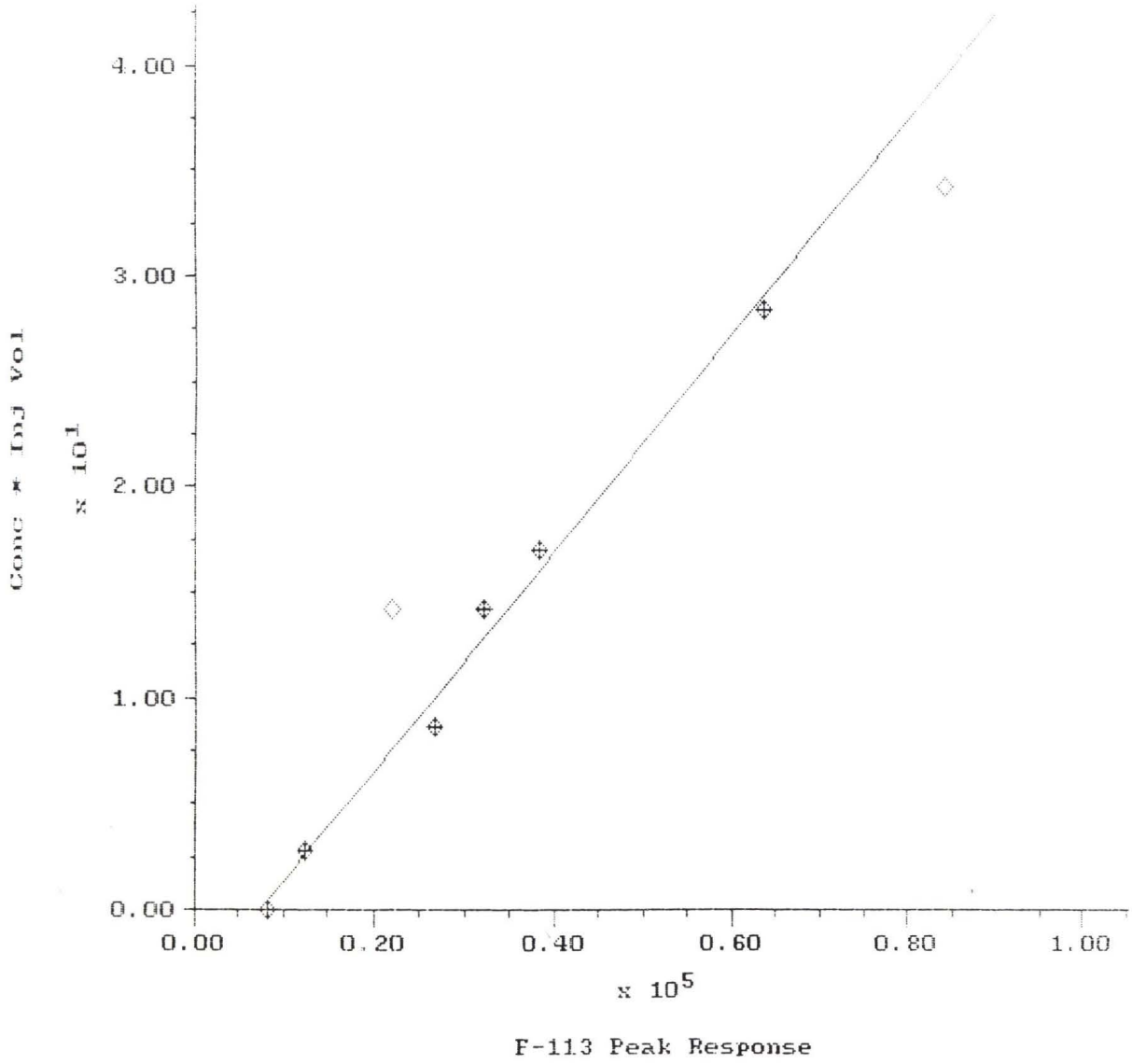
4.00
3.00
2.00
1.00
0.00
Conc * Inj Vol
x 10^1
0.00
0.20
0.40
0.60
0.80
1.00
x 10^5
F-113 Peak Response

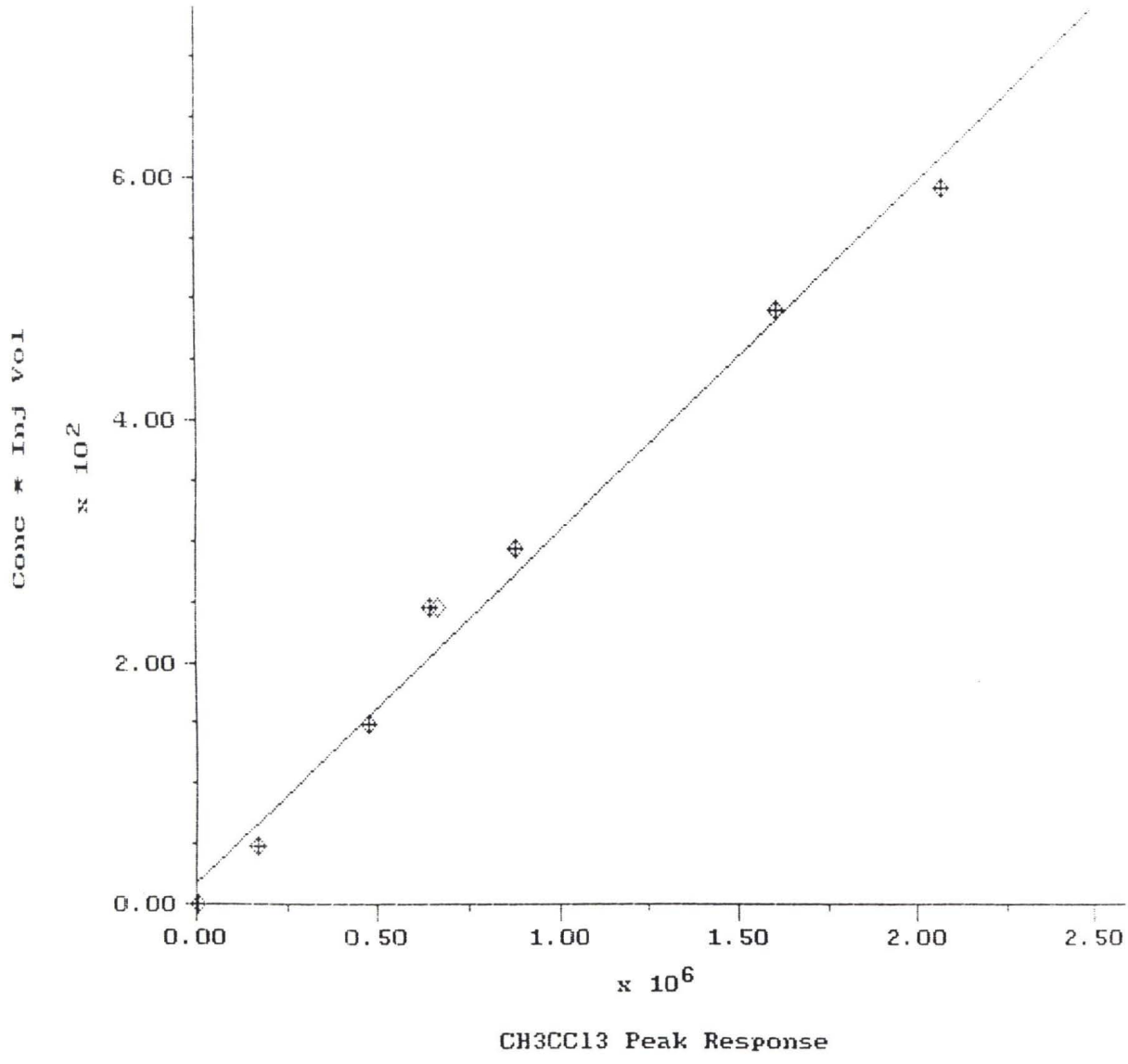
Conc * Inj Vol
x 10^2
6.00
4.00
2.00
0.00
0.00
0.50
1.00
1.50
2.00
2.50
x 10^6
CH3CCl3 Peak Response

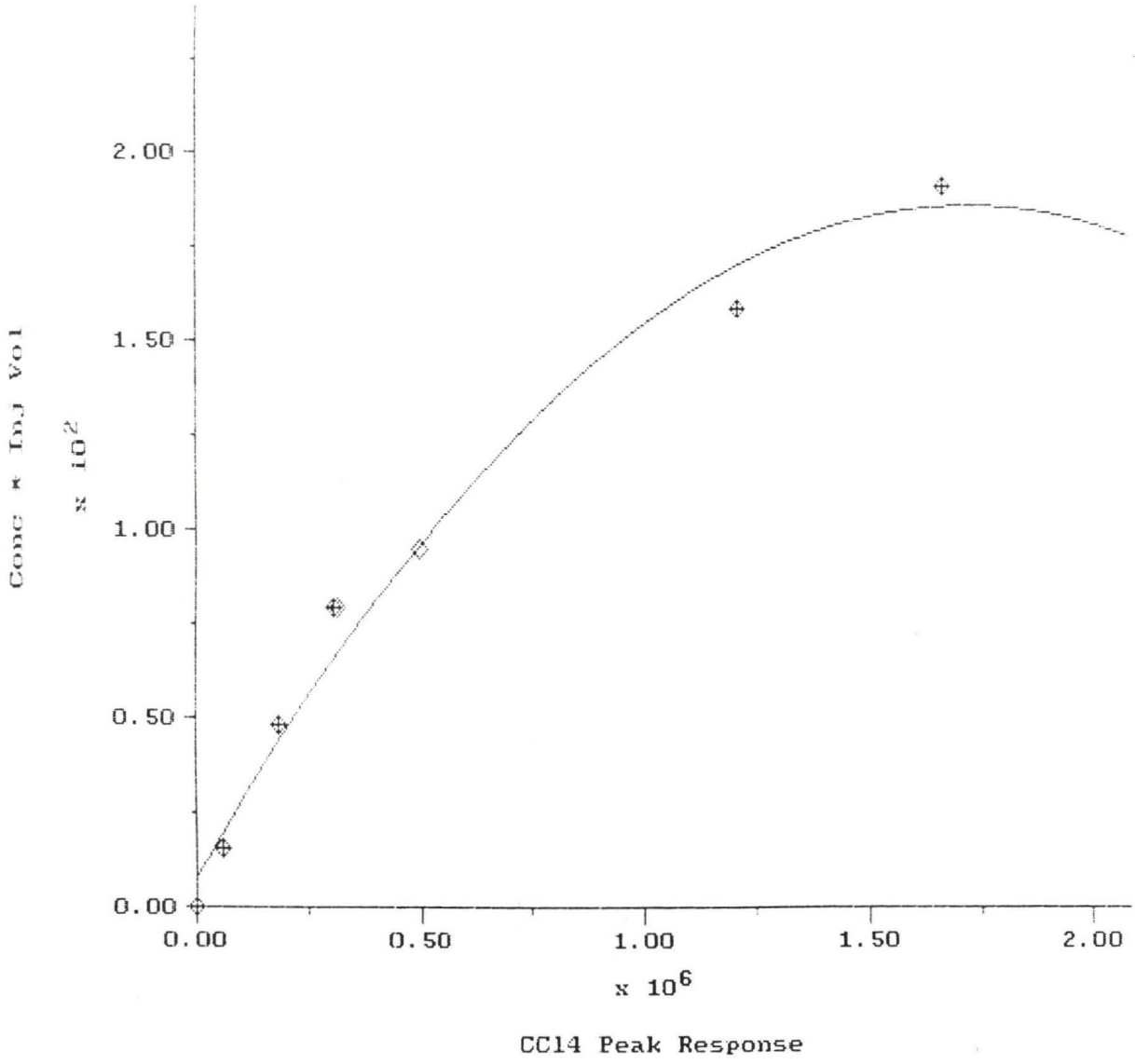
2.00
1.50
1.00
0.50
0.00
0.00
0.50
1.00
1.50
2.00
x 10^6
CCl4 Peak Response

VITA

Surname: McLaughlin Given Names: Fiona Ann

Place of birth : Kelowna, British Columbia, Canada

Educational Institutions attended:

University of Victoria	1968-72
University of Victoria	1976-77
University of Oregon	1978-79
Oregon State University	1978-79

Degrees Awarded:

B. Sc. University of Victoria 1972

Publications:

R. W. Macdonald and F. A. McLaughlin. The effect of storage by freezing on dissolved inorganic phosphate,nitrate and reactive silicate for samples from coastal and estuarine waters. Water Res., 16, 95-104, 1982.

C. S. Wong, F. A. Whitney, W. J. Cretney, K. Lee, F. McLaughlin, Jinping Wu, Tianboa Fu and Dongfa Zhuang. An experimental marine ecosystem response to crude oil and corexit 9527: Part 1 - Fate of chemically dispersed crude oil. Mar. Environ. Res., 13, 247-263, 1984.

R. W. Macdonald, F. A. McLaughlin and C. S. Wong. The storage of reactive silicate samples by freezing. Limnol. Oceanog., 31, 1139-1142, 1986.

W. J. Cretney, F. A. McLaughlin and B. R. Fowler. Implications of the solvent effect in quantitative capillary gas chromatography of minor constituents in mixtures - a study using deuterium labeled and unlabeled benzofluoranthenes. J. of H. R. C. and C. C., 10, 428-434, 1987.

Mark B. Yunker, Fiona A. McLaughlin, Robie W. Macdonald, Walter J. Cretney, Brian R. Fowler and Trevor A. Smyth. Measurement of natural trace dissolved hydrocarbons by in-situ column extraction: an intercomparison of two adsorption resins. Analyt. Chem., 61, 1333-1343, 1989.

Brian G. Whitehouse, Robie W. Macdonald, Mark B. Yunker and Fiona A. McLaughlin. Organic carbon and colloids in the Mackenzie River and Beaufort Sea. Mar. Chem., 26, 371-378, 1989.

R. W. Macdonald, E. C. Carmack, F. A. McLauhglin, K. Iseki, D. M. Macdonald and M. C. O'Brien. Composition and modification of water masses in the Mackenzie shelf estuary. J. Geophys. Res., 94, 18057-18070, 1989.

Mark B. Yunker, W. J. Cretney, B. R. Fowler, R. W. Macdonald, F. A. McLaughlin and B. G. Whitehouse. On the Distribution of Dissolved Hydrocarbons in Natural Water. Organic Geochem., 17, No. 3, 301-307, 1991.

Mark B. Yunker, Robie W. Macdonald, Brian R. Fowler, Walter J. Cretney, Scott R. Dallimore and Fiona A. McLaughlin. Geochemistry and Fluxes of Hydrocarbons to the Beaufort Sea Shelf: A Multivariate Comparison of Fluvial Inputs and Coastal Erosion of Peat Using Principal Component Analysis. Geochim. et Cosmochim. Acta, 55, 255-273, 1991.

Mark B. Yunker, Robie W. Macdonald, Walter J. Cretney, Brian R. Fowler and Fiona A. McLaughlin. Alkane, terpene and polycyclic aromatic hydrocarbon geochemistry of the Mackenzie River and Mackenzie shelf: Riverine contributions to Beaufort Sea coastal sediment. Geochim. et Cosmochim. Acta, 57, 3041-3061, 1993.

Eddy C. Carmack, Robie W. MAcdonal, Ronald G. Perkin, Fiona A. McLaughlin and Richard J. Pearson. Evidence for warming of Atlantic water in the southern Canadian Basin of the Arctic Ocean: Results from the LArsen-93 expedition. Geophys. Res. Lett., 22, 1061-1064, 1995.

Fiona A. McLaughlin, Eddy C. Carmack, Robie W. Macdonald and James K. B. Bishop. Physical and Geochemical properties across the Atlantic/Pacific water mass front in the southern Canadian Basin, J. Geophys. Res., 101, 1183-1197, 1996.

Mark B. Yunker, Lloyd R. Snowdon, Robie W. Macdonald, John N. Smith, Martin G. Fowler, Donald N. Skibo, Fiona A. McLaughlin, A. I. Danyushevskaya, V. I. Petrova and G. I. Ivanov. Polycyclic aromatic hydrocarbon composition and potential sources for sediment samples from the Beaufort and Barents Seas. Environ. Sci. Technol., 30, 1310-1320, 1996.

PARTIAL COPYRIGHT LICENSE

I hereby grant the right to lend my theisis to users of the University of Victoria Library, and to make single copies only for such users or in response to a request from the Library of any other university, or silmilar institution, on its behalf or for one of its users. I further agree that permission for extensive copying of this thesis for scholarly purposes may be granted by me or a member of the University designated by me. It is understood that copying or publication of this thesis for financila gain shall not be allowed without my written permission.

Title of thesis:

Geochemical and Physical Water Mass Properties and Halocarbon Ventilation in the Southern Canadian Basin of the Arctic Ocean

Author [redacted]

Fiona McLaughlin

April 25, 1996